IMMUNE-MEDIATED MECHANISMS OF (MAL)ADAPTIVE RENAL TISSUE REPAIR

Alessandra Tammaro

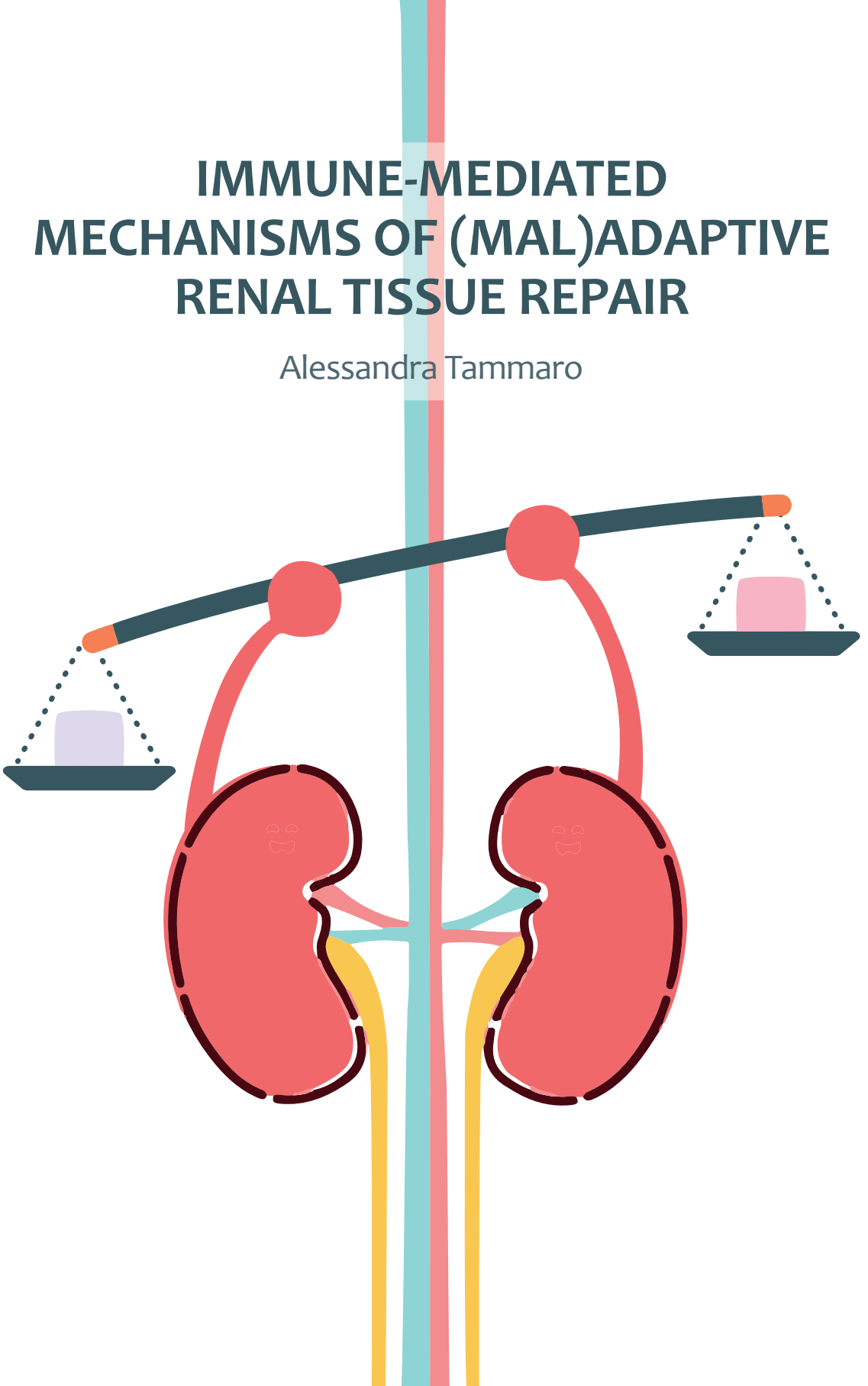

IMMUNE-MEDIATED MECHANISMS OF (MAL)ADAPTIVE RENAL TISSUE REPAIR

Alessandra Tammaro

IMMUNE-MEDIATED MECHANISMS OF (MAL)ADAPTIVE RENAL TISSUE REPAIR

Academic thesis, University of Amsterdam, Amsterdam, The Netherlands

ISBN	978-94-6375-062-2
Author	Alessandra Tammaro
Cover design	Ridderprint and Alessandra Tammaro
Layout	Wim van Est
Print	Ridderprint BV, Ridderkerk

Financial support by INOTREM for the publication of this thesis is gratefully acknowledged.

Publication of this thesis was kindly supported by the Dutch kidney foundation, HycultBiotech, Astellas Pharma and the department of pathology of the Academic Medical Center

IMMUNE-MEDIATED MECHANISMS OF (MAL)ADAPTIVE RENAL TISSUE REPAIR

ACADEMISCH PROEFSCHRIFT

ter verkrijging van de graad van doctor

aan de Universiteit van Amsterdam

op gezag van de Rector Magnificus

prof. dr. ir. K.I.J. Maex

ten overstaan van een door het College voor Promoties ingestelde commissie,

in het openbaar te verdedigen in de Agnietenkapel

op vrijdag 9 november 2018, te 14:00 uur

door **Alessandra Tammaro**

geboren te Napels, Italië

Promotiecommissie:

Promotor:	Prof. dr. S. Florquin	AMC-UvA
Copromotor(es):	dr. M.C. Dessing	AMC-UvA
	dr. J.C. Leemans	AMC-UvA
Overige leden:	Prof. dr. E.M.A. Aronica	AMC-UvA
	Prof. dr. F.J. Bemelman	AMC-UvA
	dr. M. Eikmans	Universiteit Leiden
	Prof. dr. C. van Kooten	Universiteit Leiden
	dr. B. Smeets	Radboudumc
	Prof. dr. C.J.M. de Vries	AMC-UvA
	Prof. dr. M.P.J. de Winther	AMC-UvA

Faculteit der Geneeskunde

Alla mia famiglia,
fonte inesauribile di sostegno e amore

Table of contents

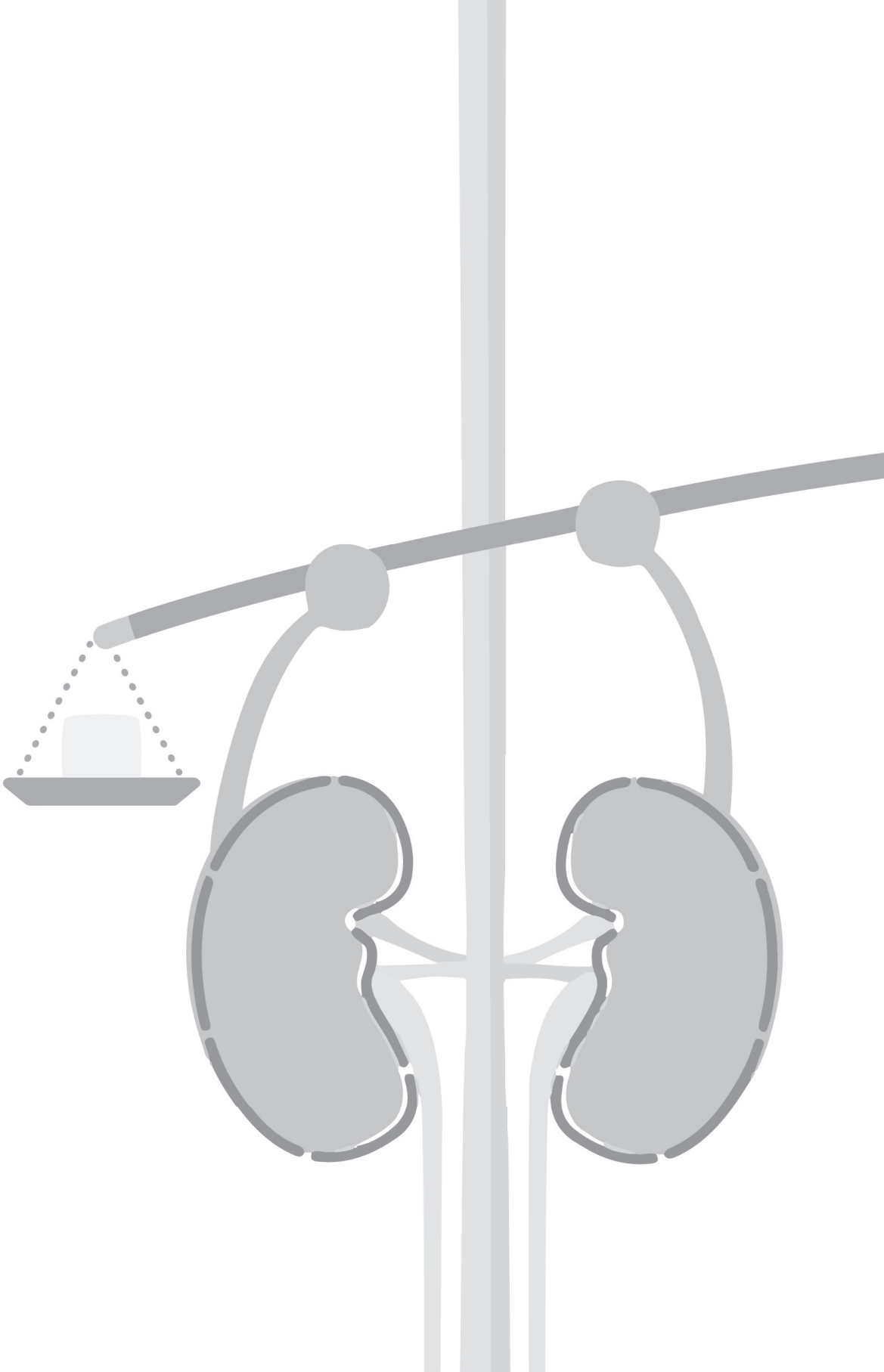

Chapter 1

General introduction and scope of the thesis

General introduction and scope of the thesis

This thesis aims to gain more insight into the role of the innate immune system in renal inflammatory diseases, focusing on the danger ligands S100A8/A9 (i.e. calprotectin) and the innate immune receptor TREM-1. Before elaborating on the evidences obtained during the last 5 years of research, I will briefly introduce the renal diseases I have been working on and the inflammatory mediators studied in this thesis.

Renal homeostasis and disease

The kidney's primary function is to maintain the volume and composition of body fluids. By excreting water and solutes through the urine, the kidney removes excess water and waste products. Moreover, the kidney also functions as a regulatory organ, by producing and secreting important hormones and controlling blood pressure. The functional unit of the kidney is the nephron, which consists of the glomerulus, the proximal tubule, the loop of Henle, the distal tubule and the collecting duct system.

Urine formation begins with blood filtration in the glomerular capillaries. The capillary endothelium, glomerular basement membrane and podocyte foot processes form the filtration barrier. The glomerulus is encased in Bowman's capsule, which connects the glomerulus to the proximal tubule. The proximal tubule is the powerhouse of the kidney; it reabsorbs the majority of the filtered water, Na+, Cl-, K+ and other solutes, in an energy-demanding manner. The key element in this process is represented by the Na+/K+ ATPase pump, present in the basolateral membrane of the proximal tubular epithelial cells (TECs).

These cells are equipped with a brush border on the apical membrane, whereas the basolateral membrane is densely packed with mitochondria, in order to meet the high energy requirement of the Na+/K+ ATPase pump. Due to their high metabolic demand, proximal TECs, especially those present in the S3 segment of the cortico-medullary area, represent the section of the nephron most susceptible to oxygen deprivation[1]. Along the nephron, the loop of Henle is responsible for the reabsorption of NaCl and water, whereas the distal segment of the nephron (distal tubules and collecting duct) makes the final adjustments in the composition and volume of the urine.

Once urine leaves the renal pelvis, it flows through the ureters and enters the urinary bladder, where it is stored. Renal function can be clinically assessed by evaluating the glomerular filtration rate (GFR) and the plasma levels of urea and creatinine. Renal diseases are associated with high morbidity and mortality[2,3]. Additionally, renal replacement therapies, which include dialysis and transplantation, although having been shown to extend life expectancy in patients with renal failure, still represent a financial burden for the healthcare system[4]. This, highlights the need for new avenues for therapeutic

intervention and the development of novel biomarkers, to provide specific treatments or earlier diagnosis. Renal diseases can manifest in two forms: acute or chronic.
Acute Kidney Injury (AKI) can be considered a reversible clinical condition, if not lethal. It is primarily characterized by rapid loss of renal function due to tubular destruction. AKI can be caused by transient ischemia, due to decreased or interrupted renal blood flow, followed by the reperfusion phase, such as during kidney transplant procedures. This is the so-called Ischemia/Reperfusion (IR)-induced acute kidney injury (AKI), which is one of the major causes of AKI[5,6]. Therefore, in our research, we studied experimental renal IR both in mice and in vitro, as a preclinical model of AKI. Conversely, chronic kidney disease (CKD) is a slower process, characterized by progressive loss of renal function due to the development of fibrosis. Tubular atrophy and interstitial fibrosis are the hallmarks of CKD and include tubular injury, chronic inflammation, myofibroblast activation and extracellular matrix deposition[7,8]. To investigate the roles of S100A8/A9 and TREM-1 in the development of progressive renal fibrosis, we used the well-established experimental model of Unilateral Ureteral Obstruction (UUO)[9].

AKI and CKD are interconnected

Epidemiological studies show that the incidence of AKI is greatly increasing in hospitalized patients[10-12]. The risk factors for AKI and CKD are quite similar. It was previously believed that patients who recovered from AKI had benign long term renal outcomes. However, since 2008, multiple observational studies, with follow up in patients who suffered from AKI, have shown a strong association between AKI and subsequent development of CKD[13]. It appears that, although patients who suffered from acute tubular necrosis are able to regain stable renal function, they later develop chronic sequelae of AKI, with progression to advanced stages of CKD, thereby increasing the risk of developing end stage renal disease (ESRD)[14-17]. This indicates that AKI is not only linked to, but may also be a primary cause of, CKD and its progression.
Animal studies have described different pathways that enhance organ dysfunction leading to fibrosis, including maladaptive repair, impaired tubular regeneration or a combination of the two[18-20]. However, the appropriate first-line and follow-up treatment for patients who survive an episode of AKI, regardless of whether they have CKD, is unclear. In light of this, novel biomarkers may be helpful to identify specific targets or the most effective moment for intervention. More importantly, particular attention should be taken to identify risk factors for progression, as this is a key element in prevention.

(Mal)adaptive repair after AKI

Most of the pre-clinical models studied to evaluate the pathophysiological events mediating the progression of AKI to CKD have used ischemia/reperfusion (IR) injury[13].

Nephrotoxic models and reversible ureteral obstruction have also been described, with fibrosis as the primary end point. However, a better animal model should be developed, one that mimics several aspects of human AKI, including the comorbidities, which represent a great risk for progression.

During ischemia, the kidney experiences a shortage of oxygen and glucose due to hypoperfusion. This is generally followed by restoration of blood flow, which is accompanied by renal injury and the initiation of inflammatory responses[21,22]. Within the nephron, the cells most susceptible to oxygen deprivation and ATP depletion are the proximal TECs, because of their high metabolic rate. Hence, IR induces severe damage in TECs, which gives rise to an altered morphology and cell death by necrosis or apoptosis[23-25]. Damaged TECs do not respond passively to injury but, instead, participate in the activation of the inflammatory response. Necrosis induces the release of pro-inflammatory mediators by TECs. This first results in infiltration of granulocytes, followed by macrophages in the renal parenchyma, which aid in the digestion and removal of necrotic material[26,27]. M1 macrophages are the first players in the tubular injury response. Granulocytes and macrophages release pro-inflammatory cytokines, including TNFα, which further fuels cell death in TECs. Hence, in this so-called "injury phase" there is a vicious cycle in which injury-induced cell death enhances inflammation, thereby promoting further cell death.

Renal regeneration, accomplished by active tissue repair, depends on the presence of an appropriate microenviroment in which surviving TECs can re-differentiate and proliferate, in order to replace lost cells. During the initial repair, macrophages switch from an M1 to M2 phenotype, which plays a beneficial role in wound healing as M2 macrophages function as scavengers of cell debris and promote tubular regeneration[28-31]. M2 macrophages secrete growth factors and other molecules, often associated with fibrosis, which support tubular repair[32]. During repair, the surviving TECs upregulate different markers, many of which are associated with fibroblasts or fibrosis markers. This, together with their expression of proliferation marker Ki67, suggests that the de-differentiated pool of TECs is actively proliferating in order to re-establish tubular morphology and function[33-35].

The abovementioned mechanism is the so-called 'adaptive repair' after AKI, which leads to the regaining of normal renal function over the course of few days, without scarring. However, it also suggests that fibrosis functions as a kind of a scaffold to facilitate the proliferation and re-differentiation of TECs. The progression of AKI into CKD, is often the result of a maladaptive repair response. Recent evidences have unraveled the different mechanisms underlying this detrimental process.

One of the main discoveries was that TECs can undergo cell cycle arrest in G2/M and senescence[18,36]. This is similar to what occurs in the aged kidney, which suffers nephron loss due to a failure in TEC re-differentiation and tubular senescence[37-39]. The mechanisms involved in this aberrant wound healing response that leads to CKD include: (a) altered growth factor expression, mainly pro-fibrotic, such as TGFβ and CTGF, secreted from G2/M-arrested TECs[40]. These pro-fibrotic factors stimulate (b) fibroblast activation and proliferation, which in turn leads to (c) increased interstitial collagen deposition. The failure to re-differentiate induces (d) chronic expression of KIM-1 on surviving TECs and increases (e) tubular loss[41]. Injured TECs retain pro-inflammatory capacities, thus, as a defense mechanism they stimulate (e) chronic inflammatory infiltration. As we mentioned earlier, macrophages play an important role in tubular repair[42]. However, when tubular injury is persistent, M2 macrophages accumulate in the renal parenchyma and gain a pro-fibrotic role, by secreting large amounts of pro-fibrotic factors, such as TGFβ[43]. Interestingly, kidney progression towards CKD, displays many characteristics associated with natural ageing, including the abovementioned pathological responses, but most importantly, tubular senescence[44,45]. Senescence is the result of a cellular stress response that results in a permanent growth arrest after acute or chronic triggers. Senescent cells are not inactive but, instead, retain the ability to propagate their senescent phenotype through a peculiar secretome. This so called "senescence-associated secretory phenotype" (SASP) is a mix of pro-inflammatory and fibrotic mediators, which can further promote chronic inflammation and fibrosis[46,47]. There is growing evidence that senescence promotes tissue degeneration during ageing and in several pathophysiological contexts[48], including multiple kidney diseases[49]. Accelerated senescence may promote pathologic alterations in kidneys, including AKI-CKD progression and shorten healthy lifespan[50].

The proximal tubule is the target of many injuries which drive the development of renal fibrosis. Proximal TECs require proper mitochondrial function in order to regulate a plethora of metabolic functions and signaling pathways[51]. Impaired mitochondrial homeostasis in TECs, is often associated with enhanced oxidative stress and accumulation of ROS, which is cytotoxic and may induce cell cycle arrest[52,53]. Recently, it has been described that mitochondrial dysfunction can also induce a senescent state termed MiDAS (mitochondrial dysfunction-associated secretory phenotype). This senescent state causes a mitotic arrest[54], suggesting that energy metabolism is an important factor in cell cycle arrest and senescence.
These evidences highlight the fact that new metabolic mechanisms should be investigated in order to prevent tubular senescence and reduce the risk of developing chronic disease after acute injury.

Inflammatory mediators in tissue injury

The Danger Theory elegantly describes that ischemia or trauma trigger an inflammatory response in different organs, just as a pathogen would[55]. Injured cells release damage-associated molecular patterns (DAMPs), which are recognized by Pattern Recognition Receptor (PRRs) that, in turn, activate an inflammatory response. Both ligands and receptors that activate the innate immune response have been shown to play a role in the pathophysiology of renal diseases.

In this thesis, we focused our attention on one class of DAMPs, the protein complex S100A8/A9, also known as calprotectin, and the innate immune receptor TREM-1. We explored the contribution of these two components of the innate immune system in the pathogenesis of acute and chronic kidney diseases.

S100A8/A9 protein complex

The S100 proteins were discovered in 1965 and identified in bovine brain fractions as proteins of the nervous system[56,57]. The genes encoding the majority of S100 proteins are located in the chromosomal region 1q21. In humans, the S100 family belongs to the Ca^{2+}-binding protein superfamily, that comprises circa 25 members. The majority of these proteins, including the S100A8/A9 complex, form heterodimers in vitro and in vivo, which confer protein function.

S100A8 and S100A9 are primarily expressed in myeloid cells, specifically neutrophils and monocyte/macrophages. However, increasing evidences describe their expression in epithelial cells, under inflammatory conditions[58].

Two forms are described for the complex protein: a secreted form and an intracellular form, which represents circa 60% of the cytosolic portion in neutrophils but is less abundant in monocytes. The secreted form can occur during translocation from the cytosol to the plasma membrane (active way), or as an extracellular release from the cytosol, as a result of tissue damage and cellular necrosis. In this last case, S100A8/A9 acts as DAMPs and modulate the inflammatory response by promoting innate immune cell recruitment to the site of injury. Moreover, the S100A8/A9 protein complex signals through Toll Like Receptor (TLR)-4 and Receptor of Advanced glycated end products (RAGE), to promote effector functions of the inflammatory response[59-61].

Additionally, extracellular S100A8/A9 can induce loss of integrity and cell death in endothelial cells and has an apoptotic effect in many cancer cell lines.

Elevated levels of the protein are present in sera and fluids of patients with several inflammatory conditions; it is, indeed, used as a reliable biomarker for arthritis, inflammatory bowel diseases, renal allograft rejection and cardiovascular diseases.

Given its high expression during inflammation in many organs, blocking S100A8/A9

represents an innovative approach to modulate the local inflammatory response, while avoiding systemic effects.

*Triggering receptor expressed on myeloid cells-1 (adapted from **Chapter 4**)*

The TREM-family comprises both activating and inhibitory receptors. Among the family members, TREM-1 represents the most widely studied activating receptor. Activation of TREM-1 is known to trigger and amplify inflammation, especially through synergism with TLR signaling.

Experiments performed by Colonna and colleagues where the first to show that TREM-1 is mainly expressed on myeloid cells, such as monocytes/macrophages and granulocytes. However, ongoing research shows that during inflammation, TREM-1 is also detected on parenchymal cell types, such as bronchial, corneal, gastric epithelial cells and hepatic endothelial cells[62-65]. TREM-1 is present in 2 forms: as a membrane-bound receptor and as a soluble protein. Membrane TREM-1 associates with the adaptor molecule TYROBP (TYRO protein tyrosine kinase-binding protein, more frequently called DAP12: DNAX activating protein of 12 kDa)[66] for signal transduction. TREM-1 activation stimulates the production of pro-inflammatory cytokines, chemokines and cell-surface molecules. In addition, TREM activation can promote mitochondrial integrity and cell survival by inactivating pro-apoptotic factors and inhibiting CytoC (Cytochrome-C) release from mitochondria[67,68]. Besides the membrane receptor, a soluble form of TREM-1 (sTREM-1) has been described. Although the origin and function of sTREM-1 is still elusive, its relevance as both a biomarker and a therapeutic target is high in both sterile and infectious disease settings. During infection or inflammation, sTREM-1 can be detected in biological fluids. In sterile inflammation, increased sTREM-1 levels have been reported during renal IR, in chronic kidney disease patients on hemodialysis, myocardial infarction, inflammatory bowel diseases, acute gouty inflammation and rheumatoid arthritis. The biological relevance of sTREM-1 in sterile inflammation is still unclear in contrast to its significance as a predictor of infection and inflammation in infectious diseases. In many inflammatory conditions, TREM-1 intervention shows a beneficial effect in murine studies, however, the precise mechanism underlying this protection is unknown, and the mechanism-of-action should be further investigated before proposing TREM-1 as a target for intervention therapy[69].

Outline of the thesis

The general aim of this thesis is to increase our knowledge into the immunopathogenesis of renal sterile inflammatory diseases, with a focus on the innate immune response activation by the danger protein S100A8/A9 and the receptor TREM-1. The different research topics covered in this thesis are illustrated in Figure 1.

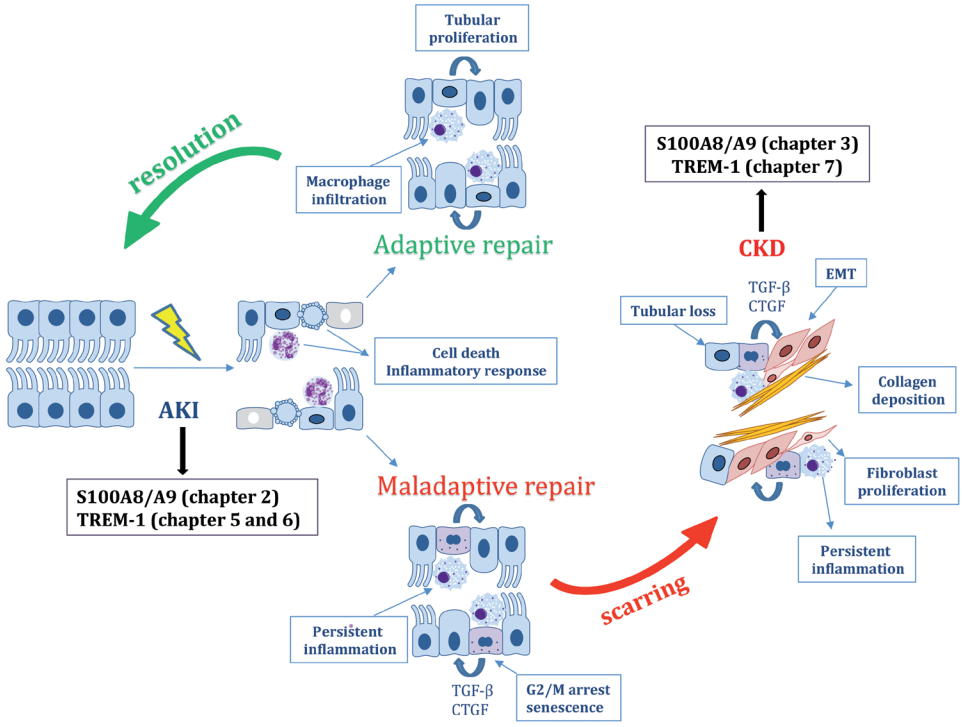

Figure 1: Thesis outline and simplified overview of maladaptive repair mechanisms post-AKI. The various research questions are depicted in black. AKI (acute kidney injury), TREM-1 (triggering receptor expressed on myeloid cells-1), TGFβ (transforming growth factor β), CTGF (connective tissue growth factor),EMT (epithelial mesenchymal transition) and CKD (chronic kidney disease).

In **Chapter 2,** the role of S100A8/A9 in the pathogenesis of IR-induced AKI was investigated. Mice lacking the S100A9 protein were subjected to IR and the injury and repair processes were evaluated. To increase our insight into S100A8/A9 signaling in the development of CKD, we used a murine model of obstructive nephropathy to induce tubulointerstitial fibrosis in WT and S100A9 KO animals in **Chapter 3**.

TREM-1 belongs to a family of receptors which are expressed on myeloid cells and is well-known to be activated during infection. However, increasing evidences describe its role during sterile inflammation. Hence, in **Chapter 4,** we reviewed the current evidences and understanding of TREM-1's role, specifically in sterile inflammatory diseases.

In **Chapter 5** we contributed to this knowledge by describing the role of TREM-1 in a pre-clinical model of AKI and in human kidney transplant patients. We subjected WT mice to renal IR injury and used different TREM-1 inhibitors to modulate its function, in order to evaluate the inflammatory response and renal damage in the acute phase of injury after ischemia. In transplanted kidney patients, we evaluated whether TREM-1 Single Nucleotide Variants (SNVs) were associated with any pathological consequences after transplantation.

An extensive research into the role of TREM-1 in the pathology of ischemic acute disease was performed in **Chapter 6,** where we used TREM-1/3 KO animals and subjected them to renal IR. In this study we set out to dissect the role of TREM-1 in kidney regeneration after injury.

Renal fibrosis can be a consequence of impaired renal regeneration, thus, in **Chapter 7,** we evaluated the specific role of TREM-1 signaling in a chronic model of renal injury. We investigated the roles of both TREM-1 role and DAP12, the signaling adapter molecule for TREM-1, in the development of renal fibrosis caused by unilateral ureteral obstruction.

Finally, in **Chapter 8**, we discuss our findings.

References

1. Liu, B.-C., Tang, T.-T., Lv, L.-L. & Lan, H.-Y. Renal tubule injury: a driving force toward chronic kidney disease. Kidney Int. **93**, 568–579 (2018).
2. Levin, A. et al. Global kidney health 2017 and beyond: a roadmap for closing gaps in care, research, and policy. Lancet **390**, 1888–1917 (2017).
3. Vanmassenhove, J., Kielstein, J., Jörres, A. & Biesen, W. Van. Management of patients at risk of acute kidney injury. Lancet **389**, 2139–2151 (2017).
4. Vanholder, R., Lameire, N., Annemans, L. & Van Biesen, W. Cost of renal replacement: how to help as many as possible while keeping expenses reasonable? Nephrol. Dial. Transplant. **31**, 1251–1261 (2016).
5. Sharfuddin, A. A. & Molitoris, B. A. Pathophysiology of ischemic acute kidney injury. Nat. Rev. Nephrol. **7**, 189–200 (2011).
6. Zuk, A. & Bonventre, J. V. Acute Kidney Injury. Annu. Rev. Med. **67**, 293–307 (2016).
7. Duffield, J. S. Cellular and molecular mechanisms in kidney fibrosis. J. Clin. Invest. **124**, 2299–306 (2014).
8. Zhou, D. & Liu, Y. Renal fibrosis in 2015: Understanding the mechanisms of kidney fibrosis. Nat. Rev. Nephrol. **12**, 68–70 (2016).
9. Chevalier, R. L., Forbes, M. S. & Thornhill, B. A. Ureteral obstruction as a model of renal interstitial fibrosis and obstructive nephropathy. Kidney Int **75**, 1145–1152 (2009).
10. Ishani, A. et al. Acute kidney injury increases risk of ESRD among elderly. J. Am. Soc. Nephrol. **20**, 223–8 (2009).
11. Xue, J. L. et al. Incidence and mortality of acute renal failure in Medicare beneficiaries, 1992 to 2001. J. Am. Soc. Nephrol. **17**, 1135–42 (2006).
12. Chawla, L. S., Eggers, P. W., Star, R. A. & Kimmel, P. L. Acute Kidney Injury and Chronic Kidney Disease as Interconnected Syndromes. N. Engl. J. Med. **371**, 58–66 (2014).
13. Basile, D. P. et al. Progression after AKI: Understanding Maladaptive Repair Processes to Predict and Identify Therapeutic Treatments. J. Am. Soc. Nephrol. **27**, 687–97 (2016).
14. Rifkin, D. E., Coca, S. G. & Kalantar-Zadeh, K. Does AKI truly lead to CKD? J. Am. Soc. Nephrol. **23**, 979–84 (2012).
15. Chawla, L. S. & Kimmel, P. L. Acute kidney injury and chronic kidney disease: an integrated clinical syndrome. Kidney Int **82**, 516–524 (2012).
16. Coca, S. G., Singanamala, S. & Parikh, C. R. Chronic kidney disease after acute kidney injury: a systematic review and meta-analysis. Kidney Int. **81**, 442–448 (2012).
17. Thakar, C. V, Christianson, A., Himmelfarb, J. & Leonard, A. C. Acute kidney injury episodes and chronic kidney disease risk in diabetes mellitus. Clin. J. Am. Soc. Nephrol. **6**, 2567–72 (2011).
18. Yang, L., Besschetnova, T. Y., Brooks, C. R., Shah, J. V & Bonventre, J. V. Epithelial cell cycle arrest in G2/M mediates kidney fibrosis after injury. Nat. Med. **16**, 535–543 (2010).
19. Grgic, I. et al. Targeted proximal tubule injury triggers interstitial fibrosis and glomerulosclerosis. Kidney Int. **82**, 172–183 (2012).

20. Ferenbach, D. A. & Bonventre, J. V. Mechanisms of maladaptive repair after AKI leading to accelerated kidney ageing and CKD. Nat. Publ. Gr. **11**, 264–276 (2015).
21. Kumar, S. Cellular and molecular pathways of renal repair after acute kidney injury. Kidney Int. **93**, 27–40 (2018).
22. Bonventre, J. & Yang, L. Cellular pathophysiology of ischemic acute kidney injury. J. Clin. Invest. **121**, (2011).
23. Kers, J., Leemans, J. C. & Linkermann, A. An Overview of Pathways of Regulated Necrosis in Acute Kidney Injury. Semin. Nephrol. **36**, 139–152 (2016).
24. Havasi, A. & Borkan, S. C. Apoptosis and acute kidney injury. Kidney Int. **80**, 29–40 (2011).
25. Linkermann, A. et al. Regulated cell death in AKI. J. Am. Soc. Nephrol. **25**, 2689–701 (2014).
26. Clements, M. et al. Differential Ly6C Expression after Renal Ischemia-Reperfusion Identifies Unique Macrophage Populations. J. Am. Soc. Nephrol. ASN.2014111138- (2015). doi:10.1681/ASN.2014111138
27. Sachet, M., Liang, Y. Y. & Oehler, R. The immune response to secondary necrotic cells. Apoptosis **22**, 1189–1204 (2017).
28. Zhang, M.-Z. et al. CSF-1 signaling mediates recovery from acute kidney injury. J. Clin. Invest. **122**, 4519–32 (2012).
29. Kinsey, G. R. Macrophage dynamics in AKI to CKD progression. J. Am. Soc. Nephrol. **25**, 209–11 (2014).
30. Lee, S. et al. Distinct macrophage phenotypes contribute to kidney injury and repair. J. Am. Soc. Nephrol. **22**, 317–26 (2011).
31. Lin, S.-L. et al. Macrophage Wnt7b is critical for kidney repair and regeneration. Proc. Natl. Acad. Sci. U. S. A. **107**, 4194–9 (2010).
32. Vinuesa, E. et al. Macrophage involvement in the kidney repair phase after ischaemia/reperfusion injury. J. Pathol. **214**, 104–113 (2008).
33. Kusaba, T., Lalli, M., Kramann, R., Kobayashi, A. & Humphreys, B. D. Differentiated kidney epithelial cells repair injured proximal tubule. Proc. Natl. Acad. Sci. U. S. A. **111**, 1527–32 (2014).
34. Guan, Q., Nguan, C. Y. C. & Du, C. Expression of Transforming Growth Factor-β1 Limits Renal Ischemia-Reperfusion Injury. Transplantation **89**, 1320–1327 (2010).
35. Berger, K. et al. Origin of regenerating tubular cells after acute kidney injury. Proc. Natl. Acad. Sci. **111**, 1533–1538 (2014).
36. Krishnamurthy, J. et al. Ink4a/Arf expression is a biomarker of aging. J. Clin. Invest. **114**, 1299–1307 (2004).
37. Berkenkamp, B. et al. In Vivo and In Vitro Analysis of Age-Associated Changes and Somatic Cellular Senescence in Renal Epithelial Cells. PLoS One **9**, e88071 (2014).
38. Chkhotua, A. B. et al. Increased expression of p16(INK4a) and p27(Kip1) cyclin-dependent kinase inhibitor genes in aging human kidney and chronic allograft nephropathy. Am. J. Kidney Dis. **41**, 1303–13 (2003).

39. Baisantry, A. et al. Autophagy Induces Prosenescent Changes in Proximal Tubular S3 Segments. 1–8 (2015). doi:10.1681/ASN.2014111059
40. Qi, W. et al. Integrated actions of transforming growth factor-β 1 and connective tissue growth factor in renal fibrosis. Am. J. Physiol. Physiol. **288**, F800–F809 (2005).
41. Humphreys, B. D. et al. Chronic epithelial kidney injury molecule-1 expression causes murine kidney fibrosis. J. Clin. Invest. **123**, 4023–4035 (2013).
42. Lin, S. L. et al. Macrophage Wnt7b is critical for kidney repair and regeneration. Proc. Natl. Acad. Sci. U. S. A **107**, 4194–4199 (2010).
43. Braga, T. T., Agudelo, J. S. H. & Camara, N. O. S. Macrophages During the Fibrotic Process: M2 as Friend and Foe. Front. Immunol. **6**, 602 (2015).
44. Luo, C. et al. Wnt9a Promotes Renal Fibrosis by Accelerating Cellular Senescence in Tubular Epithelial Cells. J. Am. Soc. Nephrol. **29**, 1238–1256 (2018).
45. Clements, M. E., Chaber, C. J., Ledbetter, S. R. & Zuk, A. Increased Cellular Senescence and Vascular Rarefaction Exacerbate the Progression of Kidney Fibrosis in Aged Mice Following Transient Ischemic Injury. PLoS One **8**, e70464 (2013).
46. Gewin, L. & Zent, R. How does TGF-β mediate tubulointerstitial fibrosis? Semin. Nephrol. **32**, 228–35 (2012).
47. Rodier, F. et al. Persistent DNA damage signalling triggers senescence-associated inflammatory cytokine secretion. Nat. Cell Biol. **11**, 973–979 (2009).
48. Muñoz-Espín, D. & Serrano, M. Cellular senescence: from physiology to pathology. Nat. Rev. Mol. Cell Biol. **15**, 482–496 (2014).
49. Valentijn, F. A., Falke, L. L., Nguyen, T. Q. & Goldschmeding, R. Cellular senescence in the aging and diseased kidney. J. Cell Commun. Signal. **12**, 69–82 (2018).
50. Sturmlechner, I., Durik, M., Sieben, C. J., Baker, D. J. & van Deursen, J. M. Cellular senescence in renal ageing and disease. Nat. Rev. Nephrol. **13**, 77–89 (2017).
51. Bhargava, P. & Schnellmann, R. G. Mitochondrial energetics in the kidney. Nat. Rev. Nephrol. **13**, 629–646 (2017).
52. Brooks, C., Wei, Q., Cho, S.-G. & Dong, Z. Regulation of mitochondrial dynamics in acute kidney injury in cell culture and rodent models. J. Clin. Invest. **119**, 1275–1285 (2009).
53. Small, D. M. et al. Oxidative stress and cell senescence combine to cause maximal renal tubular epithelial cell dysfunction and loss in an in vitro model of kidney disease. Nephron. Exp. Nephrol. **122**, 123–30 (2012).
54. Wiley, C. D. et al. Mitochondrial Dysfunction Induces Senescence with a Distinct Secretory Phenotype. Cell Metab. **23**, 303–314 (2016).
55. Matzinger, P. Tolerance, Danger, and the Extended Family. Annu. Rev. Immunol. **12**, 991–1045 (1994).
56. Moore, B. W. A soluble protein characteristic of the nervous system. Biochem. Biophys. Res. Commun. **19**, 739–44 (1965).

57. Pruenster, M., Vogl, T., Roth, J. & Sperandio, M. S100A8/A9: From basic science to clinical application. Pharmacol. Ther. **167**, 120–131 (2016).
58. Donato, R. et al. Functions of S100 proteins. Curr. Mol. Med. **13**, 24–57 (2013).
59. Vogl, T. et al. Mrp8 and Mrp14 are endogenous activators of Toll-like receptor 4, promoting lethal, endotoxin-induced shock. Nat Med **13**, 1042–1049 (2007).
60. Ehlermann, P. et al. Increased proinflammatory endothelial response to S100A8/A9 after preactivation through advanced glycation end products. Cardiovasc. Diabetol. **5**, 6 (2006).
61. Narumi, K. et al. Proinflammatory Proteins S100A8/S100A9 Activate NK Cells via Interaction with RAGE. J. Immunol. **194**, 5539–48 (2015).
62. Barrow, a. D. et al. Cutting Edge: TREM-Like Transcript-1, a Platelet Immunoreceptor Tyrosine-Based Inhibition Motif Encoding Costimulatory Immunoreceptor that Enhances, Rather than Inhibits, Calcium Signaling via SHP-2. J. Immunol. **172**, 5838–5842 (2004).
63. Rigo, I. et al. Induction of triggering receptor expressed on myeloid cells (TREM-1) in airway epithelial cells by 1,25(OH) 2 vitamin D 3. Innate Immun. **18**, 250–257 (2012).
64. Schmausser, B. et al. Triggering receptor expressed on myeloid cells-1 (TREM-1) expression on gastric epithelium: implication for a role of TREM-1 in Helicobacter pylori infection. Clin Exp Immunol **152**, 88–94 (2008).
65. Chen, L. C., Laskin, J. D., Gordon, M. K. & Laskin, D. L. Regulation of TREM expression in hepatic macrophages and endothelial cells during acute endotoxemia. Exp Mol Pathol **84**, 145–155 (2008).
66. Colonna, M. & Facchetti, F. TREM-1 (triggering receptor expressed on myeloid cells): a new player in acute inflammatory responses. J. Infect. Dis. **187** Suppl, S397-401 (2003).
67. Yuan, Z. et al. Triggering receptor expressed on myeloid cells 1 (TREM-1)-mediated Bcl-2 induction prolongs macrophage survival. J Biol. Chem **289**, 15118–15129 (2014).
68. Yuan, Z. et al. TREM-1-accentuated lung injury via miR-155 is inhibited by LP17 nanomedicine. Am. J Physiol Lung Cell Mol. Physiol **310**, L426–L438 (2016).
69. Tammaro, A. et al. TREM-1 and its potential ligands in non-infectious diseases: from biology to clinical perspectives. Pharmacol. Ther. **177**, (2017).

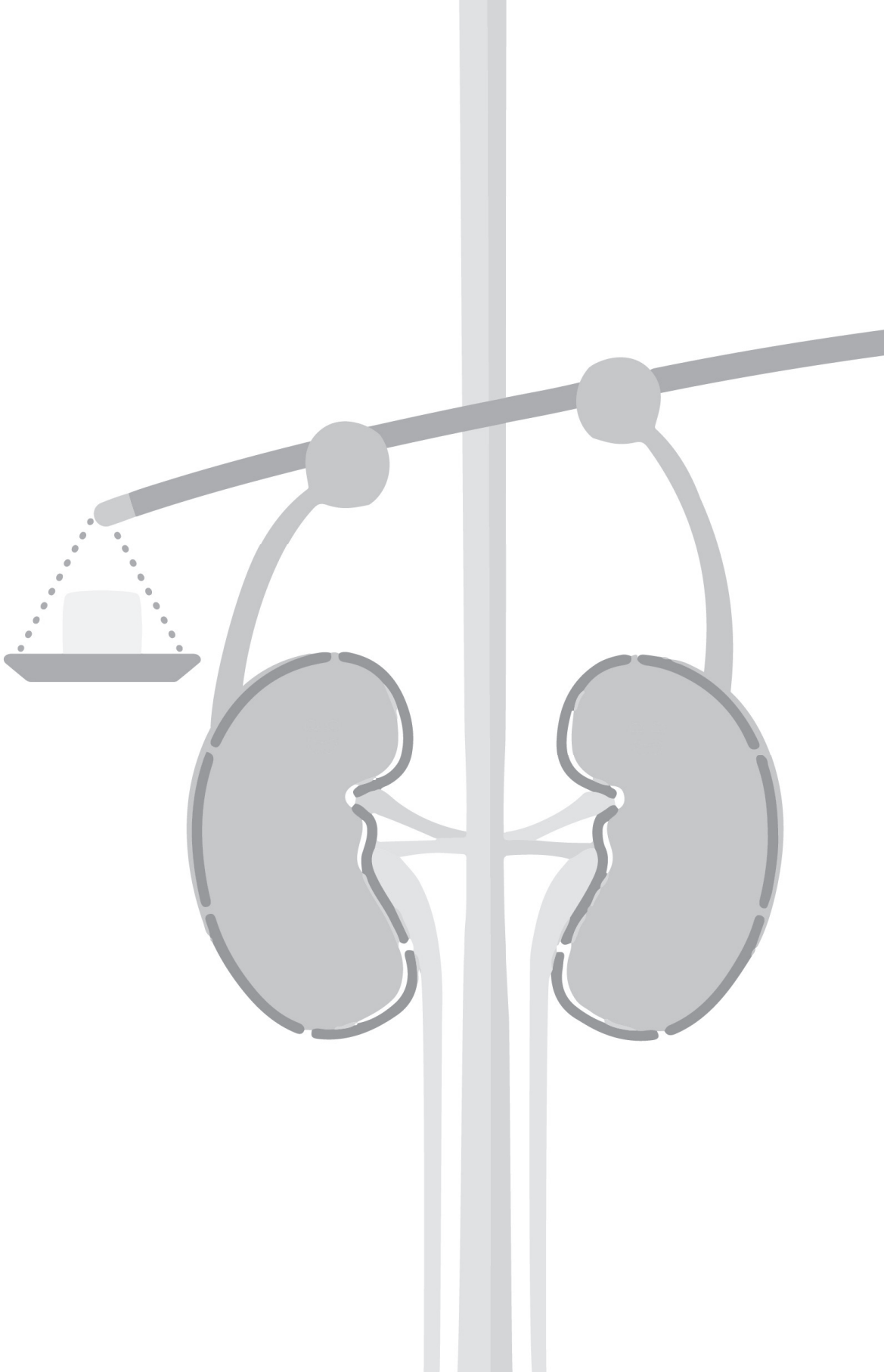

Chapter 2

The calcium-binding protein complex S100A8/A9 has a crucial role in controlling macrophage-mediated renal repair following ischemia/reperfusion

Kidney International (2015) 87, 85–94

The calcium-binding protein complex S100A8/A9 has a crucial role in controlling macrophage-mediated renal repair following ischemia/reperfusion

Mark C. Dessing[1], Alessandra Tammaro[1], Wilco P. Pulskens[1], Gwendoline J. Teske[1], Loes M. Butter[1], Nike Claessen[1], Marco van Eijk[2], Tom van der Poll[3], Thomas Vogl[4], Johannes Roth[4], Sandrine Florquin[1,5,6] and Jaklien C. Leemans[1,6]

[1]Department of Pathology, Academic Medical Center, University of Amsterdam, Amsterdam, The Netherlands; [2]Department of Medical Biochemistry, Academic Medical Center, University of Amsterdam, Amsterdam, The Netherlands; [3]Center for Infection and Immunity Amsterdam (CINIMA) and Center for Experimental and Molecular Medicine, Academic Medical Center, University of Amsterdam, Amsterdam, The Netherlands; [4]Institute of Immunology, University of Muenster, Muenster, Germany and [5]Department of Pathology, Radboud University Nijmegen Medical Center, Nijmegen, The Netherlands

Upon ischemia/reperfusion (I/R)-induced injury, several damage-associated molecular patterns are expressed including the calcium-binding protein S100A8/A9 complex. S100A8/A9 can be recognized by Toll-like receptor-4 and its activation is known to deleteriously contribute to renal I/R-induced injury. To further test this, wild-type and S100A9 knockout mice (deficient for S100A8/A9 complex) were subjected to renal I/R. The expression of S100A8/A9 was significantly increased 1 day after I/R and was co-localized with Ly6G (mouse neutrophil marker)-positive cells. These knockout mice displayed similar renal dysfunction and damage and neutrophil influx compared with wild-type mice at this early time point. Interestingly, S100A9 knockout mice displayed altered tissue repair 5 and 10 days post I/R, as reflected by increased renal damage, sustained inflammation, induction of fibrosis, and increased expression of collagens. This coincided with enhanced expression of alternatively activated macrophage (M2) markers, while the expression of classically activated macrophage (M1) markers was comparable. Similarly, S100A9 deficiency affected M2, but not M1 macrophage polarization *in vitro*. During the repair phase following acute kidney injury, S100A9 deficiency affects M2 macrophages in mice leading to renal fibrosis and damage. Thus, S100A8/A9 plays a crucial part in controlling macrophage-mediated renal repair following I/R.

Kidney International (2015) **87,** 85–94; doi:10.1038/ki.2014.216; published online 18 June 2014

KEYWORDS: acute kidney injury; inflammation; immunology and pathology; ischemia/reperfusion; macrophages; renal ischemia/reperfusion

Correspondence: *Mark C. Dessing, Department of Pathology, Academic Medical Center, University of Amsterdam, Room L2-111, Meibergdreef 9, Amsterdam 1105 AZ, The Netherlands. E-mail: m.c.dessing@amc.uva.nl*

[6]These authors contributed equally to this work.

Received 25 January 2013; revised 30 April 2014; accepted 8 May 2014; published online 18 June 2014

Renal ischemia/reperfusion (I/R)-induced injury is a major clinical problem and is the most common cause of acute renal failure after renal transplantation, shock, sepsis, and renal artery stenosis.[1] Upon I/R-induced renal injury, several damage-associated molecular patterns are released like heat shock proteins, high mobility group box 1, hyaluronan, biglycan, and S100 calcium-binding proteins.[2,3] These proteins can be recognized by several pattern recognition receptors including Toll-like receptor (TLR)2 and TLR4, and signaling through these receptors are known to play a deleterious role in renal I/R-induced injury.[2,4–7] S100A8 and S100A9 proteins were characterized as new endogenous TLR4 activators.[8] S100A8 (also named myeloid-related protein 8) and S100A9 (myeloid-related protein 14) are members of the S100 calcium-binding proteins and exist mainly as a biologically functional S100A8/A9 heterodimer. S100A8 and S100A9 are constitutively expressed by granulocytes, monocytes, and early differentiation stages of macrophages and can be released upon necrosis or actively secreted by phagocytes during inflammation.[9,10] S100A8/A9 proteins were linked to innate immunity because of the ability to activate TLR4.[8] S100A8/A9 amplified endotoxin-mediated inflammatory response thought TLR4 and S100A9-deficient mice were resistant to endotoxin-induced lethal shock and abdominal sepsis.[8] Next to sepsis, S100A8/A9 has been associated with several human diseases including renal transplantation.[10–14] In a microarray study to identify genes of which expression during acute rejection is associated with progression to chronic allograft nephropathy, Eikmans *et al.*[12] showed that S100A8 and S100A9 expression could distinguish between patients with graft loss later on due to chronic allograft nephropathy and those who retained stable graft function. Relatively higher S100A8 and S100A9 mRNA and protein levels in infiltrating cells were associated with a favorable prognosis supporting the interest for S100A8/A9 in renal disease. Recently, Fujiu *et al.*[15] showed that S100A8/A9

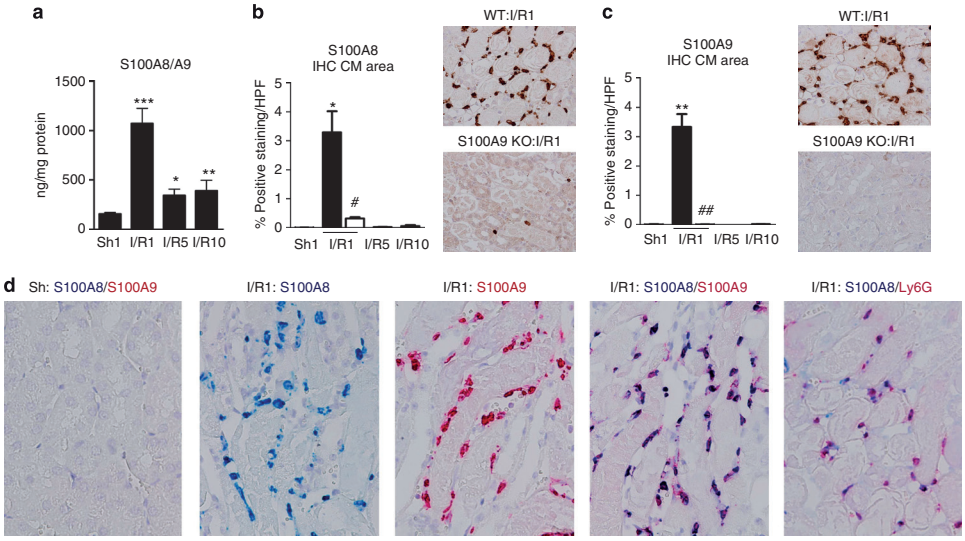

Figure 1 | S100A8 and S100A9 expression in renal tissue during renal ischemia/reperfusion (I/R) injury. Protein complex S100A8/A9 (**a**) in kidney tissue from sham (Sh) wild-type (WT) mice or WT mice 1, 5, or 10 days following I/R. Quantification and representative photos from S100A8 (**b**) or S100A9 (**c**) single staining in corticomedular region (CM) in kidney tissue slides from WT mice (black bars) and S100A9 knockout (KO) mice (white bars). (**d**) Representative photos from kidney tissue sections with staining for S100A8 and/or S100A9 or Ly6/S100A8 (original magnification ×400). Protein complex S100A8/A9 expression (**a**) was corrected for total protein level in tissue. HPF, high-power field. Graph data are mean ± s.e.m. $^{*}P<0.05$, $^{**}P<0.005$, $^{***}P<0.0005$ versus WT sham, $^{\#}P<0.05$, $^{\#\#}P<0.01$ versus WT I/R 1. (**a**): $N=8$ individuals mice per group, (**b**, **c**): $N=3$ individuals mice per group.

is induced in a model for progressive renal injury and contributes in monocyte recruitment and development. The role for S100A8/A9 in acute kidney injury is unknown. To determine the contribution of S100A8/A9 in acute renal damage, we subjected wild type (WT) and S100A9 knockout (KO) mice to renal I/R. We showed for the first time that S100A9 deficiency affects M2 macrophage polarization both *in vitro* and *in vivo*. *In vivo*, S100A9 deficiency leads to an uncontrolled repair phase resulting in renal fibrosis through an unrestrained M2 macrophage polarization.

RESULTS

Renal I/R-induced injury leads to increased S100A8/A9 levels in the kidney

Compared with sham WT mice, renal protein level of the biologically relevant S100A8/A9 heterodimer[8,16,17] was elevated in renal tissue, especially 1 day post I/R (Figure 1a). In plasma from WT mice, S100A8/A9 levels remained similar at all time points (sham: 859 ± 132, I/R day 1: 980 ± 127, I/R day 5: 814 ± 114, I/R day 10: 619 ± 131, data are ng/ml with mean ± s.e.m., $N=7$–8 per group). We further determined S100A8 and S100A9 expression in detail. Renal S100A8 and/or S100A9 staining was observed especially 1 day after I/R in corticomedular region, which is most susceptible to I/R (Figure 1 and Supplementary Figure S1 online). S100A8 and S100A9 co-localized with Ly6G-positive cells, most presumably granulocytes (Figure 1d). Only very few S100A8 cells were observed in S100A9 KO mice, 1 day after I/R (Figure 1b). As expected[8,18], renal S100A8/A9 heterodimer and S100A9 staining was undetectable in sham and I/R-treated S100A9 KO mice (Figure 1c and data not shown).

S100A8/A9 deficiency leads to reduced recovery of renal dysfunction and sustained damage following I/R

In order to unravel the role of S100A8/A9 in renal I/R, WT and S100A9 KO mice were subjected to bilateral renal I/R. Naïve WT and S100A9 KO mice displayed similar renal function (plasma creatinine and urea; Figure 2), renal collagen deposition (Figure 3), urinary albumin levels, and without occurrence of tubular damage or glomerular scenescence (data not shown). One day after I/R, WT and S100A9 KO mice displayed similar renal dysfunction (Figure 2a and b). In contrast to WT mice, several parameters of renal damage in S100A9 KO mice did not return to basal level. Serum creatinine and urea levels remained increased pointing toward an impaired renal function after I/R. In addition, tubular damage remained severe in S100A9 KO mice as displayed by a higher renal necrosis injury score, KIM1 and NGAL expression and increasing amount of apoptotic tubular epithelial cells (Figure 2c–g). Strikingly, in S100A9 KO mice, tubules remained damaged and cast formation was still present 10 days after I/R, whereas in

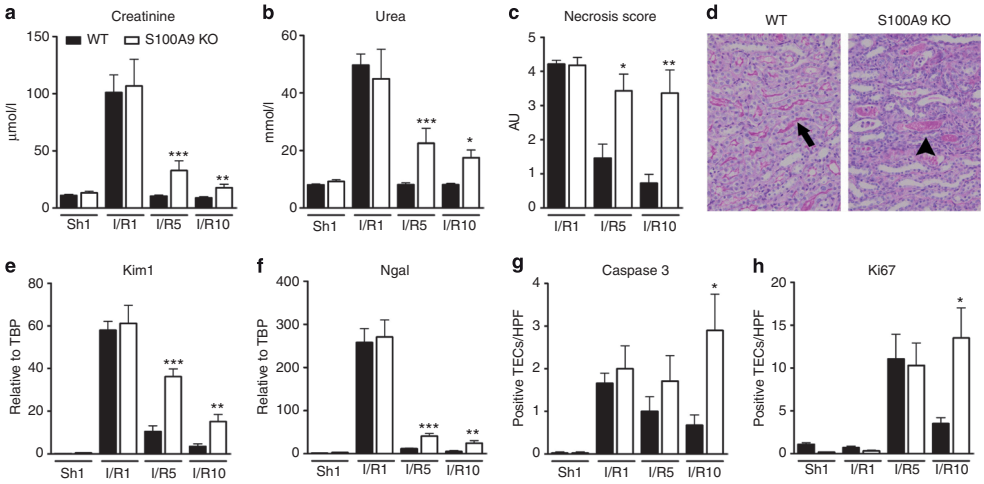

Figure 2 | Renal function and damage in wild-type (WT) and S100A9 knockout (KO) mice during renal ischemia/reperfusion (I/R) injury. Renal function as displayed by serum creatinine (**a**) and urea (**b**), renal damage markers as displayed by tubular necrosis score (**c**, **d**), Kim1 mRNA (**e**) and Ngal mRNA (**f**), apoptotic TECs (**g**) and proliferating TECs (**h**) in kidneys from WT (black bars) and S100A9 KO mice (white bars) 1, 5, or 10 days after I/R and in sham (Sh) mice. (**d**) Representative photos of periodic acid-Schiff diastase (PASD) staining on renal tissue slides from WT and S100A9 KO mice 10 days after I/R. Arrow shows brush border; arrowhead shows cast formation (original magnification ×200). Necrosis score was graded according to a severity score of '0' to '5' as described in Materials and Methods section and displayed as arbitrary units (AU). Amounts of caspase-3- or Ki67-positive TECs were counted in 10 nonoverlapping high-power fields (HPFs). mRNA levels of Kim1 and Ngal (**e**, **f**) are expressed relative to housekeeping gene TATA box-binding protein (TBP). Graph data are mean ± s.e.m. *$P<0.01$, **$P<0.005$, ***$P<0.001$ versus WT (**a**–**c**, **e**–**h**). TECs, tubular epithelial cells.

WT mice, kidney tissue was repaired with functional, brush-border-positive tubuli (Figure 2d). Caspase-3- and Ki67-positve cells were mainly tubular epithelial cells and not characterized as macrophages or fibroblasts (data not shown). In S100A9 KO mice, ongoing tissue damage and apoptosis of tubular epithelial cells was in line with ongoing proliferating tubular epithelial cells, most likely because of the necessity for tissue repair in these mice (Figure 2g and h).

S100A9 KO mice develop renal fibrosis and sustained inflammation following I/R

The impaired renal tissue repair in S100A9 KO mice upon I/R could lead to renal fibrosis. Therefore, we determined major markers for fibrosis. Transforming growth factor (TGF)-β and hepatocyte growth factor (HGF) are important opposite key players in fibrosis during the progression of renal disease with TGF-β being profibrotic and HGF anti-fibrotic.[19,20] Total TGF-β levels were elevated in S100A9 KO mice 5 and 10 days after I/R, whereas HGF levels were lower in S100A9 KO mice 5 days after I/R (Figure 3a and b). TGF-β is a known inducer of myofibroblast accumulation, which is characterized by induced expression of α-smooth muscle actin (α-SMA) and production of collagens.[21] In S100A9 KO mice, more renal α-SMA staining was observed compared with WT mice, 5 days after I/R (WT versus S100A9 KO mice: 1.5 ± 0.5 vs. 3.7 ± 0.7% positive area/HPF, $P<0.05$). In line with collagen type I and type III mRNA data, S100A9 KO mice displayed more collagens in renal tissue compared with WT mice 5 and 10 days following I/R (Figure 3e–h and data not shown). These data showed that S100A9 KO mice displayed and altered repair phase following I/R leading to the development of fibrosis. The enhanced fibrosis was in line with ongoing inflammation in S100A9 KO mice as displayed by enhanced production of pro-inflammatory mediators (Figure 4). The elevated levels of pro-inflammatory mediators could be related to the increased renal expression of damage-associated molecular patterns biglycan and HSP60 in S100A9 KO mice which are known to induce a TLR-mediated inflammatory response (Supplementary Figure S2 online).

S100A9 KO mice display elevated M2 macrophage-related gene profile during repair phase

To further determine which cell type could be involved in the observed phenotype in S100A9 KO mice, we determined granulocyte, dendritic cell (DC) and macrophage content. Granulocyte content and activation (as determined by myeloperoxidase levels and superoxide dismutase (SOD) activity in renal homogenate) increased similarly in WT and S100A9 KO mice 1 day after I/R (Supplementary Figure S3 online) and granulocyte content decreased thereafter in similar manner to sham level implicating no direct difference

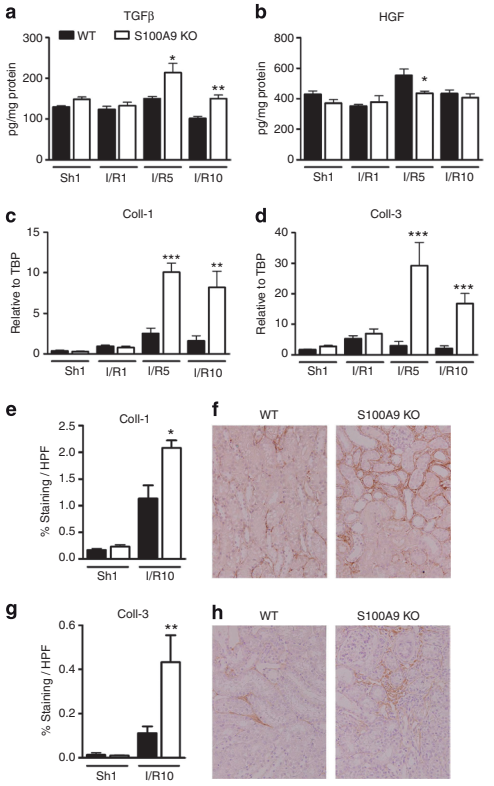

Figure 3 | Renal fibrosis in wild-type (WT) and S100A9 knockout (KO) mice during renal ischemia/reperfusion (I/R) injury. Markers of fibrosis transforming growth factor-beta (TGF-β) (**a**), hepatocyte growth factor (HGF) (**b**), collagen type 1 (**c**, **e**, and **f**), and collagen type 3 (**d**, **g**, and **h**) in kidney tissue from WT mice (black bars) and S100A9 KO mice (white bars). TGF-β and HGF expression was corrected for total protein level in tissue. Collagen type 1 and type 3 mRNA levels are expressed relative to housekeeping gene TATA box-binding protein (TBP). Collagen type 1 (**e**) and type 3 (**g**) staining on renal tissue slides were digitally analyzed and presented as % positive staining per high-power field (HPF). Representative photos of collagen type 1 (**f**) and type 3 (**h**) staining on renal tissue slides from WT and S100A9 KO, 10 days after I/R (original magnification ×200). Graph data are mean ± s.e.m. $*P<0.05$, $**P<0.005$, $***P<0.001$ versus WT.

in renal granulocyte migration and function between the two strains. Next, we quantified renal CD11c cells, presumably DC. CD11c mRNA levels increased in WT and S100A9 KO mice 5 days after I/R, which remained high in S100A9 KO mice 10 days after I/R (Supplementary Figure S4 online). Increased mRNA levels in S100A9 KO mice were confirmed on protein level by immunohistochemistry. In addition, we determined activation state of renal DC in kidney single cells. DC activation state was similar between WT and S100A9 KO mice 10 days after I/R, as reflected by similar MHC-II expression on CD45 + CD11c + F4/80 cells (MFI WT versus S100A9 KO: 1168 ± 32 vs. 1205 ± 60). We also observed increased level of F4/80-positive cells, presumably macrophages, in kidneys from S100A9 KO mice during late repair phase compared with WT mice (Figure 5). Most F4/80-positive cells were Ki67 negative implicating that F4/80-positive cells were not proliferating but infiltrating cells (data not shown). Macrophages can roughly be categorized into so-called 'classically activated' (M1) or 'alternatively activated' (M2) macrophages, depending on their stimuli and/or environment.[22–24] To determine if S100A9 KO mice displayed a different profile in macrophage phenotypes in their kidneys, several markers involved in M1 polarization or M2 polarization were analyzed (M1: nitric oxide synthase-2 and interferon-regulating factor-5: IRF5,[25] M2: arginase-1: Arg1, macrophage galactose-type C-type lectin-1 and IRF4[26]). Emr1 mRNA levels (Figure 6a), which encode for macrophage F4/80 gene expression, reflected the influx of renal F4/80 + macrophages in kidneys of WT and S100A9 KO mice with similar pattern (Figure 5). The level of Emr1 mRNA and number of macrophages in the kidney of WT mice peaked at day 5 and declined thereafter, whereas these parameters remained higher in the S100A9 KO mice. M1 markers nitric oxide synthase-2 and IRF5 increased similarly in WT and S100A9 KO mice during the repair phase (Figure 6b and c). Interestingly, M2-associated macrophage markers macrophage galactose-type C-type lectin-1, IRF4, and especially Arg1 were elevated in S100A9 KO mice 5 days after I/R (Figure 6d–f). The difference in Arg1 mRNA was confirmed at protein level (Figure 6g). Arg1 protein expression co-localized with F4/80 staining (Figure 6h). These data implicate that M2, but not M1 polarization, is affected in S100A9 KO mice.

Endogenous S100A8 and S100A9 does not induce M2-type macrophage

We determined S100A8 and S100A9 mRNA kinetics during macrophage development *in vitro*. Expression of S100A8 and S100A9 mRNA reduced during differentiation of bone marrow cells into macrophages (Figure 7a and b). However, M1 polarization increased S100A8 mRNA level whereas M2 polarization further decreased S100A8 and S100A9 mRNA levels (Figure 7c and d). To determine effect of extracellular S100A8 and/or S100A9 on macrophage development, WT bone marrow–derived macrophages (BMDMs) were incubated with recombinant S100A8, S100A9, or S100A8/A9 complex. S100A8, S100A9, and S100A8/A9 induced a dose-dependent tumor necrosis factor-α response and nitric oxide synthase-2 mRNA expression (Figure 8a and data not shown). In contrast, S100A8 and/or S100A9 did not affect Arg1 mRNA expression (Figure 8b and c). These data showed that *in vitro*, endogenous S100A8 and S100A9 does not induce M2-type macrophage markers, but is involved in macrophage M1 activation.

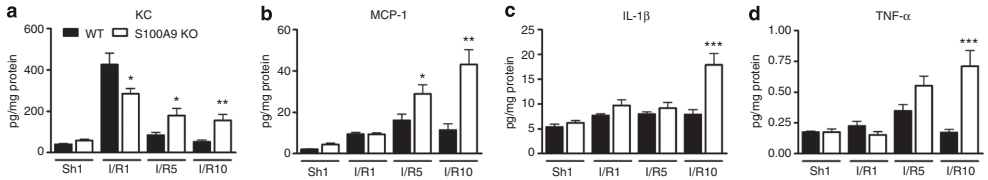

Figure 4 | Cytokine and chemokine levels in wild-type (WT) and S100A9 knockout (KO) mice during renal ischemia/reperfusion (I/R) injury. Inflammatory mediators keratinocyte-derived chemokine (KC) (**a**), monocyte chemoattractant protein (MCP)-1 (**b**), interleukin (IL)-1β (**c**), and tumor necrosis factor (TNF)-α (**d**) in kidney homogenate from WT mice (black bars) and S100A9 KO mice (white bars) 1, 5, or 10 days after I/R and in sham (Sh) mice. Protein expression was corrected for total protein level in tissue. Data are mean ± s.e.m. $^{*}P<0.05$, $^{**}P<0.01$, $^{***}P<0.005$ versus WT.

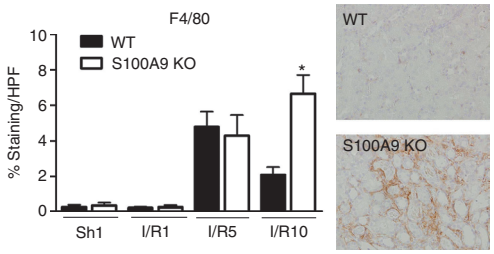

Figure 5 | Macrophage influx in kidneys from wild-type (WT) and S100A9 knockout (KO) mice during renal ischemia/reperfusion (I/R) injury. F4/80 staining on kidney tissue from WT mice (black bars) and S100A9 KO mice (white bars) was digitally analyzed and presented as % positive staining per high-power field (HPF). Representative photos of kidney tissue slides from WT and S100A9 KO mice stained for F4/80, 10 days after I/R (original magnification ×200). Graph data are mean ± s.e.m. $^{*}P<0.005$ versus WT.

S100A8/A9 deficiency exceeds M2 polarization

We further investigated the contribution of S100A9 deficiency in macrophage polarization *in vitro*. Nitric oxide synthase-2 mRNA levels increased similarly in WT and S100A9 KO macrophages during M1 polarization (Figure 9a and c). During M2 polarization, a striking induction of Arg1 mRNA level was observed in S100A9 KO macrophages compared with WT macrophages (Figure 9b and d) which matched our *in vivo* Arg1 findings. Similar results were observed in a second independent experiment (data not shown). *In vitro*, IRF4 but not macrophage galactose-type C-type lectin-1 mRNA levels were higher in M2-polarized peritoneal macrophages from S100A9 KO mice compared with WT mice (Supplementary Figure S5 online) indicating that the characteristics of M2 polarization of S100A9 KO mice *in vitro* and *in vivo* did not perfectly match. These data showed that *in vitro*, S100A9 deficiency intrinsically predisposes macrophages to sustain a M2 phenotype. We then determined which T helper type 2-related response *in vivo* was involved in M2 polarization during the repair phase. Renal interleukin (IL)-2, IL-4, and IL-5 protein level and IL-13 and Gata3 (transcription factor T helper type 2 cells) mRNA levels remained similar at all time points in all groups (data not shown). It remains to be determined which mediator *in vivo* contributes to M2 polarization following I/R in S100A9 KO mice.

DISCUSSION

The recent discovery of S100A8/A9 as a TLR4 activator leads to new interest in its contribution during inflammatory.[8] In renal I/R, TLR-induced inflammation plays a deleterious role. Unexpectedly, S100A8/A9 did not contribute to renal I/R-induced acute injury. By contrast, at later stages, S100A9 KO mice displayed a phenotype with enhanced renal dysfunction, damage, fibrosis, and inflammation that is associated with an enhanced polarization of macrophages into a M2 subtype. We showed that S100A8/A9 plays a crucial part in controlling macrophage-mediated renal repair following I/R.

Following renal I/R, granulocytes infiltrate the tissue which are known to play a detrimental role in I/R-induced injury. Granulocytes abundantly express S100A8 and S100A9[9,10] and apoptotic granulocytes are able to release S100A9,[27] a known DAMP and activator of TLR4.[8] TLR4 plays part in renal I/R-induced injury[2,28] and we hypothesized that S100A8/A9–TLR4 signaling could play part in the mechanism behind renal I/R-induced injury. Unexpectedly, WT and S100A9 KO mice displayed similar granulocyte influx and activation, renal dysfunction and damage, 1 day after I/R. Compared with WT mice, S100A9 KO mice displayed a mild reduction in renal keratinocyte-derived chemokine levels implicating a limited role for TLR4-S100A8/A9 signaling at this time point. In a study by Ziegler *et al.*,[29] S100A9 KO mice displayed less I/R-induced cerebral damage, most likely by absence of S100A8/A9-induced inflammation when signaling through TLR4.[30] However, unlike in cerebral I/R,[29] we did not observe a protective phenotype in S100A9 KO mice possibly because TLR4-S100A8/A9 signaling plays a limited role in the induction of inflammation during renal I/R. Ziegler *et al.*[29] did not investigate long-term effect of S100A9 deficiency during I/R-induced cerebral injury which could be comparable with our observed phenotype. Our data implicate that the direct role of S100A9-deficient granulocytes in renal I/R injury is limited. However, we cannot exclude that S100A9-deficient granulocytes affect functions of other inflammatory cells like

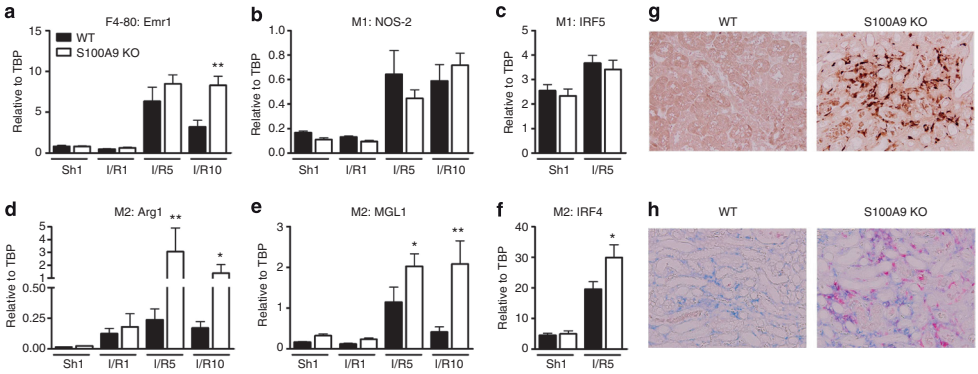

Figure 6 | Classical and alternative macrophage markers in ischemia/reperfusion (I/R)-damaged kidney from wild-type (WT) and S100A9 knockout (KO) mice. mRNA levels of general macrophage marker Emr1 (**a**), classical macrophage marker nitric oxide synthase-2 (NOS-2) (**b**), interferon-regulating factor-5 (IRF5) (**c**), and alternative macrophage marker arginase-1 (Arg1) (**d**), macrophage galactose-type C-type lectin-1 (MGL1) (**e**), and interferon-regulating factor-4 (IRF4) (**f**) in kidneys from WT mice (black bars) and S100A9 KO mice (white bars) after I/R or in sham (Sh) mice. mRNA levels are expressed relative to housekeeping gene TATA box-binding protein (TBP). (**g**) Representative photos for Arg1 single staining on kidney tissue slides from WT and S100A9 KO mice, 5 days after I/R (original magnification ×200). (**h**) Representative photos for co-localization of Arg1 (red) and F4-80 (blue) on kidney tissue slides from WT and S100A9 KO mice, 5 days after I/R (original magnification ×200). Graph data are mean ± s.e.m. $*P<0.05$, $**P<0.005$ versus WT.

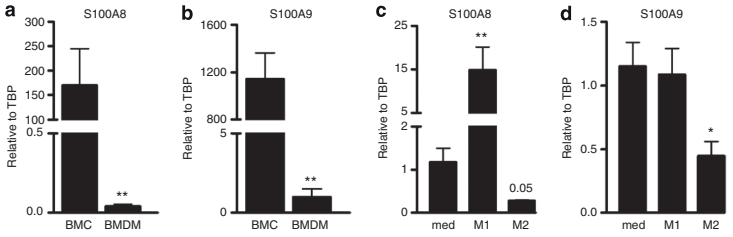

Figure 7 | S100A8 and S100A9 mRNA levels during macrophage development and polarization. S100A8 and S100A9 mRNA levels in bone marrow cells (BMCs) and bone marrow–derived macrophages (BMDMs) from wild-type (WT) mice (**a**, **b**). S100A8 and S100A9 mRNA levels in BMDMs from WT mice, 48 h after stimulation with medium (med), lipopolysaccharide + interferon (IFN)-γ (M1 polarization), or interleukin (IL)-4 + IL-13 (M2 polarization) (**c** and **d**). mRNA levels are expressed relative to housekeeping gene TATA box-binding protein (TBP). Data are mean ± s.e.m. (**a**, **b**): $**P<0.005$ versus BMCs, (**c**, **d**): $*P<0.05$, $**P<0.005$ versus medium ($N=6$ individuals mice per group).

macrophages,[31] which accumulate into the kidney during repair phase.

During macrophage development, S100A8 and S100A9 mRNA levels drastically decrease and S100A8/A9 expression is differentially affected during M1 or M2 polarization as described before.[32–35] We showed that S100A8/A9 deficiency intrinsically affects merely M2 polarization, whereas extracellular recombinant S100A8 and/or S100A9 plays part in M1 but not M2 macrophage activation/polarization. Although M2 macrophages contribute to repair mechanisms in damaged organs like kidney,[36] numerous studies have also implicated M2 macrophages in the pathogenesis of fibrosis.[37] Possibly, intrinsic functions in S100A9-deficient M2 macrophages are altered leading to excessive production of wound-healing factors with different candidates like collagens, TGF-β, or other factors. In the kidney, macrophages are a main source of profibrotic mediators including TGF-β that directly activate fibroblast to differentiate into myofibroblasts which produce collagens.[22] However, macrophages may also synthesize and secrete collagens themselves.[38] Ultimately, this process becomes pathological resulting in irreversible fibrosis, tissue destruction and progressive kidney disease as we see in the S100A9 KO mice.

In the kidney, resident DCs form an extensive network and contribute to induction of inflammation following I/R,[39] and S100A9-deficient bone marrow–derived DCs showed enhanced inflammatory response to TLR ligands.[35] Enhanced presence of renal DCs and damage-associated molecular patterns in S100A9 KO mice may account for the elevated renal cytokine/chemokine levels in these mice. This could explain the apparent paradox of increased pro-inflammatory mediators (which are linked to M1-type macrophage) with

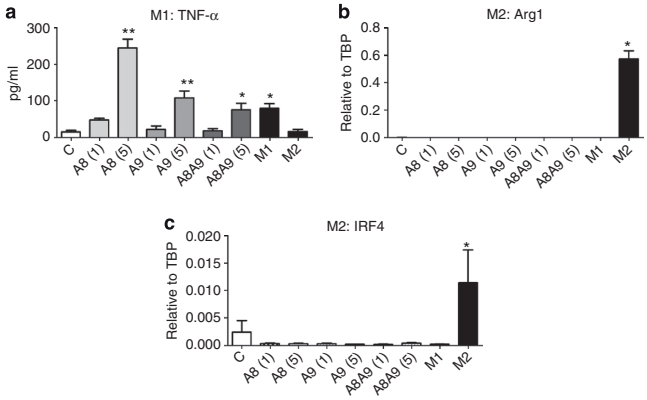

Figure 8 | Macrophage response to recombinant S100A8 and/or S100A9. Wild-type bone marrow–derived macrophages (WT BMDMs) were cultured *in vitro* and incubated with medium, 1 or 5 μg/ml S100A8 (A8), S100A9 (A9), S100A8/A9 (A8/A9), lipopolysaccharide + interferon (IFN)-γ (M1 polarization), or interleukin (IL)-4 + IL-13 (M2 polarization) for 48 h. Tumor necrosis factor (TNF)-α was measured in supernatant (**a**); arginase-1 (Arg1) (**b**) and interferon-regulating factor 4 (IRF4) (**c**) were measured on mRNA level. Data are mean ± s.e.m. $*P<0.05$, $**P<0.01$ versus control ($N=3$ individuals mice per group).

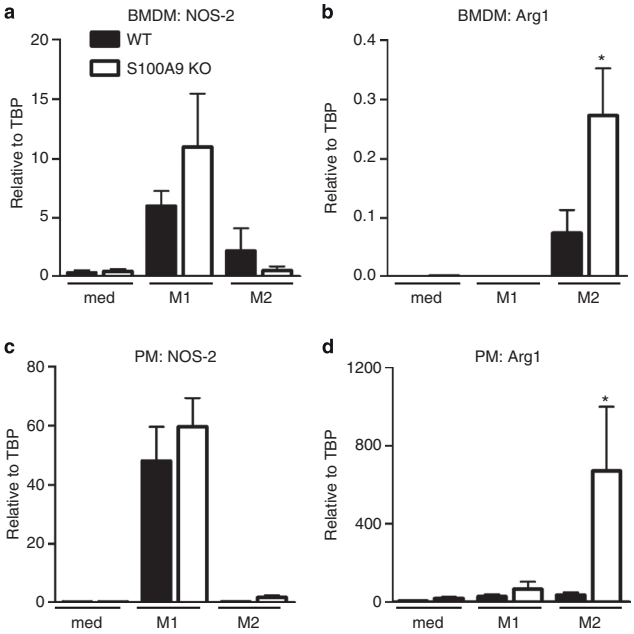

Figure 9 | *In vitro* macrophage polarization in wild-type (WT) and S100A9 knockout (KO) mice. Classical macrophage marker nitric oxide synthase-2 (NOS-2) (**a**, **c**) and alternative macrophage marker arginase-1 (Arg1) (**b**, **d**) in bone marrow–derived macrophages (BMDM; (**a**, **b**)) and peritoneal macrophages (PM; (**c**, **d**)) from WT mice (black bars) and S100A9 KO mice (white bars) 48 h after stimulation with medium (med), lipopolysaccharide + interferon (IFN)-γ (M1 polarization), or interleukin (IL)-4 + IL-13 (M2 polarization). mRNA levels are expressed relative to housekeeping gene TATA box-binding protein (TBP). Data are mean ± s.e.m. $*P<0.05$ versus WT ($N=6$ individuals mice per group).

the simultaneous shift to a more M2-type polarization in S100A9 KO mice. Thus, S100A9 KO deficiency could lead to potential dual phenotype following renal I/R with ongoing inflammation and excessive M2 marker expression.

The expression and contribution of S100A8 and/or S100A9 has been reported before in renal transplant patients showing the importance of S100A8/A9 in renal disease and transplantation biology. Urinary S100A8/A9 is a promising biomarker in the differentiation of pre-renal and intrinsic acute kidney injury.[13,14] Goebeler *et al.*[11] showed that macrophages displayed heterogeneity with respect to S100A8 and S100A9 expression during acute and chronic rejection. In acute rejection, CD68 + S100A8/A9 + macrophages were related to acute, while CD68 + S100A8/A9 − macrophages were related to chronic rejection.[11] In a microarray study to identify genes of which expression during acute rejection is associated with progression to chronic allograft nephropathy, Eikmans *et al.*[12] showed that S100A8 and S100A9 expression upon acute rejection could distinguish between patients developing chronic allograft dysfunction later on and those who retained stable graft function. mRNA and protein levels of S100A8 and S100A9 in infiltrating monocytes/macrophages were higher in patients with stable graft function over time compared with patients who lost their graft through chronic allograft nephropathy. Relative high expression of S100A8 and S100A9 during acute rejection was associated with a favorable prognosis. Interestingly, the number of infiltrating monocytes/macrophages was similar between the two groups. These studies implicate that during acute kidney injury, S100A8/A9-positive monocytes/macrophages are (functionally) different from S100A8/A9-negative monocytes/macrophages and may be involved in tissue-repair mechanisms. Our study provides an explanation as to why high S100A8/A9 mRNA and protein level in infiltrating cells is associated with a favorable prognosis of renal transplant patients. We found profound renal dysfunction, damage, fibrosis, and inflammation in S100A9 KO mice after renal I/R injury due to an enhanced polarization of macrophages into a M2 phenotype.

In summary, we found that S100A8/A9 deficiency affects M2 polarization, renal fibrosis, inflammation, and damage after ischemia reperfusion injury. We show, for the first time, a crucial role of S100A8/A9 in controlling macrophage-mediated renal repair following I/R.

MATERIALS AND METHODS

Mice

Deletion of the S100A8 gene in mice results in a lethal embryonically phenotype.[40] Therefore, we used S100A9 KO mice.[18,41] S100A9 KO mice were generated by target gene disruption of the *Mrp14* gene as described (C57BL/6 genetic background).[8,18] S100A9 KO mice developed normally. Kidneys revealed no morphological or histological alterations and the number/morphology of leukocytes in the peripheral blood (including Ly6C-positive/negative cells) of WT and S100A9 KO mice were normal. S100A8 is almost not detectable at the protein level in mature phagocytes of S100A9 KO mice despite normal S100A8 mRNA levels. Thus, targeted deletion of S100A9 leads to a complete lack of a functional S100A8/A9 complex in the mouse.[8,18] Pathogen-free 9–10-week-old male C57BL/6 wild-type mice were purchased from Charles River Laboratories (Cologne, Germany). All mice were bred in the animal facility of the Academic Medical Center in Amsterdam, The Netherlands. Age/sex-matched mice were used in all experiments. The Animal Care and Use Committee of the University of Amsterdam approved all experiments.

Renal I/R injury model

Renal I/R injury was induced as described previously.[4,42] Briefly, 30 min of bilateral clamping of renal arteries was performed using microaneurysm clamps through a midline abdominal incision under general anesthesia (1.25 mg/ml midazolam (Actavis, Dublin, Ireland), 0.08 mg/ml fentanyl citrate, and 2.5 mg/ml fluanisone (VetaPharma, Leeds, UK), which induces profound renal damage and dysfunction without inducing mortality.[43] All mice received a subcutaneous injection of 50 μg/kg buprenorphin (Temgesic; Schering-Plough, Amstelveen, The Netherlands) for analgetic purposes. Sham mice underwent the same procedure without clamping and were killed 1 day after surgery. Groups of mice were killed 1, 5, or 10 days after surgery by exsanguinations under general anesthesia.

Plasma biochemical analysis

The recovery of renal function was determined by measuring creatinine and urea in plasma samples obtained after intervention by enzyme reactions involving urease and creatinase and using standard autoanalyzer methods by our hospital research services.

Preparation of renal tissue and assays

For cytokine measurements, snap-frozen kidneys were diluted in lysis buffer (300 mmol/l NaCl, 30 mmol/l Tris, 2 mmol/l $MgCl_2$, 2 mmol/l $CaCl_2$, 1% Triton X-100, and 1% protease inhibitor cocktail II (Sigma-Aldrich, Zwijndrecht, The Netherlands), homogenized and incubated at 4 °C for 30 min. Homogenates were subsequently centrifuged at 1500 g at 4 °C for 15 min, and supernatants were stored at − 70 °C until assays were performed. S100A8/A9 was measured by enzyme-linked immunosorbent assay.[8] Keratinocyte-derived chemokine, monocyte chemoattractant protein-1, IL-1β, TGF-β and HGF were measured using specific enzyme-linked immunosorbent assays (R&D Systems, Abingdon, UK). Tumor necrosis factor-α, IL-2, IL-4, and IL-5 were measured using cytometric bead array (BD Biosciences, Breda, The Netherlands) all according to manufacturer's instructions. Myeoloperoxidase and antioxidant SOD activity was measured by enzyme-linked immunosorbent assay (Hycult Biotechnology BV, Uden, The Netherlands, and SOD assay kit-WST, Sigma-Aldrich, respectively). The rate of the reduction with superoxide anion is inhibited by SOD. Therefore, SOD activity can be determined by measuring the inhibition rate. Protein parameters *in vivo* were corrected for the amount of total protein content present in tissue homogenate supernatant using the Bio-Rad protein assay (Bio-Rad Laboratories, Veenendaal, The Netherlands).

Histology and immunohistochemistry

Renal tissue was fixed and processed as described before.[4,42] Paraffin-embedded sections were used for periodic acid-Schiff diastase staining and immunohistochemistry. The degree of tubular damage was assessed on periodic acid-Schiff diastase-stained 4-μm-thick sections by scoring tubular cell necrosis in 10 nonoverlapping high-power fields (magnification ×40) in the corticomedullary junction. The degree of injury was scored by a pathologist in a blinded fashion on a 5-point scale: 0 = no damage, 1 = 10% of the corticomedullary

junction injured, 2 = 10–25%, 3 = 25–50%, 4 = 50–75%, 5 = more than 75%. Tissue sections were incubated with specific antibodies for granulocytes (fluorescein isothiocyanate-labeled anti-mouse Ly6G mAb; BD Biosciences–Pharmingen, Breda, The Netherlands), macrophages (rat anti-mouse F4/80 IgG2b mAb; Serotec, Puchheim, Germany), apoptosis (rabbit anti-human active caspase-3; Cell Signaling Technology, Leiden, The Netherlands), proliferation (rabbit-anti-Ki67 antibody, Thermo Scientific, Landsmeer, The Netherlands), myofibroblast α-smooth muscle actin (α-SMA, DAKO, Heverlee, Belgium), collagen I and III (GeneTex, Aachen, Germany) followed by appropriate secondary antibodies as described before.[4,6,42,44-47] Immunohistochemical sequential double alkaline phosphatase (AP) staining was performed essentially as previously described.[48-50] Briefly, sections were incubated overnight at 4 °C with rat-anti-mouse-Ly6G-FITC (BD Pharmingen, Breda, The Netherlands) or rabbit-anti-mouse Arginase-1 (gift from Prof W.H. Lammers; Tytgat Institute for Liver and Intestinal Research, Academic Medical Center, Amsterdam, The Netherlands) followed by rabbit anti-FITC antibody (DAKO) or goat-anti-rabbit and subsequently PowerVision anti-rabbit AP (ImmunoLogic, Duiven, The Netherlands). AP activity was visualized in blue, using Vector Blue (Vector Labs, Amsterdam, The Netherlands). Next, a second heat-induced epitope retrieval step was applied to remove the antibodies from the first staining sequence. Sections were incubated with rat-anti-mouse S100A8 or S100A9 (R&D systems) or rat anti-mouse F4/80 for 3 h followed by goat-anti-rat IgG AP. AP activity was visualized in red using Vector Red (Vector Labs). To quantify the amount of apoptotic and proliferating tubular epithelial cells, the number of positive cells was counted within 10 nonoverlapping high-power fields. CD11c staining was performed on cryosections. Briefly, cryosections were fixed in acetone, and incubated with CD11c (hamster anti-mouse; Novus Biologicals 1/100, Huissen, The Netherlands) followed by rabbit-anti-hamster (1/500) and PowerVision anti-rabbit (ImmunoLogic). The amount of S100A8, S100A9, macrophages, CD11c, α-SMA, collagen type I-positive staining was quantified digitally with ImageJ software version 1.46r (NIH, Bethesda, MD).

Flow cytometric analysis

To isolate cells from kidney, whole kidney was cut into small pieces in ice-cold phosphate-buffered saline and collected by centrifugation (250 g). Collected tissue was incubated for 30 min at 37 °C in collagenase 1 (1 mg/ml, Sigma-Aldrich) and DNAse 1 (0.1 mg/ml, Roche, Woerden, The Netherlands) in RPMI 1640 medium (Gibco BRL, Bleiswijk, The Netherlands) supplemented with 100 IU/ml penicillin, 100 μg/ml streptomycin (Invitrogen, Bleiswijk, The Netherlands) but without serum. Thereafter, cells were passed through 40-μmol/l filter, centrifuged, and collected in cold fluorescence-activated cell sorting buffer (3% fetal calf serum, 2 mmol/l EDTA, azide). Cells were incubated with Fc block (CD16/32 BD Pharmingen), viability tracker efluor 780 (eBioscience, Vienna, Austria), CD45.2 Percp Cy5.5 (BD Pharmingen), F4/80 Alexa 647 (eBioscience), MHC-II-FITc (eBioscience), and CD11c-bio (eBioscience) followed by secondary antibody streptavidin-RPE (DAKO). Cells were measured using FACSCantoII (BD Biosciences) and analyzed using FlowJo v10 (Ashland, OR).

Isolation and stimulation of peritoneal- and bone marrow-derived macrophages

Peritoneal macrophages were isolated as described before.[51] Briefly, 2×5 ml cold phosphate-buffered saline was injected intraperitoneal, after which peritoneal lavage was retracted. Cells were counted using hemocytometer (Beckman Coulter Counter, Woerden, The Netherlands) and a total of 1×10^5 cells per well in a 24-well plate (tissue-culture treated) were let to adhere 2 h and washed thereafter to remove non-adherent cells. Isolation and culturing of BMDMs were performed as partly described before.[52,53] Mononuclear phagocyte progenitor cells were derived by flushing of the femoral and tibial bone marrow with ice-cold sterile phosphate-buffered saline. Cells were transferred to bone marrow macrophage medium containing RPMI 1640 medium supplemented with 10% FCS, 2 mmol/l L-glutamine, 100 IU/ml penicillin, 100 μg/ml streptomycin (Invitrogen), and 15% LCM (L929 conditioned medium) and cultured for 8 days at 37 °C and 5% CO_2 in 145×20-mm Petri dishes (Greiner, Alphen a/d Rijn, The Netherlands). Thereafter, BMDMs were detached from Petri dishes using sterile Lidocaine (Sigma-Aldrich) solution (4 mg/ml sterile phosphate-buffered saline), harvested, and counted using a hemocytometer. A total of 5×10^5 cells per well in a 24-well plate were used. Recombinant S100A8, S100A9, and S100A8/A9 were purified as described before (8). Cells were stimulated with 1 or 5 μg/ml recombinant S100A8, S100A9, or S100A8/A9 protein complex. BMDMs and peritoneal macrophages were incubated with both lipopolysaccharide (10 ng/ml; Sigma-Aldrich) and mouse interferon-γ (50 ng/ml; ProSpec, East Brunswick, NJ) to initiate M1 activation, or incubated with mouse IL-4 and IL-13 (both 50 ng/ml; ProSpec) to initiate M2 activation.[22,23]

RNA purification and reverse transcriptase-PCR

Total RNA was extracted from snap-frozen renal tissue sections and isolated from peritoneal macrophages and BMDMs using TRIzol reagent (Invitrogen) and subsequently converted to cDNA. mRNA level was analyzed by reverse transcriptase-PCR with SYBR green PCR master mix (Roche). SYBR green dye intensity was analyzed with linear regression analysis (LinRegPCR v12.4, developed by Heart Failure Research Center, Amsterdam, The Netherlands). Specific gene expression was normalized to mouse housekeeping gene TATA box-binding protein. Primer sequences are displayed in Supplementary Table S1 online.

Statistics

Differences between groups were analyzed using Mann–Whitney *U*-test. Values are expressed as mean ± s.e.m. ($N = 8$ individuals mice per group unless mentioned otherwise). A value of $P < 0.05$ was considered statistically significant.

DISCLOSURE

All the authors declared no competing interests.

ACKNOWLEDGMENTS

This study has been funded by the Dutch Kidney Foundation.

SUPPLEMENTARY MATERIAL

Figure S1. Renal S100A8 and S100A9 expression during renal I/R injury.
Figure S2. Renal biglycan and HSP60 expression in WT and S100A9 KO mice during repair following I/R.
Figure S3. Neutrophil content and SOD activity in WT and S100A9 KO mice during renal I/R injury.
Figure S4. CD11c expression in WT and S100A9 KO mice during renal I/R.
Figure S5. IRF4 and MGL1 mRNA expression in WT and S100A9 KO macrophages.
Table S1. Primers used for determination of specific genes.
Supplementary material is linked to the online version of the paper at http://www.nature.com/ki

REFERENCES

1. Alkhunaizi AM, Schrier RW. Management of acute renal failure: new perspectives. *Am J Kidney Dis* 1996; **28**: 315–328.
2. Wu H, Chen G, Wyburn KR *et al.* TLR4 activation mediates kidney ischemia/reperfusion injury. *J Clin Invest* 2007; **117**: 2847–2859.
3. Zhang PL, Lun M, Schworer CM *et al.* Heat shock protein expression is highly sensitive to ischemia-reperfusion injury in rat kidneys. *Ann Clin Lab Sci* 2008; **38**: 57–64.
4. Leemans JC, Stokman G, Claessen N *et al.* Renal-associated TLR2 mediates ischemia/reperfusion injury in the kidney. *J Clin Invest* 2005; **115**: 2894–2903.
5. Shigeoka AA, Holscher TD, King AJ *et al.* TLR2 is constitutively expressed within the kidney and participates in ischemic renal injury through both MyD88-dependent and -independent pathways. *J Immunol* 2007; **178**: 6252–6258.
6. Pulskens WP, Teske GJ, Butter LM *et al.* Toll-like receptor-4 coordinates the innate immune response of the kidney to renal ischemia/reperfusion injury. *PLoS ONE* 2008; **3**: e3596.
7. Kruger B, Krick S, Dhillon N *et al.* Donor Toll-like receptor 4 contributes to ischemia and reperfusion injury following human kidney transplantation. *Proc Natl Acad Sci USA* 2009; **106**: 3390–3395.
8. Vogl T, Tenbrock K, Ludwig S *et al.* Mrp8 and Mrp14 are endogenous activators of Toll-like receptor 4, promoting lethal, endotoxin-induced shock. *Nat Med* 2007; **13**: 1042–1049.
9. Foell D, Wittkowski H, Vogl T *et al.* S100 proteins expressed in phagocytes: a novel group of damage-associated molecular pattern molecules. *JLeukoc Biol* 2007; **81**: 28–37.
10. Ehrchen JM, Sunderkotter C, Foell D *et al.* The endogenous Toll-like receptor 4 agonist S100A8/S100A9 (calprotectin) as innate amplifier of infection, autoimmunity, and cancer. *J Leukoc Biol* 2009; **86**: 557–566.
11. Goebeler M, Roth J, Burwinkel F *et al.* Expression and complex formation of S100-like proteins MRP8 and MRP14 by macrophages during renal allograft rejection. *Transplantation* 1994; **58**: 355–361.
12. Eikmans M, Roos-van Groningen MC, Sijpkens YW *et al.* Expression of surfactant protein-C, S100A8, S100A9, and B cell markers in renal allografts: investigation of the prognostic value. *J Am Soc Nephrol* 2005; **16**: 3771–3786.
13. Heller F, Frischmann S, Grunbaum M *et al.* Urinary calprotectin and the distinction between prerenal and intrinsic acute kidney injury. *Clin J Am Soc Nephrol* 2011; **6**: 2347–2355.
14. Seibert FS, Pagonas N, Arndt R *et al.* Calprotectin and neutrophil gelatinase-associated lipocalin in the differentiation of pre-renal and intrinsic acute kidney injury. *Acta Physiol (Oxf)* 2013; **207**: 700–708.
15. Fujiu K, Manabe I, Nagai R. Renal collecting duct epithelial cells regulate inflammation in tubulointerstitial damage in mice. *J Clin Invest* 2011; **121**: 3425–3441.
16. Vogl T, Roth J, Sorg C *et al.* Calcium-induced noncovalently linked tetramers of MRP8 and MRP14 detected by ultraviolet matrix-assisted laser desorption/ionization mass spectrometry. *J Am Soc Mass Spectrom* 1999; **10**: 1124–1130.
17. Vogl T, Ludwig S, Goebeler M *et al.* MRP8 and MRP14 control microtubule reorganization during transendothelial migration of phagocytes. *Blood* 2004; **104**: 4260–4268.
18. Manitz MP, Horst B, Seeliger S *et al.* Loss of S100A9 (MRP14) results in reduced interleukin-8-induced CD11b surface expression, a polarized microfilament system, and diminished responsiveness to chemoattractants in vitro. *Mol Cell Biol* 2003; **23**: 1034–1043.
19. Stahl PJ, Felsen D. Transforming growth factor-beta, basement membrane, and epithelial-mesenchymal transdifferentiation: implications for fibrosis in kidney disease. *Am J Pathol* 2001; **159**: 1187–1192.
20. Liu Y. Hepatocyte growth factor in kidney fibrosis: therapeutic potential and mechanisms of action. *Am J Physiol* 2004; **287**: F7–16.
21. Zeisberg M, Neilson EG. Mechanisms of tubulointerstitial fibrosis. *J Am Soc Nephrol* 2010; **21**: 1819–1834.
22. Ricardo SD, van Goor H, Eddy AA. Macrophage diversity in renal injury and repair. *J Clin Invest* 2008; **118**: 3522–3530.
23. Gordon S. Alternative activation of macrophages. *Nat Rev Immunol* 2003; **3**: 23–35.
24. Gordon S, Martinez FO. Alternative activation of macrophages: mechanism and functions. *Immunity* 2010; **32**: 593–604.
25. Krausgruber T, Blazek K, Smallie T *et al.* IRF5 promotes inflammatory macrophage polarization and TH1-TH17 responses. *Nat Immunol* 2011; **12**: 231–238.
26. Satoh T, Takeuchi O, Vandenbon A *et al.* The Jmjd3-Irf4 axis regulates M2 macrophage polarization and host responses against helminth infection. *Nat Immunol* 2010; **11**: 936–944.
27. Voganatsi A, Panyutich A, Miyasaki KT *et al.* Mechanism of extracellular release of human neutrophil calprotectin complex. *J Leukoc Biol* 2001; **70**: 130–134.
28. Pulskens WP, Rampanelli E, Teske GJ *et al.* TLR4 promotes fibrosis but attenuates tubular damage in progressive renal injury. *J Am Soc Nephrol* 2010; **21**: 1299–1308.
29. Ziegler G, Prinz V, Albrecht MW *et al.* Mrp-8 and -14 mediate CNS injury in focal cerebral ischemia. *Biochim Biophys Acta* 2009; **1792**: 1198–1204.
30. Lehnardt S, Massillon L, Follett P *et al.* Activation of innate immunity in the CNS triggers neurodegeneration through a Toll-like receptor 4-dependent pathway. *Proc Natl Acad Sci USA* 2003; **100**: 8514–8519.
31. De Lorenzo BH, Godoy LC, Novaess e Brito *et al.* Macrophage suppression following phagocytosis of apoptotic neutrophils is mediated by the S100A9 calcium-binding protein. *Immunobiology* 2009; **215**: 341–347.
32. Xu K, Geczy CL. IFN-gamma and TNF regulate macrophage expression of the chemotactic S100 protein S100A8. *J Immunol* 2000; **164**: 4916–4923.
33. Cheng P, Corzo CA, Luetteke N *et al.* Inhibition of dendritic cell differentiation and accumulation of myeloid-derived suppressor cells in cancer is regulated by S100A9 protein. *J Exp Med* 2008; **205**: 2235–2249.
34. Lagasse E, Weissman IL. Mouse MRP8 and MRP14, two intracellular calcium-binding proteins associated with the development of the myeloid lineage. *Blood* 1992; **79**: 1907–1915.
35. Averill MM, Barnhart S, Becker L *et al.* S100A9 differentially modifies phenotypic states of neutrophils, macrophages, and dendritic cells: implications for atherosclerosis and adipose tissue inflammation. *Circulation* 2011; **123**: 1216–1226.
36. Lee S, Huen S, Nishio H *et al.* Distinct macrophage phenotypes contribute to kidney injury and repair. *J Am Soc Nephrol* 2011; **22**: 317–326.
37. Wynn TA, Barron L. Macrophages: master regulators of inflammation and fibrosis. *Semin Liver Dis* 2010; **30**: 245–257.
38. Bronte V, Zanovello P. Regulation of immune responses by L-arginine metabolism. *Nat Rev Immunol* 2005; **5**: 641–654.
39. Dong X, Swaminathan S, Bachman LA *et al.* Resident dendritic cells are the predominant TNF-secreting cell in early renal ischemia-reperfusion injury. *Kidney Int* 2007; **71**: 619–628.
40. Passey RJ, Williams E, Lichanska AM *et al.* A null mutation in the inflammation-associated S100 protein S100A8 causes early resorption of the mouse embryo. *J Immunol* 1999; **163**: 2209–2216.
41. Hobbs JA, May R, Tanousis K *et al.* Myeloid cell function in MRP-14 (S100A9) null mice. *Mol Cell Biol* 2003; **23**: 2564–2576.
42. Stokman G, Leemans JC, Claessen N *et al.* Hematopoietic stem cell mobilization therapy accelerates recovery of renal function independent of stem cell contribution. *J Am Soc Nephrol* 2005; **16**: 1684–1692.
43. Iyer SS, Pulskens WP, Sadler JJ *et al.* Necrotic cells trigger a sterile inflammatory response through the Nlrp3 inflammasome. *Proc Natl Acad Sci USA* 2009; **106**: 20388–20393.
44. Roelofs JJ, Rouschop KM, Leemans JC *et al.* Tissue-type plasminogen activator modulates inflammatory responses and renal function in ischemia reperfusion injury. *J Am Soc Nephrol* 2006; **17**: 131–140.
45. Rouschop KM, Roelofs JJ, Claessen N *et al.* Protection against renal ischemia reperfusion injury by CD44 disruption. *J Am Soc Nephrol* 2005; **16**: 2034–2043.
46. Sadis C, Teske G, Stokman G *et al.* Nicotine protects kidney from renal ischemia/reperfusion injury through the cholinergic anti-inflammatory pathway. *PLoS ONE* 2007; **2**: e469.
47. Leemans JC, Butter LM, Pulskens WP *et al.* The role of Toll-like receptor 2 in inflammation and fibrosis during progressive renal injury. *PLoS ONE* 2009; **4**: e5704.
48. Teeling CM. A generally applicable sequential alkaline phosphatase immunohistochemical double staining. *J Histotechnol* 2008; **31**: 119–127.
49. van der Loos CM. Multiple immunoenzyme staining: methods and visualizations for the observation with spectral imaging. *J Histochem Cytochem* 2008; **56**: 313–328.
50. Dessing MC, Butter LM, Teske GJ *et al.* S100A8/A9 is not involved in host defense against murine urinary tract infection. *PLoS ONE* 2011; **5**: e13394.
51. Weijer S, Florquin S, van der Poll T. Endogenous interleukin-12 improves the early antimicrobial host response to murine Escherichia coli peritonitis. *Shock* 2005; **23**: 54–58.
52. van Eijk M, van Roomen CP, Renkema GH *et al.* Characterization of human phagocyte-derived chitotriosidase, a component of innate immunity. *Int Immunol* 2005; **17**: 1505–1512.
53. Koning N, van Eijk M, Pouwels W *et al.* Expression of the inhibitory CD200 receptor is associated with alternative macrophage activation. *J Innate Immun* 2010; **2**: 195–200.

Supplementary informations

The calcium-binding protein complex S100A8/A9 has a crucial role in controlling macrophage-mediated renal repair following ischemia/reperfusion

Mark C. Dessing[1], Alessandra Tammaro[1] , Wilco P. Pulskens[1], Gwendoline J. Teske[1], Loes M. Butter[1], Nike Claessen[1], Marco van Eijk[2], Tom van der Poll[3], Thomas Vogl[4], Johannes Roth[4], Sandrine Florquin[1,5*] and Jaklien C. Leemans[1*]

[1] Department of Pathology, [2] Medical Biochemistry, [3] Center for Infection and Immunity Amsterdam (CINIMA) and Center for Experimental and Molecular Medicine Academic Medical Center, University of Amsterdam, the Netherlands and [4] Institute of Immunology, University of Muenster, Muenster, Germany, [5] Department of Pathology, Radboud University Nijmegen Medical Center, Nijmegen, the Netherlands. *Contributed equally to manuscript

Supplementary figures

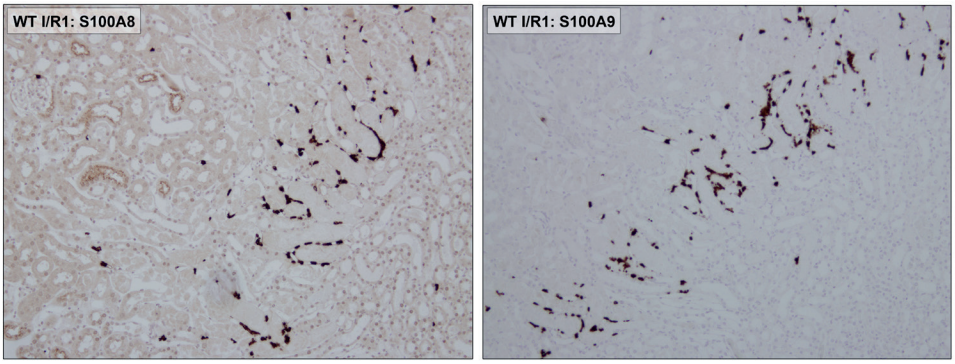

Supplementary Figure 1: renal S100A8 and S100A9 expression during renal I/R injury.
Representative photos from WT kidney tissue slides stained for S100A8 or S100A9, 1 day after I/R (magnification x100).

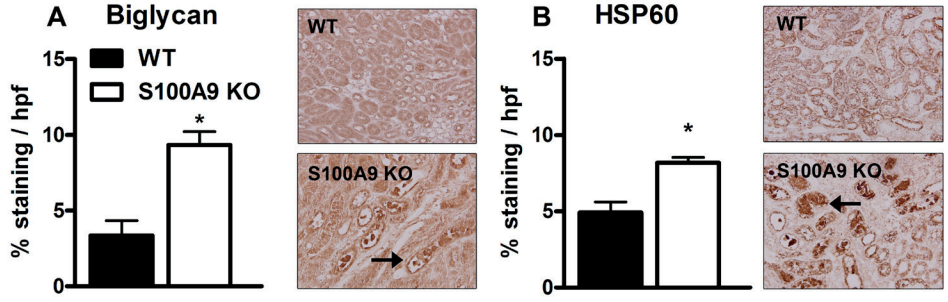

Supplementary Figure 2: Renal biglycan and HSP60 expression in WT and S100A9 KO mice during repair following I/R.
Digital quantification with representative photos taken from biglycan (**A**) and HSP60 (**B**) staining on kidney tissue slides of WT (black bars) and S100A9 KO mice (white bars), 5 days after I/R. Data is presented as % positive staining per high power field (hpf). Arrows indicate biglycan and HSP60 expression in renal tissue slides (magnification x400). Graph data are mean ± SEM (N=3 individual mice per group) *P<0.05 versus WT mice.

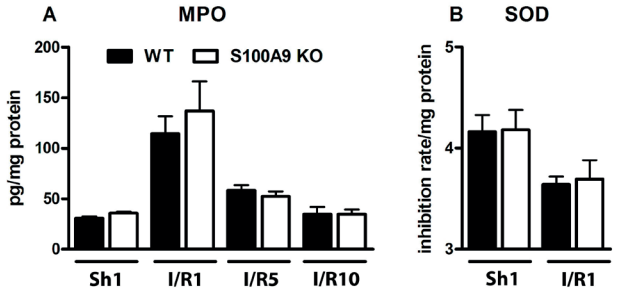

Supplementary Figure 3: Neutrophil content and SOD activity in WT and S100A9 KO mice during renal I/R injury. Neutrophil content (as reflected by MPO; A) and SOD activity (B) in kidney tissue from WT mice (black bars) and S100A9 KO mice (white bars) after I/R and from sham (sh) mice. MPO and SOD was corrected for total protein level in tissue. Data are mean ± SEM. *P<0.05 versus WT.

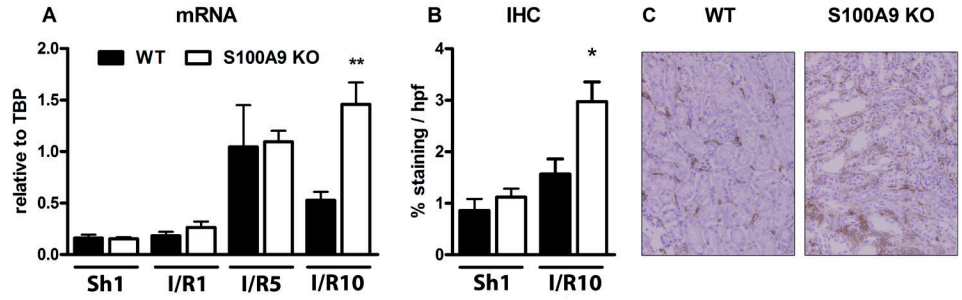

Supplementary Figure 4: CD11c expression in WT and S100A9 KO mice during renal I/R.
CD11c mRNA (**A**) and protein level (**B-C**) in WT mice (black bars) and S100A9 KO mice (white bars). A: mRNA levels are expressed relatively to housekeeping gene TBP. B: Digital quantification of CD11c staining on kidney tissue slides in sham WT (black bars) and S100A9 KO mice (white bars) 10 days after I/R. Data is presented as % positive staining per high power field (hpf). Representative photos of CD11c staining on renal tissue slides from WT and S100A9 KO mice 10 days after I/R (magnification x200). Data are mean ± SEM *P<0.05 versus WT mice.

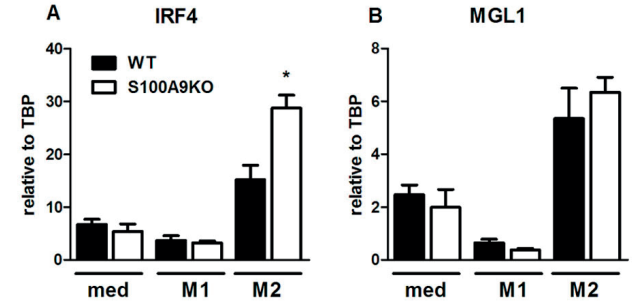

Supplementary Figure 5: IRF4 and MGL1 mRNA expression in WT and S100A9 KO macrophages. Alternative macrophage marker IRF4 (**A**) and MGL1 (**B**) in peritoneal macrophages from WT mice (black bars) and S100A9 KO mice (white bars) 48 hours after stimulation with medium (med), LPS+IFNγ (M1 polarization) or IL4+IL13 (M2 polarization). mRNA levels are expressed relatively to housekeeping gene TBP. Data are mean ± SEM. *P<0.05 versus WT (N=6 individual mice per group).

supplementary Table 1: Primers used for determination of specific genes.

S100A8	F: 5'- GGAAATCACCATGCCCTCTA R: 5'- ATCACCATCCGAAGGAACTC
S100A9	F: 5'- GAAGGAAGGACACCCTGACA R: 5'- AGCTGATTGTCCTGGTTTGTG
Kidney injury molecule (KIM)-1	F: 5'- TGGTTGCCTTCCGTGTCTCT R: 5'- TCAGCTCGGGAATGCACAA
Neutrophil gelatinase-associated lipocalin (NGAL)	F: 5'- GCCTCAAGGACGACAACATC R: 5' - CTGAACCATTGGGTCTCTGC
Collagen I	F: 5'- ACCTAAGGGTACCGCTGGA R: 5'- TCCAGCTTCTCCATCTTTGC
Collagen III	F: 5'- GTGGTTTTCAGTTCAGCTATG R: 5'- TCCCCAGTGTGTTTAGTACAG
Epidermal growth factor module-containing mucin-like receptor (Emr)-1	F: 5'- CTTTGGCTATGGGCTTCCAGTC R: 5'- GCAAGGAGGACAGAGTTTATCGTG
Nitric oxide synthase (NOS)-2	F: 5'- CCAAGCCCTCACCTACTTCC R: 5'- CTCTGAGGGCTGACACAAGG
Interferon regulatory factor (IRF)-4	F: 5'- CGGCCAGCACCGAGATTCCA R: 5'- AATGACGGAGGGAGCGGTGG
IRF5	F: 5'- CTTGGCCCATGGCTCCTGCC R: 5'- AGCAACCGGGCTGCAACAGG
Arginase (Arg)-1	F: 5'- CTCCAAGCCAAAGTCCTTAGAG R: 5'- AGGAGCTGTCATTAGGGACATC
Macrophage galactose-type C-type lectin (MGL) 1	F: 5'- TGAGAAAGGCTTTAAGAACTGGG R: 5'- GACCACCTGTAGTGATGTGGG
Interleukin -13	F: 5'- AGGCCCCCACTACGGTCTCC R: 5'- AAGGGGCCGTGGCGAAACAG
Integrin, Alpha X (ItgaX, or CD11C)	F: 5'- CTGGATAGCCTTTCTTCTGCTG R: 5'- GCACACTGTGTCCGAACTC
Transacting T-cell-specific transcription factor (GATA)-3	F: 5'- CTGGAGGAGGAACGCTAATG R: 5'- GTTGAAGGAGCTGCTCTTGG
TATA box binding protein (TBP)	F: 5'- GGAGAATCATGGACCAGAACA R: 5'- GATGGGAATTCCAGGAGTCA

F: forward primer, R: reverse primer

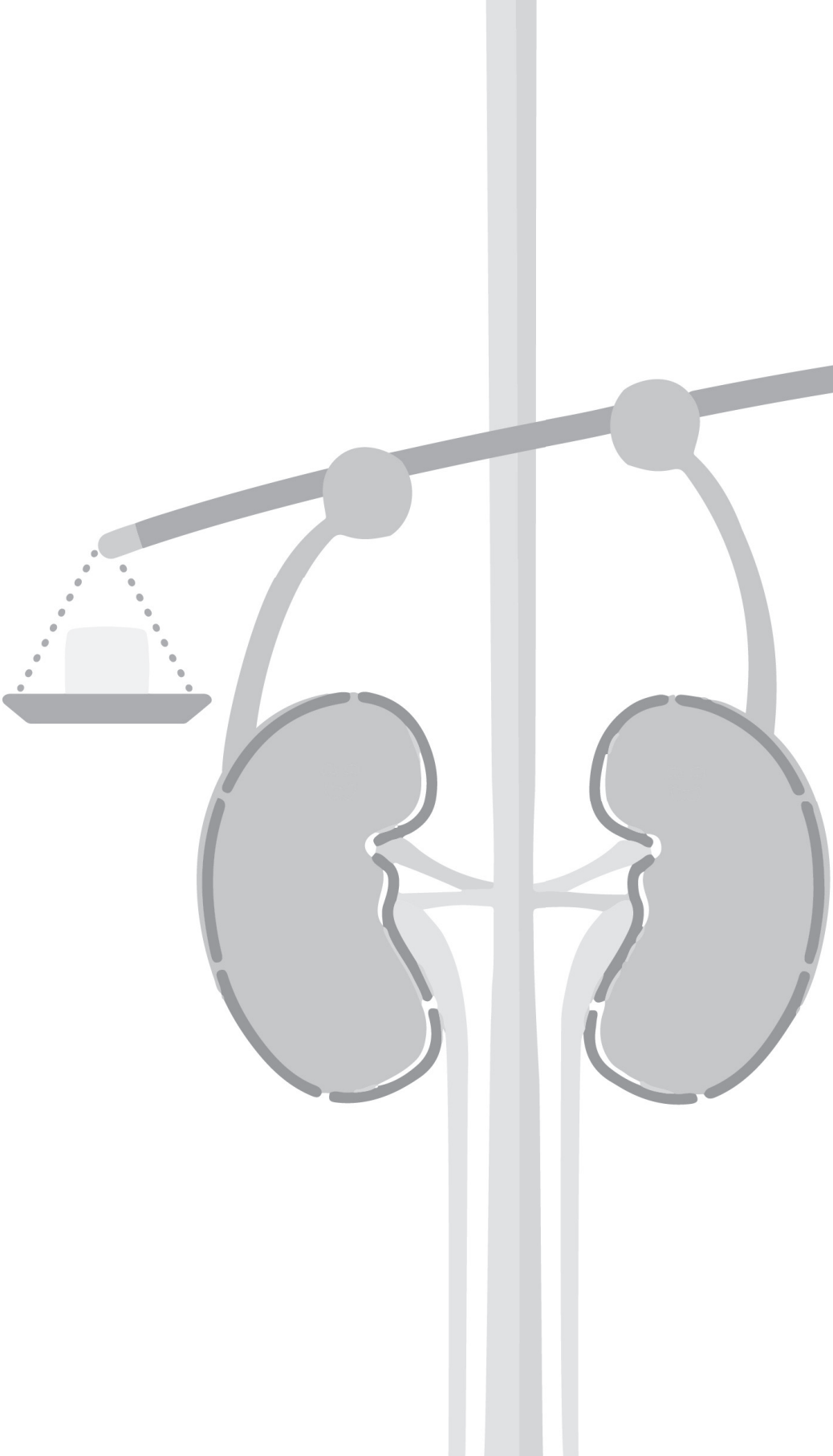

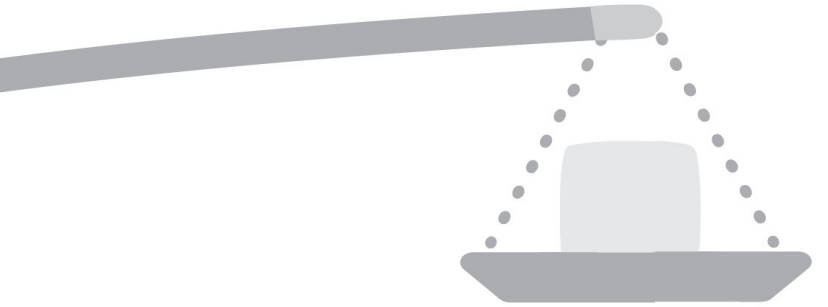

Chapter 3

S100A8/A9 promotes parenchymal damage and renal fibrosis in obstructive nephropathy

Clinical & Experimental Immunology 2018, 193: 359–373

Clinical and Experimental Immunology ORIGINAL ARTICLE doi: 10.1111/cei.13154

S100A8/A9 promotes parenchymal damage and renal fibrosis in obstructive nephropathy

A. Tammaro,* S. Florquin,* M. Brok,* N. Claessen,* L. M. Butter,* G. J. D. Teske,* O. J. de Boer,* T. Vogl,† J. C. Leemans*[1] and M. C. Dessing*[1]

*Department of Pathology, Amsterdam UMC, Univ(ersity) of Amsterdam, Amsterdam, the Netherlands, and †Institute of Immunology, University of Münster, Münster, Germany

Summary

Despite advances in our understanding of the mechanisms underlying the progression of chronic kidney disease and the development of fibrosis, only limited efficacious therapies exist. The calcium binding protein S100A8/A9 is a damage-associated molecular pattern which can activate Toll-like receptor (TLR)-4 or receptor for advanced glycation end-products (RAGE). Activation of these receptors is involved in the progression of renal fibrosis; however, the role of S100A8/A9 herein remains unknown. Therefore, we analysed S100A8/A9 expression in patients and mice with obstructive nephropathy and subjected wild-type and S100A9 knock-out mice lacking the heterodimer S100A8/A9 to unilateral ureteral obstruction (UUO). We found profound S100A8/A9 expression in granulocytes that infiltrated human and murine kidney, together with enhanced renal expression over time, following UUO. S100A9 KO mice were protected from UUO-induced renal fibrosis, independently of leucocyte infiltration and inflammation. Loss of S100A8/A9 protected tubular epithelial cells from UUO-induced apoptosis and critical epithelial–mesenchymal transition steps. *In-vitro* studies revealed S100A8/A9 as a novel mediator of epithelial cell injury through loss of cell polarity, cell cycle arrest and subsequent cell death. In conclusion, we demonstrate that S100A8/A9 mediates renal damage and fibrosis, presumably through loss of tubular epithelial cell contacts and irreversible damage. Suppression of S100A8/A9 could be a therapeutic strategy to halt renal fibrosis in patients with chronic kidney disease.

Keywords: damage-associated molecular patterns, innate immunity, renal fibrosis, S100 proteins, tubular integrity

Accepted for publication 26 April 2018
Correspondence: A. Tammaro, Department of Pathology, Amsterdam UMC, Univ(ersity) of Amsterdam, Room L2-112, Meibergdreef 09, Amsterdam 1105AZ, the Netherlands. E-mail: a.tammaro@amc.uva.nl

[1]These authors contributed equally to this study.

Introduction

Fibrotic diseases, including progressive renal diseases, lead to loss of function and organ failure. They represent a major socioeconomic burden and account for at least one-third of deaths worldwide [1]. Renal fibrosis is the final common pathway leading to end-stage renal disease (ESRD), a condition for which no effective treatments exist except for life-long dialysis or renal transplantation [2]. The pathophysiological mechanisms driving the loss of renal function involve four cellular protagonists: myofibroblasts, tubular epithelial cells (TECs), immune cells and endothelial cells which, upon (mal)adaptive activation, induce the progression of tubulo-interstitial fibrosis [3]. Although progress has been made in understanding the molecular mechanisms underlying the development of fibrosis, the failure to limit this process is undeniable. Thus, new avenues need to be explored in order to offer a therapeutic potential for preventing renal fibrosis.

Calprotectin, or the S100A8/S100A9 protein complex, belongs to the S100 calcium-binding protein family. This heterodimer protein is expressed and released by activated phagocytes, mainly neutrophils and macrophages, and has been shown to induce cytoskeleton reorganization [4], chemotaxis [5] and cytokine expression [6,7]. Apart from the above-mentioned intracellular functions, S100A8/A9 is also released upon tissue injury, thereby acting as a damage-associated molecular pattern (DAMP), which mediates the activation of the inflammatory response [8,9]. In the context of obstructive nephropathy, damaged cells

release DAMPs such as S100A8/A9 to alert the immune system [10,11]. In response to the insult, S100A8/A9 functions as an endogenous ligand which binds to pattern recognition receptors (PRRs), including Toll-like receptor (TLR)-4 [12,13] and the receptor for advanced glycation end-products (RAGE) [14,15]. Both receptors are expressed by macrophages and TECs following ureteral obstruction [16,17], which can initiate the inflammatory response and are involved in processes related to tissue repair. Also, chronic inflammation may perpetuate tissue injury leading to the development of fibrosis [3]. Indeed, several studies have demonstrated that TLR-4 and RAGE represent key factors of chronic kidney disease (CKD) progression through modulation of interstitial fibrosis [17,18]. As these receptors are crucial for host defence it might be more interesting to target their ligands instead. Thus, we investigated the role of their shared ligand S100A8/A9 in the pathogenesis of renal fibrosis. To assess the contribution of S100A8/A9 in the progression of renal fibrosis we subjected wild-type (WT) and S100A9 knock-out (KO) mice to UUO and determined its expression, location and function.

Materials and methods

Patients

Renal biopsies (n = 3) were obtained from patients diagnosed with obstructive hydronephrosis, characterized by extensive fibrosis and tubular atrophy or healthy renal tissue, at the Academic Medical Center (University of Amsterdam), as described previously [19]. All biopsies were taken for diagnostic purposes only. For the present study, only left-over biological material was used, delinked from patient records, and as such was not subjected to any requirement for ethical review or approval according to Dutch law when patients have made no objection (Article 7:467 BW Book 7). We have only used the material of patients with no objection.

Experimental animals and procedure

The Institutional Animal Care and Use Committee of the University of Amsterdam approved all experiments for the animal study, in compliance with the Animal Research: Reporting of In Vivo Experiments (ARRIVE) guidelines (NC3Rs). The study was designed with two experimental groups: (1) C57Bl/6 WT controls (n = 8) and (2) S100A9 KO animals (n = 8) and four time-points (from days 1, 3, 7 and 14 of sacrificed) for each experimental group. Each experimental group was divided into two cages of three and five animals. The total number of mice for the experi-mental group was 32. Genetic deletion of S100A8 leads to embryonic lethality [20]. We therefore used S100A9-deficient mice that lack functional calprotectin complex and display almost undetectable levels of S100A8 protein. These mice were generated as described previously [21] and back-crossed to a C57Bl/6 genetic background. Animals were bred in the animal facility of the Academic Medical Center (AMC) in Amsterdam, the Netherlands. Eight to 10-week-old male mice were used in the experiments. Age- and sex-matched WT C57Bl/6 mice were purchased from Charles River Laboratories (Cologne, Germany). Mice weighed approximately 25 g/mouse. Animals were kept in standard environmental conditions (temperature, humidity, ventilation, light/dark cycle), housed in specific pathogen-free conditions (SPF) with *ad libitum* access to water and food, and allowed to acclimatize for a week before starting the experiment. WT C57Bl/6 and S100A9 KO mice were subjected to progressive renal injury by UUO, as described previously [19]. Briefly, the right ureter was ligated (near the ureteropelvic junction) with suture (6.0 Tyco healthcare) under 2·5% isoflurane-induced anaesthesia and oxygen (via inhalation) through an abdominal incision. The surgical procedure was carried out in the morning under the laminar flow cabinet with a temperature-controlled heating pad. Upon completing surgery, muscle and skin layers were closed with surgical sutures (6.0, Tyco healthcare). Fifty μg/kg buprenorphine was administered through a subcutaneous injection for analgesic purposes (Temgesic, Schering-Plough, Kenilworth, NJ, USA). Animals were sacrificed via cardiac exsanguination followed by cervical dis-location at days 1, 3, 7 and 14 post-surgery. Sham mice were sacrificed at day 1 post-UUO. Contralateral/unobstructed left kidneys were also used as controls.

RNA isolation and reverse transcriptase–polymerase chain reaction (RT–PCR)

Total RNA was isolated from snap-frozen renal tissue using Trizol reagent (Invitrogen, Waltham, MA, USA), according to the manufacturer's protocol. RNA was converted into cDNA by the use of oligo-dT as a primer. Gene expression was analysed by reverse transcriptase-polymerase chain reaction (RT–PCR) with SYBR green PCR master mix on a Lightcycler 480 (Hoffmann-Roche, Basel, Switzerland). Relative expression was analysed using LinRegPCR (developed by Hearth Failure Research Center, University of Amsterdam, the Netherlands). Gene expression was normalized to mouse TATA box-binding protein (*Tbp*) housekeeping gene, n = 7/8 animals per group; see Supporting information, Table S1 for primer sequences.

Plasma biochemical analysis

Plasma levels of creatinine were measured by standard autoanalyser methods at our hospital research services.

Enzyme-linked immunosorbent assay (ELISA) and immunoblot

In order to measure renal S100A8/A9 and transforming growth factor (TGF)-β1 protein, snap-frozen kidney (n = 7/8) tissues were homogenized in Greenberger lysis buffer (150 mM NaCl, 15 mM Tris, 1 mM $MgCl_2$ pH 7.4, 1 mM $CaCl_2$, 1% Triton X-100 and 1% protease inhibitor cocktail (Sigma-Aldrich, Zwijndrecht, the Netherlands). The S100A8/A9 Heterodimer DuoSet and TGF-β1 ELISA kit (R&D Systems, Minneapolis, MN, USA) were used according to the manufacturer's protocol.

Snap-frozen kidneys or cell lysates were used for immunoblotting (n = 2/4). Protein lysates were obtained from snap-frozen kidney tissue or primary TECs derived from *in-vitro* assays. Tissue and cells were lysed in radioimmunoprecipitation assay (RIPA) buffer [50 m M T ris pH 7.5, 0·15 M NaCl, 2 mM ethylenediamine tetraacetic acid (EDTA), 1% deoxycholic acid, 1% NP-40, 4 mM sodium orthovanadate, 10 mM sodium fluoride], s upplemented with 1% of protease inhibitor cocktail (Sigma-Aldrich, Zwijndrecht, the Netherlands). Lysates were loaded on a 4–12% Nupage gel and blotted onto a polyvinylidene difluoride (PVDF) membrane. After blocking aspecific signal, blots were incubated overnight at 4°C with differ-ent antibodies, as listed in Supporting information, Table S2. Blots were incubated with horseradish peroxidase-conjugated secondary antibodies and detected with enhanced chemiluminescence (ECL) (Pierce, Waltham, MA, USA).

Immunostaining

Renal tissues were fixed in 10% formalin for 24 h, pro-cessed and paraffin-embedded. For immunohistochemical staining, 4-µm-thick sections of murine renal tissues (n = 7/8) or human biopsies (n = 3) were treated for 30 min with 0·25% pepsin in 0·1 M HCl at 37°C (for Ly6G) or boiled for 10 min in 10 mM citrate (pH 6.0) (other antibodies), incubated overnight with different pri-mary antibodies, as described in Supporting information, Table S2, and developed using diaminobenzidine (DAB) (Sigma). For collagen staining, slides were incubated with 0·2% Picro Sirius Red (PSR) solution (pH 2.0) for 1 h followed by incubation within 0·01 M HCl. Periodic acid–Schiff diastase (PAS-D) was used to quantify the number of intact tubules, based on morphology, dimensions and brush border presence, as described previously [2]. To quantify the number of apoptotic and proliferating TECs only tubules (not interstitial cells) surrounding glomeruli were included in the count, as shown by the white drawings in the picture. The number of intact tubules and those positive for cleaved caspase-3 or Ki67 were counted within 10 non-overlapping high-power fields (HPF) (×40 magnification) in a blinded manner. The amount of positive staining for F4/80, alpha smooth muscle actin (αSMA), collagen I, PSR, intercellular adhesion molecule 1 (ICAM-1), S100A8 and S100A9 was quantified with ImageJ software, Fiji (National Institutes of Health, Bethesda, MD, USA), a computer-based imaging analysis for reliable biomarker quantitation which is applied widely for tissue-based research.

For sequential immunohistochemistry, sections were labelled and stained with NovaRed, as described previously [22]. After each staining slides were acquired on a digital slide scanner (IntelliSite Pathology Ultra Fast Scanner; Philips, Eindhoven, the Netherlands). Afterwards, coverslips were removed and the sections were stripped by incubation for 30 min in 1 M Tris–HCl (pH 7.5) supplemented with 2% (v/v) sodium dodecyl sulphate and 0·7% (v/v) β-mercaptoethanol at 50°C, followed by rinsing with tap water. Complete removal of the stain was ensured by visual inspection. Three sequential stainings (mouse: S100A8, S100A9 and Ly6G/F480; human: S100A8/S100A9, CD15 and CD68) were performed on the same section. Overlay images were obtained as described previously by our group [22].

For immunofluorescence staining, paraffin-embedded tissues from T14 post-UUO were incubated with biotin–dolichos biflorus agglutinin (DBA: collecting duct marker) and lotus tetragonolobus lectin (LTL: proximal tubule marker) followed by streptavidin fluorescein isothiocyanate (FITC). Primary antibodies incubation followed the lectin staining. Rat-anti-S100A8 and S100A9 primary antibodies were detected by rabbit anti-rat Texas Red. Nuclei were stained with Hoechst. Pictures were taken with a fluorescence light microscope (Leica, Wetzlar, Germany; magnification ×40).

Reagents were used according to the manufacturer's protocol.

In-vitro assays

For *in-vitro* assays, primary, immortalized proximal TECs (IM-PTEC) and polarized TECs [Madin–Darby canine kidney cells (MDCK)] were used. Primary TECs were isolated from kidneys of C57Bl/6 WT mice (n = 4), as described previously [23]. IM-PTECs were cultured in hexokinase 2 (HK2) medium supplemented with interferon gamma at 33°C. A week before the experiment, IM-PTEC cells were transferred to a 37°C incubator in order to lose SV40 expression [24]. MDCK cells were cultured on collagen-coated coverslips in HK2 medium. Cells were stimulated with different concentrations of recombinant S100A8/A9 (rS100A8/A9) (kindly provided by T. Vogl) and/or recombinant TGF-β1 (rTGF-β1) (Pepscan, Lelystad, the Netherlands), as described in the figure legends, for 24 h.

Cell death assays were performed as follows. Cells were detached with trypsin, washed once with phosphate-buffered saline (PBS) followed by washing with annexin V buffer [500 ml: 1·19 g HEPES, 4·4 g NaCl, 0·19 g KCl, 0·1 g $CaCl_2$, 0·1 g $MgCl_2$, 1 ml/ml glucose and 0·5% bovine serum albumin (BSA), pH 7.3]. Subsequently, cells were incubated with annexin V for 20 min on ice in the dark. Propidium iodide (PI) or To-Pro3 (Thermo Fisher,

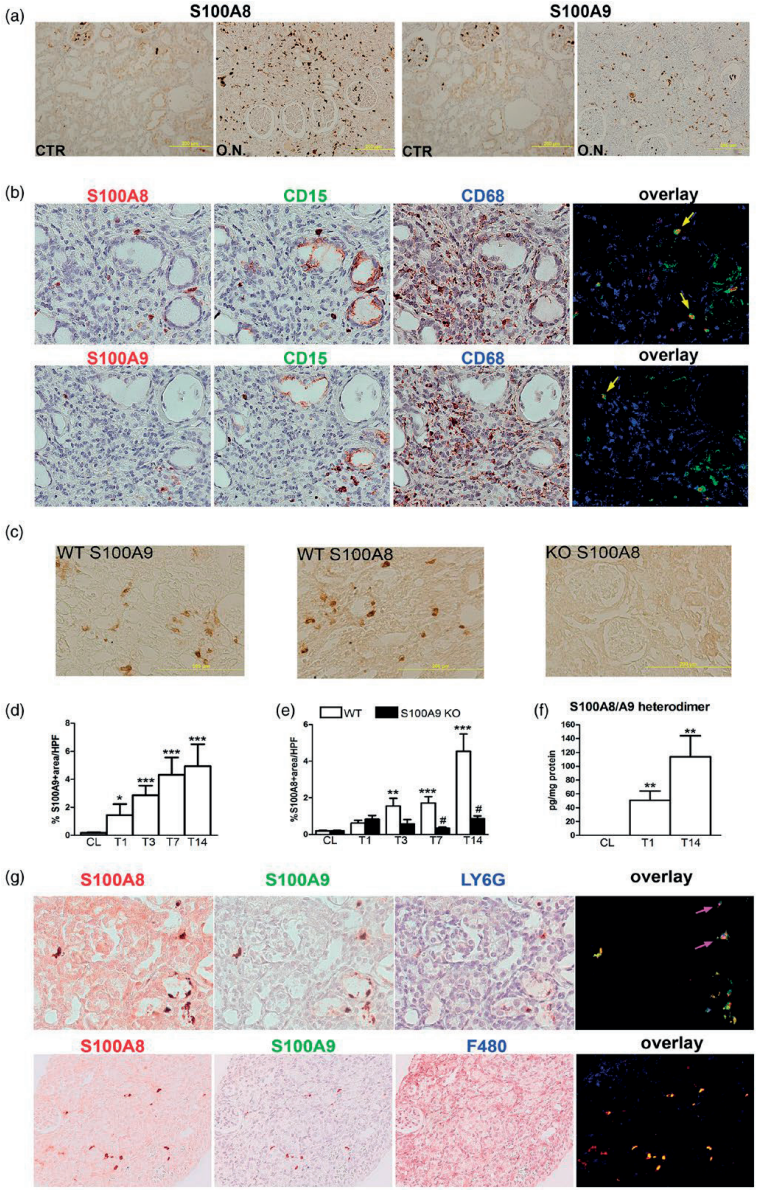

Fig. 1. Human and murine S100A8/A9 expression during obstructive nephropathy. (a) Immunohistochemistry for human S100A8 and S100A9 on healthy tissue (CTR) and from kidney biopsies of patients with obstructive hydronephrosis (ON). (b) Representative examples of original immunostaining and composite overlays for S100A8 or S100A9 (red), CD15 (green) and CD68 (blue) on obstructive nephropathy biopsies. Composite images, obtained with Image J, reveal only the triple overlay between S100A8/S100A9 and CD15 (yellow cells and arrow) (magnification ×40). (c) Representative pictures of murine S100A8/A9 staining in kidney sections from wild-type (WT) and S100A9 knock-out (KO) mice. (d) Quantification of S100A9 in contralateral kidneys (CL) (grey bar) and WT mice (white bars) upon 1, 3, 7 and 14 days of unilateral ureteral obstruction (UUO). (e) Quantification of S100A8 in CL kidneys and upon 1, 3, 7 and 14 days of UUO in sham WT and S100A9 KO mice. (f) Murine S100A8/A9 protein complex levels in CL kidneys or following 1 and 14 days of UUO in WT mice as measured by enzyme-linked immunosorbent assay (ELISA). Protein expression was corrected for total protein levels in renal tissue. (g) Representative examples of original immunostaining and composite overlays for S100A8 (red), S100A9 (green) and Ly-6G or F480 (blue) in WT mouse kidney after 14 days of UUO. Overlay pictures were obtained by sequential immunostaining technique as described in Material and methods. Co-localization of murine S100A8/A9 are shown in yellow. Triple overlay is shown in pink/purple colour and indicated with pink arrows (S100A8, S100A9 and LY6G) (magnification ×40). Graph data are mean ± standard error of the mean (s.e.m.). #$P < 0{\cdot}05$ *versus* WT at the same time-point, *$P < 0{\cdot}05$, **$P < 0{\cdot}005$, ***$P < 0{\cdot}0005$ *versus* CL unobstructed kidney. Scale bar 200 μm; $n = 3$ for human data. For statistical analysis of murine data the Mann–Whitney U-test was used for comparison between two groups; $n = 7/8$ mice per group. [Colour figure can be viewed at wileyonlinelibrary.com]

Fremont, CA, USA) was added to the cells prior to acquisition. Cells were acquired on a fluorescence activated cell sorter (FACS)Canto (Becton Dickinson, San Jose, CA, USA) and analysed with Flow-Jo software (TreeStar, Inc., Ashland, OR, USA).

The activity of caspase-3 was measured in cell lysates, using the fluorogenic substrate Ac-DEVD-AMC (Enzo Life Sciences, Exeter, UK), in the caspase assay buffer [HEPES 20 mM, dimethyl [3-(propyl)] azaniumyl propane-1-sulphonate (CHAPS) 5 mM, dithiothreitol (DTT) 5 mM, EDTA 5 mM]. Fluorescence was measured with a 360-nm excitation wavelength and 460-nm emission wavelength.

For immunofluorescence on MDCK cells cultured on coverslips, cells were fixed and permeabilized before incubation with primary antibodies followed by AlexaFluor 488-conjugated secondary antibody. Pictures were taken with a fluorescence light microscope (Leica; magnification ×40).

Statistics

Comparisons between two groups were analysed using the Mann–Whitney *U*-test or between more than two groups with the Kruskal–Wallis test, unless mentioned otherwise in the figure legend. For *in-vitro* experiments, comparison between two groups was analysed using the two-tailed Student's *t*-test. Values are expressed as mean ± standard error of the mean (s.e.m.). *P*-values < 0·05 were considered statistically significant.

Results

Increased S100A8/A9 expression in human biopsies and murine renal tissue with obstructive nephropathy

We first investigated the expression of S100A8 and S100A9 in renal biopsies of patients with obstructive hydronephrosis. As a control we used the healthy area in renal tissue derived from nephrectomy for malignancy. Using immunohistochemistry (IHC) we observed that S100A8 and S100A9 expression is increased during obstructive nephropathy and is localized to the tubulo-interstitial compartment (Fig. 1a). It is noteworthy that non-myeloid cells such as tubular cells did not show any positivity for S100A8/A9 as described previously after stress conditions [8]. The S100A8/A9-positive cells were identified as granulocytes and not macrophages, as displayed by co-localization (overlay displayed in yellow and highlighted with arrow) of S100A8/A9 (red) with CD15 (green), a marker for granulocytes but not with CD68 (macrophage marker: blue) (Fig. 1b).

Next, we evaluated expression and localization in the experimental model of obstructive nephropathy UUO, which mimics the various stages of progressive renal injury and fibrosis [25]. Similar to human staining, in murine kidney we detected S100A8- and S100A9- positive cells mainly within the interstitial compartment (Fig. 1c). Digital quantification of stained tissue revealed an increased expression of S100A8/A9 over time (Fig. 1d,e). Staining for S100A8 was almost undetectable in S100A9 KO mice (Fig. 1c,e). As S100A8/A9 functions as a heterodimer, we measured this by enzyme-linked immunosorbent assay (ELISA). S100A8/A9 complex is expressed significantly 14 days after surgery, compared to contralateral tissue (Fig. 1f).

As in the human study, sequential immunostaining was used to determine the cellular source of S100A8/A9 expression in kidney post-UUO at day 14. We found that S100A8 (red) co-localizes with S100A9 (green) (overlay in yellow) suggesting that the functional heterodimer is present. Moreover, and in line with human data, the complex co-localizes with the granulocyte marker Ly6G (blue) (overlay: pink positive cells highlighted with pink arrow) but not with the macrophage marker F480 (blue) (Fig. 1g). Of note, staining for granulocyte influx (Ly6G) in renal tissue was similar between WT and S100A9 KO mice 1 and 14 days following UUO (WT *versus* S100A9

KO mice, day 1: 1·1 ± 0·3 *versus* 1.9 ± 0·4 and day 14: 7 ± 1·8 *versus* 8·6 ± 4·4% positive staining/HPF). The small percentage of S100A8/A9-positive cells, which do not express the Ly6G marker, appears to be positive for DBA but not for LTL (Supporting information, Fig. S1). Together, these human and experimental data suggest a potential role for S100A8/A9 in progressive renal injury.

S100A9 deficiency dampens renal fibrosis independently of leucocyte infiltration

To directly assess the contribution of S100A8/A9 to renal interstitial fibrosis, we analysed the presence of α-SMA-positive myofibroblasts and collagen deposits in WT and S100A9 KO mice after UUO. We have described previously that, in untreated conditions, levels of α-SMA, collagen-1 and macrophage polarization markers were similar between WT and KO mice [21].

Differences were found at time-points where we observed the highest expression of the S100A8/A9 monomer (such as days 7 and 14). We did not detect any differences in these parameters at days 1 and 3 following UUO (data not shown). Seven days following UUO, kidneys of S100A9 KO mice showed less accumulation of myofibroblasts compared to WT mice, whereas no differences were observed at day 14 (Fig. 2a). A reduction of collagen deposition, detected by IHC, was observed in S100A9 KO mice compared to WT at 7 and 14 days of UUO (Fig. 2b). The latter finding was also verified by PSR staining, which confirmed that KO mice have reduced collagen deposits 14 days post-UUO (Fig. 2c).

The reduced extent of fibrosis in the S100A9 KO animals also affected the expression of the profibrotic growth factor platelet-derived growth factor (*Pdgfa*) and collagen-1 genes (*col1a1*), particularly 14 days after UUO (Fig. 2d,e). During progression of fibrosis, particularly 14 days upon UUO, TGF-β1 is expressed and activated in WT mice, whereas in S100A9 KO animals appears to be significantly decreased (Fig. 2f). The rescue in renal fibrosis was accompanied by a functional renal improvement, as shown by decreased levels of creatinine (Fig. 2g).

Sustained inflammation is a hallmark of progressive renal fibrosis [3]. In particular, macrophages modulate tubulo-interstitial damage after UUO [26]. Accumulation of F4/80$^+$ macrophages and the transcript expression of proinflammatory mediators such as C-C motif chemokine ligand 2 (CCL2), interleukin (IL)-6 and tumour necrosis factor (TNF)-α was comparable between WT and S100A9 KO mice at days 7 and 14 post-UUO (Fig. 3a–d). S100A8/A9 can modulate macrophage polarization [21,27]. However, we found no differences in the expression of M1- and M2-differentiated macrophages markers (*Nos2*, *Irf5*, *Ly6c* and *Arg1*, *Irf4* and *Mrc1*, respectively) between WT and KO mice (Fig. 3e,f).

Altogether, these results suggest that S100A8/A9 has a detrimental effect on the development of UUO-induced renal fibrosis, which was not associated with a difference in inflammatory cytokine response or modulation of gene expression, indicative of macrophage polarization.

S100A9 deficiency preserves tubular epithelial cells integrity following UUO

Next, we evaluated whether differences in fibrosis between WT and S100A9 KO mice could be ascribed to an effect on TECs injury. Thus, we analysed TECs apoptosis, proliferation and morphology at days 7 and 14 post- UUO. Compared to WT mice, S100A9 KO mice display decreased tubular apoptosis, as shown by cleaved caspase-3 positive tubular cells (Fig. 4a,d). In addition, the proliferation of tubular cells, as verified by Ki67 positivity, was increased in S100A9 KO mice compared to WT animals (Fig. 4b,e). These findings were corroborated by the presence of an increased number of intact tubules in S100A9 KO mice, as detected by the presence of brush border and regular morphology with PAS-D staining (Fig. 4c,f). Epithelial mesenchymal transition (EMT) occurs in TECs in response to injury and can lead to the progression of tubulo-interstitial fibrosis [3,25]. Critical molecular events in EMT are characterized by loss of expression of adhesion molecule E-cadherin and by the induction of the transcription factor Twist [28]. Compared to WT mice, S100A9 KO mice display increased expression of the E-cadherin transcript 14 days post-surgery (Fig. 4g). E-cadherin expression is regulated negatively by Twist, which was decreased in S100A9 KO animals compared to WT upon 14 days of UUO (Fig. 4h). Given the decreased activation of the key transition steps leading to EMT, together with the development of fibrosis, we investigated whether these observations correlated with the level of renoprotective cytokine IL-10, shown recently to have anti-fibrotic effects in the context of UUO [29]. Indeed, IL-10 was increased significantly in S100A9 KO mice compared to WT 14 days after UUO (Fig. 4i). Altogether, these data suggest that S100A9 deficiency ameliorates renal fibrosis by preserving tubular health, possibly via the suppression of critical molecular events in EMT.

S100A9 deficiency is associated with down-regulation of RAGE and its interacting receptor ICAM-1

S100A8/A9 can bind either TLR-4 or RAGE receptors, which are both up-regulated in epithelial cells following UUO [17]. We therefore analysed and normalized the expression of TLR-4 and RAGE protein in murine kidneys of WT and S100A9 KO mice 14 days post-UUO,

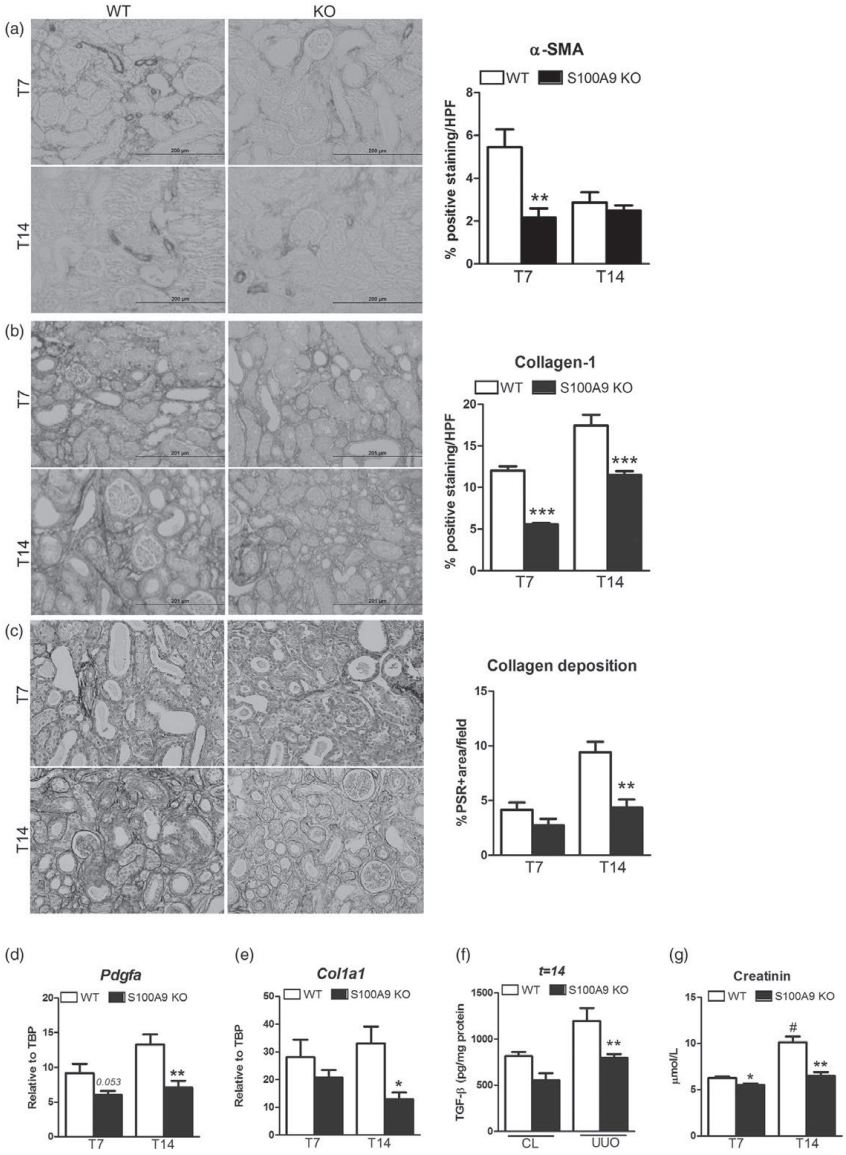

Fig. 2. Renal fibrosis in wild-type (WT) and S100A9 knock-out (KO) mice during unilateral ureteral obstruction (UUO). Renal fibrosis as displayed by representative pictures and quantification of (a) α-smooth muscle actin (SMA), (b) collagen 1 and (c) Picro Sirius Red (PSR) staining on renal tissue slides from WT and S100A9 KO mice 7 and 14 days after UUO. (d,e) Transcript expression of pro-fibrotic genes *Pdgfa* and Col1a1 measured by reverse transcriptase–polymerase chain reaction (RT–PCR). Data are expressed relative to the housekeeping gene *Tbp in* WT and S100A9 KO mice 7 and 14 days after UUO. (f) Transforming growth factor (TGF)-β protein detected by enzyme-linked immunosorbent assay (ELISA) in contralateral (CL) and obstructed kidney from WT and S100A9 KO mice, 14 days post-UUO. (g) Plasma levels of creatinine in WT and S100A9 KO animals, 7 and 14 days after UUO. HPF = high-power field. Magnification ×20. The Mann–Whitney *U*-test was used for comparisons between two groups; $n = 7/8$ mice per group. Graph data are mean ± standard error of the mean (s.e.m.). $^{*}P < 0{\cdot}05$, $^{**}P < 0{\cdot}005$, $^{***}P < 0{\cdot}0005$ *versus* WT at the same time-point. $\#P < 0{\cdot}005$ compared to WT at T7. Scale bar 200 μm.

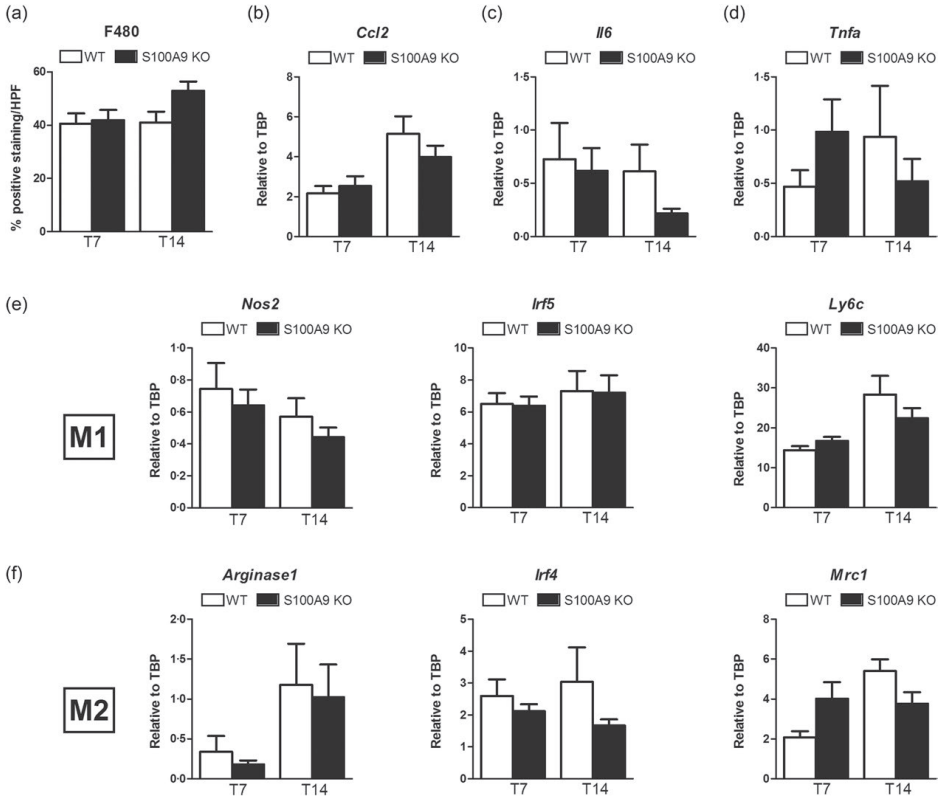

Fig. 3. Inflammatory parameters in WT and S100A9 KO mice. (a) Renal macrophages accumulation shown as percentage of F480 positive area detected by IHC, in renal tissues 7 and 14 days post- unilateral ureteral obstruction (UUO). Next, transcript expression in renal tissue of (b) *Ccl2* (the gene for MCP-1), (c) *Il6* and (d) *Tnfa* measured by reverse transcriptase–polymerase chain reaction (RT–PCR). (e) Transcript expression in renal tissue of M1 markers, *Nos2*, *Irf5*, *Ly6c* and (f) M2 macrophage markers, *Arginase-1, Irf4, Mrc1* measured by reverse transcription–polymerase chain reaction (RT–PCR). Values are relative to the housekeeping gene *Tbp*. Data are expressed as mean ± standard error of the mean (s.e.m.); $n = 7/8$ samples per group.

as more consistent results were obtained at this time-point. TLR-4 and RAGE proteins showed a similar down-regulated pattern in kidney lysates after UUO in the absence of S100A9, with statistical significance for RAGE (Fig. 5a–c).

As, together with intracellular adhesion molecule-1 (ICAM-1), RAGE may mediate interstitial fibrosis by modulating epithelial integrity during UUO [17], we inves-tigated the expression of ICAM-1. Our results show that besides RAGE, ICAM-1 is also reduced in KO kidneys 14 days post-UUO compared to WT tissue at mRNA and protein levels (Fig. 5d,e). It is conceivable that the S100A8/A9 may induce tubular injury via RAGE and its interacting receptor ICAM-1.

Recombinant S100A8/A9 directly affects TECs de-differentiation and cell death *in vitro*

In order to unravel the mechanism by which S100A8/A9 contributes to tubular injury, TECs were stimulated with different concentrations of recombinant S100A8/A9 protein. As previous studies have shown that S100A8/A9 impairs endothelial cell integrity by down-regulation of cell junction protein [30,31], which leads to cell death, we measured the expression of cell junction protein zonula occludens-1 (ZO-1) and adhesion molecule E-cadherin in TECs stimulated with a low concentration of S100A8/A9. Our results show that S100A8/A9 induces a profound down-regulation of ZO-1 protein expression and a trend

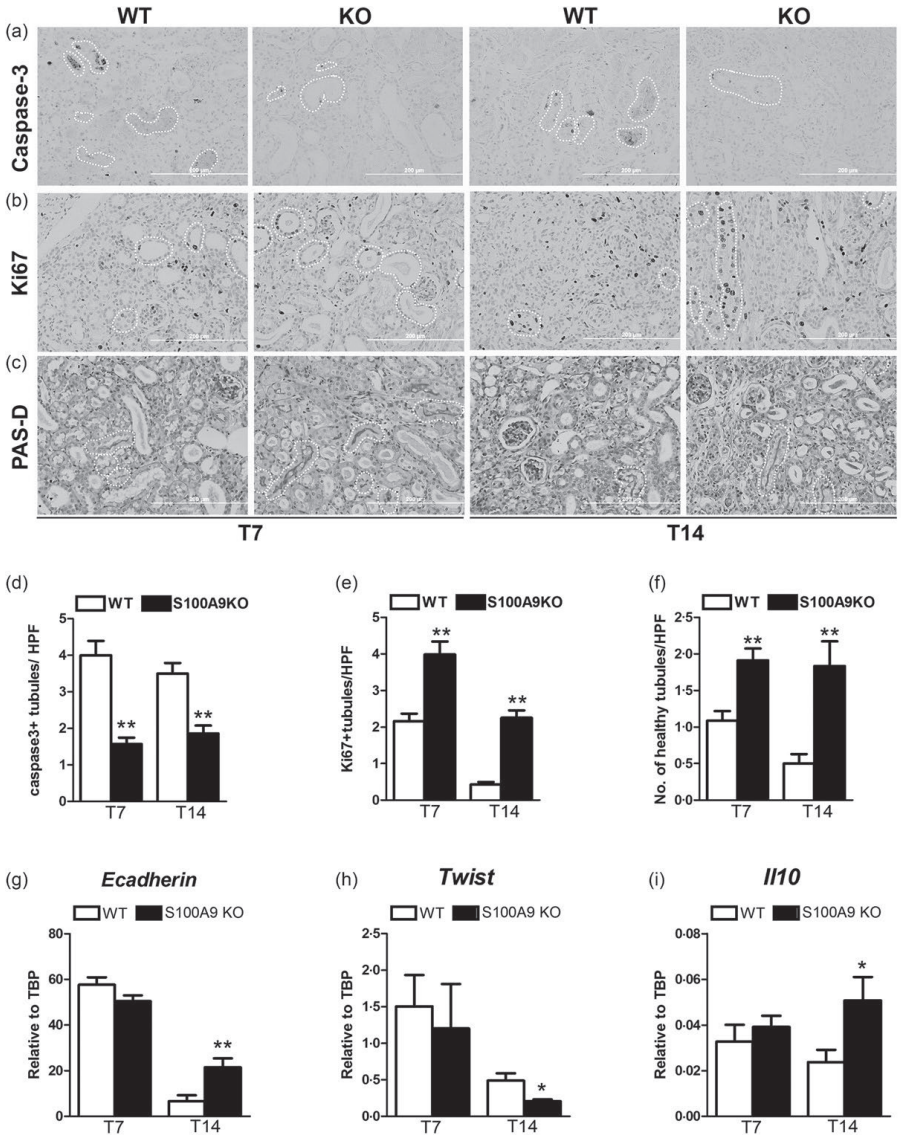

Fig. 4. Tubular injury and epithelial mesenchymal transition (EMT) in wild-type (WT) and S100A9-deficient mice, 7 and 14 days post-unilateral ureteral obstruction (UUO). (a,d) Tubular apoptosis as displayed by representative pictures and quantification of cleaved caspase-3 positive tubules on renal tissue slides from WT and S100A9 knock-out (KO) mice. (b,e) Tubular proliferation as displayed by representative pictures and quantification of Ki-67. No interstitial Ki-67-positive cells were included in the count. (c,f) Periodic acid–Schiff-diastase (PAS-D) staining of renal tissue was used to quantify the number of healthy tubules (by presence of brush border) in WT and S100A9 KO mice 7 and 14 days after UUO. Only tubules surrounding glomeruli were considered for the above analysis. White drawing in the pictures show an example of tubular cells included in the count. The number of caspase-3, Ki67-positive and healthy tubular epithelial cells (TECs) (measured by PAS-D) were counted in 10 non-overlapping high-power fields (HPFs), having glomerular cells as reference, in a blind manner, with a ×40 magnification. (g–i) Transcript expression of *E-cadherin*, *Twist* and *Il10* measured by reverse transcriptase–polymerase chain reaction (RT–PCR) in WT and S100A9 KO, 7 and 14 days upon UUO. Values are normalized to the housekeeping gene Tbp. The Mann–Whitney *U*- test was used for comparison between two groups; $n = 7/8$ mice per group. Graph data are expressed as mean ± standard error of the mean (s.e.m.). $^{*}P < 0{\cdot}05$, $^{**}P < 0{\cdot}005$, *versus* WT at the same time-point. Scale bar 200 μm.

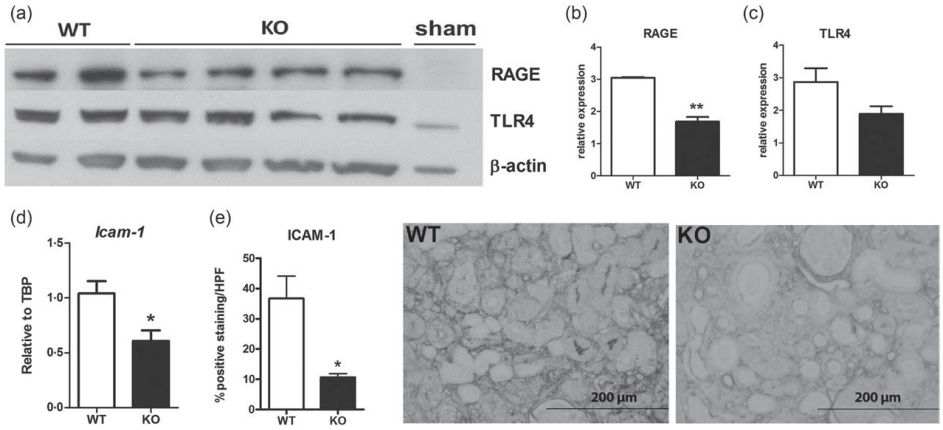

Fig. 5. Expression of S100A8/A9 receptors, Toll-like receptor (TLR)-4 and receptor for advanced glycation end-products (RAGE). (a–c) Expression of RAGE and TLR-4 protein measured by Western blot. Quantification of RAGE and TLR-4 in wild-type (WT) ($n = 2$) and knock-out (KO) ($n = 4$) kidney lysates from day 14 after unilateral ureteral obstruction (UUO). Values were normalized to the levels of β-actin. Statistical difference were analysed by two-tailed Student's *t*-test. (d,e) Intercellular adhesion molecule 1 (ICAM-1) transcript and protein expression as measured by reverse transcriptase–polymerase chain reaction (RT–PCR)and immunohistochemistry (IHC), respectively, in tissue of WT and KO mice, 14 days after UUO; $n = 5$ mice per group. (e) Representative pictures of ICAM-1 IHC. Percentage of positive staining was measured by ImageJ software. The Mann–Whitney *U*-test was used for comparison between these groups. Graph data are mean ± standard error of the mean (s.e.m.). $^{*}P < 0{\cdot}05$, $^{**}P < 0{\cdot}005$ *versus* WT. Scale bar 200 μm.

in E-cadherin decrease, which was also confirmed in a polarized cellular system of TECs (Fig. 6a and Supporting information, Fig. S2). Moreover, rS100A8/A9 affects not only cell–cell junction, but the expression of mitotic cyclin B1 (Fig. 6a), the latter suggesting a proliferation arrest. Of note, the cell-cycle arrest did not induce full EMT in TECs, measured by expression of α-SMA (data not shown).

To study whether extracellular S100A8/A9 can affect cell death, TECs were stimulated with increasing concentrations of rS100A8/A9 and apoptosis/necrosis was measured by FACS analysis with annexin V/PI staining. S100A8/A9 induced late apoptosis/necrosis in TECs, as shown by an increased percentage of PI/annexin V^+ cells in a concentration-dependent manner (Fig. 6b). This cytotoxic effect of S100A8/A9 was not reversed by treatment with a Pan-caspase inhibitor Q-VD-OPh hydrate (QVD), suggesting that S100A8/A9 induces a caspase-independent cell death, most probably necrosis, as observed by PI uptake (Fig. 6c). In support of this observation, we found that caspase-3 activity was not affected by incubation with rS100A8/A9 or upon ligand activation of TLR-4 or RAGE receptor (Supporting information, Fig. S3).

However, to further mimic a UUO-like model *in vitro*, we co-stimulated cells with rTGF-β1 and rS100A8/A9 and evaluated the effect on TEC cell death. Surprisingly, we noticed that the fibrotic trigger in combination with S100A8/A9 leads to increased early apoptosis and not necrosis, as observed by increased annexin V^+ cells (Fig. 6d).

Altogether, these *in-vitro* data indicate that S100A8/A9 induces polarity changes in TECs which might disrupt the interaction between epithelial cells, driving subsequent cell death and tubular atrophy during progressive renal fibrosis.

Discussion

CKD is a pathological condition with different aetiologies characterized by a progressive loss of nephrons and renal fibrosis. Treatments to prevent renal fibrosis still rely upon regimes targeting the underlying disease processes, such as diabetes and hypertension [1]. Identifying novel targets which delay, arrest or reverse the progression of tissue fibrosis may lead to treatment opportunities for patients suffering from CKD. Increasing evidence suggests that DAMPs released during tissue injury, together with the innate immune receptors involved in their recognition [9], contribute to the development of renal fibrosis [10,11]. However, the role of the damage molecule S100A8/A9 in the pathogenesis of obstructive nephropathy has not yet been unravelled. This study provides evidence that S100A8/A9 protein may emerge as a target for novel therapeutic interventions to preserve parenchymal integrity

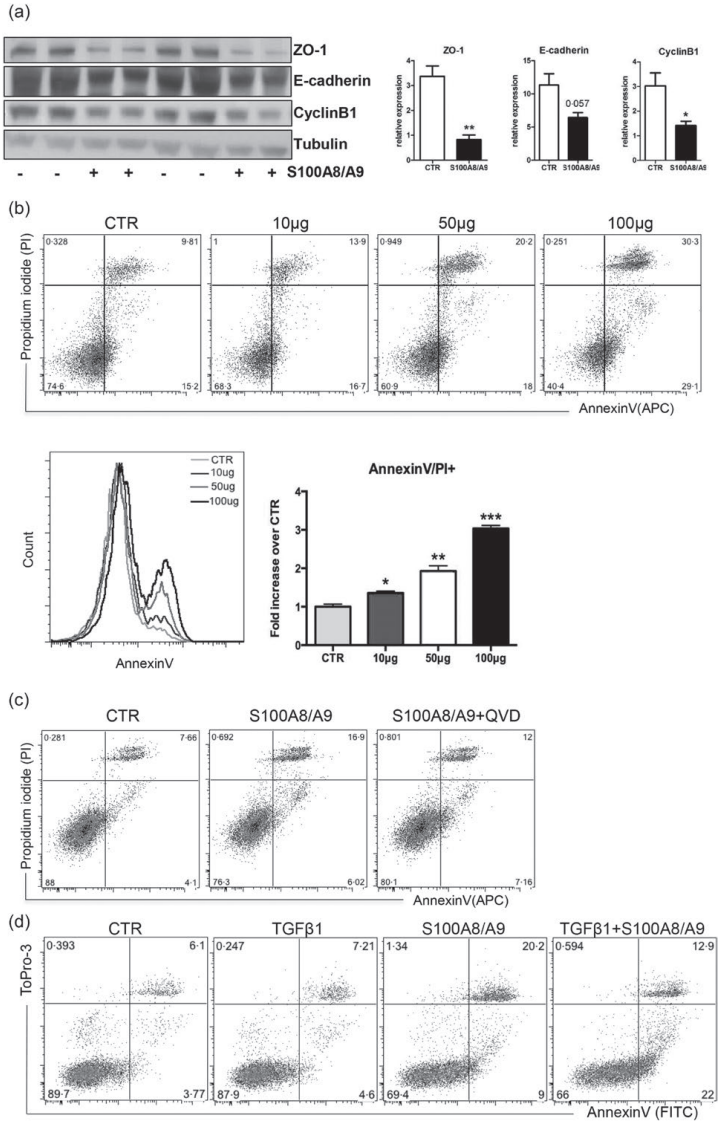

Fig. 6. Effect of extracellular S100A8/A9 on tubular epithelial cells. (a) Western blot analysis of primary tubular epithelial cells (TECs) isolated from four wild-type WT) mice (Charles River) and stimulated with a low concentration of rS100A8/A9 (5 µg/ml) for 24 h in HK2 medium. Protein expression of ZO-1, E-cadherin and cyclin B1 are calculated relatively to the levels of tubulin. (b) Fluorescence activated cell sorter (FACS) plots and histograms relative to cell death measured by annexin V/propidium iodide (PI) staining in stimulated immortalized proximal TEC (IM-PTEC) cells with S100A8/A9 (10, 50 and 100 µg/ml) for 24 h in hexokinase 2 (HK2) medium. The percentage of late apoptotic cells/necrotic (double-positive) are showed in the graph. (c) Representative plots of IM-TEC stimulated with S100A8/A9 (50 µg/ml) in the presence or absence of the Q-VD-OPh hydrate (ApexBio), a pan-caspase inhibitor (20 µM). (d) Representative plots of IM-TEC stimulated with rS100A8/A9 (100 µg/ml) and/or recombinant human transforming growth factor (rhTGF)-β1 (20 ng/ml). Cells were treated for 24 h and harvested for annexin V/PI or To-Pro3 staining. FACS data are representative of three independent experiments. Statistical difference were analysed by two-tailed Student's *t*-test. Data are expressed as mean ± standard error of the mean (s.e.m.). $^{*}P < 0{\cdot}05$, $^{**}P < 0{\cdot}005$, $^{***}P < 0{\cdot}0005$ versus unstimulated control.

as chronic fibrotic disease progresses. We found that S100A8/A9 mediates renal fibrosis, activation of critical molecular events in EMT and tubular apoptosis independently of leucocyte infiltration in the kidney after UUO. *In vitro*, we showed that S100A8/A9 has a deleterious effect on TEC morphology, by inducing loss of cell junction proteins and arrest of cell proliferation, possibly driving subsequent irreversible tubular damage. These changes in tubular morphology result eventually in cell death by apoptosis, when S100A8/A9 is combined with a pro-fibrotic trigger such as TGF-β1.

S100A8/A9 is a critical player during inflammatory responses [32]. Previous studies have shown that, in human diseases, S100A8/A9 can be detected in serum, aspirates or faeces of patients with rheumatoid arthritis [33], acute rejection [34,35], inflammatory bowel disease [36], lung disease [37], systemic sclerosis [38] and atherosclerosis [39]. In the context of renal fibrosis, we are the first to show that S100A8/A9 expression is increased in patients with obstructive nephropathy and localizes uniquely to interstitial granulocytes and not to other parenchymal cells, such as epithelial cells [40]. These human findings were corroborated by the experimental data where we observed increased expression of S100A8/A9 in WT mice following UUO, and its localization was similar to that observed in human samples. Despite similar experimental conditions, Fujiu *et al.* [27], showed that S100A8/A9 expression is high in collecting duct cells and that expression peaks at day 1 post-UUO, whereas in our experiment S100A8/A9 seems to be expressed mainly by granulocytes and only with a low percentage in collecting duct cells, with a peak at day 14 post-UUO. These contrasting results may be related to differences in the technical method used to identify these cells. We performed immunohistochemical staining, whereas Fujiu *et al*. looked at the transcript expression of sorted cells from UUO kidney. The results of two techniques may not be fully comparable, as protein and mRNA might have discordant results in similar pathological conditions [41].

Although we detected S100A8/A9 expression mainly on infiltrating granulocytes, mice lacking S100A9 displayed similar granulocyte numbers compared to WT mice, as shown previously by our group in the acute model of injury [21], suggesting a limited role of S100A8/A9 in granulocyte infiltration in both acute and chronic models of renal injury. Nonetheless, the role of granulocytes in the progression of renal fibrosis is not as pronounced as the role of macrophages [42]. Instead, the latter play a pivotal role in the development of tubulo-interstitial injury, due to the activation of an excessive inflammatory response [26,43]. Previously, in renal ischaemia reperfusion (IR), we showed a beneficial role of S100A8/A9 in controlling macrophage-mediated renal repair by preventing excessive M2 polarization and renal fibrosis [21]. Supporting this study, Rekers *et al*. showed that high levels of S100A8/A9 correlated with improved graft outcome after kidney transplantation [35]. Thus, we hypothesized that S100A8/A9 would dampen macrophage-induced inflammation and the development of renal fibrosis following UUO. Surprisingly, in sharp contrast to the results obtained in renal IR and allograft rejection, we found that S100A9 KO mice were protected against renal fibrosis, independently of the activation of the inflammatory response, macrophage infiltration and polarization, which suggests a deleterious role for S100A8/A9 in renal fibrogenesis.

In the UUO model, one study demonstrated that Klf5 controls macrophage polarity via S100A8/A9, thereby controlling tissue remodelling and limiting fibrosis [27]. These findings were obtained in mice aploinsufficient for Klf5 which, although not specific for S100A8/A9, is known to regulate other cellular processes such as growth and differentiation [27]. Apparently, S100A8/A9 is a beneficial player in the progression of acute renal disease, but shows contrasting results in the context of obstructive nephropathy. We speculate that in the renal IR model the functional S100A8/A9 signalling in non-parenchymal cells is necessary to recognize the initial damage from ischaemic cells and initiate a proper wound-healing response from macrophages. Indeed, the aberrant innate immune response observed in the KO animals after IR may be responsible for an altered wound-healing process with progression to renal fibrosis.

If S100A8/A9 protein reduces the risk of maladaptive renal repair following renal IR, low levels of the protein during the progression of renal fibrosis may prevent perpetuation to irreversible damage. This dual role of S100A8/A9 might be dependent upon the primary insult driving the progression of renal fibrosis. In the UUO model, S100A8/A9 signalling in immune cells seems to be dispensable for the progression of renal fibrosis, as demonstrated in mice over-expressing S100A12/A8/A9 specifically in myeloid cells and subjected to UUO ligation. These mice displayed no differences in interstitial inflammation and fibrosis/tubular atrophy in the kidney, suggesting a dispensable role for inflammatory cell-associated S100A8/A9 in renal fibrosis [44]. Interestingly, similar to our study, a study on cardiac fibrosis, showed that inhibition of S100A8/A9 via a neutralizing antibody suppressed angiotensin II (AngII)-induced perivascular and interstitial fibrosis [45].

This would suggest that, in the absence of S100A8/A9, other DAMPs are released during chronic damage which

may compensate for the activation of the inflammatory response. S100A8/A9 signals via RAGE and TLR-4. Mice deficient for both receptors show a phenotype similar to that of S100A9 KO mice, namely decreased fibrosis independently of leucocyte infiltration and reduced nuclear factor kappa B (NF-κB) activation [17]. Thus, it appears that S100A8/A9 and its interacting receptors modulate the extent of fibrosis via pathological mechanisms activated in parenchymal cells, instead of regulating the inflammatory response [46]. Hence, blocking DAMPs might be a great alternative for targeting the multiple receptors associated with immunopathology, as it will not hinder pathogen detection.

Following UUO, TECs become injured and start to lose their functionality. As a survival mechanism, TECs start an EMT programme with myofibroblast recruitment and subsequent collagen deposits [2,47]. S100A9 KO mice displayed decreased recruitment of myofibroblasts, collagen deposits and pro-fibrotic mediators, suggesting that injury was contained in TECs, as the inflammatory compartment was unaffected. Indeed, S100A9KO mice displayed improved renal function and decreased tubular injury, which resulted in decreased activation of critical EMT steps in TECs. Among S100A8/A9 receptors, RAGE and its interacting receptor ICAM-1 have been shown to mediate renal fibrosis via the loss of epithelial cell integrity and by modulating cellular apoptosis [17]. Other members of the S100 family are known to trigger cell death in cancer cells by binding to RAGE [48]. Expression of RAGE and its interacting receptor ICAM-1 was dampened in the absence of S100A9 after UUO. However, more experiments are needed to ascertain whether S100A8/A9-mediated tubular injury and renal fibrosis may be dependent upon the RAGE-ICAM-1 interaction. Our data argue in favour of a possible involvement.

Finally, we explored the mechanism by which S100A8/A9 may contribute to tubular injury and fibrosis. We found that tubular epithelial cell lines stimulated with low concentrations of rS100A8/A9 displayed down-regulation of tight junction protein ZO-1 and adhesion molecule E-cadherin, together with cell-cycle arrest. Extracellular S100A8/A9 can affect cell growth and have cytotoxic/apoptotic effects on different cell types in a dose-dependent manner [30,31,49,50]. Our results are in unison with these studies, as a high concentration of rS100A8/A9 induced a caspase-independent cell death in TECs, most probably necrosis. However when rS100A8/A9 is combined with a pro-fibrotic trigger, tubular apoptosis is pronounced. Increasing evidence describes a relationship between cell-cycle arrest and renal fibrosis [51]. The reduction of fibrosis observed in S100A9 KO mice may be explained partially by the decreased tubular apoptosis and destruction.

We believe that treatment with recombinant protein induces dissolution of the cell–cell junction, which is essential for maintaining tubular structure and may lead to cell death by necrosis. Consistent with our results, S100A8/A9 was shown to induce loss of endothelial cell contact which triggered subsequent cell death, not exclusively via the apoptotic pathway [30]. However, during progression of fibrosis, S100A8/A9 affects mainly tubular apoptosis, as confirmed *in vivo* and *in vitro*.

In conclusion, our study demonstrates that S100A8/A9 mediates tubular apoptosis and renal fibrosis presumably through the loss of TECs contacts and activation of EMT transition steps. Targeting the TLR-4 and RAGE shared ligand, S100A8/A9, could be a therapeutic strategy to halt renal fibrosis and parenchymal damage in patients with CKD.

Acknowledgements

The authors would like to acknowledge Angelique Scantlebery for proof-reading the paper. This work was supported further by the Dutch Kidney Foundation and the Netherlands Organization for Health Research and Development (ZonMw) to M. D. (Meer Kennis met Minder Dieren; no. 114024040) and J. C. L. (Vidi #91712386), (ASPASIA no. 015.008.044).

Disclosure

The authors declare no potential conflicts of interest to disclose.

References

1 Rockey DC, Bell PD, Hill JA. Fibrosis: a common pathway to organ injury and failure. N Engl J Med 2015;**372**:1138–49.

2 Lovisa S, LeBleu VS, Tampe B *et al*. Epithelial-to-mesenchymal transition induces cell cycle arrest and parenchymal damage in renal fibrosis. Nat Med 2015;**21**:998–1009.

3 Lovisa S, Zeisberg M, Kalluri R. Partial epithelial-to-mesenchymal transition and other new mechanisms of kidney fibrosis. Trends Endocrinol Metab 2016;**27**:681–95.

4 Vogl T, Ludwig S, Goebeler M *et al*. MRP8 and MRP14 control microtubule reorganization during transendothelial migration of phagocytes. Blood 2004;**104**:4260–8.

5 Lackmann M, Rajasekariah P, Iismaa SE *et al*. Identification of a chemotactic domain of the pro-inflammatory S100 protein CP-10. J Immunol. 1993;**150**:2981–91.

6 Simard J-C, Cesaro A, Chapeton-Montes J *et al*. S100A8 and S100A9 induce cytokine expression and regulate the NLRP3 inflammasome via ROS-dependent activation of NF-κB1. PLOS ONE 2013;**8**:e72138.

7 Donato R. Intracellular and extracellular roles of S100 proteins. Microsc Res Tech 2003;**60**:540–51.

8 Donato R, Cannon BR, Sorci G *et al.* Functions of S100 proteins. Curr Mol Med 2013;**13**:24–57.

9 Matzinger P. Tolerance, danger, and the extended family. Annu Rev Immunol 1994;**12**:991–1045.

10 Leemans JC, Kors L, Anders H-J, Florquin S. Pattern recognition receptors and the inflammasome in kidney disease. Nat Rev Nephrol 2014;**10**:398–414.

11 Anders H-J, Schaefer L. Beyond tissue injury-damage-associated molecular patterns, toll-like receptors, and inflammasomes also drive regeneration and fibrosis. J Am Soc Nephrol 2014;**25**:1387–400.

12 Johnson GB, Brunn GJ, Platt JL. Activation of mammalian toll-like receptors by endogenous agonists. Crit Rev Immunol. 2003;**23**:15–44.

13 Vogl T, Tenbrock K, Ludwig S *et al.* Mrp8 and Mrp14 are endogenous activators of toll-like receptor 4, promoting lethal, endotoxin-induced shock. Nat Med 2007;**13**:1042–9.

14 Ehlermann P, Eggers K, Bierhaus A *et al.* Increased proinflammatory endothelial response to S100A8/A9 after preactivation through advanced glycation end products. Cardiovasc Diabetol 2006;**5**:6.

15 Narumi K, Miyakawa R, Ueda R *et al.* Proinflammatory proteins S100A8/S100A9 activate NK cells via interaction with RAGE. J Immunol 2015;**194**:5539–48.

16 Yiu WH, Lin M, Tang SCW. Toll-like receptor activation: from renal inflammation to fibrosis. Kidney Int 2014;**4**:20–5.

17 Gasparitsch M, Arndt A-K, Pawlitschek F *et al.* RAGE-mediated interstitial fibrosis in neonatal obstructive nephropathy is independent of NF-κB activation. Kidney Int 2013;**84**:911–9.

18 Pulskens WP, Rampanelli E, Teske GJ *et al.* TLR4 promotes fibrosis but attenuates tubular damage in progressive renal injury. J Am Soc Nephrol 2010;**21**:1299–308.

19 Tammaro A, Stroo I, Rampanelli E *et al.* Role of TREM1-DAP12 in renal inflammation during obstructive nephropathy. PLOS ONE 2013;**8**:e82498.

20 Passey RJ, Williams E, Lichanska AM *et al.* A null mutation in the inflammation-associated S100 protein S100A8 causes early resorption of the mouse embryo. J Immunol 1999;**163**:2209–16.

21 Dessing MC, Tammaro A, Pulskens WP *et al.* The calcium-binding protein complex S100A8/A9 has a crucial role in controlling macrophage-mediated renal repair following ischemia/reperfusion. Kidney Int 2015;**87**:85–94.

22 Stokman G, Kers J, Yapici Ü *et al.* Predominant tubular interleukin-18 expression in polyomavirus-associated nephropathy. Transplantation 2016;**100**:e88–95.

23 Pulskens WP, Teske GJ, Butter LM *et al.* Toll-like receptor-4 coordinates the innate immune response of the kidney to renal ischemia/reperfusion injury. PLOS ONE 2008;**3**:e3596.

24 Stokman G, Qin Y, Genieser H-G *et al.* Epac-rap signaling reduces cellular stress and ischemia-induced kidney failure. J Am Soc Nephrol 2011;**22**:859–72.

25 Bascands J-L, Schanstra JP. Obstructive nephropathy: insights from genetically engineered animals. Kidney Int 2005;**68**:925–37.

26 Meng X-M, Nikolic-Paterson DJ, Lan HY. Inflammatory processes in renal fibrosis. Nat Rev Nephrol 2014;**10**:493–503.

27 Fujiu K, Manabe I, Nagai R. Renal collecting duct epithelial cells regulate inflammation in tubulointerstitial damage in mice. J Clin Invest 2011;**121**:3425–41.

28 Lamouille S, Xu J, Derynck R. Molecular mechanisms of epithelial-mesenchymal transition. Nat Rev Mol Cell Biol 2014;**15**:178–96.

29 Jin Y, Liu R, Xie J, Xiong H, He JC, Chen N. Interleukin-10 deficiency aggravates kidney inflammation and fibrosis in the unilateral ureteral obstruction mouse model. Lab Invest 2013;**93**:801–11.

30 Viemann D, Barczyk K, Vogl T *et al.* MRP8/MRP14 impairs endothelial integrity and induces a caspase-dependent and -independent cell death program. Blood 2007;**109**:2453.

31 Viemann D, Strey A, Janning A *et al.* Myeloid-related proteins 8 and 14 induce a specific inflammatory response in human microvascular endothelial cells. Blood 2005;**105**:2955–62.

32 Pruenster M, Vogl T, Roth J, Sperandio M. S100A8/A9: From basic science to clinical application. Pharmacol Ther 2016;**167**:120–31.

33 Perera C, McNeil HP, Geczy CL. S100 Calgranulins in inflammatory arthritis. Immunol Cell Biol 2010;**88**:41–9.

34 Eikmans M, Roos-van Groningen MC, Sijpkens YW *et al.* Expression of surfactant protein-C, S100A8, S100A9, and B cell markers in renal allografts: investigation of the prognostic value. J Am Soc Nephrol 2005;**16**:3771–86.

35 Rekers NV, Bajema IM, Mallat MJK *et al.* Beneficial immune effects of myeloid-related proteins in kidney transplant rejection. Am J Transplant 2016;**16**:1441–55.

36 Ikhtaire S, Shajib MS, Reinisch W, Khan WI. Fecal calprotectin: its scope and utility in the management of inflammatory bowel disease. J Gastroenterol 2016;**51**:434–46.

37 Kuipers MT, Vogl T, Aslami H *et al.* High levels of S100A8/A9 proteins aggravate ventilator-induced lung injury via TLR4 signaling. PLOS ONE 2013;**8**:e68694.

38 Xu X, Wu W, Tu W *et al.* Increased expression of S100A8 and S100A9 in patients with diffuse cutaneous systemic sclerosis. A correlation with organ involvement and immunological abnormalities. Clin Rheumatol. 2013;**32**:1501–10.

39 Xu X, Wu W-y, Tu W-z *et al.* S100A8 and S100A9 in cardiovascular biology and disease. Arterioscler Thromb Vasc Biol 2013;**32**:1501–229.

40 Henke MO, Renner A, Rubin BK, Gyves JI, Lorenz E, Koo JS. UP-regulation of S100A8 and S100A9 protein in bronchial epithelial cells by lipopolysaccharide. Exp Lung Res 2006;**32**:331–47.

41 Chen G, Gharib TG, Huang C-C *et al.* Discordant protein and mRNA expression in lung adenocarcinomas. Mol Cell Proteomics 2002;**1**:304–13.

42 Höchst B, Mikulec J, Baccega T *et al.* Differential induction of Ly6G and Ly6C positive myeloid derived suppressor cells in chronic kidney and liver inflammation and fibrosis. PLOS ONE 2015;**10**:e0119662.

43 Nikolic-Paterson DJ, Wang S, Lan HY. Macrophages promote renal fibrosis through direct and indirect mechanisms. Kidney Int Suppl 2014;**4**:34–8.

44 Yan L, Mathew L, Chellan B *et al.* S100/Calgranulin-mediated inflammation accelerates left ventricular hypertrophy and aortic valve sclerosis in chronic kidney disease in a receptor for advanced glycation end products-dependent manner. Arterioscler Thromb Vasc Biol 2014;**34**:1399–411.
45 Wu Y, Li Y, Zhang C *et al.* S100a8/a9 released by CD11b+Gr1+ neutrophils activates cardiac fibroblasts to initiate angiotensin II-Induced cardiac inflammation and injury. Hypertension 2014;**63**:1241–50.
46 Leemans JC, Stokman G, Claessen N *et al.* Renal-associated TLR2 mediates ischemia/reperfusion injury in the kidney. J Clin Invest 2005;**115**:2894–903.
47 Grande MT, Sánchez-Laorden B, López-Blau C *et al.* Snail1-induced partial epithelial-to-mesenchymal transition drives renal fibrosis in mice and can be targeted to reverse established disease. Nat Med 2015;**21**:989–97.
48 Jin Q, Chen H, Luo A, Ding F, Liu Z. S100A14 stimulates cell proliferation and induces cell apoptosis at different concentrations via receptor for advanced glycation end products (RAGE). PLoS One 2011;**6**:e19375.
49 Yui S, Mikami M, Tsurumaki K, Yamazaki M. Growth-inhibitory and apoptosis-inducing activities of calprotectin derived from inflammatory exudate cells on normal fibroblasts: regulation by metal ions. J Leukoc Biol 1997;**61**:50–7.
50 Yui S, Nakatani Y, Mikami M. Calprotectin (S100A8/S100A9), an inflammatory protein complex from neutrophils with a broad apoptosis-inducing activity. Biol Pharm Bull 2003;**26**:753–60.
51 Yang L, Besschetnova TY, Brooks CR, Shah JV, Bonventre JV. Epithelial cell cycle arrest in G2/M mediates kidney fibrosis after injury. Nat Med 2010;**16**:535–43.

Supplementary Information

S100A8/A9 promotes parenchymal damage and renal fibrosis in obstructive nephropathy

Alessandra Tammaro[1], Sandrine Florquin[1], Mascha Brok[1], Nike Claessen[1], Loes M. Butter[1], Gwendoline J. D. Teske[1], Onno J. de Boer[1], Thomas Vogl[2], Jaklien C. Leemans[1*] and Mark C. Dessing[1*].

[1]Department of Pathology, Academic Medical Center, University of Amsterdam, Amsterdam, The Netherlands; [2]Institute of Immunology, University of Muenster, Muenster, Germany. * These authors contributed equally.

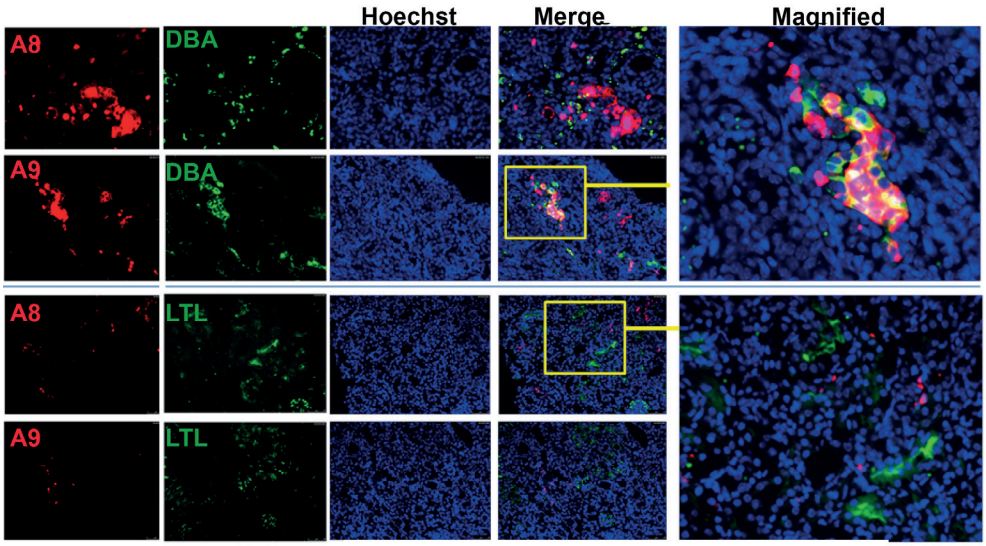

Figure S1: Cellular expression of S100A8/A9 after 14 days of UUO.
Representative pictures of immunofluorescence staining on kidney tissue from WT mice, 14 days post-UUO, with S100A8 or S100A9 (red), DolichosBiflorus Agglutinin (DBA:collecting duct marker) and lotus tetragonolobus lectin (LTL: proximal tubule marker), both in green. Nuclei were stained with Hoechst (blue). S100A8 or S100A9, DBA and Hoechst positive staining are merged (magnification 40X).

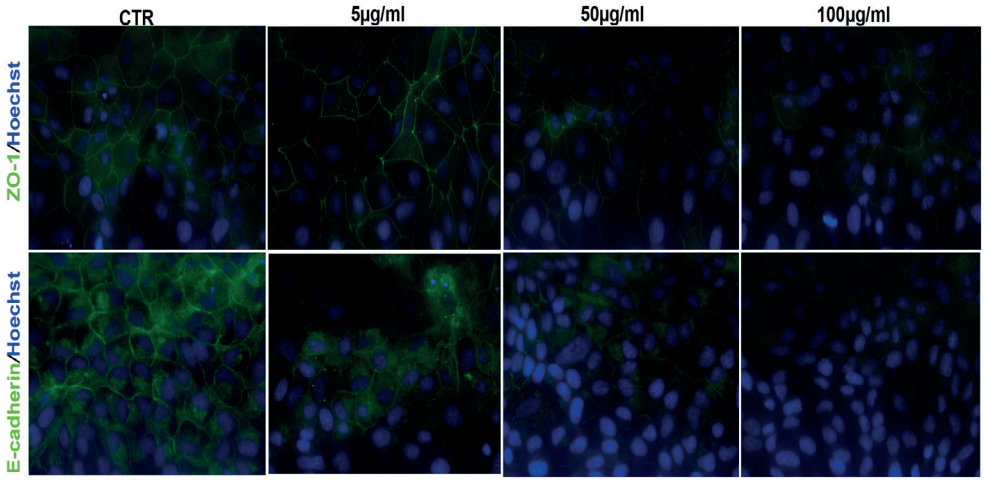

Figure S2: Effect of S100A8/A9 on a polarized system of tubular epithelial cells.
Representative pictures of ZO-1 and E-cadherin immunofluorescence staining of Madin-Darby canine kidney (MDCK) cell line, cultured on collagen-coated coverslip in HK2 medium and stimulated with increasing concentration of rS100A8/A9, for 24 hours. Both primary antibodies were detected with an Alexa-fluor 488 conjugated secondary antibody. Hoechst was used for nuclear staining. Magnification 40X.

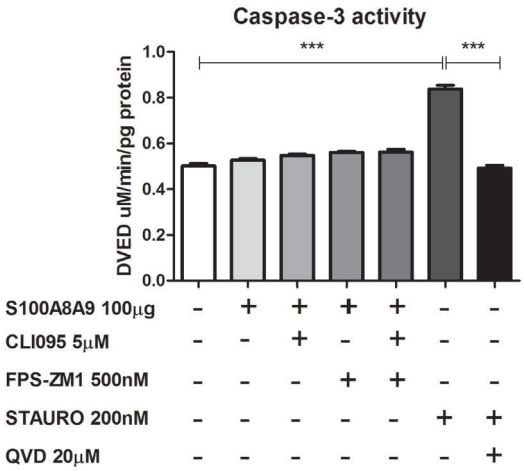

Figure S3: Effect of S100A8/A9 on epithelial cell death after ligand activation.
Caspase-3 enzyme activity measurement by DEVD-AMC cleavage. IM-TECs were stimulated for 24 hours with rS100A8/A9 in presence or not of TLR4 inhibitor (CLI095) and RAGE antagonist (FPSZM-1). Staurosporine (stauro) and a PAN-caspase inhibitor Q-VD-OPh hydrate (QVD) were used as experimental controls. Statistical difference were analyzed by two-tailed student t-test Data are expressed as mean±s.e.m. ***P<0.0005 versus unstimulated control (white bar).

Supplementary Tables

Table S1

RT-PCR primer sequences

TATA-box binding protein (Tbp)	Forward: 5'-GGAGAATCATGGACCAGAACA Reverse: 5'-GATGGGAATTCCAGGAGTCA
C-C motif chemokine ligand 2 (Ccl2)	Forward: 5′-CATCCACGTGTTGGCTCA Reverse: 5′-GATCATCTTGCTGGTGAATGAGT
Interleukin 6 (Il6)	Forward: 5′-GCTACCAAACTGGATATAATGGA Reverse: 5′-CCAGGTAGCTATGGTACTCCAGAA
Tumor necrosis factor a (Tnfa)	Forward: 5′-CTGTAGCCCACGTCGTAGC Reverse: 5′-TTGACATCCATGCCGTTG
E-cadherin	Forward: 5'-CTTCATCGATGAAAACCTGAAG Reverse: 5'-TCGTTCAGATAATCGTAGTCCTG
Twist	Forward: 5'-GGCTCAGCTACGCCTTCTC Reverse: 5'-TCTCTGGAAACAATGACATCTAGG
interleukin 10 (Il10)	Forward: 5'-TTTGAATTCCCTGGGTGAGAA Reverse: 5'-ACAGGGGAGAAATCGATGACA
intercellular adhesion molecule 1 (Icam1)	Forward: 5'-TTCACACTGAATGCCAGCTC Reverse: 5'-GTCTGCTGAGACCCCTCTTG
nitric oxide synthase 2 (Nos2)	Forward: 5'- CCAAGCCCTCACCTACTTCC Reverse: 5'- CTCTGAGGGCTGACACAAGG
Interferon regulatory factor 5 (Irf5)	Forward: 5'- CTTGGCCCATGGCTCCTGCC Reverse: 5'- AGCAACCGGGCTGCAACAGG
Ly6C	Forward: 5'-TCTTGTGGCCCTACTGTGTG Reverse: 5'-GCAATGCAGAATCCATCAGA
Arginase-1(Arg1)	Forward: 5'- CTCCAAGCCAAAGTCCTTAGAG Reverse: 5'- AGGAGCTGTCATTAGGGACATC
Interferon regulatory factor 4 (Irf4)	Forward: 5'- CGGCCAGCACCGAGATTCCA Reverse: 5'- AATGACGGAGGGAGCGGTGG
Mannose receptor C-type 1 (Mrc1)	Forward: 5'-GGACGAGCAGGTGCAGTT Reverse: 5'-CAACACATCCCGCCTTTC
Platelet-derived growth factor (Pdgfa)	Forward: 5'- CCAGCGACTCTTGGAGATAGA Reverse: 5'- GGGCTCTCAGGCTTGTCTC
Collagen-1 (Col1a1)	Forward: 5'- ACCTAAGGGTACCGCTGGA Reverse: 5'- TCCAGCTTCTCCATCTTTGC

Table S2

Antibodies list Western Blot

Antibody	Company
Rabbit polyclonal RAGE	Novusbio
Goat polyclonal TLR4	Santa Cruz
Rabbit polyclonal ZO-1	Thermo
Rabbit polyclonal E-cadherin	Cell signaling
Rabbit polyclonal Cyclin B1	Cell signaling
Rabbit monoclonal β-actin	Merck
Rabbit monoclonal Tubulin	Sigma

Antibodies list IHC

Staining	Antibody	Company
Granulocytes (m)	Rat-anti-mouse Ly6G-FITC	BD pharmigen
Apoptotis	Rabbit-anti-caspase 3 Asp175	Cell signalling
Proliferation	Rabbit-anti-Ki67 Sp6	Neomarkers
Macrophages (m)	Rat-anti-mouse F4/80	BD pharmigen
Myofibroblasts	Mouse-anti-human αSMA clone 1A4	DAKO
Collagen Type-1	Rabbit-polyclonal collagen type 1	Genetex
S100A8, S100A9 (m)	Rat-anti-mouse S100A8, S100A9	R&D
ICAM-1	Goat-anti-ICAM-1	R&D
Macrophages (h)	Mouse-anti-human CD68	DAKO
Granulocytes (h)	Mouse-anti-human CD15	DAKO
S100A8, S100A9 (h)	Mouse anti human S100A8, S100A9	R&D

(m)= mouse; (h)= human

Chapter 4

TREM-1 and its potential ligands in non-infectious diseases: from biology to clinical perspectives

Pharmacology & therapeutics 2017 Sep;177:81-95

Contents lists available at ScienceDirect

Pharmacology & Therapeutics

journal homepage: www.elsevier.com/locate/pharmthera

TREM-1 and its potential ligands in non-infectious diseases: from biology to clinical perspectives

Alessandra Tammaro [a,*], Marc Derive [b], Sebastien Gibot [c,d], Jaklien C. Leemans [a], Sandrine Florquin [a,e], Mark C. Dessing [a]

[a] Department of Pathology, Academic Medical Center, University of Amsterdam, Amsterdam, The Netherlands
[b] INOTREM, Nancy, France
[c] Medical Intensive Care Unit, Hôpital Central, CHU Nancy, Nancy, France
[d] Inserm UMR_S1116, Faculté de Médecine, Université de Lorraine, Nancy, France
[e] Department of Pathology, Radboud University Nijmegen Medical Center, Nijmegen, The Netherlands

ARTICLE INFO

Available online 27 February 2017

Associate Editor: S. Enna

Keywords:
Triggering receptor expressed on myeloid cells-1
TLR/NLR pathway
TREM-1 ligands
Non-infectious inflammatory diseases
TREM-1 inhibitors

ABSTRACT

Triggering receptor expressed on myeloid cells-1 (TREM-1) is expressed on the majority of innate immune cells and to a lesser extent on parenchymal cells. Upon activation, TREM-1 can directly amplify an inflammatory response. Although it was initially demonstrated that TREM-1 was predominantly associated with infectious diseases, recent evidences shed new light into its role in sterile inflammatory diseases. Indeed, TREM-1 receptor and its signaling pathways contribute to the pathology of several non-infectious acute and chronic inflammatory diseases, including atherosclerosis, ischemia reperfusion-induced tissue injury, colitis, fibrosis and cancer. This review, aims to give an extensive overview of TREM-1 in non-infectious diseases, with the focus on the therapeutic potential of TREM-1 intervention strategies herein. In addition, we provide the reader with a functional enrichment analysis of TREM-1 signaling pathway and potential TREM-1 ligands in these diseases, obtained via *in silico* approach. We discuss pre-clinical studies which show that TREM-1 inhibition, via synthetic soluble TREM-1 protein mimickers, is effective in treating (preventing) specific inflammatory disorders, without significant effects on antibacterial response. Further research aimed at identifying specific TREM-1 ligands, in different inflammatory disorders, is required to further unravel the role of this receptor, and explore new avenues to modulate its function.

Contents

Abbreviations: AGA, acute gouty arthritis; AP-1, activator protein-1; BAL, bronchial alveolar lavage; BD, intestinal Behcet's disease; BPAR, biopsy proven acute rejection; CAD, coronary artery disease; CARD, caspase recruitment domain-containing protein; CAT, colitis-associated tumorigenesis; CD, Crohn's disease; CIA, collagen-induced arthritis; DAMPs, damage associated molecular patterns; DGF, delayed graft function; ERK, extracellular signal-regulated; HMGB1, high mobility group box-1; HSP, heat shock proteins; IBD, inflammatory bowel disease; IFTA, interstitial fibrosis/tubular atrophy; IR, ischemia-reperfusion; IRAK, IL-1R-associated kinases; LPS, lipopolysaccharide; MAPK, mitogen-activated protein kinase; Myd88, myeloid differentiation primary response; Nf-κB, nuclear factor-κB; NLR, Nod-like receptor; NOD, nucleotide-binding oligomerization domain; NSCLC, non-small cell lung cancer; PAMPs, pathogen-associated molecular patterns; PBC, peripheral blood cells; PGN, peptidoglycan; PI3K, phosphatidylinositol 3-kinase; PRR, pattern recognition receptors; RA, rheumatoid arthritis; RIP2, receptor-interacting serine/threonine-protein 2; SNV, single nucleotide variants; sTREM-1, soluble TREM-1; TLR, Toll like receptor; TREM-1, triggering receptor expressed on myeloid cells-1; UC, ulcerative colitis; UO, ureteral obstruction.

* Corresponding author at: Academic Medical Center (AMC), University of Amsterdam, Department of Pathology, Room L2–112, Meibergdreef 09, 1105AZ Amsterdam, The Netherlands.
E-mail address: a.tammaro@amc.uva.nl (A. Tammaro).

http://dx.doi.org/10.1016/j.pharmthera.2017.02.043

1. Introduction

Innate immune cells are key players in the recognition of invading pathogens or alarming the host during tissue damage. The magnitude of inflammation relies on the activation of pattern recognition receptors (PRR). One family of PRRs is the family of Toll-like receptors (TLRs), which are well known for their role in innate immunity during infectious and non-infectious diseases. More recently, another family of innate immune receptors was described to interact with TLRs and influence the extent of the inflammatory response: the triggering receptors expressed on myeloid cells (TREMs) (Arts, Joosten, van der Meer, & Netea, 2012; Klesney-Tait, Turnbull, & Colonna, 2006). The TREM-family comprises both activating and inhibitory receptors. Among these family members, TREM-1 represent the most studied activating receptor, whereas TREM-2 is widely known as an inhibitor of the inflammatory response. Activation of TREM-1 is known to trigger and amplify inflammation, especially through synergism with TLR signaling. Early after the discovery of TREM-1, it was believed that TREM-1 was merely involved in non-infectious diseases, and research was mainly focused on TREM-pathogen interaction as described in several elegant reviews (Gibot, 2005, 2006; Roe, Gibot, & Verma, 2014; Sharif & Knapp, 2008). However, more recent research shows that TREM-1 is also involved in non-infectious diseases and this review aims to give an overview of the expression, and function of TREM-1 receptor and its ligands herein. Moreover, intervention studies that examined TREM-1 receptor modulation in non-infectious diseases, were included. Lastly, because several research questions regarding the TREM-1 ligand and pathway synergism, are still unanswered, we performed an *in silico* analysis of putative TREM1-ligand expression and pathway enrichment in several sterile inflammatory diseases.

2. TREM-1 signaling pathway

2.1. TREM-1 pathway

First experiments performed by Colonna and colleagues showed that TREM-1 is mainly expressed on myeloid cells such as monocytes/macrophages and granulocytes. However, ongoing research shows that during inflammation, TREM-1 is also detected on parenchymal cell types such as bronchial, corneal, gastric epithelial cells, and hepatic endothelial cells (Barrow et al., 2004; Chen, Laskin, Gordon, & Laskin, 2008; Rigo et al., 2012; Schmausser et al., 2008). TREM-1 is present in 2 forms: as a membrane-bound receptor and as soluble protein (Figs. 1 and 2). Membrane TREM-1 features 3 distinct domains: an Ig-like structure (most likely responsible for ligand binding), a transmembrane part and a cytoplasmic tail which associates with the adaptor molecule TYROBP (TYRO protein tyrosine kinase-binding protein, more frequently called DAP12: DNAX activating protein of 12 kDa) (Colonna, 2003). This complex is stabilized through a unique electrostatic interaction between a negatively charged (−) aspartic acid in DAP12, and a positively charged (+) lysine in TREM-1 intracytoplasmic tail, which is necessary for signal transduction. Following TREM-1 engagement, the cytoplasmic part of DAP12 containing ITAMs (Immunoreceptor tyrosine-based activation motif) becomes phosphorylated at its tyrosine residue, providing a docking site for protein tyrosine kinases: ZAP70 (Zeta-chain-associated protein kinase 70) and SYK (Spleen Tyrosine Kinase). SYK promotes the recruitment and tyrosine phosphorylation of adaptor complexes that contain Cbl (Casitas B-lineage Lymphoma), SOS (Son of sevenless) and GRB2 (Growth Factor Receptor Binding Protein-2), which results in downstream signal transduction through PI3K, PLC-Gamma (Phospholipase-C-Gamma) and the ERK pathways. These pathways induce Ca^{2+} mobilization, rearrangement of the actin cytoskeleton and activation of transcription factors such as Elk1 (ETS domain-containing protein), NFAT (Nuclear Factor of Activated T-Cells), AP1, c-Fos, c-Jun and Nf-κB, which transcribe genes that encode pro-inflammatory cytokines, chemokines and cell-surface molecules. In addition, TREM1-induced PI3K and ERK pathway activation can promote mitochondrial integrity and cell survival by inactivating pro-apoptotic factors: BID (BH3-Interacting Domain Death agonist), BAD (BCL-2-Antagonist of cell Death) and BAX (BCL-2-Associated X-Protein) and inhibiting CytoC (Cytochrome-C) release from mitochondria (Yuanet al., 2014, 2016).

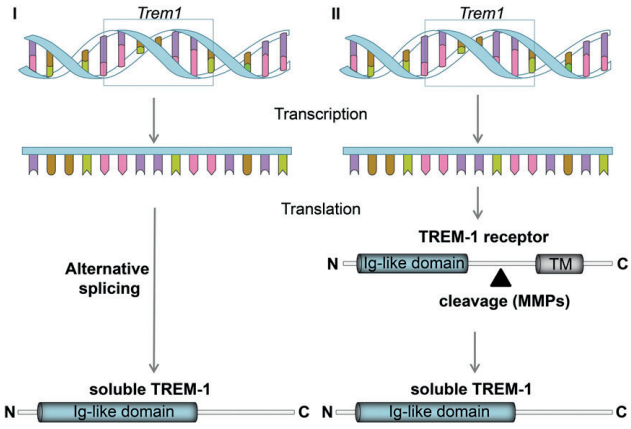

Fig. 1. TREM-1 receptor and soluble protein regulation. Graphical representation of the two hypotheses of soluble TREM-1 protein (*s*TREM-1) origins. Upon transcription, alternative splicing of the *Trem1* gene can result in the synthesis of a smaller protein, which contains only the immuoglobulin-like domain (Ig-like domain). This protein is referred to as sTREM-1 (I: left). The canonical translation process produces the TREM-1 receptor protein, which consists of the Ig-like domain and a transmembrane domain (TM). This receptor, upon proteolytic cleavage by metalloproteinases (MMPs), results in sTREM-1 protein generation (II: right).

Besides the membrane receptor, a soluble form of TREM-1 (sTREM-1) has been described (Klesney-Tait et al., 2006). Although the origin and function of sTREM-1 are still elusive, its relevance as both biomarker and therapeutic target is high, in both sterile and infectious disease settings. In terms of molecular structure, sTREM-1 lacks the transmembrane and intracellular domain; hence its lack of signal transduction properties. It exhibits the extracellular part of the receptor (Ig-like domain), also known as ectodomain, proposed as the site responsible for ligand binding. The firsts to propose the origin of sTREM-1 were Gingras et al., who described an alternatively spliced form of TREM-1 (TREM-1sv) (Gingras, Lapillonne, & Margolin, 2002). The protein produced in this case was 17.5 kDa in size, compared to the typical 27 kDa of TREM-1 membrane receptor. This isoform was isolated from CD34+ bone marrow cells and mature monocytes. Consistent with this study, a novel splice variant of TREM-1 was recently described in human neutrophil granules (Baruah et al., 2015). This isoform, with a molecular weight of 15 kDa, was isolated from the α and β neutrophil fractions, rich in primary and secondary granules, respectively. According to Baruah et al. the release of TREM-1sv may modulate the inflammatory response by inhibiting neutrophil migration regulated from membrane TREM-1, and by acting as a decoy receptor in the circulation (Baruah et al., 2015). Beside the splice variant hypothesis, another theory has emerged, which postulate that the proteolytic cleavage of membrane bound receptor by metallo-proteinases (MMPs) is an alternative source of sTREM-1. Monocytes treated with Lipopolysaccharide (LPS) in the presence of a metalloproteinases inhibitor displayed increased expression of the membrane receptor while sTREM-1 levels decreased (Gomez-Pina et al., 2007). Thus far, the main function of sTREM-1 appears to be the neutralization of TREM-1 inflammatory activity (Roe et al., 2014). Once secreted, sTREM-1 can be detected in biological fluid, during infection or inflammation. In sterile

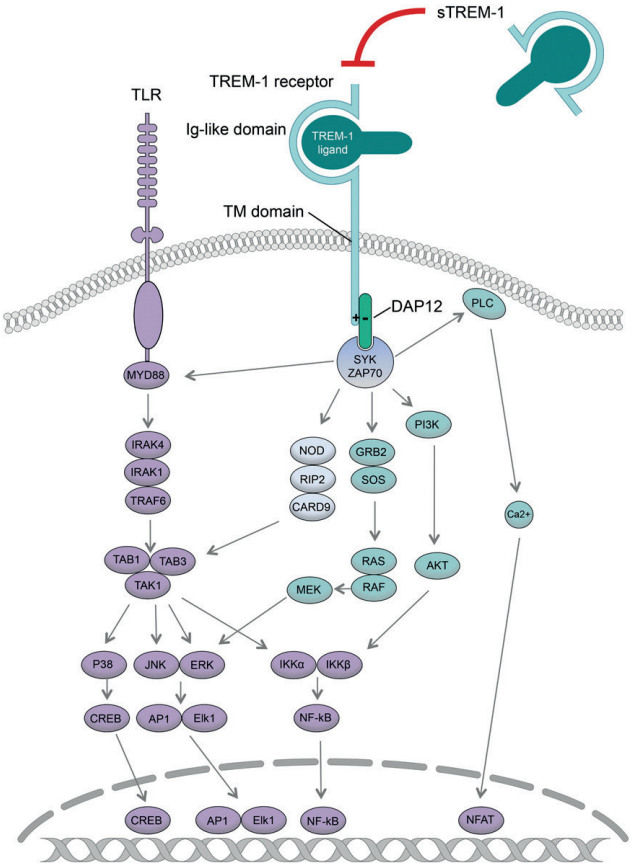

Fig. 2. TREM-1/TLR/sTREM-1 pathway interaction. Schematic illustration of TREM-1, TLR and NLR combined signaling pathways. TREM-1 belongs to the immunoglobulin superfamily of receptors and is located on the plasma membrane. The Immunoglobulin-like (Ig) domain, in the extracellular part, is responsible for ligand binding, while the transmembrane (TM) domain associates with the adaper molecule DAP12. Upon binding to DAP12, the protein tyrosine kinases SYK and ZAP70 are recruited, leading to the activation of PLC, PI3K and ERK pathways, upstream regulators of inflammatory gene transcription. The tyrosine kinases SYK/ZAP70 can also activate the NLR pathway, which will merge with the TLR pathway, initiated by Myd88. The TREM-1 pathway can synergize with the TLR pathway (in) dependently of Myd88. Engagement of Myd88 stimulates downstream signaling pathways that involve IRAKs and another family of adaptor molecules, namely TNF receptor-associated factors (TRAFs). This leads to the activation of the MAPKs, Janus N-terminal kinase (JNK) and p38, as well as the activation of transcription factors. The main families of transcription factors that are activated downstream of TLR signaling, are NF-κB, cyclic AMP-responsive element-binding protein (CREB), AP, and Elk, responsible for the transcription of proinflammatory cytokines and chemokines. sTREM-1 by scavenging TREM-1 ligand is able to inhibit the perpetuation of this inflammatory pathway.

inflammation, sTREM-1 has been described to increase during renal IR, chronic kidney disease patients on hemodialysis, myocardial infarction, inflammatory bowel disease, acute gouty inflammation and rheumatoid arthritis, suggesting the potential for biological activity of the soluble receptor (Table 1). However, the biological relevance of sTREM-1 in sterile inflammation is still unclear in contrast to its significance as predictor of infection and inflammation in infectious diseases. Whether sTREM-1 may be a novel biomarker candidate, experiments to unveil its function in sterile inflammation are necessary.

2.2. TREM-1-TLR connection

TLRs are PRRs that recognize distinct pathogen-associated molecular patterns (PAMPs) that play a critical role in innate immune responses. The fact that TLRs also recognize endogenous ligands released after sterile tissue injury (called damage-associated molecular patterns; DAMPs) led to new mechanistic insights on the role of TLRs in the induction of inflammation. Activation of TLRs leads to association of the cytoplasmic Toll/IL-1 receptor (TIR) domain with a TIR domain-containing adaptor, MyD88 that recruits

Table 1.
(Soluble) Trem-1 expression in mice and human.

		Expression upon inflammation *vs* control **1) Soluble form, 2) Circulating leukocytes, 3) Tissue**	
Location	**Model/Disease**	**Mouse**	**Human**
Circulation	Atherosclerosis	1. Increased during high cholesterol/high fat diet (Joffre, Potteaux, et al., 2016; Zysset et al., 2016) 2. Enhanced expression on myeloid cells after high cholesterol/high fat diet (Joffre, Potteaux, et al., 2016; Zysset et al., 2016) 3. Enhanced mRNA in aortic arch after high cholesterol/high fat diet (Zysset et al., 2016)	1. n.d. 2. Enhanced expression on monocytes with oxLDL (Joffre, Potteaux, et al., 2016; Zysset et al., 2016) 3. Enhanced mRNA and protein in severe condition (Joffre, Potteaux, et al., 2016; Zysset et al., 2016)
Heart	Myocardial IR	1. Increased 2. Increased 3. Enhanced mRNA/protein by infiltrating granulocytes (Boufenzer et al., 2015)	1. Enhanced and associated with mortality and recurrence of cardiovascular events (Boufenzer et al., 2015) 2. n.d. 3. Enhanced number of TREM-1-expressing granulocytes (Boufenzer et al., 2015)
Intestine	IBD/Colitis	1. n.d. 2. Enhanced number of Trem-1 expressing granulocytes (Liu et al., 2015) 3. Enhanced mRNA/protein (Schenk et al., 2007)	1. n.d. 2. n.d. 3. Enhanced number of TREM-1-expressing macrophages (Schenk et al., 2007)
	Mesenteric IR	1. Elevated in plasma (Gibot et al., 2008) 2. n.d. 3. n.d.	1. n.d. 2. n.d. 3. n.d.
Joint	Gout (AGA)	1. n.d. 2. n.d. 3. n.d.	1. Elevated in synovial fluid (Lee et al., 2016) 2. Enhanced expression on monocytes in synovial fluid (Lee et al., 2016) 3. Presence of TREM-1-expressing macrophages in tophaceous tissue (Lee et al., 2016)
	RA	1. n.d. 2. n.d. 3. n.d.	1. n.d. 2. Enhanced mRNA expression (PBC) (Lee, Sugino, Aoki, & Nishimoto, 2011)* 3. Presence of TREM-1-expressing macrophages in synovial tissue (Murakami et al., 2009)
Kidney	Renal fibrosis (UO/IFTA)	1. n.d. 2. n.d. 3. Enhanced mRNA/protein (Campanholle et al., 2013; Lech et al., 2012; Lo et al., 2014; Tammaro et al., 2013)	1. n.d. 2. n.d. 3. Enhanced mRNA (Maluf et al., 2014)*. Presence of TREM-1-expressing cells (Lo et al., 2014; Tammaro et al., 2013)
	Renal IR	1. Elevated in plasma (Tammaro et al., 2016) 2. Increased on monocytes (Tammaro et al., 2016) 3. Enhanced mRNA/protein (Campanholle et al., 2013; Lech et al., 2012; Liu et al., 2014; Tammaro et al., 2016)	1. n.d. 2. n.d. 3. mRNA n.s. [ATN (Famulski et al., 2012)*]
Lung	Cystic fibrosis	1. n.d. 2. n.d. 3. n.d.	1. Similar (Del et al., 2008) 2. Reduced expression on monocytes (Del et al., 2008) 3. n.d.
	NSCLS	1. n.d. 2. n.d. 3. n.d.	1. Elevated in pleural effusion (Ho et al., 2008) 2. n.d. 3. Enhanced mRNA in tissue and number of TREM-1-expressing macrophages (Ho et al., 2008; Kadara et al., 2014; Yuan, Mehta, et al., 2014)*
	Pulmonary contusion	1. n.d. 2. n.d. 3. n.d.	1. Elevated in BAL: higher in severe *vs* no/mild/moderate (Bingold et al., 2011) 2. n.d. 3. n.d.
Pancreas	Pancreatitis	1. Elevated in plasma (Dang, Shen, Yin, & Zhang, 2012; Kamei et al., 2010) 2. n.d. 3. Enhanced mRNA/protein (Dang et al., 2012; Kamei et al., 2010)	1. Elevated in plasma: higher in non-survivors *vs* survivors (Ferat-Osorio et al., 2009; Yasuda et al., 2008) 2. Enhanced expression on monocytes (Ferat-Osorio et al., 2009) 3. Enhanced mRNA/protein (Wang, Qin, Liu, Gupta, & Chang, 2004)
Skin	Psoriasis	1. n.d. 2. Increased in splenic mononuclear cells (Joffre, Hau, et al., 2016) 3. Enhanced mRNA expression (Suarez-Farinas et al., 2013)	1. Elevated in plasma (Hyder et al., 2013) 2. n.d. 3. Enhanced number of TREM-1 expressing myeloid cells (Hyder et al., 2013)

n.d.: not determined, n.s.: not significant (or unknown). * Data was obtained through Nextbio.

IL-1 receptor-associated kinase-4 (IRAK-4). This leads to IRAK-1 phosphorylation and association with TRAF6, thereby activating the IKK complex and leading to activation of MAP kinases (JNK, p38 MAPK). Finally, nuclear translocation of CREB, Nf-κB and AP1 leads to induction of diverse gene transcription, including inflammatory mediators (Fig. 2). TLR activation also leads to upregulation of TREM-1 expression which is MyD88-dependent and involves transcription factors Nf-kB, PU.1 and AP1 (Bouchon, Dietrich, & Colonna, 2000; Gibot et al., 2005; Knapp et al., 2004). Following LPS stimulation of neutrophils, TREM-1 was found to be recruited to M1-lipid rafts and co-localized with TLR4 (Fortin, Lesur, & Fulop, 2007). TREM-1 knock down induces down-regulation of several genes implicated in the TLR4 pathway including MyD88, CD14 and IκBα, even when TLR4 expression is unaltered (Ornatowska et al., 2007; Tammaro et al., 2016). Simultaneous activation of TREM-1 and TLR4 leads to synergistic production of pro-inflammatory mediators through common signaling pathway activation including PI3K, ERK1/2, IRAK1 and Nf-κB activation (Tessarz & Cerwenka, 2008) (Fig. 2). TREM-1 inhibition by means of inhibitory peptides is linked to a decrease in the production of LPS-induced cytokines including MCP-1, IL-8 and IL-10 (Derive et al., 2012; Ornatowska et al., 2007; Zeng, Ornatowska, Joo, & Sadikot, 2007). Interestingly, TREM-1 ligation alone does not lead to sustained inflammation, which confirms that TREM-1 amplifies the inflammatory response initiated by TLR engagement.

2.3. TREM-1-NLR connection

Next to TLRs, NLRs (nucleotide-binding oligomerization domain – NOD - receptors) are members of the PRR family that can detect microbial infection, but also sterile tissue damage. NLRs can cooperate with TLRs and regulate inflammatory and apoptotic responses. Among the NLRs, NOD1 and NOD2 are two well defined cytosolic PRR that specifically recognize diaminopimelatic acid (DAP)-containing muropeptide found primarily in Gram-negative bacteria (NOD1) and muramyl dipeptide (MDP) moieties (NOD2). However, NOD1/2 are also activated by molecules induced from dead or dying cells, as consequence of endoplasmic reticulum stress, through an intracellular pathway involving the activating receptor EIF1 and TRAF2. Many conditions that impose stress on cells, including hypoxia, starvation and changes in secretory needs, promote endoplasmic reticulum stress (Iurlaro & Muñoz-Pinedo, 2016). Thus, this finding provides a new link between inflammatory disease which involve ER stress and NOD1/2 (Keestra-Gounder et al., 2016). Both NOD1 and NOD2 contain ligand binding regions LRR (C-terminal leucine-rich repeats), a central nucleotide-binding oligomerization domain (NACHT) and N-terminal caspase recruitment domains (CARDs). NOD activation results in oligomerization of the NACHT domains, which results in CARD binding of downstream proteins such as RIP2 (receptor-interacting protein 2) which is important for NOD-induced Nf-κB activation. Very little is known about the effect of TREM-1 and NLRs. TREM-1 has a synergistic effect on the production of pro-inflammatory mediators induced by NOD1 and NOD2 ligands (Netea et al., 2006; Prufer et al., 2014). Monocytes stimulation with TREM-1 agonist and TLR or NOD1/2 ligands leads to phosphorylation of Akt and MAPK p38 and synergistic production of cytokines (Netea et al., 2006; Prufer et al., 2014). Mechanistically, TREM-1 activation/crosslinking can lead to enhanced NOD2 expression, caspase activation and RIP2/CARD9 related NF-kB activation and cytokine production like IL-1β which in addition induces other pro-inflammatory mediators like IL-6 in an autocrine loop (Netea et al., 2006) (Fig. 2). It remains to be determined if and how TREM-1 and (other) NLRs interact in different inflammatory diseases and if this interaction is of significance compared to other synergistic pathways with TREM-1.

3. Identifying TREM-1 ligands

3.1. Methods

The identification of TREM-1 ligands remains a difficult, yet essential task. The reason behind this lies in the low affinity and rapid dissociation between receptor and ligand, common phenomena for innate immune receptors. Most of the functional studies on TREM-1 were performed in murine models. A crystallography study has shown that, unlike human TREM-1, mouse TREM-1 extracellular immunoglobulin domain, lacks conserved residues at the complementary determining region (CDR), crucial domain part for ligand binding. Hence, this means that no obvious binding sites for the ligand are observed. This raises the question as to whether the CDR regions are involved in direct ligand recognition and binding (Kelker, Debler, & Wilson, 2004). It is not excluded indeed, that indirectly, *via* a carrier molecule for example, TREM-1 ligand can engage the receptor. In order to describe low affinity ligands, several strategies have been proposed either by immunoprecipitation assays, mass spectroscopy and/or by using cell reporter assays (Read et al., 2015). Some of these methods have been successfully used to propose two candidates as TREM-1 ligands (see below).

3.1.1. Method: TREM-1 fluorescent-labeled tetramer

This method uses a construct in which the extracellular domain of TREM-1 is biotinylated and subsequently assembled to a scaffold of streptavidin, conjugated with a fluorescent dye. As streptavidin contains 4 binding sites for biotin, the resulting molecule is a TREM-1 tetramer with 4 available ectodomains; hence this strategy is expected to increase the affinity for TREM-1 ligand.

3.1.2. Method: functional assay with TREM-1 reporter cells

A cell-based TREM-1 reporter has been described, which can be used to identify TREM-1 activating factor/s. This cell line was derived from BWZ.36 mouse T cell lymphoma line and contains a NFAT-driven LacZ reporter gene. These cells were stably transfected with a TREM-1/DAP12 chimera protein composed of a fusion between TREM-1 (aa1-200) and DAP12. These cells were shown to be robustly activated by the agonistic anti-TREM-1 antibody MAB1278 (R&D Systems) (Campanholle et al., 2013).

3.1.3. Method: surface plasmon resonance (SPR)

This is a powerful technique used to study ligand-binding interactions with membrane proteins. SPR is capable of measuring real-time binding affinities and kinetics of two interacting molecules. It is based on the immobilization of one of the components to a chip that is connected to a sensor, whereas the other interacting molecule is allowed to flow over the surface of the sensor. The detection of the binding is based on the optical phenomena, that measure the changes in the refractive index at the surface of the sensor. Whenever an interaction is detected there will be a change in signal intensity. The increase of the signal is expressed in response unit (RU). SPR is performed using the Biacore technology (Patching, 2014).

TREM-1 receptor can be immobilized on the sensor chip and solutions with putative ligands may be flowed over it. Two recent works have identified HMGB1 and PGLRP1 as potential ligands of TREM-1 receptor using this technique (see below) (Read et al., 2015; Wu et al., 2012).

3.2. High mobility group Box 1 (HMGB1)

HMGB1 is a ubiquitous nuclear protein, that interacts with nucleosomes, transcription factors and histones, to regulate transcription. During inflammation, HMGB1 is actively secreted by activated myeloid cells and is released by dying and necrotic cells (Magna & Pisetsky, 2014; Stephenson, Herzig, & Zychlinsky, 2016; Tsung, Tohme, & Billiar, 2014; Venereau, Ceriotti, & Bianchi, 2015). HMGB1 has been shown to signal

Box 1

Future research questions

- Which ligand is responsible for TREM-1 signaling in different inflammatory diseases?
- Does the TREM-1 and TLR signaling pathways work synergistically or independently in acute and chronic inflammatory disease? Does TREM-1 signal through other (innate) PRRs?
- During inflammation, is TREM-1 expressed on other non-myeloid cells, besides those that are currently known?
- What is the phenotype of TREM-1 polymorphisms in humans?
- Is sTREM-1 a biomarker for non-infectious diseases?

through several receptors, including TLRs and RAGE (receptor for advanced glycation end products), to induce a pathogenic inflammatory response, thereby functioning as a DAMP molecule. HMGB1 has been suggested as a TREM-1 ligand. Indeed, a direct interaction between TREM-1 and HMGB1 was observed by Wu and colleagues, using different approaches like immunoprecipitation and cross-linking assays (Wu et al., 2012). Necrotic cell lysates (NCL), from activated human monocyte cell line THP1, and murine hepatocytes, containing HMGB1, were able to induce an inflammatory response that was blocked by recombinant, soluble TREM-1 (El Mezayen et al., 2007; Wu et al., 2012). However, HMGB1 alone seems unable to trigger TREM-1 activation and possibly needs co-activating molecules (Lo et al., 2014). HMGB1 is considered an inducer of inflammation through activation of diverse PRR and its expression in inflammatory diseases has been observed during colitis, ischemia, arthritis, fibrosis, pancreatitis and cancer (Table 2). Currently, several clinical trials are ongoing to determine its association with outcome and potential for intervention strategies (https://clinicaltrials.gov). It is unknown if HMGB1-TREM1 signaling is of significance compared to signaling of HMGB1 through other PRRs in non-infectious diseases. An additional level of complexity in HMGB1 biology is that it is a redox-sensitive protein containing three conserved cysteine residues, whose redox status dictates the extracellular chemokine- or cytokine-inducing properties of the protein. Ample evidence suggests that HMGB1 is released as a mixture of several isoforms, with distinct post-translational modifications (Yang, Antoine, Andersson, & Tracey, 2013).

3.3. Peptidoglycan recognition receptor 1 (PGLYRP1)

Recently, Read and colleagues identified PGLYRP1 as a potential TREM-1 ligand (Read et al., 2015). The PGLYRP1 protein is primarily found in the granules of granulocytes and is known for its bactericidal properties, namely binding to peptidoglycan (PGN) and other microbial cell wall components such as LPS, and inducing lethal membrane depolarization and oxidative stress in bacteria. It was already known that neutrophils activated by bacteria can release a TREM-1 ligand (Gibot, Buonsanti, et al., 2006). Supernatants from neutrophils activated by PGN (but not by other TLR/NOD-ligands) were able to activate the TREM-1 reporter cell line and this was inhibited with TREM-1 blocking antibodies (Read et al., 2015). Since PGN by itself did not induce activation of the TREM-1 reporter cell line, the authors further investigated the presumed TREM-1 ligand on PGN-activated neutrophils using immunoprecipitation with a tetramer of TREM-1 and mass spectrometry. PGLYRP1 was found to bind TREM-1 (Read et al., 2015). Interestingly, stimulation with soluble PGLYRP1 alone did not induce TREM-1 activation and crosslinking of PGLYRP1 by PGN was required to stimulate TREM-1, suggesting a role of PGLYRP1 as a TREM-1 ligand in infectious diseases. Similar to TREM-1, PGLYRP1 mRNA expression is upregulated in tissue following diverse inflammatory diseases; however its protein expression has not yet been investigated (Table 2). PGLYRP1 was proven to be beneficial in several inflammatory diseases. Mice lacking *Pglyrp1* are more sensitive to colitis and variants in the *PGLYRP1* gene are associated with ulcerative colitis in patients (Saha et al., 2010; Zulfiqar et al., 2013). It remains to be investigated if this is due to the bactericidal properties of PGLYRP1 or its signaling *via* TREM-1 (Yashin et al., 2015).

3.4. Heat shock protein 70-kDA (Hsp70)

Endogenous danger signals released by stressed or necrotic cells, are represented mostly by HMGB1 and HSP70. Eukariotics Hsps are evolutionarily conserved molecules present in all intracellular organelles. They mainly function as molecular chaperones and participate in maintenance of protein homeostasis in normal and stressful conditions. Hsp70 is one of the most frequently studied Hsps because of its potential anti-inflammatory properties. NCLs prepared from LPS-treated THP-1 cells, contain endogenous danger signals, including Hsp70, which are able to induce pro-inflammatory response (El Mezayen et al., 2007; Wu et al., 2012). This effect was reduced by blocking Hsp70 and/or TREM-1, most likely due to a reduction of the p38 MAPK (and not Nf-κB) pathway (El Mezayen et al., 2007). In contrast to the direct interaction observed with HMGB1, Hsp70 did not directly bind TREM-1 (Wu et al., 2012), suggesting that possibly HMGB1 has stronger affinity and might compete for the binding. Of note, Hsp70 seems to display beneficial properties in several pathophysiological conditions; colitis was ameliorated in Hsp70 transgenic mice compared to normal mice, and variants in *HSP70* are associated with Crohn's disease and ulcerative colitis (Debler et al., 2003; Esaki et al., 1999; Klausz et al., 2005; Nam et al., 2007; Tanaka et al., 2007). In addition, Hsp70 plays a protective role in IR-induced injury, fibrosis, cancer and pancreatitis (Bellaye, Burgy, Causse, Garrido, & Bonniaud, 2014; Feng & Li, 2010; Jones, Voegeli, Li, Chen, & Currie, 2011; Murphy, 2013; O'Neill, Harrison, Ross, Wigmore, & Hughes, 2014; Sherman & Gabai, 2015). In conclusion, it appears that only blocking antibodies experiments support the hypothesis that TREM-1 and HSP70 are functionally related (El Mezayen et al., 2007). Further experiments are required to confirm whether TREM-1 activation, in other models of non-infectious diseases, is HSP70-dependent.

3.5. Ligand on platelets

Platelets (thrombocytes) are blood components without nuclei that play a major role in coagulation. Platelets express a wide range of receptors including TLT-1 (TREM-Like Transcript-1, see below) (Haselmayer, Grosse-Hovest, von Landenberg, Schild, & Radsak, 2007). Authors used a recombinant soluble fusion protein consisting of the extracellular domain of human TREM-1 fused to the Fc part of human IgG (rsTREM-1), to demonstrate the binding of TREM-1 on human platelets. In addition to the receptor, platelets also express a TREM-1 ligand on the surface of platelets, both in resting condition and after thrombin activation. Binding of the fusion protein to platelets was inhibited by competing soluble protein or LP17 (Haselmayer et al., 2007). However, the soluble TREM-1 construct did not activate platelets as determined by platelet-dependent aggregation and degranulation (Haselmayer et al., 2007). Interestingly, and in contrast to earlier reports (Gibot, Alauzet, et al., 2006; Gibot, Buonsanti, et al., 2006), TREM-1 ligand was not found on neutrophils.

4. TREM-1 deficient mice

In absence of a specific TREM-1 ligand in sterile inflammatory disorders, genetic models with TREM-1 deficiency represent a valid tool to unveil TREM-1 function *in vivo*. To study this, two different genetic modified murine models are available: TREM1/3 double KO and TREM-1 single KO. Colonna and colleagues postulated that murine *Trem1* lies adjacent to *Trem3* gene and that the 2 genes are likely to have complementary functions. Additionally *TREM-3* is a pseudogene

Table 2
Role for Trem-1 in murine non-infectious disease and potential ligands.

Location	Model	Modulation: phenotype (species, dose)	Potential TREM-1 ligands
Circulation	Hemorrhagic shock	- LP17: protective (rat: 1.0 mg) (Gibot et al., 2009)	- HMGB1 (Yang & Tracey, 2010) - HSP70 (Yang & Tracey, 2010), HSP70 (mRNA lung/liver ↑) (Feinman et al., 2007; Moran et al., 2011)* - CD177 (mRNA liver ↑, lung/liver n.s.) (Edmonds et al., 2011; Feinman et al., 2007; Moran et al., 2011) * - PGLYRP1 (mRNA lung/liver ↑) (Feinman et al., 2007; Moran et al., 2011)*
	Atherosclerosis	- Apoe/Trem-1 KO mice: protective compared to Apoe KO mice (Joffre, Potteaux, et al., 2016; Zysset et al., 2016) - Ldlr/Trem-1 KO mice: protected compared to Ldlr KO mice (Joffre, Potteaux, et al., 2016) - LR12: protective (mice: 5 mg/kg) (Joffre, Potteaux, et al., 2016)	- HMGB1 (Kanellakis et al., 2011) - HSP70 (Xie et al., 2016; Zhou et al., 2004) - CD177 (mRNA n.s.) (Beer et al., 2011; Grabner et al., 2009; Yin et al., 2015)* - PGLYRP1 (mRNA n.s.) (Beer et al., 2011; Grabner et al., 2009; Yin et al., 2015)*
Heart	Myocardial IR	- LR12: protective (mice: 5 mg/kg) (Boufenzer et al., 2015) - Trem-1 KO: Protective (Boufenzer et al., 2015) (mice)	- HMGB1 (de Haan, Smeets, Pasterkamp, & Arslan, 2013) - HSP70 (de Haan et al., 2013) - CD177 (mRNA n.s.) (Harpster et al., 2006; Hunt et al., 2012; Roy et al., 2006; Tarnavski et al., 2004)* - PGLYRP1 (mRNA↑) (Harpster et al., 2006; Hunt et al., 2012; Tarnavski et al., 2004)*
Intestine	Colitis/CAT	- LP17: protective (mice: 0.2 mg, rat: 1.0 mg) (Schenk et al., 2007; Zhou et al., 2013)	- HMGB1 (Hu et al., 2015; Yang & Tracey, 2010) - HSP70 (Tanaka et al., 2007) - CD177 (mRNA ↑; GSE64658)* - PGLYRP1 (mRNA ↑; GSE64658) (Gao et al., 2013)*
	Mesenteric IR	- LP17: protective (rat: 3.5 mg/kg) (Gibot et al., 2008)	- HMGB1 (Kojima et al., 2012)
Joint	CIA	- LP17: protective (mice: 0.2 mg) (Murakami et al., 2009) - Trem1-adenovirus: protective (mice: Trem1 adenovirus 10e8–9 PFU) (Murakami et al., 2009)	- HMGB1 (Yang & Tracey, 2010) - HSP70 (mRNA ↑ Tarsal joints) (Denninger et al., 2015)* - CD177 (mRNA n.s. Tarsal Joints) (Denninger et al., 2015)* - PGLYRP1 (mRNA ↑ n.s. Tarsal Joints) (Denninger et al., 2015)*
Kidney	Renal fibrosis	- Trem-1 KO: protective (Lo et al., 2014) - Trem-1/3 KO: mild phenotype (Tammaro et al., 2013)	- HMGB1 (Yang & Tracey, 2010) - HSP70 (mRNA ↓) (Wu & Brooks, 2012) * - CD177 (mRNA n.s.) (Wu & Brooks, 2012)* - PGLYRP1 (mRNA ↑) (Wu & Brooks, 2012)*
	Renal IR	- LP17: no effect (mice; 0.05–0.2 mg) (Tammaro et al., 2016) - LR12: no effect (mice: 0.2 mg) (Tammaro et al., 2016) - Fc Trem1: no effect (mice; 0.04–5 mg) (Campanholle et al., 2013; Tammaro et al., 2016)	- HMGB1 (Leemans, Kors, Anders, & Florquin, 2014; Yang & Tracey, 2010) - HSP70 (mRNA n.s.) (Liu et al., 2014)* - CD177 (mRNA ↑ interstitial/vascular) (Liu et al., 2014)* - PGLYRP1 (mRNA myeloid cells↑) (Liu et al., 2014)*
Liver	Hepatocellular Carcinoma	- Trem-1 KO: protective (Wu et al., 2012)	- HMGB1 (Wang et al., 2015; Zhou et al., 2014) - HSP70 (mRNA ↑) (Dapito et al., 2012)* - CD177 (mRNA n.s.) (Dapito et al., 2012)* - PGLYRP1 (mRNA ↑) (Dapito et al., 2012)*
Pancreas	Pancreatitis	- LP17: protective (Rat; 1.0 mg) (Dang et al., 2012; Kamei et al., 2010)	- HMGB1 (Yang & Tracey, 2010) - HSP70 (mRNA ↑) (Siveke et al., 2008; Ulmasov, Oshima, Rodriguez, Cox, & Neuschwander-Tetri, 2013)* - CD177 (mRNA n.s.) (Siveke et al., 2008; Ulmasov et al., 2013)* - PGLYRP1 (mRNA n.s.) (Siveke et al., 2008; Ulmasov et al., 2013)
Skin	Psoriasis	- Trem-1 KO: no effect (Joffre, Hau, et al., 2016)	- HMGB1 (mRNA ↓ or n.s.) (Swindell et al., 2011)* (Suarez-Farinas et al., 2013)* - HSP70 (mRNA ↓ or n.s.) (Swindell et al., 2011)* (Suarez-Farinas et al., 2013)* - CD177 (mRNA n.s or (Swindell et al., 2011)* (Suarez-Farinas et al., 2013)* - PGLYRP1 (mRNA ↑) (Swindell et al., 2011)* (Suarez-Farinas et al., 2013)*

n.s.: not significant (or unknown).* Data obtained from Nextbio.

in human, hence mice lacking TREM1/3 receptors bear strong resemblance to the human TREM-1 system regulation *in vivo* (Klesney-Tait et al., 2013; Tammaro et al., 2013). In the context of sterile inflammatory disorders, genetic deletion of TREM1/3 showed a milder protective phenotype following obstructive-induced nephropathy compared to TREM-1 single knockout mice, indicating indeed a potential role for TREM-3 herein (Lo et al., 2014; Tammaro et al., 2013). Additionally, *Trem-1* single KO mice display protection, mostly due to decreased recruitment of inflammatory cells, in models of atherosclerosis, myocardial IR, and hepatocellular carcinoma (Boufenzer et al., 2015; Joffre, Hau, et al., 2016; Joffre, Potteaux, et al., 2016; Wu et al., 2012Zysset et al., 2016). If phenotypes are different in TREM1/3 double KO mice remains to be determined. Given the difference in phenotype observed in the 2 genetic mice, especially in the context of renal fibrosis, one could speculate that knockdown of both receptors *in vivo* might affect the expression of other receptors, located in proximity of the genes, such as TREM-2, known to have opposite functions compared to TREM-1. However, it cannot be excluded that TREM-3 plays any role in inflammation, which remains yet to be elucidated. In addition, differences in phenotype between TREM-1 and TREM1/3 KO mice during renal fibrosis could be related to different operators, different facility and local mice microbiota, with or without genetic background differences (Jenq et al., 2012). We would like to refer to Table 2 for the overview of TREM-1 function in these studies.

5. TREM-1 as a promising therapeutic target in non-infectious disease

Although the pathophysiological role of TREM-1 was first identified during infectious diseases (Bouchon et al., 2000), TREM-1 is, today,

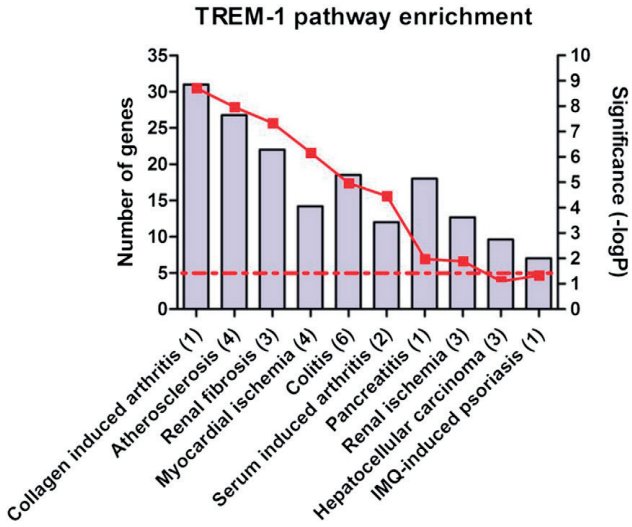

Fig. 3. TREM-1 signaling pathway enrichment in non-infectious diseases. A set of 45 genes related to TREM-1 signaling pathway (provided by Ingenuity® Pathway Analysis, Qiagen; www.ingenuity.com) was uploaded as bioset, and analyzed *in silico* by Nextbio (Illumina; www.nextbio.com). TREM-1 signaling pathway enrichment and number of overlapping genes were determined between the TREM-1 bioset and murine genome datasets related to non-infectious diseases. Number of studies included is displayed in brackets. Purple bar shows average of overlapping genes between TREM-1 bioset and selected genome datasets (× out of 45 genes, left Y-axis). Red line indicates average of significance for TREM-1 signaling pathway enrichment (−LogP; right Y-axis). Red dotted line indicates threshold for significance (−logP = 1.3). See supplementary methods for further details.

believed to play a crucial role in, both acute (ischemia-reperfusion, hemorrhagic shock,pancreatitis) and chronic (inflammatory bowel diseases, rheumatic diseases, atherosclerosis, psoriasis and cystic fibrosis) forms of aseptic inflammation. In line, DAMPs that emerged from the danger theory (Matzinger, 1994) and PAMPs are the primary triggers of non-infectious and infectious inflammation and are both recognized by PRRs. This may explain the similarities observed in the cascade of events occurring during sterile or infectious inflammation, including the activation of TREM-1 as an amplifier of TLRs. In Tables 1 and 2 we summarize current knowledge about TREM-1 expression and function respectively in the non-infectious diseases discussed in this review. In addition, we determined TREM-1 signaling pathway enrichment in several published array datasets related to acute and chronic non-infectious diseases in mice. Based on Ingenuity® Pathway Analysis (IPA, Qiagen; www.ingenuity.com), 45 genes associated to TREM-1 signaling pathway (presented in supplementary Table S1) were uploaded to Nextbio (Illumina; www.nextbio.com) and TREM-1 signaling pathway enrichment was analyzed *in silico*, in available genome datasets curated by Illumina. Relevant selected public datasets used for the analysis are displayed in supplementary Table S2. For comprehensive methods please see the supplementary methods section. Based on *in silico* analysis, we show that TREM-1 signaling pathway is enriched and TREM-1 putative ligands are expressed in multiple non-infectious diseases which suggest that TREM-1 intervention strategies could affect the diseased phenotype through interference with receptor-ligand interaction (Table 2 and Fig. 3). Moreover in Table 3, we describe the association of TREM-1 single nucleotide variance (SNVs) and non-infectious diseases, in humans.

5.1. Acute inflammatory diseases

5.1.1. Ischemia reperfusion (IR)

Reperfusion injury that follows an ischemic event is the consequence of a complex cascade of events that first implicates the components of the innate immune response and subsequently leads to an acute inflammatory reaction. IR-induced cellular and molecular processes show similarities among different organs including the release of DAMPs and inflammatory cytokines (such as HMGB-1, TNFα, IL-1β and IL-6), activation of PRRs and leukocytes influx. Although these

Table 3
Trem-1 polymorphisms in non-infectious disease.

Disease	SNV	Country (population)	Cohort (N)	Effect
CAD	rs2234237 (A/A) rs4711668 (T/T) rs6910730 (G/G) rs9471535 (C/C)	Russia (Caucasian)	CAD (702) Healthy control (300)	Elevated risk (Golovkin et al., 2014)
IBD	rs2234237 (A allele) rs3789205 (G allele) rs9471535 (C allele)	Korea	CD (202) UC (265) BD (138) Ctrl (234)	Elevated risk for BD, not CD or UC (Jung et al., 2011)
Kidney transplantation	rs2234237 (A allele)	Netherlands (Caucasian)	Donor (1260) Recipient (1260)	No effect on DGF, BPAR, graft loss, patient survival (Tammaro et al., 2016)

signals initiate the mechanisms of tissue repair, excessive and prolonged inflammation may lead to deleterious fibrosis and organ dysfunction.

5.1.1.1. Kidney: In a model of renal IR, we and others have shown an increase in TREM-1 expression as well as sTREM-1 in renal tissue 24 h after the event that was mainly due to the recruitment and *in situ* accumulation of TREM-1 expressing granulocytes (Campanholle et al., 2013; Tammaro et al., 2016). In the repair phase following renal IR, Campanholle and colleagues observed an increased expression of TREM-1 in macrophages (Campanholle et al., 2013). While TLR2/4 and MyD88 pathway impairment was associated with a decrease in monocytic TREM-1 expression and displayed beneficial effects, TREM-1 inhibition by the administration of a recombinant soluble form of TREM-1 had no impact on disease severity or macrophage activation (Campanholle et al., 2013). Similarly, we observed no effect of TREM-1 inhibition in the prevention of renal IR induced injury (Tammaro et al., 2016). In addition, we did not observe any association with allograft or host-related TREM-1 SNVs with delayed graft function, generally caused by IR induced injury (Tammaro et al., 2016). Apparently, any pathophysiological contribution of TREM-1 in IR is time-dependent and organ specific.

5.1.1.2. Intestine: During intestinal IR, the *in situ* inflammatory reaction may contribute to ischemic injury in the intestinal epithelium, which in turn might allow for the translocation of bacteria and bacterial products from the gut lumen to the blood compartment, accounting for distant organ failure with high mortality (Harward, Brooks, Flynn, & Seeger, 1993; Oldenburg, Lau, Rodenberg, Edmonds, & Burger, 2004; Panes & Granger, 1998; Swank & Deitch, 1996). In preclinical models, the pharmacological inhibition of TREM-1 by the use of synthetic peptide LP17 was shown to be associated with reduced leukocyte recruitment/activation and systemic inflammatory reaction, thus limiting intestinal injury and bacterial translocation as well as distant organ failure, and finally improving survival (Gibot et al., 2008). These results were confirmed in a similar model by the inhibition of Syk, a component of the TREM-1/DAP12 signaling pathway (Pamuk et al., 2010).

5.1.1.3. Heart: Considerable work has been performed to decipher cellular or molecular targets in myocardial infarction (MI) clinical trials, though with disappointing results (Armstrong & Granger, 2007; Christia & Frangogiannis, 2013; Faxon et al., 2002). Interestingly, the inhibition of TREM-1 is associated with protection against hyper-responsiveness without a complete abrogation of the immune response (Bouchon, Facchetti, Weigand, & Colonna, 2001; Derive et al., 2012). A crucial determinant of infarct healing and scar formation resides into the delicate balance between the type and amount of recruited leukocytes (Libby, Nahrendorf, & Swirski, 2016; Swirski & Nahrendorf, 2013). In a recent preclinical study, we demonstrated that the genetic invalidation and the pharmacological inhibition of TREM-1 using the synthetic peptide LR12 limit the recruitment of inflammatory leukocytes to the infarcted myocardium and their activation (Boufenzer et al., 2015). More precisely, TREM-1 inhibition limited neutrophil recruitment and MCP-1 production, thus reducing the mobilization of $Ly6C^{high}$ inflammatory monocytes to the heart, but without impacting the trafficking of pro-resolving $Ly6C^{low}$ monocytes. This strongly suggests that TREM-1 is a central player in the inflammatory reactions following MI that regulates leukocyte recruitment, both quantitatively and qualitatively. In a more clinically relevant model of cardiogenic shock in mini-pigs, the administration of LR12 improved hemodynamic parameters and cardiac function, concomitantly, with a reduction in infarct size as evaluated by the reduction of circulating creatinine phosphokinase and troponin I within the first hours following reperfusion (Lemarie et al., 2015).

5.1.2. Hemorrhagic shock

Hemorrhagic shock, following major trauma, results in a global IR injury. This may lead to multiple organ failure, a process in which the innate immune system plays a significant role. Numerous studies have shown that the early activation of leukocytes is responsible for the systemic release of inflammatory mediators, leading to multiple organ failure after severe hemorrhagic shock (Hierholzer et al., 1998; Meldrum et al., 1997; Meng, Dyer, Billiar, & Tweardy, 2001). Bacterial and endotoxin translocation also appear to be implicated in the development of organ failure after hemorrhagic shock and resuscitation, *via* the release of HMGB1 and activation of TLR4 of the intestinal epithelium (Benhamou et al., 2009; Kao et al., 2014; Shimizu et al., 2002; Sodhi et al., 2015). Pharmacological inhibition of TREM-1 in rats by the administration of the TREM-1inhibitor, LP17, attenuated the hemodynamic compromise and the development of lactic acidosis, prevented cytokine production, organ dysfunction and, finally, improved survival (Gibot, Massin, et al., 2009).

5.1.3. Pancreatitis

The initial injury in acute pancreatitis is characteristically sterile and results in release of DAMPs and activation of innate immunity. Severe acute pancreatitis can readily progress from a localized inflammation in the pancreas to multiple organ failure. In a mouse model for mild and severe acute pancreatitis, membrane TREM-1 on neutrophils, as well as sTREM-1 plasma levels, were correlated to severity of the model (Liu, Wu, Zhao, Feng, & Wang, 2015). Similar results were observed in patients with acute pancreatitis, in which sTREM-1 plasma levels were higher in non-survivors as compared to survivors and may be a predictive marker of organ failure (Ferat-Osorio et al., 2009; Yasuda et al., 2008). In mice, TREM-1 upregulation in injured major organs was observed in the early phases following acute pancreatitis, and inhibition of TREM1 by LP17, displayed protective effects by lowering aspartate transaminase and blood urea nitrogen (Kamei et al., 2010).

5.2. Chronic inflammatory diseases

5.2.1. Inflammatory bowel disease(IBD)

Innate immune sensors such as TLRs, possibly in collaboration with TREM-1, may be considered as an interface between the intestinal epithelial barrier and innate immunity. TREM-1 appears to be crucially involved in chronic inflammatory bowel diseases and experimental colitis. It was shown to be upregulated in $CD14^{high}$ macrophages from IBD patients. TREM-1 expression could not be detected in macrophages derived from healthy intestine. This expression correlated with an enhanced release of inflammatory mediators such as TNFα, IL-6, IL-8 and MCP-1, and enhanced disease activity (Schenk, Bouchon, Seibold, & Mueller, 2007). In parallel, serum sTREM-1 concentrations are significantly enhanced in patients with IBD (Park et al., 2009). In 2 distinct mouse models of colitis, blocking TREM-1, by LP17 administration attenuated intestinal inflammation and histological alterations. Interestingly, both early and late LP17 treatment showed the same efficacy (Schenk et al., 2007). Trem-1 KO mice displayed significantly attenuated disease that was associated with reduced inflammatory infiltrates and diminished expression of pro-inflammatory cytokines (Weber et al., 2014).

Although the phenotype of TREM-1 SNVs is not yet known, SNVs within the *TREM-1* gene are associated with elevated risk for intestinal Behçet's disease, another form of multisystemic, chronic, relapsing intestinal inflammatory disorder (Jung et al., 2011). These data suggest that TREM-1 may be a potential therapeutic target in chronic intestinal inflammatory diseases.

5.2.2. Rheumatoid arthritis/gout

Rheumatoid arthritis (RA) is a chronic, systemic autoimmune and inflammatory syndrome characterized by the destruction of synovial joints. The synovium of established RA patients is characterized by

marked synovial intimal lining hyperplasia, increased vascularity and accumulation of inflammatory cells (Smolen, Aletaha, & McInnes, 2016). TREM-1 expression was shown to be increased in $CD45^+$/$CD14^+$ cells, both in synovial samples from patients with RA and from mice with collagen-II-induced arthritis, but was not detectable in synoviocytes (Collins et al., 2009; Kuai et al., 2009). Its engagement was linked to an increase in inflammatory mediators. Indeed, *in vitro* stimulation of human primary synovial cells, isolated from RA patients (comprising synoviocytes but also infiltrated leukocytes), with an agonistic anti-TREM-1 showed increased cytokine production (TNFα, IL-8, IL-1β, GM-CSF) as compared to controls. These data suggest that TREM-1 could play a role in amplifying inflammation during arthritis, and that modulating TREM-1 activation could downregulate excessive chemokine and cytokine production. This was further demonstrated in an experimental model of collagen type II-induced arthritis model in mice: TREM-1 fusion protein or LP17 administration was associated with a sharp reduction in clinical signs, in a dose-dependent manner (Yousuke Murakami et al., 2009). Recently Fan et al. showed that Triplotide, an active component isolated from the *Tripterygium wilfordii* Hook F plant, was able to modulate the expression of several inflammatory pathways including the TREM-1 pathway. This was linked to a reduction in the arthritic score in a rat model of collagen-induced arthritis (Fan et al., 2016).

Gout is a prototype of crystal-induced acute inflammation, caused by the deposition of MonoSodium Urate Monohydrate (MSU) crystals. The innate immune system initiates inflammatory responses through the recognition of MSU crystals as a danger signal (Shi, Evans, & Rock, 2003). In line, phagocytes up-regulate TREM-1 after stimulation with MSU crystals and its engagement synergistically enhanced production of pro-inflammatory cytokines by macrophages such as IL-1β and MCP-1 (Murakami et al., 2006). TREM-1 expression was significantly upregulated among infiltrating cells in a murine air pouch model of MSU crystal-induced acute inflammation (Murakami et al., 2006). In acute gouty arthritis patients, TREM-1 expression was higher in the synovial fluid mononuclear cells than in PBMCs and profound sTREM-1 levels were measured in gout synovial fluid. Interestingly, MSU crystals were able to induce TREM-1 in PBMCs from acute gout patients, but not from chronic gout patients (Lee et al., 2016). These data show that TREM-1 is induced and participates in the amplification of inflammation in acute gouty arthritis.

5.2.3. Fibrosis

Kidney: Renal fibrosis is the hallmark of progressive renal disease and has been investigated in mice using the unilateral ureteral obstruction (UUO) model. During UUO, macrophage and TLR signaling play a role in the infiltration of several inflammatory myeloid cells into the tissue (Leemans et al., 2009; Pulskens et al., 2010). Lo and colleagues demonstrated that TREM-1 was implicated in the polarization of monocytes through classically activated (M1) macrophages, and that UUO-injured kidneys contain a TREM-1-ligand that triggers M1 macrophage differentiation. We, and others, have shown that TREM-1 is highly upregulated in renal tissue following UUO, and that TREM1 KO and TREM-1/3 double KO mice showed less tissue inflammation as compared to WT mice (Lo et al., 2014; Tammaro et al., 2013). In humans, TREM-1 expression on inflammatory cells was observed in obstructive nephropathy which was correlated with disease progression (Lo et al., 2014; Tammaro et al., 2013).

5.2.4. Atherosclerosis

Atherosclerosis is a chronic inflammatory response of the arterial wall initiated by a lesion in the endothelium, which evolve in progressive damage sustained by interaction between lipoproteins, monocyte-derived macrophages and other constituents of the arterial wall. Monocytes-derived macrophages promote atherosclerotic plaque initiation, by differentiation into foam cells, which play a role in further plaque progression and rupture (Libby & Hansson, 2015). TREM-1 controls the production of IL-8 and TNFα in U937 foam cells, suggesting a critical role for TREM-1 in the pathogenesis of atherosclerosis (Wang, Li, & Zhao, 2012). Indeed silencing of TREM-1, by means of shRNA or inhibitory peptides, leads to reduced oxLDL phagocytosis and a reduction in the release of pro-inflammatory mediators by macrophages (Li, Hong, Pan, Lei, & Yan, 2016). Recently, pre-clinical models of atherosclerosis, in unison, confirmed a pro-atherogenic role of TREM-1 receptor (Joffre, Potteaux, et al., 2016; Zysset et al., 2016). The genetic invalidation of TREM-1 in mice models of atherosclerosis (ApoE −/− and Ldlr −/−) was linked to a strong reduction in atherosclerotic plaque size, inflammation and macrophage infiltration, possibly due to decreased CXCR1 expression on circulating non-classical monocyte (Joffre, Potteaux, et al., 2016). This led to a decrease in monocyte recruitment and accumulation in plaques, a decrease in TLR4-initiated pro-inflammatory macrophages response, and decreased foam cell formation (Joffre, Potteaux, et al., 2016; Zysset et al., 2016). Macrophage with TREM-1 deletion or inhibition displayed a pronounced anti-atherogenic phenotype as displayed by CD36 decrease. Targeting TREM-1, according to the authors, would be beneficial as a double hit therapy against both and TLR and CD36 (Joffre, Potteaux, et al., 2016). However, it is still unclear how TREM-1 directly regulates CXCR1 and CD36 pathways in atherosclerosis. Unraveling these mechanisms would set the bases for a next research step.

The role of TREM-1 during atherogenesis is supported by clinical data, showing increased levels of TREM-1 in atheromatous human atherosclerotic lesions, and a significant association between high levels of circulating sTREM-1 and major adverse cardiovascular events in patients with acute myocardial infarction (Boufenzer et al., 2015; Zysset et al., 2016). Additionally, TREM-1 was reported to control plaque vulnerability. Patients with symptomatic plaque display increased TREM-1 expression on dendritic cells, vascular smooth muscle cells and macrophages, possibly as consequence of the inflammatory milieu present in the atheroma. TREM-1 activates MMPs to induce collagen degradation and hence plaque instability (Rai, Rao, Shao, & Agrawal, 2016; Rao, Rai, Stoupa, Subramanian, & Agrawal, 2016a; Rao, Rai, Stoupa, Subramanian, & Agrawal, 2016b). Although these encouraging results strongly suggest TREM-1 involvement in the initiation and progression of atherosclerosis, additional studies are required to determine the exact molecular mechanism underlying protection in absence of TREM-1.

5.2.5. Psoriasis

Psoriasis is a common inflammatory skin disease, of unknown etiology, and dendritic cells (DCs) are thought to play an important role in the pathogenesis of skin lesions (Lowes, Bowcock, & Krueger, 2007). The TREM-1 signaling pathway was identified as the third highest canonical pathway enriched in the transcriptome of inflammatory DCs derived from psoriatic lesions. The *in situ* upregulation of TREM-1 was confirmed by immunohistochemistry on $CD11c^+$ DCs and $CD31^+$ cells. Moreover, psoriatic patients displayed elevated levels of circulating sTREM-1 (Hyder et al., 2013). In psoriatic patients subjected to a 6 weeks treatment with narrow-band ultraviolet radiation (NB-UVB), the number of TREM-1^+ dermal cells was increased in non-responder patients. Contrary, a decrease in TREM-1 + dermal cells and mRNA levels, were observed in patients classified as responders to the NB-UVB treatment. In both, responders and non-responders patients, circulating levels of sTREM-1 show no profile differences (Hyder et al., 2013). In an *in vitro* and *ex vivo* model, TREM-1 blockade by TREM-1 fusion protein was linked to a decreased Th17 response, suggesting that TREM-1 blockade could reduce the effect of psoriatic DC activation of Th17 cells (Hyder et al., 2013). However, in a model of imiqimod (IMQ)-induced psoriatic lesion, an acute model of inflammation, TREM-1 deficiency did not induce any difference in T cell infiltration in the lesion as well as pathological features of psoriasis (Joffre, Hau, et al., 2016). In line, *in silico* analysis in Nextbio we show that TREM-1 signaling pathway enrichment was not significant in a dataset of skin tissue from the

back of IMQ-treated wild type mice (Swindell et al., 2011) (Fig. 2). This question whether TREM-3 might compensate for TREM-1 absence or other TLRs are predominant in this model. Of note, significance for TREM-1 signaling pathway enrichment was highly variable in datasets between different types of murine models for psoriasis that are used, including spontaneous lesions in specific knockout mice, IL-23 or IMQ-induced psoriasis (Suarez-Farinas et al., 2013; Swindell et al., 2011). In many of these murine models for psoriasis, each model displayed similarities but also differences among each other and in comparison to human psoriasis (Swindell et al., 2011). Altogether, these results suggest that future research should be conducted to investigate whether TREM-1 is a potential target in psoriasis.

5.2.6. Cystic fibrosis

Cystic fibrosis (*CF*) results from abnormalities in the gene that codes for the CFTR (Cystic Fibrosis Transmembrane Conductance Regulator), which is implicated in the regulation of chloride flux across cell membranes. In this disease, an impaired inflammatory response allows for a huge bacterial colonization of the airways (Cantin, Hartl, Konstan, & Chmiel, 2015; Montgomery, Mall, Kicic, & Stick, 2017). While lung resident macrophages and circulating monocytes from *CF* patients express levels of TLR4/MD2 similar to those of control subjects, TREM-1 expression is profoundly downregulated (Del et al., 2008). These data suggest that monocytes are maintained in a LPS-tolerant state, due to repression of TREM-1, associated with a failure to generate an appropriate inflammatory response (Del et al., 2008; Fresno et al., 2009). The active form of Vitamin D, $1,25(OH)_2D_3$, is known to strongly upregulate TREM-1 expression of in human monocytes and macrophages (Kim et al., 2013). The use of $1,25(OH)_2D_3$ to stimulate airway epithelial cells from patients with *CF* was able to induce TREM-1 expression, without affecting the expression of TREM-2, which is known to antagonize TREM-1, through DAP12 (Rigo et al., 2012). Altogether these studies demonstrate that TREM-1 repression during cystic fibrosis can lead to an impaired response to infection following TLR engagement.

5.3. Other diseases

5.3.1. Cancer

Numerous studies support the concept that inflammation is a critical component of tumor progression. Tumor cells can use the innate immune system for migration, invasion, angiogenesis, all of which enable metastasis. It has become evident that the inflammatory response observed in or around developing neoplasms can regulate tumor development. Moreover, tumor cells have co-opted some of the signaling molecules of the innate immune system (Coussens & Werb, 2002; van Kempen, de Visser, & Coussens, 2006). TREM-1 was shown to be upregulated on Tumor-Associated Macrophages (TAMs) under the control of COX2/PGE2 axis, and its engagement promotes cells' invasive ability (Ho et al., 2008; Yuan, Mehta, et al., 2014). Levels of sTREM-1 were increased in malignant pleural effusion from patients with non-small cell lung cancer (NSCLC), without infection, making sTREM-1 an independent predictor of patient survival. Moreover, an increased TREM-1 expression in tumor tissue was associated with poor outcome (Ho et al., 2008).

IBD is associated with an increased risk for the development of colorectal and small bowel cancer (Rubin, Shaker, & Levin, 2012). TREM-1 inhibition, by LP17, attenuated colitis-associated tumorigenesis in a murine model (Zhou et al., 2013). Hepatocellular carcinoma (HCC) is a well-known type of inflammation-related cancer. Deletion of *Trem1* in a murine diethylnitrosamine (DEN)-induced hepatocellular carcinogenesis model attenuated Kupffer cell activation and HCC development suggesting that TREM-1 is a pivotal determinant of Kupffer cell activation in liver carcinogenesis (Wu et al., 2012). TREM-1 expression by HCC cells has been confirmed in humans and was shown to increase the migratory ability of cells in culture (Wu et al., 2012), confirming the role of TREM-1 in cancer metastasis. The TREM-1 expression in HCC cells correlated with worse survival (Liao et al., 2012). These data underline the potential therapeutic interest in TREM-1 modulation during cancer in order to prevent tumor progression.

6. Pharmacological TREM-1 inhibitors: a novel therapeutic approach

Several strategies have been developed to inhibit TREM-1 receptor activation using small molecules and peptides. Soluble TREM-1 is used as the blueprint for the development of inhibitory peptides, that work as a scavenger receptors to bind TREM-1 ligands, and thereby prevent TREM-1 activation. Currently, these peptides are in an experimental phase, and some are under modification for potential use in clinical trials. Herein, we discuss the two potential peptides actually tested in preclinical studies.

6.1. LP17

Based on murine and human TREM-1 sequences, a highly conserved sequence was found in the ectodomain and is therefore suitable as a sTREM-1 mimics (Gibot et al., 2004).

This peptide (LQVTDSGLYRCVIYHPP), called LP17, was shown to reduce an inflammatory response in monocytes, induced by LPS or TREM-1 agonistic antibody (Gibot et al., 2004). Further studies in mice show that LPS- and caecal ligation puncture-induced mortality was reduced by LP17 treatment, prompting an interest for clinical application (Gibot, Buonsanti, et al., 2006; Gibot et al., 2004). Since then, the therapeutic potential of LP17 in several infectious and non-infectious diseases has been investigated in experimental models (Table 2).

6.2. LR12

The LR12 peptide is another pharmacological approach to inhibit TREM-1. LR12 (LQEEDAGEYGCM) represents a conserved motif from TREM-like transcript (TLT)-1. TLT-1 is a member of the TREM gene cluster 6p21.1, but more importantly, is expressed exclusively in the platelet lineage and localized in α-granules of resting platelets (Morales et al., 2010). Therefore, TLT-1 is exposed at the membrane upon platelet activation and could promote platelet aggregation by crosslinking fibrinogen (Derive et al., 2012; Morales et al., 2010; Washington et al., 2009). A soluble form of TLT-1 (sTLT-1) was found in the sera of septic shock patients which correlated with mortality (Washington et al., 2009). Moreover, mice lacking TLT-1 (Treml-1 ko mice) were more susceptible to LPS- or caecal ligation puncture-induced inflammation. In these models, administration of the LR12 peptide was able to restore a balanced immune response and improve survival (Derive et al., 2012; Washington et al., 2009). sTLT-1 controls leukocyte activation, and displays immunomodulatory properties through the specific inhibition of TREM-1 (Derive et al., 2012). The TLT-1-derived peptide LR12, was able to reduce the LPS-induced inflammatory responses and to prevent sepsis-induced tissue abnormalities and dysfunctions, which translated into a gain of survival, even in case of administration after the onset of sepsis (Derive et al., 2012). Moreover, pharmacological inhibition of TREM-1, by the use of LR12, was associated with a reduced need for norepinephrine and improved cardiac parameters in a mini-pig model of peritonitis. During experimental monkey endotoxemia, the administration of LR12 attenuated the endotoxin-induced blood pressure decrease and release of several inflammatory cytokines in blood (Derive, Boufenzer, & Gibot, 2014; Derive et al., 2013). In all preclinical models of septic shock, the administration of LR12 was linked to a strong protective effect of the cardiovascular system and an improvement in survival.

Pharmacological inhibition of TREM-1 in preclinical models of non-infectious diseases was also linked to markedly beneficial effects. Indeed, LR12 administration during acute myocardial infarction was able to control leukocyte recruitment to the infarcted area, thus limiting *in situ* inflammation, excessive cardiac remodeling and infarct size

(Boufenzer et al., 2015). Even more interesting, a recent study shows that pharmacological blockade of Trem-1 in ApoE −/− mice, using LR-12 peptide, significantly reduced the development of atherosclerosis throughout the vascular tree, and lessened plaque inflammation (Joffre, Potteaux, et al., 2016). These studies strengthen the hypothesis that LR12 exhibits potent immunomodulatory properties, by inhibiting the TREM-1 inflammatory amplification loop, which dampened, but did not completely abrogate, the inflammatory reaction. Safety and pharmacokinetics of LR12 (www.inotrem.com; MOTREM™, INN: Nangibotide, CAS number 2014384-91-7) are being evaluated in a First-in-Man study before further clinical trials in patients.

7. Conclusion and clinical perspectives

The discovery of the relatively novel TREM family has increased our repertoire of PRRs and understanding of innate immunity. Although no TREM-1 *specific* (endogenous) ligand has been discovered, TREM-1 appears to be activated by several DAMPs that are shared by other PRRs. It is unknown why these ligands, specifically, share TREM-1 activation. Neither it is known what they have in common, but this information could certainly be of use in the determination of new specific ligands.

We now know that TREM-1 is not only involved in infectious disease, but also in several non-infectious diseases. In general, TREM-1 amplifies the inflammatory response triggered by DAMPs, released upon tissue injury or stress. In many cases, TREM-1 intervention proved to be beneficial in non-infectious diseases. However, accumulating data shows that the contribution of TREM-1 in the pathophysiology can be organ or disease specific. Although, in many cases, TREM-1 intervention shows a beneficial effect in murine studies, the precise mechanism that underlies protection is unknown and mechanism-of-action should be further investigated. Several scientific questions are still unanswered and are of interest for the future use of TREM-1 as a target for intervention therapy (see Box 1).

Thus far, TREM-1 inhibitory proteins, such as LP17 and LR12 are a promising class of compounds for the inhibition of unwanted inflammation during several (non)-infectious diseases as shown in several pre-clinical studies in different murine models. Needless to say, this is only the beginning of the drug development cycle and more research, and money, is needed to go from first-in-man study to further clinical trials. Of the described TREM-1 inhibitors, LR12 is most developed and shown to be well tolerated in human without side effects in a double-blind, randomized, placebo-controlled phase I clinical trial. Currently, LR12 is being investigated in phase I trial for septic shock and acute myocardial infarction (www.inotrem.com). Based on pre-clinical studies, many more applications for LR12 are thinkable. Importantly, the main advantage of pharmacologically targeting TREM-1 over other PRRs, such as TLRs, is that such an approach does not fully abolish the inflammatory response required for a proper immune response against bacteria, pathogenic or not. This feature contributes to the safety for TREM-1 inhibitors in treating inflammatory diseases.

Conflict of interests

Marc Derive and Sebastien Gibot are co-founders of INOTREM, a company developing TREM-1 inhibitors.

Appendix A. Supplementary data

Supplementary data to this article can be found online at http://dx.doi.org/10.1016/j.pharmthera.2017.02.043.

References

Armstrong, P. W., & Granger, C. B. (2007). Pexelizumab and the APEX AMI trial. *JAMA 297*(17), 1881 (author reply 1881-2).

Arts, R. J., Joosten, L. A., van der Meer, J. W., & Netea, M. G. (2012). TREM-1: Intracellular signaling pathways and interaction with pattern recognition receptors. *Journal of Leukocyte Biology*.

Barrow, A. D., Astoul, E., Floto, A., Brooke, G., Relou, I. A. M., Jennings, N. S., ... Trowsdale, J. (2004). Cutting edge: TREM-like transcript-1, a platelet immunoreceptor tyrosine-based inhibition motif encoding costimulatory Immunoreceptor that enhances, rather than inhibits, calcium signaling via SHP-2. *The Journal of Immunology 172*(10), 5838–5842.

Baruah, S., Keck, K., Vrenios, M., Pope, M. R., Pearl, M., Doerschug, K., & Klesney-Tait, J. (2015). Identification of a novel splice variant isoform of TREM-1 in human neutrophil granules. *Journal of Immunology (Baltimore, Md.: 1950) 195*(12), 5725–5731.

Beer, M., Doepping, S., Hildner, M., Weber, G., Grabner, R., Hu, D., ... Habenicht, A. J. (2011). Laser-capture microdissection of hyperlipidemic/ApoE(−)/(−) mouse aorta atherosclerosis. *Methods in Molecular Biology 755*, 417–428.

Bellaye, P. S., Burgy, O., Causse, S., Garrido, C., & Bonniaud, P. (2014). Heat shock proteins in fibrosis and wound healing: Good or evil? *Pharmacology & Therapeutics 143*(2), 119–132.

Benhamou, Y., Favre, J., Musette, P., Renet, S., Thuillez, C., Richard, V., & Tamion, F. (2009). Toll-like receptors 4 contribute to endothelial injury and inflammation in hemorrhagic shock in mice. *Critical Care Medicine 37*(5), 1724–1728.

Bingold, T. M., Pullmann, B., Sartorius, S., Geiger, E. V., Marzi, I., Zacharowski, K., ... Scheller, B. (2011). Soluble triggering receptor on myeloid cells-1 is expressed in the course of non-infectious inflammation after traumatic lung contusion: A prospective cohort study. *Critical Care 15*(2), R115.

Bouchon, A., Dietrich, J., & Colonna, M. (2000). Cutting edge: inflammatory responses can be triggered by TREM-1, a novel receptor expressed on neutrophils and monocytes. *Journal of Immunology (Baltimore, Md.: 1950) 164*(10), 4991–4995.

Bouchon, A., Facchetti, F., Weigand, M. A., & Colonna, M. (2001). TREM-1 amplifies inflammation and is a crucial mediator of septic shock. *Nature 410*(6832), 1103–1107.

Boufenzer, A., Lemarié, J., Simon, T., Derive, M., Bouazza, Y., Tran, N., ... Gibot, S. (2015). TREM-1 mediates inflammatory injury and cardiac remodeling following myocardial infarction. *Circulation Research 116*(11), 1772–1782.

Campanholle, G., Mittelsteadt, K., Nakagawa, S., Kobayashi, A., Lin, S. L., Gharib, S. A., ... Duffield, J. S. (2013). TLR-2/TLR-4 TREM-1 signaling pathway is dispensable in inflammatory myeloid cells during sterile kidney injury. *PloS One 8*(7), e68640.

Cantin, A. M., Hartl, D., Konstan, M. W., & Chmiel, J. F. (2015). Inflammation in cystic fibrosis lung disease: Pathogenesis and therapy. *Journal of Cystic Fibrosis 14*(4), 419–430.

Chen, L. C., Laskin, J. D., Gordon, M. K., & Laskin, D. L. (2008). Regulation of TREM expression in hepatic macrophages and endothelial cells during acute endotoxemia. *Experimental and Molecular Pathology 84*(2), 145–155.

Christia, P., & Frangogiannis, N. G. (2013). Targeting inflammatory pathways in myocardial infarction. *European Journal of Clinical Investigation 43*(9), 986–995.

Collins, C. E., La, D. T., Yang, H. T., Massin, F., Gibot, S., Faure, G., & Stohl, W. (2009). Elevated synovial expression of triggering receptor expressed on myeloid cells 1 in patients with septic arthritis or rheumatoid arthritis. *Annals of the Rheumatic Diseases 68*(11), 1768–1774.

Colonna, M. (2003). TREMs in the immune system and beyond. *Nature Reviews. Immunology 3*(6), 445–453.

Coussens, L. M., & Werb, Z. (2002). Inflammation and cancer. *Nature 420*(6917), 860–867.

Dang, S., Shen, Y., Yin, K., & Zhang, J. (2012). TREM-1 promotes pancreatitis-associated intestinal barrier dysfunction. *Gastroenterology Research and Practice 2012*, 720865.

Dapito, D. H., Mencin, A., Gwak, G. Y., Pradere, J. P., Jang, M. K., Mederacke, I., ... Schwabe, R. F. (2012). Promotion of hepatocellular carcinoma by the intestinal microbiota and TLR4. *Cancer Cell 21*(4), 504–516.

de Haan, J. J., Smeets, M. B., Pasterkamp, G., & Arslan, F. (2013). Danger signals in the initiation of the inflammatory response after myocardial infarction. *Mediators of Inflammation 2013*, 206039.

Debler, J., Schiemann, U., Seybold, U., Mussack, T., Landauer, N., Ladurner, R., & Gross, M. (2003). Heat-shock protein HSP70-2 genotypes in patients with Crohn's disease: A more severe clinical course with intestinal complications in presence of the PstI-polymorphism. *European Journal of Medical Research 8*(3), 120–124.

Del, F. C., Gomez-Pina, V., Lores, V., Soares-Schanoski, A., Fernandez-Ruiz, I., Rojo, B., ... Lopez-Collazo, E. (2008). Monocytes from cystic fibrosis patients are locked in an LPS tolerance state: Down-regulation of TREM-1 as putative underlying mechanism. *PloS One 3*(7), e2667 (del).

Denninger, K. C., Litman, T., Marstrand, T., Moller, K., Svensson, L., Labuda, T., & Andersson, A. (2015). Kinetics of gene expression and bone remodelling in the clinical phase of collagen-induced arthritis. *Arthritis Research & Therapy 17*, 43.

Derive, M., Bouazza, Y., Sennoun, N., Marchionni, S., Quigley, L., Washington, V., ... Gibot, S. (2012). Soluble TREM-like transcript-1 regulates leukocyte activation and controls microbial sepsis. *Journal of Immunology 188*(11), 5585–5592.

Derive, M., Boufenzer, A., Bouazza, Y., Groubatch, F., Alauzet, C., Barraud, D., ... Gibot, S. (2013). Effects of a TREM-like transcript 1-derived peptide during hypodynamic septic shock in pigs. *Shock (Augusta, Ga.) 39*(2), 176–182.

Derive, M., Boufenzer, A., & Gibot, S. (2014). Attenuation of responses to endotoxin by the triggering receptor expressed on myeloid cells-1 inhibitor LR12 in nonhuman primate. *Anesthesiology 120*(4), 935–942.

Edmonds, R. D., Vodovotz, Y., Lagoa, C., Dutta-Moscato, J., Yang, Y., Fink, M. P., ... Billiar, T. R. (2011). Transcriptomic response of murine liver to severe injury and hemorrhagic shock: A dual-platform microarray analysis. *Physiological Genomics 43*(20), 1170–1183.

El Mezayen, R., El Gazzar, M., Seeds, M. C., McCall, C. E., Dreskin, S. C., & Nicolls, M. R. (2007). Endogenous signals released from necrotic cells augment inflammatory responses to bacterial endotoxin. *Immunology Letters 111*, 36–44.

Esaki, M., Furuse, M., Matsumoto, T., Aoyagi, K., Jo, Y., Yamagata, H., ... Fujishima, M. (1999). Polymorphism of heat-shock protein gene HSP70-2 in Crohn disease:

Possible genetic marker for two forms of Crohn disease. *Scandinavian Journal of Gastroenterology 34*(7), 703–707.
Famulski, K. S., de Freitas, D. G., Kreepala, C., Chang, J., Sellares, J., Sis, B., ... Halloran, P. F. (2012). Molecular phenotypes of acute kidney injury in kidney transplants. *Journal of the American Society of Nephrology 23*(5), 948–958.
Fan, D., He, X., Bian, Y., Guo, Q., Zheng, K., Zhao, Y., ... Lu, A. (2016). Triptolide modulates TREM-1 signal pathway to inhibit the inflammatory response in rheumatoid arthritis. *International Journal of Molecular Sciences 17*(4).
Faxon, D. P., Gibbons, R. J., Chronos, N. A., Gurbel, P. A., Sheehan, F., & Investigators, H. -M. (2002). The effect of blockade of the CD11/CD18 integrin receptor on infarct size in patients with acute myocardial infarction treated with direct angioplasty: the results of the HALT-MI study. *Journal of the American College of Cardiology 40*(7), 1199–1204.
Feinman, R., Deitch, E. A., Aris, V., Chu, H. B., Abungu, B., Caputo, F. J., ... Soteropoulos, P. (2007). Molecular signatures of trauma-hemorrhagic shock-induced lung injury: Hemorrhage- and injury-associated genes. *Shock 28*(3), 360–368.
Feng, J. Y., & Li, Y. Y. (2010). Alteration and role of heat shock proteins in acute pancreatitis. *Journal of Digestive Diseases 11*(5), 277–283.
Ferat-Osorio, E., Wong-Baeza, I., Esquivel-Callejas, N., Figueroa-Figueroa, S., Duarte-Rojo, A., Guzman-Valdivia-Gomez, G., ... Isibasi, A. (2009). Triggering receptor expressed on myeloid cells-1 expression on monocytes is associated with inflammation but not with infection in acute pancreatitis. *Critical Care 13*(3), R69.
Fortin, C. F., Lesur, O., & Fulop, T., Jr. (2007). Effects of TREM-1 activation in human neutrophils: activation of signaling pathways, recruitment into lipid rafts and association with TLR4. *International Immunology 19*(1), 41–50.
Fresno, C., Garcia-Rio, F., Gomez-Pina, V., Soares-Schanoski, A., Fernandez-Ruiz, I., Jurado, T., ... Lopez-Collazo, E. (2009). Potent phagocytic activity with impaired antigen presentation identifying lipopolysaccharide-tolerant human monocytes: Demonstration in isolated monocytes from cystic fibrosis patients. *Journal of Immunology 182*(10), 6494–6507.
Gao, Y., Li, X., Yang, M., Zhao, Q., Liu, X., Wang, G., ... Zhang, Y. (2013). Colitis-accelerated colorectal cancer and metabolic dysregulation in a mouse model. *Carcinogenesis 34*(8), 1861–1869.
Gibot, S. (2005). Clinical review: Role of triggering receptor expressed on myeloid cells-1 during sepsis. *Critical Care 9*(5), 485–489.
Gibot, S. (2006). The therapeutic potential of TREM-1 modulation in the treatment of sepsis and beyond. *Current Opinion in Investigational Drugs 7*(5), 438–442.
Gibot, S., Alauzet, C., Massin, F., Sennoune, N., Faure, G. C., Béné, M. -C., ... Lévy, B. (2006a). Modulation of the triggering receptor expressed on myeloid cells-1 pathway during pneumonia in rats. *The Journal of Infectious Diseases 194*(7), 975–983.
Gibot, S., Buonsanti, C., Massin, F., Romano, M., Kolopp-Sarda, M. N., Benigni, F., ... Levy, B. (2006b). Modulation of the triggering receptor expressed on the myeloid cell type 1 pathway in murine septic shock. *Infection and Immunity 74*(5), 2823–2830.
Gibot, S., Kolopp-Sarda, M. -N., Béné, M. -C., Bollaert, P. -E., Lozniewski, A., Mory, F., ... Faure, G. C. (2004). A soluble form of the triggering receptor expressed on myeloid cells-1 modulates the inflammatory response in murine sepsis. *The Journal of Experimental Medicine 200*(11), 1419–1426.
Gibot, S., Le Renard, P. E., Bollaert, P. E., Kolopp-Sarda, M. N., Bene, M. C., Faure, G. C., & Levy, B. (2005). Surface triggering receptor expressed on myeloid cells 1 expression patterns in septic shock. *Intensive Care Medicine 31*(4), 594–597.
Gibot, S., Massin, F., Alauzet, C., Derive, M., Montemont, C., Collin, S., ... Levy, B. (2009b). Effects of the TREM 1 pathway modulation during hemorrhagic shock in rats. *Shock (Augusta, Ga.) 32*(6), 633–637.
Gibot, S., Massin, F., Alauzet, C., Montemont, C., Lozniewski, A., Bollaert, P. -E., & Levy, B. (2008). Effects of the TREM-1 pathway modulation during mesenteric ischemia-reperfusion in rats. *Critical Care Medicine 36*(2), 504–510.
Gingras, M. C., Lapillonne, H., & Margolin, J. F. (2002). TREM-1, MDL-1, and DAP12 expression is associated with a mature stage of myeloid development. *Molecular Immunology 38*(11), 817–824.
Golovkin, A. S., Ponasenko, A. V., Khutornaya, M. V., Kutikhin, A. G., Salakhov, R. R., Yuzhalin, A. E., ... Barbarash, L. S. (2014). Association of TLR and TREM-1 gene polymorphisms with risk of coronary artery disease in a Russian population. *Gene 550*(1), 101–109.
Gomez-Pina, V., Soares-Schanoski, A., Rodriguez-Rojas, A., Del Fresno, C., Garcia, F., Vallejo-Cremades, M. T., ... Lopez-Collazo, E. (2007). Metalloproteinases shed TREM-1 ectodomain from lipopolysaccharide-stimulated human monocytes. *Journal of Immunology 179*(6), 4065–4073.
Grabner, R., Lotzer, K., Dopping, S., Hildner, M., Radke, D., Beer, M., ... Habenicht, A. J. (2009). Lymphotoxin beta receptor signaling promotes tertiary lymphoid organogenesis in the aorta adventitia of aged ApoE−/− mice. *The Journal of Experimental Medicine 206*(1), 233–248.
Harpster, M. H., Bandyopadhyay, S., Thomas, D. P., Ivanov, P. S., Keele, J. A., Pineguina, N., ... Stayton, M. M. (2006). Earliest changes in the left ventricular transcriptome postmyocardial infarction. *Mammalian Genome 17*(7), 701–715.
Harward, T. R., Brooks, D. L., Flynn, T. C., & Seeger, J. M. (1993). Multiple organ dysfunction after mesenteric artery revascularization. *Journal of Vascular Surgery 18*(3), 459–467.
Haselmayer, P., Grosse-Hovest, L., von Landenberg, P., Schild, H., & Radsak, M. P. (2007). TREM-1 ligand expression on platelets enhances neutrophil activation. *Blood 110*(3), 1029–1035.
Hierholzer, C., Harbrecht, B., Menezes, J. M., Kane, J., MacMicking, J., Nathan, C. F., ... Tweardy, D. J. (1998). Essential role of induced nitric oxide in the initiation of the inflammatory response after hemorrhagic shock. *The Journal of Experimental Medicine 187*(6), 917–928.
Ho, C. C., Liao, W. Y., Wang, C. Y., Lu, Y. H., Huang, H. Y., Chen, H. Y., ... Yang, P. C. (2008). TREM-1 expression in tumor-associated macrophages and clinical outcome in lung cancer. *American Journal of Respiratory and Critical Care Medicine 177*(7), 763–770.
Hu, Z., Wang, X., Gong, L., Wu, G., Peng, X., & Tang, X. (2015). Role of high-mobility group box 1 protein in inflammatory bowel disease. *Inflammation Research 64*(8), 557–563.
Hunt, D. L., Campbell, P. H., Zambon, A. C., Vranizan, K., Evans, S. M., Kuo, H. C., ... McCulloch, A. D. (2012). Early postmyocardial infarction survival in Murphy Roths Large mice is mediated by attenuated apoptosis and inflammation but depends on genetic background. *Experimental Physiology 97*(1), 102–114.
Hyder, L. A., Gonzalez, J., Harden, J. L., Johnson-Huang, L. M., Zaba, L. C., Pierson, K. C., ... Lowes, M. A. (2013). TREM-1 as a potential therapeutic target in psoriasis. *The Journal of Investigative Dermatology 133*(7), 1742–1751.
Iurlaro, R., & Muñoz-Pinedo, C. (2016). Cell death induced by endoplasmic reticulum stress. *The FEBS Journal 283*(14), 2640–2652.
Jenq, R. R., Ubeda, C., Taur, Y., Menezes, C. C., Khanin, R., Dudakov, J. A., ... van den Brink, M. R. (2012). Regulation of intestinal inflammation by microbiota following allogeneic bone marrow transplantation. *The Journal of Experimental Medicine 209*(5), 903–911.
Joffre, J., Hau, E., Zeboudj, L., Laurans, L., Battistella, M., Boufenzer, A., ... Ait-Oufella, H. (2016a). Trem-1 is not crucial in psoriasiform imiquimod-induced skin inflammation in mice. *Experimental Dermatology 25*(5), 400–402.
Joffre, J., Potteaux, S., Zeboudj, L., Loyer, X., Boufenzer, A., Laurans, L., ... Ait-Oufella, H. (2016b). *Genetic and pharmacological inhibition of TREM-1 limits the development of experimental atherosclerosis.*
Jones, Q., Voegeli, T. S., Li, G., Chen, Y., & Currie, R. W. (2011). Heat shock proteins protect against ischemia and inflammation through multiple mechanisms. *Inflammation & Allergy Drug Targets 10*(4), 247–259.
Jung, E. S., Kim, S. W., Moon, C. M., Shin, D. -J., Son, N. -H., Kim, E. S., ... Cheon, J. H. (2011). Relationships between genetic polymorphisms of triggering receptor expressed on myeloid cells-1 and inflammatory bowel diseases in the Korean population. *Life Sciences 89*(9–10), 289–294.
Kadara, H., Fujimoto, J., Yoo, S. Y., Maki, Y., Gower, A. C., Kabbout, M., ... Wistuba, I. I. (2014). Transcriptomic architecture of the adjacent airway field cancerization in non-small cell lung cancer. *Journal of the National Cancer Institute 106*(3), dju004.
Kamei, K., Yasuda, T., Ueda, T., Qiang, F., Takeyama, Y., & Shiozaki, H. (2010). Role of triggering receptor expressed on myeloid cells-1 in experimental severe acute pancreatitis. *Journal of Hepato-Biliary-Pancreatic Sciences 17*(3), 305–312.
Kanellakis, P., Agrotis, A., Kyaw, T. S., Koulis, C., Ahrens, I., Mori, S., ... Bobik, A. (2011). High-mobility group box protein 1 neutralization reduces development of diet-induced atherosclerosis in apolipoprotein e-deficient mice. *Arteriosclerosis, Thrombosis, and Vascular Biology 31*(2), 313–319.
Kao, R. L., Xu, X., Xenocostas, A., Parry, N., Mele, T., Martin, C. M., & Rui, T. (2014). Induction of acute lung inflammation in mice with hemorrhagic shock and resuscitation: Role of HMGB1. *Journal of Inflammation (London) 11*(1), 30.
Keestra-Gounder, A. M., Byndloss, M. X., Seyffert, N., Young, B. M., Chavez-Arroyo, A., Tsai, A. Y., ... Tsolis, R. M. (2016). NOD1 and NOD2 signalling links ER stress with inflammation. *Nature 532*(7599), 394–397.
Kelker, M. S., Debler, E. W., & Wilson, I. A. (2004). Crystal structure of mouse triggering receptor expressed on myeloid cells 1 (TREM-1) at 1.76 A. *Journal of Molecular Biology 344*(5), 1175–1181.
Kim, T. H., Lee, B., Kwon, E., Choi, S. J., Lee, Y. H., Song, G. G., ... Ji, J. D. (2013). Regulation of TREM-1 expression by 1,25-dihydroxyvitamin D3 in human monocytes/macrophages. *Immunology Letters 154*(1–2), 80–85.
Klausz, G., Molnar, T., Nagy, F., Gyulai, Z., Boda, K., Lonovics, J., & Mandi, Y. (2005). Polymorphism of the heat-shock protein gene Hsp70-2, but not polymorphisms of the IL-10 and CD14 genes, is associated with the outcome of Crohn's disease. *Scandinavian Journal of Gastroenterology 40*(10), 1197–1204.
Klesney-Tait, J., Keck, K., Li, X., Gilfillan, S., Otero, K., Baruah, S., ... Colonna, M. (2013). Transepithelial migration of neutrophils into the lung requires TREM-1. *The Journal of Clinical Investigation 123*(1), 138–149.
Klesney-Tait, J., Turnbull, I. R., & Colonna, M. (2006). The TREM receptor family and signal integration. *Nature Immunology 7*(12), 1266–1273.
Knapp, S., Gibot, S., de Vos, A., Versteeg, H. H., Colonna, M., & van der Poll, T. (2004). Cutting edge: Expression patterns of surface and soluble triggering receptor expressed on myeloid cells-1 in human endotoxemia. *Journal of Immunology (Baltimore, Md.: 1950) 173*(12), 7131–7134.
Kojima, M., Tanabe, M., Shinoda, M., Yamada, S., Miyasho, T., Suda, K., ... Kitagawa, Y. (2012). Role of high mobility group box chromosomal protein 1 in ischemia-reperfusion injury in the rat small intestine. *The Journal of Surgical Research 178*(1), 466–471.
Kuai, J., Gregory, B., Hill, A., Pittman, D. D., Feldman, J. L., Brown, T., ... Lin, L. L. (2009). TREM-1 expression is increased in the synovium of rheumatoid arthritis patients and induces the expression of pro-inflammatory cytokines. *Rheumatology (Oxford) 48*(11), 1352–1358.
Lech, M., Susanti, H. E., Rommele, C., Grobmayr, R., Gunthner, R., & Anders, H. J. (2012). Quantitative expression of C-type lectin receptors in humans and mice. *International Journal of Molecular Sciences 13*(8), 10113–10131.
Lee, J., Lee, S. Y., Lee, J., Lee, J., Baek, S., Lee, D. G., ... Park, S. H. (2016). Monosodium urate crystal-induced triggering receptor expressed on myeloid cells 1 is associated with acute gouty inflammation. *Rheumatology (Oxford, England) 55*(1), 156–161.
Lee, H. M., Sugino, H., Aoki, C., & Nishimoto, N. (2011). Underexpression of mitochondrial-DNA encoded ATP synthesis-related genes and DNA repair genes in systemic lupus erythematosus. *Arthritis Research & Therapy 13*(2), R63.
Leemans, J. C., Butter, L. M., Pulskens, W. P., Teske, G. J., Claessen, N., van der Poll, T., & Florquin, S. (2009). The role of Toll-like receptor 2 in inflammation and fibrosis during progressive renal injury. *PloS One 4*(5), e5704.
Leemans, J. C., Kors, L., Anders, H. -J., & Florquin, S. (2014). Pattern recognition receptors and the inflammasome in kidney disease. *Nature Reviews. Nephrology 10*(7), 398–414.

Lemarie, J., Huttin, O., Girerd, N., Mandry, D., Juilliere, Y., Moulin, F., ... Selton-Suty, C. (2015). Usefulness of speckle-tracking imaging for right ventricular assessment after acute myocardial infarction: A magnetic resonance imaging/echocardiographic comparison within the relation between aldosterone and cardiac remodeling after myocardial infarction. *Journal of the American Society of Echocardiography 28*(7), 818–827 (e4).

Li, H., Hong, F., Pan, S., Lei, L., & Yan, F. (2016). Silencing triggering receptors expressed on myeloid cells-1 impaired the inflammatory response to oxidized low-density lipoprotein in macrophages. *Inflammation 39*(1), 199–208.

Liao, R., Sun, T. W., Yi, Y., Wu, H., Li, Y. W., Wang, J. X., ... Fan, J. (2012). Expression of TREM-1 in hepatic stellate cells and prognostic value in hepatitis B-related hepatocellular carcinoma. *Cancer Science 103*(6), 984–992.

Libby, P., & Hansson, G. K. (2015). Inflammation and immunity in diseases of the arterial tree: Players and layers. *Circulation Research 116*(2), 307–311.

Libby, P., Nahrendorf, M., & Swirski, F. K. (2016). Leukocytes link local and systemic inflammation in ischemic cardiovascular disease: An expanded "cardiovascular continuum.". *Journal of the American College of Cardiology 67*(9), 1091–1103.

Liu, J., Krautzberger, A. M., Sui, S. H., Hofmann, O. M., Chen, Y., Baetscher, M., ... McMahon, A. P. (2014b). Cell-specific translational profiling in acute kidney injury. *The Journal of Clinical Investigation 124*(3), 1242–1254.

Liu, M., Wu, W., Zhao, Q., Feng, Q., & Wang, W. (2015). High expression levels of trigger receptor expressed on myeloid cells-1 on neutrophils associated with increased severity of acute pancreatitis in mice. *Biological & Pharmaceutical Bulletin 38*(10), 1450–1457.

Lo, T. -H., Tseng, K. -Y., Tsao, W. -S., Yang, C. -Y., Hsieh, S. -L., Chiu, A. W. -H., ... Chen, N. -J. (2014). TREM-1 regulates macrophage polarization in ureteral obstruction. *Kidney International 86*(6), 1174–1186.

Lowes, M. A., Bowcock, A. M., & Krueger, J. G. (2007). Pathogenesis and therapy of psoriasis. *Nature 445*(7130), 866–873.

Magna, M., & Pisetsky, D. S. (2014). The role of HMGB1 in the pathogenesis of inflammatory and autoimmune diseases. *Molecular Medicine 20*, 138–146.

Maluf, D. G., Dumur, C. I., Suh, J. L., Lee, J. K., Cathro, H. P., King, A. L., ... Mas, V. R. (2014). Evaluation of molecular profiles in calcineurin inhibitor toxicity post-kidney transplant: Input to chronic allograft dysfunction. *American Journal of Transplantation 14*(5), 1152–1163.

Matzinger, P. (1994). Tolerance, danger, and the extended family. *Annual Review of Immunology 12*, 991–1045.

Meldrum, D. R., Shenkar, R., Sheridan, B. C., Cain, B. S., Abraham, E., & Harken, A. H. (1997). Hemorrhage activates myocardial NFkappaB and increases TNF-alpha in the heart. *Journal of Molecular and Cellular Cardiology 29*(10), 2849–2854.

Meng, Z. H., Dyer, K., Billiar, T. R., & Tweardy, D. J. (2001). Essential role for IL-6 in postresuscitation inflammation in hemorrhagic shock. *American Journal of Physiology. Cell Physiology 280*(2), C343–C351.

Montgomery, S. T., Mall, M. A., Kicic, A., & Stick, S. M. (2017). Hypoxia and sterile inflammation in cystic fibrosis airways: Mechanisms and potential therapies. *European Respiratory Journal 49*(1).

Morales, J., Villa, K., Gattis, J., Castro, W., Colon, K., Lubkowski, J., ... Washington, A. V. (2010). Soluble TLT-1 modulates platelet-endothelial cell interactions and actin polymerization. *Blood Coagulation & Fibrinolysis 21*(3), 229–236.

Moran, A., Thacker, S. A., Arikan, A. A., Mastrangelo, M. A., Wu, Y., Yu, B., & Tweardy, D. J. (2011). IL-6-mediated activation of Stat3alpha prevents trauma/hemorrhagic shock-induced liver inflammation. *PloS One 6*(6), e21449.

Murakami, Y., Akahoshi, T., Aoki, N., Toyomoto, M., Miyasaka, N., & Kohsaka, H. (2009). Intervention of an inflammation amplifier, triggering receptor expressed on myeloid cells 1, for treatment of autoimmune arthritis. *Arthritis and Rheumatism 60*(6), 1615–1623.

Murakami, Y., Akahoshi, T., Hayashi, I., Endo, H., Kawai, S., Inoue, M., ... Kitasato, H. (2006). Induction of triggering receptor expressed on myeloid cells 1 in murine resident peritoneal macrophages by monosodium urate monohydrate crystals. *Arthritis and Rheumatism 54*(2), 455–462.

Murphy, M. E. (2013). The HSP70 family and cancer. *Carcinogenesis 34*(6), 1181–1188.

Nam, S. Y., Kim, N., Kim, J. S., Lim, S. H., Jung, H. C., & Song, I. S. (2007). Heat shock protein gene 70-2 polymorphism is differentially associated with the clinical phenotypes of ulcerative colitis and Crohn's disease. *Journal of Gastroenterology and Hepatology 22*(7), 1032–1038.

Netea, M. G., Azam, T., Ferwerda, G., Girardin, S. E., Kim, S. H., & Dinarello, C. A. (2006). Triggering receptor expressed on myeloid cells-1 (TREM-1) amplifies the signals induced by the NACHT-LRR (NLR) pattern recognition receptors. *Journal of Leukocyte Biology 80*(6), 1454–1461.

Oldenburg, W. A., Lau, L. L., Rodenberg, T. J., Edmonds, H. J., & Burger, C. D. (2004). Acute mesenteric ischemia: A clinical review. *Archives of Internal Medicine 164*(10), 1054–1062.

O'Neill, S., Harrison, E. M., Ross, J. A., Wigmore, S. J., & Hughes, J. (2014). Heat-shock proteins and acute ischaemic kidney injury. *Nephron. Experimental Nephrology 126*(4), 167–174.

Ornatowska, M., Azim, A. C., Wang, X., Christman, J. W., Xiao, L., Joo, M., & Sadikot, R. T. (2007). Functional genomics of silencing TREM-1 on TLR4 signaling in macrophages. *American Journal of Physiology. Lung Cellular and Molecular Physiology 293*(6), L1377–L1384.

Pamuk, O. N., Lapchak, P. H., Rani, P., Pine, P., Dalle Lucca, J. J., & Tsokos, G. C. (2010). Spleen tyrosine kinase inhibition prevents tissue damage after ischemia-reperfusion. *American Journal of Physiology. Gastrointestinal and Liver Physiology 299*(2), G391–G399.

Panes, J., & Granger, D. N. (1998). Leukocyte-endothelial cell interactions: Molecular mechanisms and implications in gastrointestinal disease. *Gastroenterology 114*(5), 1066–1090.

Park, J. J., Cheon, J. H., Kim, B. Y., Kim, D. H., Kim, E. S., Kim, T. I., ... Kim, W. H. (2009). Correlation of serum-soluble triggering receptor expressed on myeloid cells-1 with clinical disease activity in inflammatory bowel disease. *Digestive Diseases and Sciences 54*(7), 1525–1531.

Patching, S. G. (2014). Surface plasmon resonance spectroscopy for characterisation of membrane protein-ligand interactions and its potential for drug discovery. *Biochimica et Biophysica Acta 1838*(1 Pt A), 43–55.

Prufer, S., Weber, M., Sasca, D., Teschner, D., Wolfel, C., Stein, P., ... Radsak, M. P. (2014). Distinct signaling cascades of TREM-1, TLR and NLR in neutrophils and monocytic cells. *Journal of Innate Immunity 6*(3), 339–352.

Pulskens, W. P., Rampanelli, E., Teske, G. J., Butter, L. M., Claessen, N., Luirink, I. K., ... Leemans, J. C. (2010). TLR4 promotes fibrosis but attenuates tubular damage in progressive renal injury. *Journal of the American Society of Nephrology 21*(8), 1299–1308.

Rai, V., Rao, V. H., Shao, Z., & Agrawal, D. K. (2016). Dendritic cells expressing triggering receptor expressed on myeloid cells-1 correlate with plaque stability in symptomatic and asymptomatic patients with carotid stenosis. *PloS One 11*(5), e0154802.

Rao, V. H., Rai, V., Stoupa, S., Subramanian, S., & Agrawal, D. K. (2016a). Data on TREM-1 activation destabilizing carotid plaques. *Data in Brief 8*, 230–234.

Rao, V. H., Rai, V., Stoupa, S., Subramanian, S., & Agrawal, D. K. (2016b). Tumor necrosis factor-α regulates triggering receptor expressed on myeloid cells-1-dependent matrix metalloproteinases in the carotid plaques of symptomatic patients with carotid stenosis. *Atherosclerosis 248*, 160–169.

Read, C. B., Kuijper, J. L., Hjorth, S. A., Heipel, M. D., Tang, X., Fleetwood, A. J., ... Stennicke, V. W. (2015). Cutting edge: Identification of neutrophil PGLYRP1 as a ligand for TREM-1. *Journal of Immunology 194*(4), 1417–1421.

Rigo, I., McMahon, L., Dhawan, P., Christakos, S., Yim, S., Ryan, L. K., & Diamond, G. (2012). Induction of triggering receptor expressed on myeloid cells (TREM-1) in airway epithelial cells by 1,25(OH)(2) vitamin D(3). *Innate Immunity 18*(2), 250–257.

Roe, K., Gibot, S., & Verma, S. (2014). Triggering receptor expressed on myeloid cells-1 (TREM-1): A new player in antiviral immunity? *Frontiers in Microbiology 5*, 627.

Roy, S., Khanna, S., Kuhn, D. E., Rink, C., Williams, W. T., Zweier, J. L., & Sen, C. K. (2006). Transcriptome analysis of the ischemia-reperfused remodeling myocardium: Temporal changes in inflammation and extracellular matrix. *Physiological Genomics 25*(3), 364–374.

Rubin, D. C., Shaker, A., & Levin, M. S. (2012). Chronic intestinal inflammation: Inflammatory bowel disease and colitis-associated colon cancer. *Frontiers in Immunology 3*, 107.

Saha, S., Jing, X., Park, S. Y., Wang, S., Li, X., Gupta, D., & Dziarski, R. (2010). Peptidoglycan recognition proteins protect mice from experimental colitis by promoting normal gut flora and preventing induction of interferon-gamma. *Cell Host & Microbe 8*(2), 147–162.

Schenk, M., Bouchon, A., Seibold, F., & Mueller, C. (2007). TREM-1—Expressing intestinal macrophages crucially amplify chronic inflammation in experimental colitis and inflammatory bowel diseases. *The Journal of Clinical Investigation 117*(10), 3097–3106.

Schmausser, B., Endrich, S., Beier, D., Moran, A. P., Burek, C. J., Rosenwald, A., ... Eck, M. (2008). Triggering receptor expressed on myeloid cells-1 (TREM-1) expression on gastric epithelium: implication for a role of TREM-1 in *Helicobacter pylori* infection. *Clinical and Experimental Immunology 152*(1), 88–94.

Sharif, O., & Knapp, S. (2008). From expression to signaling: Roles of TREM-1 and TREM-2 in innate immunity and bacterial infection. *Immunobiology 213*(9–10), 701–713.

Sherman, M. Y., & Gabai, V. L. (2015). Hsp70 in cancer: Back to the future. *Oncogene 34*(32), 4153–4161.

Shi, Y., Evans, J. E., & Rock, K. L. (2003). Molecular identification of a danger signal that alerts the immune system to dying cells. *Nature 425*(6957), 516–521.

Shimizu, T., Tani, T., Endo, Y., Hanasawa, K., Tsuchiya, M., & Kodama, M. (2002). Elevation of plasma peptidoglycan and peripheral blood neutrophil activation during hemorrhagic shock: Plasma peptidoglycan reflects bacterial translocation and may affect neutrophil activation. *Critical Care Medicine 30*(1), 77–82.

Siveke, J. T., Lubeseder-Martellato, C., Lee, M., Mazur, P. K., Nakhai, H., Radtke, F., & Schmid, R. M. (2008). Notch signaling is required for exocrine regeneration after acute pancreatitis. *Gastroenterology 134*(2), 544–555.

Smolen, J. S., Aletaha, D., & McInnes, I. B. (2016). Rheumatoid arthritis. *The Lancet 388*(10055), 2023–2038.

Sodhi, C. P., Jia, H., Yamaguchi, Y., Lu, P., Good, M., Egan, C., ... Hackam, D. J. (2015). Intestinal epithelial TLR-4 activation is required for the development of acute lung injury after trauma/hemorrhagic shock via the release of HMGB1 from the gut. *Journal of Immunology 194*(10), 4931–4939.

Stephenson, H. N., Herzig, A., & Zychlinsky, A. (2016). Beyond the grave: When is cell death critical for immunity to infection? *Current Opinion in Immunology 38*, 59–66.

Suarez-Farinas, M., Arbeit, R., Jiang, W., Ortenzio, F. S., Sullivan, T., & Krueger, J. G. (2013). Suppression of molecular inflammatory pathways by Toll-like receptor 7, 8, and 9 antagonists in a model of IL-23-induced skin inflammation. *PloS One 8*(12), e84634.

Swank, G. M., & Deitch, E. A. (1996). Role of the gut in multiple organ failure: Bacterial translocation and permeability changes. *World Journal of Surgery 20*(4), 411–417.

Swindell, W. R., Johnston, A., Carbajal, S., Han, G., Wohn, C., Lu, J., ... Gudjonsson, J. E. (2011). Genome-wide expression profiling of five mouse models identifies similarities and differences with human psoriasis. *PloS One 6*(4), e18266.

Swirski, F. K., & Nahrendorf, M. (2013). Leukocyte behavior in atherosclerosis, myocardial infarction, and heart failure. *Science 339*(6116), 161–166.

Tammaro, A., Kers, J., Emal, D., Stroo, I., Teske, G. J. D., Butter, L. M., ... Dessing, M. C. (2016). Effect of TREM-1 blockade and single nucleotide variants in experimental renal injury and kidney transplantation. *Scientific Reports 6*, 38275.

Tammaro, A., Stroo, I., Rampanelli, E., Blank, F., Butter, L. M., Claessen, N., ... Dessing, M. C. (2013). Role of TREM1-DAP12 in renal inflammation during obstructive nephropathy. *PloS One 8*(12), e82498.

Tanaka, K., Namba, T., Arai, Y., Fujimoto, M., Adachi, H., Sobue, G., ... Mizushima, T. (2007). Genetic evidence for a protective role for heat shock factor 1 and heat shock protein 70 against colitis. *The Journal of Biological Chemistry 282*(32), 23240–23252.
Tarnavski, O., McMullen, J. R., Schinke, M., Nie, Q., Kong, S., & Izumo, S. (2004). Mouse cardiac surgery: Comprehensive techniques for the generation of mouse models of human diseases and their application for genomic studies. *Physiological Genomics 16*(3), 349–360.
Tessarz, A. S., & Cerwenka, A. (2008). The TREM-1/DAP12 pathway. *Immunology Letters 116*(2), 111–116.
Tsung, A., Tohme, S., & Billiar, T. R. (2014). High-mobility group box-1 in sterile inflammation. *Journal of Internal Medicine 276*(5), 425–443.
Ulmasov, B., Oshima, K., Rodriguez, M. G., Cox, R. D., & Neuschwander-Tetri, B. A. (2013). Differences in the degree of cerulein-induced chronic pancreatitis in C57BL/6 mouse substrains lead to new insights in identification of potential risk factors in the development of chronic pancreatitis. *The American Journal of Pathology 183*(3), 692–708.
van Kempen, L. C., de Visser, K. E., & Coussens, L. M. (2006). Inflammation, proteases and cancer. *European Journal of Cancer 42*(6), 728–734.
Venereau, E., Ceriotti, C., & Bianchi, M. E. (2015). DAMPs from cell death to new life. *Frontiers in Immunology 6*, 422.
Wang, Y. S., Li, X. J., & Zhao, W. O. (2012). TREM-1 is a positive regulator of TNF-alpha and IL-8 production in U937 foam cells. *Bosnian Journal of Basic Medical Sciences 12*(2), 94–101.
Wang, D. Y., Qin, R. Y., Liu, Z. R., Gupta, M. K., & Chang, Q. (2004). Expression of TREM-1 mRNA in acute pancreatitis. *World Journal of Gastroenterology 10*(18), 2744–2746.
Wang, X., Xiang, L., Li, H., Chen, P., Feng, Y., Zhang, J., ... Cao, F. (2015). The role of HMGB1 signaling pathway in the development and progression of hepatocellular carcinoma: A review. *International Journal of Molecular Sciences 16*(9), 22527–22540.
Washington, A. V., Gibot, S., Acevedo, I., Gattis, J., Quigley, L., Feltz, R., ... McVicar, D. W. (2009a). TREM-like transcript-1 protects against inflammation-associated hemorrhage by facilitating platelet aggregation in mice and humans. *The Journal of Clinical Investigation 119*(6), 1489–1501.
Weber, B., Schuster, S., Zysset, D., Rihs, S., Dickgreber, N., Schürch, C., ... Mueller, C. (2014). TREM-1 deficiency can attenuate disease severity without affecting pathogen clearance. *PLoS Pathogens 10*(1), e1003900.
Wu, B., & Brooks, J. D. (2012). Gene expression changes induced by unilateral ureteral obstruction in mice. *The Journal of Urology 188*(3), 1033–1041.
Wu, J., Li, J., Salcedo, R., Mivechi, N. F., Trinchieri, G., & Horuzsko, A. (2012). The proinflammatory myeloid cell receptor TREM-1 controls Kupffer cell activation and development of hepatocellular carcinoma. *Cancer Research 72*(16), 3977–3986.
Xie, F., Zhan, R., Yan, L. C., Gong, J. B., Zhao, Y., Ma, J., & Qian, L. J. (2016). Diet-induced elevation of circulating HSP70 may trigger cell adhesion and promote the development of atherosclerosis in rats. *Cell Stress & Chaperones 21*(5), 907–914.
Yang, H., Antoine, D. J., Andersson, U., & Tracey, K. J. (2013). The many faces of HMGB1: Molecular structure-functional activity in inflammation, apoptosis, and chemotaxis. *Journal of Leukocyte Biology 93*(6), 865–873.
Yang, H., & Tracey, K. J. (2010). Targeting HMGB1 in inflammation. *Biochimica et Biophysica Acta 1799*(1–2), 149–156.
Yashin, D. V., Ivanova, O. K., Soshnikova, N. V., Sheludchenkov, A. A., Romanova, E. A., Dukhanina, E. A., ... Sashchenko, L. P. (2015). Tag7 (PGLYRP1) in complex with Hsp70 induces alternative cytotoxic processes in tumor cells via TNFR1 receptor. *The Journal of Biological Chemistry 290*(35), 21724–21731.
Yasuda, T., Takeyama, Y., Ueda, T., Shinzeki, M., Sawa, H., Takahiro, N., ... Ohyanagi, H. (2008). Increased levels of soluble triggering receptor expressed on myeloid cells-1 in patients with acute pancreatitis. *Critical Care Medicine 36*(7), 2048–2053.
Yin, C., Mohanta, S., Ma, Z., Weber, C., Hu, D., Weih, F., & Habenicht, A. (2015). Generation of aorta transcript atlases of wild-type and apolipoprotein E-null mice by laser capture microdissection-based mRNA expression microarrays. *Methods in Molecular Biology 1339*, 297–308.
Yuan, Z., Mehta, H. J., Mohammed, K., Nasreen, N., Roman, R., Brantly, M., & Sadikot, R. T. (2014a). TREM-1 is induced in tumor associated macrophages by cyclo-oxygenase pathway in human non-small cell lung cancer. *PloS One 9*(5), e94241.
Yuan, Z., Syed, M., Panchal, D., Joo, M., Bedi, C., Lim, S., ... Sadikot, R. T. (2016). TREM-1-accentuated lung injury via miR-155 is inhibited by LP17 nanomedicine. *American Journal of Physiology. Lung Cellular and Molecular Physiology 310*(5), L426–L438.
Yuan, Z., Syed, M. A., Panchal, D., Joo, M., Colonna, M., Brantly, M., & Sadikot, R. T. (2014b). Triggering receptor expressed on myeloid cells 1 (TREM-1)-mediated Bcl-2 induction prolongs macrophage survival. *The Journal of Biological Chemistry 289*(21), 15118–15129.
Zeng, H., Ornatowska, M., Joo, M. S., & Sadikot, R. T. (2007). TREM-1 expression in macrophages is regulated at transcriptional level by NF-kappaB and PU.1. *European Journal of Immunology 37*(8), 2300–2308.
Zhou, J., Chai, F., Lu, G., Hang, G., Chen, C., Chen, X., & Shi, J. (2013). TREM-1 inhibition attenuates inflammation and tumor within the colon. *International Immunopharmacology 17*(2), 155–161.
Zhou, R. R., Kuang, X. Y., Huang, Y., Li, N., Zou, M. X., Tang, D. L., & Fan, X. G. (2014). Potential role of high mobility group box 1 in hepatocellular carcinoma. *Cell Adhesion & Migration 8*(5), 493–498.
Zhou, J., Werstuck, G. H., Lhotak, S., de Koning, A. B., Sood, S. K., Hossain, G. S., ... Austin, R. C. (2004). Association of multiple cellular stress pathways with accelerated atherosclerosis in hyperhomocysteinemic apolipoprotein E-deficient mice. *Circulation 110*(2), 207–213.
Zulfiqar, F., Hozo, I., Rangarajan, S., Mariuzza, R. A., Dziarski, R., & Gupta, D. (2013). Genetic association of peptidoglycan recognition protein variants with inflammatory bowel disease. *PloS One 8*(6), e67393.
Zysset, D., Weber, B., Rihs, S., Brasseit, J., Freigang, S., Riether, C., ... Mueller, C. (2016). TREM-1 links dyslipidemia to inflammation and lipid deposition in atherosclerosis. *Nature Communications 7*, 13151.

Supplementary Information

TREM-1 and its potential ligands in non-infectious diseases: from biology to clinical perspectives

Tammaro Alessandra[1], Derive Marc[2], Gibot Sebastien[3,4], Leemans Jaklien C.[1], Florquin Sandrine[1,5] and Dessing Mark C.[1]

[1]Department of Pathology, Academic Medical Center, University of Amsterdam, Amsterdam, the Netherlands. [2]INOTREM, Nancy, France. [3]Medical Intensive Care Unit, Hôpital Central, CHU Nancy, Nancy, France. [4]Inserm UMR_S1116, Faculté de Médecine, Université de Lorraine, Nancy, France. [5]Department of Pathology, Radboud University Nijmegen Medical Center, Nijmegen, the Netherlands. *Correspondence and requests for materials should be addressed to A.T. (email: a.tammaro@amc.uva.nl)

Supplementary Methods

TREM-1 signaling pathway enrichment based on Ingenuity Pathway Analysis

Using IPA (Ingenuity® Pathway Analysis, Qiagen; www.ingenuity.com) we obtained a report of 45 genes related to TREM-1 signaling pathway, chosen by Qiagen. This list of genes was uploaded to Nextbio (Illumina; www.nextbio.com) as a bioset, analyzed and compared to public genome data sets curated by Illumina. Obtained studies were further selected based on several filters including species (mus musculus), keywords relative to acute or chronic non-infectious diseases, genetic background (exclusion of knockout animals), RNA profiling performed in the tissue related to specific disease and acceptable sample size. The keywords to identify the studies included ischemia, colitis, arthritis, fibrosis, hepatocellular carcinoma, pancreatitis or atherosclerosis. The source and GSE numbers of the final selected studies are displayed in supplementary Table S2. Among the selected studies, Nextbio analyzed the number of overlapping genes between the TREM-1 bioset and selected genome datasets (x out of 45 genes). Purple bars show the number of genes belonging to TREM-1 signaling pathway which overlap with the gene dataset of each selected study. The significance for the enrichment is calculated using the Fisher's exact test for the overlap between the two datasets. The average of overlapping genes and significance for pathway enrichment was calculated if multiple datasets per disease group were available.

Supplementary Table S1: TREM-1 signaling pathway. Genes related to TREM-1 signaling pathway provided by IPA (Ingenuity® Pathway Analysis, Qiagen; www.ingenuity.com/).

Official symbol	Entrez Gene Name
AKT1	v-akt murine thymoma viral oncogene homolog 1
DEFB4A	defensin beta 4A
CASP1	caspase 1
CASP5	caspase 5
ITGB1	integrin subunit beta 1
FCGR2A	Fc fragment of IgG receptor IIa
FCGR2B	Fc fragment of IgG receptor IIb
FCGR2C	Fc fragment of IgG receptor IIc
CD40	CD40 molecule
ICAM1	intercellular adhesion molecule 1
CD83	CD83 molecule
CD86	CD86 molecule
ITGAX	integrin subunit alpha X
ITGA5	integrin subunit alpha 5
TYROBP	TYRO protein tyrosine kinase binding protein
MAPK3	mitogen-activated protein kinase 3
MAPK1	mitogen-activated protein kinase 1
CSF2	colony stimulating factor 2
GRB2	growth factor receptor bound protein 2
IL6	interleukin 6
CXCL8	chemokine (C-X-C motif) ligand 8
IL10	interleukin 10
IL18	interleukin 18
IL1B	interleukin 1 beta
IRAK1	interleukin 1 receptor associated kinase 1
JAK2	Janus kinase 2
CCL2	chemokine (C-C motif) ligand 2
CCL7	chemokine (C-C motif) ligand 7
CXCL3	chemokine (C-X-C motif) ligand 3
CCL3	chemokine (C-C motif) ligand 3
MPO	myeloperoxidase
MYD88	myeloid differentiation primary response 88
NFKB1	nuclear factor of kappa light polypeptide gene enhancer in B-cells 1
NFKB2	nuclear factor of kappa light polypeptide gene enhancer in B-cells 2
NOD2	nucleotide binding oligomerization domain containing 2
LAT2	linker for activation of T-cells family member 2
SIGIRR	single immunoglobulin and toll-interleukin 1 receptor (TIR) domain
IL1RL1	interleukin 1 receptor like 1
STAT3	signal transducer and activator of transcription 3
STAT5A	signal transducer and activator of transcription 5A
STAT5B	signal transducer and activator of transcription 5B
TLR2	toll-like receptor 2
TLR4	toll-like receptor 4
TNF	tumor necrosis factor
TREM1	triggering receptor expressed on myeloid cells 1

Supplementary Table S2: Datasets selected for TREM-1 signaling pathway enrichment. GSE number of public genome datasets selected for in silico analysis available in Nextbio (Illumina; www.nextbio.com). Available studies were filtered by species (mus musculus), keywords related to specific disease, genetic background (exclusion of knockout animals), acceptable sample size and when RNA profiling was done in tissue related to specific disease. GSE: Genomic Spatial Event database

Tissue	Disease	GSE
Heart	Myocardial ischemia	GSE775
		GSE4105
		GSE23294
		GSE19322
Circulation	Atherosclerosis	GSE21419
		GSE38574
		GSE40156
		GSE10000
Intestine	IBD / Colitis	GSE9293
		GSE18163
		GSE64658
		GSE36806
		GSE9281
		GSE19793
Joint	Collagen-induced arthritis	GSE13071
	Serum-induced arthritis	GSE22971
		GSE27492
Kidney	Renal fibrosis	GSE36496
		GSE38117
		GSE55808
	Renal ischemia	GSE39548
		GSE52004
		GSE34351
Liver	Hepatocellular carcinoma	GSE32244
		GSE50431
		GSE37129
		GSE44356
		GSE33446
Pancreas	Pancreatitis	GSE41418
Skin	Imiquimod-induced Psoriasis	GSE2768

Chapter 5

Effect of TREM-1 blockade and single nucleotide variants in experimental renal injury and kidney transplantation

Scientific Reports 2016 Dec 8;6:38275

SCIENTIFIC REPORTS

OPEN

Received: 21 April 2016
Accepted: 07 November 2016
Published: 08 December 2016

Effect of TREM-1 blockade and single nucleotide variants in experimental renal injury and kidney transplantation

Alessandra Tammaro[1,*], Jesper Kers[1,*], Diba Emal[1], Ingrid Stroo[1], Gwendoline J. D. Teske[1], Loes M. Butter[1], Nike Claessen[1], Jeffrey Damman[1], Marc Derive[2], Gerjan J. Navis[3], Sandrine Florquin[1,4], Jaklien C. Leemans[1] & Mark C. Dessing[1]

Renal ischemia reperfusion (IR)-injury induces activation of innate immune response which sustains renal injury and contributes to the development of delayed graft function (DGF). Triggering receptor expressed on myeloid cells-1 (TREM-1) is a pro-inflammatory evolutionary conserved pattern recognition receptor expressed on a variety of innate immune cells. TREM-1 expression increases following acute and chronic renal injury. However, the function of TREM-1 in renal IR is still unclear. Here, we investigated expression and function of TREM-1 in a murine model of renal IR using different TREM-1 inhibitors: LP17, LR12 and TREM-1 fusion protein. In a human study, we analyzed the association of non-synonymous single nucleotide variants in the *TREM1* gene in a cohort comprising 1263 matching donors and recipients with post-transplant outcomes, including DGF. Our findings demonstrated that, following murine IR, renal TREM-1 expression increased due to the influx of *Trem1* mRNA expressing cells detected by *in situ* hybridization. However, TREM-1 interventions by means of LP17, LR12 and TREM-1 fusion protein did not ameliorate IR-induced injury. In the human renal transplant cohort, donor and recipient *TREM1* gene variant p.Thr25Ser was not associated with DGF, nor with biopsy-proven rejection or death-censored graft failure. We conclude that TREM-1 does not play a major role during experimental renal IR and after kidney transplantation.

Kidney transplantation is at present the most optimal renal replacement therapy for patients with end-stage renal disease (ESRD). Following transplantation, renal ischemia reperfusion (IR)-induced injury is a major cause of delayed graft function (DGF). DGF is associated with an increased risk for acute rejection and decreased survival of the allograft[1,2]. Innate immunity plays an important role in the mechanism underlying IR-induced injury. Following kidney injury, damage-associated molecular patterns (DAMPs) are released from necrotic cells and recognized by pattern recognition receptors (PRRs) that include toll like receptors (TLRs). Activation of TLRs is known to induce inflammation that affects renal function following IR[3,4]. Over the past decade, an additional family of innate immune receptors has been identified: the triggering receptors expressed on myeloid cells (TREMs)[5–7]. TREM-1 is mainly expressed on granulocytes and monocyte/macrophages in mouse and human[8]. TREM-1 is an activating receptor, which associates with its adaptor molecule TYRO protein tyrosine kinase-binding protein (TYROBP) to induce cytokine production[5–7]. Besides from activating its own intracellular pathway, TREM-1 synergizes with diverse TLRs, leading to an amplified inflammatory responses[5–8]. Most of the studies addressing the pathogenic role of TREM-1 have been performed in infectious disease models[9,10]. The general concept thus far is that TREM-1 is specifically involved in anti-microbial immune responses[11]. Recent evidence, however, has also pointed towards a beneficial effect of TREM-1 inhibition during sterile inflammation, like IR[12,13]. Murine studies have shown that TREM-1 expression increases upon chronic obstructive nephropathy and renal IR[14–16].

[1]Department of Pathology, Academic Medical Center, University of Amsterdam, Amsterdam, the Netherlands. [2]Inserm UMR_S1116, Faculté de Médecine de Nancy, Université de Lorraine, Vandoeuvre-les-Nancy, France. [3]Department of Internal Medicine, Division of Nephrology, University Medical Center Groningen, University of Groningen, Groningen, the Netherlands. [4]Department of Pathology, Radboud University Nijmegen Medical Center, Nijmegen, the Netherlands. *These authors contributed equally to this work. Correspondence and requests for materials should be addressed to A.T. (email: a.tammaro@amc.uva.nl)

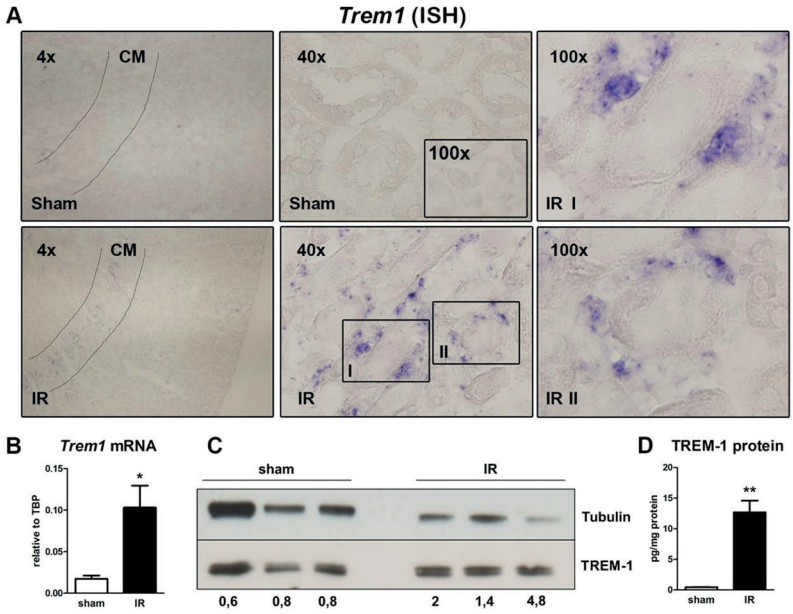

Figure 1. TREM-1 expression is increased in the kidney after IR. *Trem1* transcript expression visualized by using *in situ* hybridization (ISH) in sham and 1 day after bilateral IR. Lines in sham and IR (4× magnification) indicate the cortico-medullary (CM) area. Sham pictures (40×) shows an inset with 100× magnification. From the IR (40×) picture we selected two areas (I and II) to show in higher magnification (100×). Original magnification 4×, 40× and 100× (**A**). Intrarenal *Trem1* transcript quantified by RT-PCR (n = 6–7/group) (**B**) and protein expression as determined by western blot (n = 3) and ELISA (n = 6–7/group) (**C**,**D**). Values are expressed as mean ± SEM. *P < 0.05 vs sham; **P < 0.005 versus sham.

In humans, renal TREM-1 expression has been observed on interstitial cells of patients with obstruction-related hydronephrosis[15]. Blockade of the TREM-1 signaling by a short inhibitory peptide (LP17 and LR12) reduced tissue injury during mesenteric IR and myocardial infarction, emphasizing the potential therapeutic benefit of TREM-1 inhibition in sterile inflammation[12,13]. Currently, the treatment of patients with acute kidney injury in the context of DGF is purely supportive, whereas manipulation of innate immunity during necroinflammation might further reduce alloimmune priming, leading to a reduction in rejection. Moreover, genetic variation may also determine the course of graft injury and be linked to the risk of DGF. In the current study we investigated whether TREM-1 could be a potential target during experimental and human renal IR-induced injury.

We therefore investigated (1) the expression and function of TREM-1 in murine renal IR and (2) determined the association between non-synonymous single nucleotide variants (SNVs) in the *TREM1* gene and outcomes following renal transplantation, with a particular interest for the risk to develop DGF.

Results

Renal ischemic injury leads to increased TREM-1 expression. The S3 segment of the proximal tubules located in the cortico-medullary (CM) area is the most sensitive to ischemic injury[17]. Moreover, the interstitial cells surrounding the ischemic tubules are rich in granulocytes that accumulate in the kidney after reperfusion. Since TREM-1 is expressed on the plasma membrane of granulocytes, we determined renal *Trem1* mRNA expression 24 hours after renal IR. Using *in situ* hybridization, we localized *Trem1* transcript expression in kidney tissues from mice one day after IR. Sham tissues were used as control. *Trem1* mRNA-positive interstitial cells were detected in the CM area, after IR and absent in sham kidney. Noteworthy, baseline or damaged tubular epithelial cells did not stain positive for *Trem1* transcripts (Fig. 1A). Moreover, we quantified renal *Trem1* transcription by RT-PCR (Fig. 1B) and observed an increased expression in IR kidneys compared to sham tissues, which was confirmed on the protein level by western blot and ELISA (Fig. 1C,D). Following IR, inflammatory cells appear in the circulation to subsequently migrate to the site of injury[17]. By FACS analysis, we detected an increased percentage of circulating granulocytes (Fig. 2A) identified as Ly6C/Gr-1 high populations, following IR. Percentage of circulating monocytes (Ly6C/Gr-1 positive-F4-80 low population as shown in Supplementary Fig. S1) instead, were similar between sham and IR mice (Fig. 2B). This suggests that renal *Trem1* mRNA-expressing cells are most likely infiltrating granulocytes. We then checked the surface expression of TREM-1 receptor on circulating

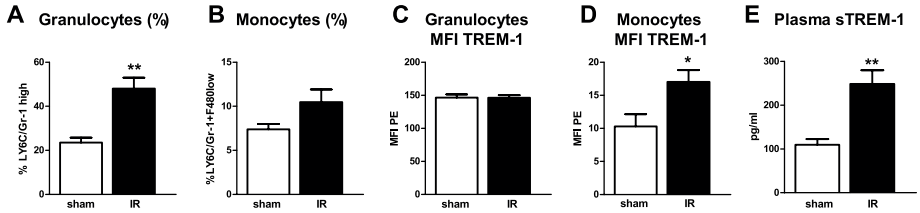

Figure 2. Renal IR increases circulating soluble TREM-1 expression. Percentage of circulating Ly6C/Gr-1 high granulocytes (**A**) and Ly6C/Gr-1+ F4-80 low monocytes (**B**) of total leukocytes, 1 day after IR (the gating strategy can be found as Supplementary Fig. S2). Membrane TREM-1 expression on granulocytes (**C**) and monocytes (**D**) as displayed by mean fluorescence intensity (MFI) (n = 5–8/group). Circulating TREM-1 soluble protein in sham and one day after IR, measured by ELISA (n = 7/group) (**E**). Values are expressed as mean ± SEM. *P < 0.05 vs sham. **P < 0.005 versus sham.

granulocytes and monocytes from sham and IR mice. Renal IR leads to up-regulation of TREM-1 receptor on the plasma membrane of circulating monocytes, but not granulocytes (Fig. 2C,D) and also to increased expression of the soluble form of TREM-1 in the plasma (Fig. 2E). These findings indicate that renal IR may modulate the inflammatory response by regulation of TREM-1 surface expression.

Administration of TREM-1 inhibitors reduces *Trem1* and *Myd88* transcription. Once we established that TREM-1 expression is indeed increased following IR, we aimed to determine the functional role of TREM-1 in renal IR. We tested the hypothesis that blocking the ligand-receptor binding by various strategies could affect renal IR-induced injury. Mice were treated with different types and doses of TREM-1 inhibitors (as indicated in the methods section) and underwent uni- or bilateral clamping of the renal artery. To confirm that the TREM-1 pathway was indeed blocked by the treatment with the various inhibitors, we measured renal *Trem1* mRNA expression in the different groups. The majority of TREM-1 inhibitors led to downregulation of renal *Trem1* transcription (see Supplementary Fig. S2A) as was previously shown[13]. Because there is evidence that TREM-1 activation regulates MYD-88 signaling and hence it controls the extent of the inflammatory response via this signaling pathway[18–21], we measured *Myd88* mRNA transcription in renal tissue as downstream readout of TREM-1 blockade[18]. In line with the previous results, we could show that following renal IR, treatment with Fc-TREM1, LR12 and LP17 affect *Myd88* mRNA expression (see Supplementary Fig. S2B), whereas *Trif* transcript levels were relatively unchanged (data not shown)[18].

Modulation of TREM-1 function affects renal cytokine and chemokine transcription profiles. TREM-1 is a well-known amplifier of the inflammatory response, thus we investigated whether TREM-1 blockade may affect renal inflammation. The expression of cytokines and chemokines that play a role during renal inflammation were measured in renal tissues by RT-PCR. The renal inflammatory reaction was mostly dampened by different doses of recombinant TREM-1 pre-treatment. Expression of *Cxcl1* (the gene for KC), *Ccl2* (the gene for MCP-1), *Il6*, *Il1b* and *Tnfa* was impaired compared to renal ischemic tissue receiving the isotype control treatment (Fig. 3A). Next, we investigated the more potent TREM-1 inhibitor LR12[22]. Due to the short half-life of LR12[23], mice were treated every 8 hours until sacrifice. Sham mice received the same treatment to exclude any detrimental effect due to repeated injections. Unlike Fc-TREM-1, LR12 treatment only downregulated *Tnfa* transcription (Fig. 3B). Finally, we evaluated the function of LP17 peptide, the TREM-1 inhibitor proposed as a therapeutic tool to dampen TREM-1 induced inflammation in several disease settings[12,20–24]. We found that LP17 affects *Cxcl1* (KC) transcription, but not the transcription of the other inflammatory mediators (Fig. 3C).

We next evaluated the inflammatory mediators on the protein level to check whether the transcript expression was translated into protein. We measured the concentrations of KC, MCP-1, IL-6 and IL-1β protein by ELISA and found that compared to sham mice, KC and IL-1β concentrations were significantly elevated 24 hours after IR. TREM-1 inhibition did not lead to any change in majority of cytokine and chemokine protein levels. The only difference we detected was related to LR12 treatment. We found that IL-1 β was significantly decreased in the LR12-treated mice that underwent IR as compared to their IR controls with levels comparable to the sham treated animals (P = 0.02, Table 1).

Administration of TREM-1 inhibitors does not prevent the development of renal injury. Renal IR injury after 24 hours is characterized by tubular injury and infiltration of granulocytes. In unilateral IRI, mice pre-treated with different doses of Fc-TREM1 or matching isotype control did not display a change in renal damage (morphologically by PAS-D staining), infiltration of Ly6G-positive granulocytes and tubular epithelial cell apoptosis (detected by immuno-histochemical staining of cleaved caspase 3) (Fig. 4A–C).

Consistent with the results obtained for Fc-TREM1 treatment, LR12 treatment did not lead to any change in terms of renal damage, granulocyte infiltration or tubular apoptosis compared to mice receiving scramble protein (Fig. 4D–F). The same results were observed for LP17-treated mice (Fig. 4G–I). Renal function as measured by plasma creatinine and urea, due to contralateral filtration, was not affected (data not shown).

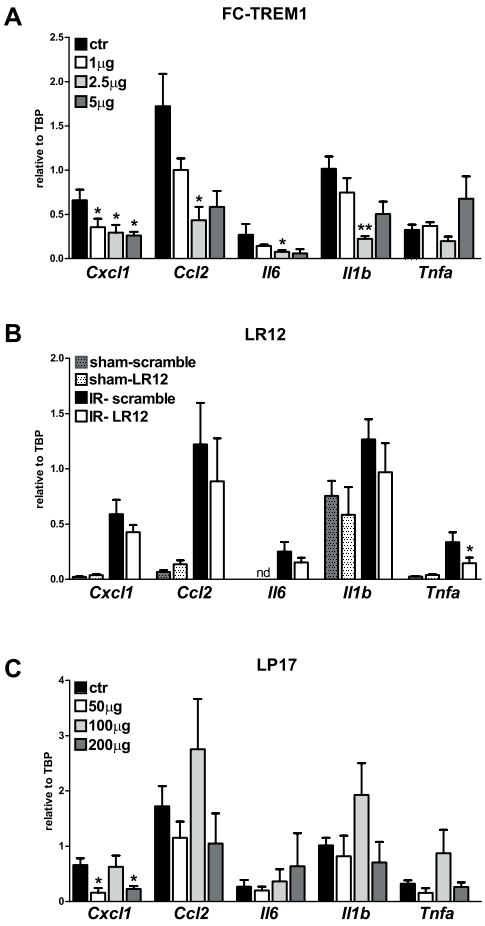

Figure 3. Renal cytokine transcripts are differentially affected by TREM-1 inhibitors following IR. Gene expression of *Cxcl1* (the gene for KC), *Ccl2* the gene for (MCP-1), *Il6*, *Il1b* and *Tnfa* in kidney of mice treated with recombinant Fc-TREM1 (n = 4/group) (**A**). In (**B**) the level of pro-inflammatory transcripts in mice treated with LR12 or scramble protein (n = 6–8/group). In the last panel (**C**) the inflammatory results of LP17 injections (n = 4/group). Values are normalized to the housekeeping gene *Tbp*. Data are expressed as mean ± SEM, *P < 0.05 versus control. **P < 0.005 versus control.

Because the potential therapeutic significance of LP17 treatment has been extensively shown by many other groups and especially in sterile inflammation settings[12,20], we tested whether the neutral results obtained were dependent on the degree of damage. Thus we induced a more severe damage model with bilateral renal IR surgery and prior treatment with LP17 or scramble peptide. In the bilateral model, renal dysfunction parameters (plasma creatinine and urea) increased compared to sham mice. LP17 treated mice did not display any significant effect on plasma urea and creatinine concentrations, renal damage score (PAS-D) or inflammation (renal granulocyte influx) compared to control-peptide treated mice (see Supplementary Fig. S3).

Taken together, our experiments indicate that modulation of TREM-1 function in the course of renal IR leads to partial downregulation of the inflammatory response, but this did not significantly affect tubular damage, renal granulocyte influx, tubular apoptosis or renal function.

Study characteristics and distribution of the *TREM1* SNVs in donors and recipients. We investigated whether SNVs in the human *TREM1* gene were associated with outcome following renal transplantation,

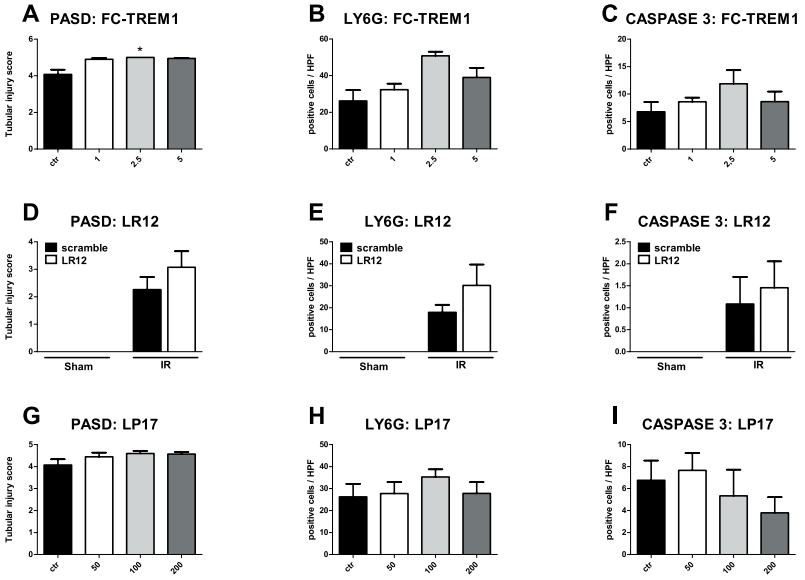

Figure 4. TREM-1 modulation does not prevent unilateral renal IR-induced injury. Renal damage (PAS-D score: **A**,**D**,**G**), influx of granulocytes (Ly6G positive cells/HPF: **B**,**E**,**H**) and tubular apoptosis (cleaved caspase 3 positive tubular epithelial cell/HPF: **C**,**E**,**H**) in mice 24 hours after unilateral IR. In order from the top row, results of Fc-TREM1 (n = 4/group), LR12 (n = 6–8/group) and LP17 treatment (n = 4/group). Data are expressed as mean ± SEM, *P < 0.05 versus control.

Cytokine fraction	Treatment			
		Fc-TREM-1		
	Control	1 μg	2.5 μg	5 μg
KC (pg/mg)	407 ± 19	443 ± 64	400 ± 123	259 ± 78
MCP-1 (pg/mg)	242 ± 45	176 ± 21	132 ± 16	152 ± 18
IL-6 (pg/mg)	27 ± 2	29 ± 4	21 ± 2	27 ± 3
IL-1β (pg/mg)	31 ± 3	38 ± 6	31 ± 4	43 ± 9
	Scramble	LR12	Scramble	LR12
	Sham	Sham	IR	IR
KC (pg/mg)	45 ± 7	48 ± 4	251 ± 64$^{\$}$	200 ± 40$^{\&}$
MCP-1 (pg/mg)	280 ± 16	301 ± 27	284 ± 24	249 ± 20
IL-6 (pg/mg	78 ± 10	79 ± 6	91 ± 7	91 ± 4
IL-1β (pg/mg)	86 ± 5	92 ± 6	172 ± 55$^{\#}$	86 ± 7$^{@}$
		LP17		
	Control	50 μg	100 μg	200 μg
KC (pg/mg)	407 ± 19	373 ± 63	447 ± 38	390 ± 23
MCP-1 (pg/mg)	267 ± 44	189 ± 14	411 ± 120	164 ± 58
IL-6 (pg/mg)	27 ± 2	40 ± 1	74 ± 22	39 ± 3
IL-1β (pg/mg)	31 ± 3	46 ± 4	127 ± 69	40 ± 1

Table 1. No differences in cytokines and chemokine protein in kidney homogenates of mice treated with different TREM-1 inhibitors. Data are presented as mean ± SEM and analysed with non-parametric tests. Fc-TREM1 (n = 4), LR12 (n = 8) and LP17 (n = 4). $^{\$}$P = 0.001 versus sham scramble. $^{\&}$P = 0.0007 versus sham LR12. $^{\#}$P = 0.01 versus sham LR12. $^{@}$P = 0.02 versus IR scramble. KC, keratinocyte-derived chemokine (= CXCL-1, chemokine C-X-C motif ligand 1); MCP-1, monocyte chemoattractant protein 1 (=CCL-2, chemokine C-C motif ligand 2); IL-6, interleukin 6; IL-1β, interleukin 1β.

Parameter	Value
N	1263
Donor characteristics	
Age (mean years ± SE)	44 ± 14
Male N (%)	645 (51%)
Donortype N (%)	
Cadaveric donor	989 (78%)
−DBD	787 (62%)
−DCD	202 (16%)
Donor cause of death N (%)	
−CVA	549 (43%)
−Trauma	305 (24%)
−Other	135 (11%)
−Unknown	282 (22%)
Recipient characteristics	
Age (mean years ± SE)	48 ± 14
Male N (%)	739 (58%)
Primary kidney disease N (%)	
−Glomerulonephritis	271 (21%)
−Adult polycyctic kidney disease	167 (13%)
−Renal vascular disease	124 (10%)
−IgA nephropathy	98 (8%)
−Pyelonephritis	148 (12%)
−Diabetic nephropathy	51 (4%)
−End-stage renal disease with unknown etiology	168 (13%)
−Other	244 (19%)
Initial immunosuppression N (%)	
−Corticosteroids	1201 (95%)
−Mycophenolic acid	907 (71%)
−Cyclosporine A	1085 (85%)
Azithioprine	72 (6%)
−Tacrolimus	97 (8%)
−Sirolimus	38 (3%)
Induction therapy N (%)	103 (8%)
−ATG	19 (2%)
−Anti-CD3 moab	199 (16%)
−Interleukin-2 RA	
First renal transplant N (%)	1142 (90%)
Transplant characteristics	
Cold ischemia time (mean hours ± SE)	
−Living donor	3 ± 2
−Cadaveric donor	21 ± 7
HLA no. of 0 mismatches N (%)	241/1050 (23%)

Table 2. Characteristics of study groups. DBD = deceased brain death, DCD = deceased cardiac death, CVA = cerebrovasculair accident, ATG = antithymocyte globulin RA = receptor antagonist, SE = standard error.

with DGF in particular. The cohort characteristics are shown in Table 2. The minor allele frequency of the two non-synonymous SNVs in the *TREM1* gene for donors and recipients were respectively 0.078 and 0.085 for p.Thr25Ser and 0.001 and 0.000 for p.Phe214Leu without statistical differences between donors and recipients ($P > 0.8$ Table 3). Donors and recipients significantly deviated from Hardy-Weinberg equilibrium ($P = 0.003$ and $P = 0.002$ for donors and recipients), but both distributions were not different from the frequency distribution found in the HapMap-CEU population of the 1000 Genomes sequencing data.

***TREM1* single nucleotide variants do not associate with renal transplant outcomes.** DGF occurred in 411/1263 patients (33%), of which 60 resulted in primary non-function and were therefore excluded from analyses. The majority (97%) of patients who experienced DGF were recipient of a deceased donor. For the p.Phe214Leu variant, we acquired insufficiently high MAFs for further analyses. In the full cohort, the *TREM1* p.Thr25Ser variant was not significantly associated with DGF in donors ($OR_{heterozygosity} = 1.08$, 95% CI = 0.77–1.52, $P = 1$) and recipients ($OR_{heterozygosity} = 0.91$, 95% CI = 0.64–1.27, $P = 1$). Five renal transplant recipients were

HGVS (rs number)	Phenotype (SNVinfo)	A/a	1000Genomes	Donor[1]				Recipient[1]				P^2
			MAF	A/A	A/a	a/a	MAF	A/A	A/a	a/a	MAF	
p.Thr25Ser (rs2234237)	Unknown (benign[5])	A/t	**0.080**[3]	0.845	0.155	0.000	**0.078**	0.836	0.159	0.005	**0.085**	0.8
p.Phe214Leu (rs2234245)	Unknown (benign[5])	G/c	**0.028**[4]	0.999	0.001	0.000	**0.001**	1.000	0.000	0.000	**0.000**	1

Table 3. Donor and recipient genotype distribution of *TREM1* single nucleotide variants. [1]Donor and recipient genotype are displayed as homyzgous dominant (A/A), heterozygous (A/a) or homozygous recessive (a/a). MAF = minor allele frequency. [2]P-value for logistic regression between donor and recipient allele frequencies in a genetic additive model, adjusted for age and donor-recipient relatedness (DFAM algorithm). [3]HapMap-CEU population. [4]Overall 1000 Genomes population. [5]Predicted benign by Polyphen (most likely lacking a phenotypical effect).

	Donor		Recipient	
Delayed graft function				
Cohort	**$OR_{heterozygosity}$ (95% CI)**	***P*-value[1]**	**$OR_{heterozygosity}$ (95% CI)**	***P*-value[1]**
Full	1.08 (0.77–1.52)	1	0.91 (0.64–1.27)	1
DBD	1.07 (0.68–1.65)	1	1.03 (0.66–1.59)	1
DCD	0.77 (0.31–2.11)	1	0.69 (0.28–1.90)	1
Biopsy-proven acute rejection				
	$HR_{heterozygosity}$ (95% CI)	***P*-value[1]**	**$HR_{heterozygosity}$ (95% CI)**	***P*-value[1]**
Full	0.72 (0.54–0.96)	0.15	0.81 (0.62–1.07)	0.84
DBD	0.70 (0.49–1.00)	0.29	0.86 (0.62–1.20)	1
DCD	1.10 (0.56–2.16)	1	1.04 (0.53–2.04)	1
Death-censored graft failure				
Full	0.75 (0.50–1.13)	1	0.87 (0.59–1.27)	1
DBD	0.89 (0.57–1.41)	1	0.84 (0.53–1.34)	1
DCD	0.50 (0.18–1.39)	1	1.18 (0.52–2.64)	1

Table 4. Association of *TREM1* single nucleotide variant p.Thr25Ser with renal outcomes. [1]After Bonferroni correction. $OR_{heterozygosity}$ = odds ratio (homozygous recessive were not sufficiently represented for statistical analyses), CI = confidence interval. DBD = deceased brain death donor, DCD = deceased cardiac death donor.

homozygous recessive for the *TREM1* variant p.Thr25Ser. None of these patients developed DGF, but due to the small group, statistical analysis was not performed (Supplementary Table S1). On follow-up, 430/1263 (34%) of recipients encountered a first episode of biopsy proven acute rejection. The median (interquartile range) time to rejection was 51 months (1–105 months). Neither donor nor recipient *TREM1* p.Thr25Ser variants associated with the cumulative incidence of biopsy proven acute rejection in donors ($HR_{heterozygosity}$ = 0.72, 95% CI = 0.54–0.96, P = 0.15 and $HR_{heterozygosity}$ = 0.81, 95% CI = 0.62–1.07, P = 0.84, respectively). Death censored graft failure occured in 215/1263 (17%) at a median (interquartile range) of 5.5 years (2.9–8.7 years) after transplantation.

Corroborating on the results obtained for death censored graft failure and biopsy proven acute rejection, neither donor nor recipient *TREM1* p.Thr25Ser associated with the cumulative incidence of death censored graft failure in donors or recipients ($HR_{heterozygosity}$ = 0.75, 95% CI = 0.50–1.13, P = 1 and $HR_{heterozygosity}$ = 0.87, 95% CI = 0.59–1.27, P = 1, respectively). When we stratified patients for donation type (DBD or DCD), similar results were obtained (Table 4). In conclusion, we did not acquire evidence for a potential effect of SNVs in the *TREM1* gene for post-transplant renal outcomes, including DGF.

Discussion

Infiltrating inflammatory cells contribute to the development of acute kidney injury following IR, which increases the risk of DGF[17]. Increasing evidence suggest that TREM-1 plays an essential role in modulating the innate immune response in (non) sterile acute and chronic inflammation[10,11,13,21]. TREM-1 enhances the inflammatory response through synergism with TLR pathway signaling[7]. The contribution of TLRs in sterile renal injury has been broadly investigated in mice and humans[4,25]. However, the role of TREM-1 herein is still unclear. Interestingly, blockade of TREM-1 activation by synthetic analogues reduced pathology in mesenteric IR and myocardial infarction[12,13]. In the current study we showed that synthetic TREM-1 inhibition in murine renal IR-induced injury does not appear to be a therapeutic target to prevent injury and/or improve function. Consistent with the results of the experimental study, we found no association of the p.Thr25Ser heterozygous variant with renal outcome following kidney transplantation.

Our findings demonstrated that renal IR induced a significant increase in *Trem1* transcripts in renal tissue. This up-regulation was in line with the increased number of circulating granulocytes, well known to express TREM-1 and to accumulate in the kidney tissue as early as 30 minutes after reperfusion[26]. We speculate that

Trem1 mRNA expressing cells, as detected by *in situ* hybridization, are most probably infiltrating granulocytes. Blood monocytes are recruited into the kidney in response to a gradient of chemokines, especially monocyte chemoattractant protein-1 (MCP-1), which peaks in IR kidney later than 24 hours[27]. Thus, no differences were observed in the number of circulating monocytes between sham and IR mice, probably because of timing of the necropsies after reperfusion. However, we found that IR leads to up-regulation of TREM-1 surface expression on circulating monocytes. Blood monocytes infiltrate inflamed kidney tissues and differentiate into macrophages and dendritic cells[17]. Thus, our data would suggest a role for TREM-1 in macrophage-mediated renal injury. This hypothesis has previously been discussed in the literature[14]. Together with an increased membrane receptor expression, we detected increased levels of plasma soluble TREM-1. The soluble protein can originate from proteolytic cleavage from monocytes[28] or new splice variant synthesis[29]. The latter hypothesis is conceivable with our results.

The increased circulating sTREM-1 protein concentration following IR is in line with other studies showing that the soluble protein can be detected in plasma, fluids and urine during infection and inflammation[30–33]. Functionally, the soluble protein acts as a counter regulatory molecule by scavenging available TREM-1 ligand thus preventing further amplification of the inflammatory signal. Nevertheless, in renal IR, the significance of this increased concentration of sTREM-1 appears to be dispensable in modulating the inflammatory response. Several studies have shown that treatment with TREM-1 inhibitors represents a therapeutic strategy to prevent excessive inflammation resulting in decreased pathology and mortality. The inhibitory peptide LP17 was shown to successfully reduce the inflammatory responses in the context of infection, mesenteric IR-induced injury, hemorrhagic shock, colitis, autoimmune arthritis and acute pancreatitis[12,20,34–39]. In addition, TREM-1 fusion protein and LR12 reduced the disease severity in sepsis and in models of acute myocardial infarction[13,23,24,40–42]. These previous studies and the significantly elevated TREM-1 expression during renal IR would suggest a potential benefit from TREM-1 interventions to reduce renal IR-induced injury. In our study, we relied on the administration of commercial available TREM-1 synthetic inhibitors. We showed that treatment with different inhibitors is able to modulate *Trem1* mRNA expression and more interestingly, TREM-1 blocking resulted in a decreased *Myd88* transcription, as previously showed by[18]. Nevertheless, the reduced transcription of pro-inflammatory markers as measured by RT-PCR as a result of decreased *Myd88* expression, was not mirrored by a significant decrease in protein concentrations. Because of discrepancy between mRNA and protein, we believe that in this study, given the final readout, protein levels are biological relevant. Indeed, in line with these findings and contrary to the above-mentioned studies addressing the pathogenic role of TREM-1, our results have shown that interventions that modulate TREM-1 function did not prevent renal IR.

Supporting our results, Campanholle *et al.* in a recent study have shown that administration of TREM-1 fusion protein did not have any effect during recovery from renal IR[14]. However, the authors aimed to answer a different research question: unraveling the therapeutic potential of TREM-1 in macrophage activation and fibrosis, a later stage of renal inflammation compared to our study. Granulocytes and macrophages have a different temporal distribution and play a distinct role in renal IR[27]. Thus, our results are not fully comparable with those of Campanholle *et al.*, but provide more evidence that blocking TREM-1 signaling at the early stage of renal IR does not represent a suitable therapeutic target. Thus far it appears that TREM-1 blocking agents provide controversial findings in sterile inflammatory disorders. Although we observed TREM-1 up-regulation following renal IR, this functional study showed that TREM-1 does not play a pivotal role in granulocyte- and monocyte-induced renal inflammation. We speculate that divergent results obtained by TREM-1 inhibitors might be dependent on affinity ligand availability. In our model of sterile renal injury, we detected *Trem1* mRNA expression in inflammatory cells rather than tubular cells. Previous study emphasized that in sterile ischemic injury, renal parenchyma-associated TLR-2 and TLR-4, rather than inflammatory cell-associated TLRs contribute to renal dysfunction[3,4,43]. The neutral results observed in terms of renal outcome could be related to the dispensable role of innate immune receptor expression on inflammatory cells in this disease setting. Additionally, renal DAMPs that are released by damaged parenchymal cells, might have higher affinity for TLRs as compared to TREM-1. In the presence of a low abundance of or a low affinity for TREM-1 ligand, TLR signaling might be dominant, thus the inflammatory response in renal IR would then be TREM-1 independent or the TREM-1 signaling pathway would be of low significance. However, it cannot be excluded that the ligands, through redundancy, could activate the inflammatory cells through an alternative receptor, for instance TREM-3, which most likely can compensate for TREM-1 blockade because of comparable function[14]. In other models of sterile inflammation where TREM-1 inhibition had a beneficial effect, the amplification of the inflammatory response might have been TREM-1 dependent.

Over the past years, soluble TREM-1 has gained interest as biomarker of several human disease settings including renal dysfunction[29,44,45]. Since then, also genetic studies that aimed at finding an association between variants in the *TREM1* gene and outcomes in various clinical settings were conducted, however with conflicting (or disease-specific) results. SNVs in the *TREM1* gene were shown to associate with intestinal Behcet's disease, pneumonia in burn patients, risk for coronary artery disease but not with inflammatory bowel diseases or infectious endocarditis[46–50]. There is no consensus on the association of *TREM1* variants with (the outcome after) sepsis with Chen *et al.*[51] indicating no association in a Chinese population comprising 175 patients with sepsis and Su *et al.* describing a significant correlation with the incidence of sepsis in 80 Chinese patients[48]. Interestingly, Su *et al.* did not describe an association between the p.Thr25Ser variant of *TREM1* with the (dynamic) concentrations of sTREM-1[48], which questions whether there truly is a biochemical consequence of this non-synonymous variant. To the best of our knowledge, the current study is the first on *TREM1* genetic variants in renal transplant patients. The lack of association between the *TREM1* p.Thr25Ser heterozygous variant and renal outcomes with DGF in particular is in line with the lack of beneficial potential in the preclinical mouse studies of IR-induced injury. However, even though this was a large study, we cannot exclude that patients with homozygosity for the p.Thr25Ser variant are in fact protected from IR-induced injury after transplantation (N = 5, Supplementary Table S1).

From these studies we conclude that (1) TREM-1 increases during experimental renal IR due to *Trem1* gene transcription by infiltrating leukocytes, (2) various interventions aiming at modulating the function of murine TREM-1 downregulated the inflammatory response, but did not prevent renal damage, leukocyte influx or organ dysfunction and (3) genetic variants in the *TREM1* gene do not associate with the development of delayed graft function, biopsy proven acute rejection or subsequent graft failure. Taken together, these experiments question TREM-1 as a potential target of therapy in these particular disease settings.

Materials and Methods

Surgical procedure of murine ischemia reperfusion. Pathogen-free 8-to 12 week-old male C57BL/6 WT were purchased from Charles River Laboratories. The Animal Care and Use Committee of the University of Amsterdam approved all the experiments in compliance with the ARRIVE guidelines (NC3Rs). Renal IR was induced as described previously with small alterations[26]. The renal pedicles were clamped for 25 minutes (uni- or bilaterally) through an abdominal incision under 2.5% isoflurane-induced anaesthesia. Mice received an injection of 50 μg/kg buprenorphin (Shering-Plough) for analgesic purposes. Sham mice underwent the same procedure without clamping of the renal pedicles. Successful reperfusion was validated by regain of the initial color of the kidney after clamp removal. Methods were carried out in accordance with the relevant guidelines and regulations.

TREM-1 inhibitors. We used 3 previously validated approaches to modulate TREM-1 function[12,13,40]. LP17 (LQVTDSGLYRCVIYHPP), LR12 (LQEEDTGEYGCV) and LP17/LR12–scramble protein (TDSRCVIG LYHPPLQVY/YQDVELCETGED) were chemically synthesized (Pepscan) based on the extracellular domain of TREM-1 and TREM-like transcript 1 (TLT1) respectively. TREM-1 fusion protein (Fc-TREM1) and control IgG were purchased from R&D. Endotoxin-free TREM-1 inhibitors or respective controls were dissolved in sterile NaCl 0.9%. WT mice received an intraperitoneal (i.p.) injection (100 μl) of Fc-TREM1 fusion protein (1, 2.5 and 5 μg) or matching isotype control, 1 hour before surgery. For LR12 experiment mice received 200 μg of LR12/control protein (100 μl total volume) i.p., starting 2 hours before the surgery and every 8 hours until the sacrifice (24 hours). Sham mice received the same treatment with scramble peptide/LR12. In the LP17 treatment, mice received different doses (50, 100 and 200 μg) of LP17 or scramble protein, 1 hour before surgery through an i.p. injection (100 μl). Mice were sacrificed 24 hours after reperfusion.

Biological parameters related to murine kidney function, damage and inflammation. Murine renal function in the bilateral experiment was determined by plasma urea and creatinine as described before[26]. The degree of tubular damage was assessed on periodic acid-Schiff after diastase treatment (PAS-D)-stained tissue sections The PAS-D score was obtained by a nephropathologist in a blinded fashion as previously described[26]. For granulocyte staining, we used FITC-labeled anti-mouse Ly6G mAb (BD Biosciences) followed by appropriate secondary antibodies as described before[26]. Ly6G positive cells were counted in 10 high power fields (HPF). Tubular apoptosis was detected with staining for cleaved caspase-3 (Cell signalling) as previously described[26]. Positive nuclei within the tubular cells were counted in 10 HPF.

ELISA and western blot. Circulating level of sTREM-1 were measured in plasma by ELISA (R&D). Renal levels of sTREM-1, KC, MCP-1, IL-6 and IL-1β (R&D) were measured in snap-frozen and lysed kidney homogenates (300 mM NaCl, 15 mM Tris, 2 mM MgCl, 1 mM $CaCl_2$ and 1% Triton X100, pH 7.4 with 100 μg/ml pepstatin A, leupeptin and aprotinin mix)[26]. Protein levels in renal tissue were corrected for total protein level using BioRad protein assay (Bio-Rad). For western blots, kidney lysates were prepared from 10 frozen sections (20 μm thick), incubated at 4 °C for 30 min in RIPA buffer containing 50 mM Tris pH7.5, 0.15 M NaCl, 2 mM EDTA, 1% deoxycholic acid, 1% NP-40, 4 mM sodium orthovanadate, 10 mM sodium fluoride, 1% protease inhibitor cocktail (P8340, Sigma). The lysates were then centrifuged at 14000 rpm for 10 minutes and the supernatants were collected and stored at −20 °C. SDS-polyacrylamide gel electrophoresis was carried out in 4–12% gradient gels (Invitrogen) and proteins were electrophoretically transferred onto methanol-activated polyvinylidene fluoride (PVDF) microporous membranes (Millipore). Membrane was blocked for one hour with 5% milk in Tris-buffered saline containing 0.1% Tween 20 (TBS-T), followed by overnight incubation at 4 °C with primary rabbit antibody anti-TREM-1 (ab104413, 1:1500, Abcam). HRP-conjugated secondary antibodies (DAKO) were incubated for two hours at room temperature, and HRP activity was visualized with ECL-reagent (Amersham Pharmacia Biotech). Tubulin was used as loading control. Densitometric quantification analysis was performed on imagines of scanned films using the image processing program ImageJ (NIH, US).

Flow cytometry. Peripheral blood was drawn via a cardiac puncture and red blood cells were lysed (Erythrocyte lysis solution: 160 mM NH_4Cl, 10 mM $KHCO_3$ and 0.1 mM EDTA, pH 7.4). Cell suspensions were stained with FITC-labeled anti-mouse Ly6C/Gr-1 (BD Pharmingen) and Alexa Fluor 647-labeled anti mouse F4/80 (eBioscience) to determine granulocytes and monocyte populations. PE-labeled rat anti-mouse TREM-1 (R&D) was used to determine TREM-1 positive cells within the identified leukocyte populations. Stained cells were acquired on FACS Calibur (BD Biosciences). Data analysis was performed using FlowJo v10 (FlowJo LLC).

mRNA purification and reverse transcriptase PCR. Total RNA was isolated from 10–15 renal frozen tissue slides (20 μM) using Trizol reagent (Invitrogen) according to manufacturer's protocol. mRNA samples were converted to cDNA (complementary DNA) using oligo-dT. Tata box-binding protein (*Tbp*), *Trem1*, *Cxcl1*, *Ccl2*, *Il6*, *Il1b*, *Tnfa and Myd88* mRNA expression was analyzed by reverse transcriptase PCR with SYBR green PCR master mix on a Light Cycler 480 (Hoffmann-La Roche). Relative expression was analyzed using LinRegPCR (developed by Hearth failure research center, University of Amsterdam). Gene expression of *Trem1* was normalized to housekeeping gene (*Tbp*). Primer sequences are *Trem1* forward: 5′-GCGTCCCATCCTTATTACCA, reverse: 5′-AAACCAGGCTCTTGCTGAGA; *Tbp* forward:

5′-GGAGAATCATGGACCAGAACA, reverse: 5′-GATGGGAATTCCAGGAGTCA; *Cxcl1* forward: 5′ATAATGGGCTTTTACATTCTTTAACC, reverse: 5′-AGTCCTTTGAACGTCTCTGTCC; *Ccl2* forward: 5′-CATCCACGTGTTGGCTCA, reverse: 5′-GATCATCTTGCTGGTGAATGAGT; *Myd88* forward: 5′-TGGCCTTGTTAGACCGTGA; reverse: 5′-AAGTATTTCTGGCAGTCCTCCTC; *Il1b* forward: 5′-CTGCAGCTGGAGAGTGTGGAT; reverse: 5′-GCTTGTGCTCTGCTTGTGAG; *Il6* forward: 5′-GCTACCAAACTGGATATAATGGA; reverse: 5′-CCAGGTAGCTATGGTACT6CCAGAA; *Tnfa* forward: 5′-CTGTAGCCCACGTCGTAGC; reverse: 5′-TTGACATCCATGCCGTTG.

***Trem1 in situ* hybridization.** *In situ* hybridization was performed on frozen tissue sections as described before[15,52] with minor adjustments. A DNA template was generated by nested PCR incorporation of T7 RNA polymerase promoters using *mTrem1* primers (forward: 5′-GCGTGTTCTTTGTCTCAGAAGT and reverse 5′-taatacgactcactataggg AGGAGAGGAAACAACCGCAG). Kidneys were perfused with PBS, fixated in 4% PFA and placed in 30% sucrose overnight at 4 °C. The next day, the tissues was placed in O.C.T. compound (Tissue-Tek). The kidney tissue sections (5 μm) were permeabilised with proteinase K (10 μg/ml), fixated and next acetylated. Riboprobe concentration of 0.5 μg/ml was used for hybridization. For riboprobe detection, sections were pre-treated with blocking buffer (20% heat inactivated sheep serum, 2% blocking reagent; Hoffmann-La Roche) and incubated with anti–DIG-AP antibody (Hoffmann-La Roche) at 4 °C overnight. The next day, a chromogenic substrate (BM Purple; Hoffmann-La Roche) was used to visualize the signal. Sections were fixated in 4% PFA and mounted with Glycergel (Dako).

Renal transplant study population. We included samples from the Renal Genetics Transplantation (REGaTTA) cohort collected from the University Medical Center Groningen, Groningen, The Netherlands[25]. Matched donors and recipients from 1430 transplantations were assessed for eligibility. Patients with more than two re-transplantations, simultaneous kidney/pancreas- or kidney/liver transplantations, unavailability of DNA for genotyping, technical problems or patients that were lost to follow-up, were excluded. The final cohort on which statistical analyses was performed comprised of 1263 donor-recipient pairs. A detailed flow diagram is shown in Supplementary Fig. S5. The medical ethics committee of the University Medical Center Groningen approved the study under file n° METc 2014/077 and written informed consent was acquired from all living transplant donors. By Dutch jurisdiction, deceased donors provide informed consent upon registration of their donation status. No living donors from a vulnerable population were used. The study was conducted according to the Declarations of Helsinki and Istanbul.

DNA isolation and *TREM1* variant selection. Peripheral blood mononuclear cells were used to acquire donor and recipient DNA. Based on a 1000 Genomes minor allele frequency (MAF) of >1%, 2 non-synonymous SNVs in the *TREM1* gene were selected: rs2234237 (p.Thr25Ser) and rs2234245 (p. Phe214Leu). Genotyping of the SNVs was performed using the Illumina VeraCode GoldenGate Assay kit (Illumina) according to the manufacturer's instructions. Genotype clustering and calling were performed using BeadStudio Data Analysis Software (Illumina).

Renal transplantation study outcomes. The primary outcome used in this study was DGF, defined as the requirement for dialysis within the first week after transplantation (patients with primary non-function of the graft[53], were excluded, since these cases most probably represent arterial and venous thrombosis instead of IR). Secondary outcomes were time-to-first episode of biopsy-proven acute rejection (BPAR) and death-censored graft survival (DCGF: defined as the need for indefinite dialysis or re-transplantation).

Statistical analyses. In the murine studies, differences between groups were analysed using non-parametric Mann-Whitney (2 groups) or Kruskal-Wallis tests (>2 groups) followed by Mann Whitney (treatment compared to control) using Prism (GraphPad Software). Results are expressed as mean ± SEM. Values of $P < 0.05$ were considered significant. For the human renal transplantation study, deviation from Hardy-Weinberg equilibria were tested with PLINK[54]. Differences in allele frequencies between donors and recipients were tested by logistic regression analyses in a genetic additive model construction. Results were adjusted for age and donor-recipient relatedness with the DFAM algorithm. Minor allele frequencies between the HapMap-CEU (a population from Utah with Northern and Western European ancestry) that was genotyped in the context of the 1000 Genomes study were compared by Fisher exact tests or χ^2 tests where appropriate. The association between *TREM1* SNVs and DGF were tested with logistic regression models with stratification for donor type. The association with biopsy-proven acute rejection and death-censored graft survival was tested with Cox proportional hazard models. An insufficient amount of patients had a homozygous recessive genotype and we therefore only calculated odds (OR) and hazard (HR) ratios for the heterozygous genotype. Two-sided *P*-values below 0.05 after Bonferroni correction were considered significant. Data were analyzed with the R computing environment.

References

1. Siedlecki, A., Irish, W. & Brennan, D. C. Delayed graft function in the kidney transplant. *Am. J. Transplant* **11,** 2279–96 (2011).
2. Cooper, J. E. & Wiseman, A. C. Acute kidney injury in kidney transplantation. *Curr. Opin. Nephrol. Hypertens.* **22,** 698–703 (2013).
3. Leemans, J. C. *et al.* Renal-associated TLR2 mediates ischemia/reperfusion injury in the kidney. *J. Clin. Invest.* **115,** 2894–903 (2005).
4. Pulskens, W. P. *et al.* Toll-like receptor-4 coordinates the innate immune response of the kidney to renal ischemia/reperfusion injury. *PLoS One* **3,** e3596 (2008).
5. Colonna, M. TREMs in the immune system and beyond. *Nat. Rev. Immunol.* **3,** 445–53 (2003).
6. Sharif, O. & Knapp, S. From expression to signaling: roles of TREM-1 and TREM-2 in innate immunity and bacterial infection. *Immunobiology* **213,** 701–13 (2008).
7. Arts, R. J. W., Joosten, L. A. B., van der Meer, J. W. M. & Netea, M. G. TREM-1: intracellular signaling pathways and interaction with pattern recognition receptors. *J. Leukoc. Biol.* **93,** 209–15 (2013).

8. Bouchon, A., Dietrich, J. & Colonna, M. Cutting edge: inflammatory responses can be triggered by TREM-1, a novel receptor expressed on neutrophils and monocytes. *J. Immunol.* **164,** 4991–5 (2000).
9. Klesney-Tait, J. *et al.* Transepithelial migration of neutrophils into the lung requires TREM-1. *J. Clin. Invest.* **123,** 138–49 (2013).
10. Hommes, T. J. *et al.* Role of Triggering Receptor Expressed on Myeloid Cells-1/3 in Klebsiella-Derived Pneumosepsis. *Am. J. Respir. Cell Mol. Biol.* **53,** 647–55 (2015).
11. Weber, B. *et al.* TREM-1 deficiency can attenuate disease severity without affecting pathogen clearance. *PLoS Pathog.* **10,** e1003900 (2014).
12. Gibot, S. *et al.* Effects of the TREM-1 pathway modulation during mesenteric ischemia-reperfusion in rats. *Crit. Care Med.* **36,** 504–10 (2008).
13. Boufenzer, A. *et al.* TREM-1 Mediates Inflammatory Injury and Cardiac Remodeling Following Myocardial Infarction. *Circ. Res.* **116,** 1772–82 (2015).
14. Campanholle, G. *et al.* TLR-2/TLR-4 TREM-1 signaling pathway is dispensable in inflammatory myeloid cells during sterile kidney injury. *PLoS One* **8,** e68640 (2013).
15. Tammaro, A. *et al.* Role of TREM1-DAP12 in Renal Inflammation during Obstructive Nephropathy. *PLoS One* **8,** e82498 (2013).
16. Lo, T.-H. *et al.* TREM-1 regulates macrophage polarization in ureteral obstruction. *Kidney Int.* **86,** 1174–86 (2014).
17. Bonventre, J. & Yang, L. Cellular pathophysiology of ischemic acute kidney injury. *J. Clin. Invest.* **121,** (2011).
18. Ornatowska, M. *et al.* Functional genomics of silencing TREM-1 on TLR4 signaling in macrophages. *Am. J. Physiol. Lung Cell. Mol. Physiol.* **293,** L1377–84 (2007).
19. Klesney-Tait, J. & Colonna, M. Uncovering the TREM-1-TLR connection. *Am. J. Physiol. Lung Cell. Mol. Physiol.* **293,** L1374–6 (2007).
20. Schiechl, G. *et al.* Inhibition of Innate Co-Receptor TREM-1 Signaling Reduces CD4(+) T Cell Activation and Prolongs Cardiac Allograft Survival. *Am. J. Transplant* **13,** 1168–80 (2013).
21. Wu, J. *et al.* The proinflammatory myeloid cell receptor TREM-1 controls Kupffer cell activation and development of hepatocellular carcinoma. *Cancer Res.* **72,** 3977–86 (2012).
22. Derive, M. *et al.* Effects of a TREM-like transcript 1-derived peptide during hypodynamic septic shock in pigs. *Shock* **39,** 176–82 (2013).
23. Derive, M., Boufenzer, A. & Gibot, S. Attenuation of responses to endotoxin by the triggering receptor expressed on myeloid cells-1 inhibitor LR12 in nonhuman primate. *Anesthesiology* **120,** 935–42 (2014).
24. Gibot, S. *et al.* Modulation of the triggering receptor expressed on the myeloid cell type 1 pathway in murine septic shock. *Infect. Immun.* **74,** 2823–30 (2006).
25. Dessing, M. C. *et al.* Toll-Like Receptor Family Polymorphisms Are Associated with Primary Renal Diseases but Not with Renal Outcomes Following Kidney Transplantation. *PLoS One* **10,** e0139769 (2015).
26. Dessing, M. C. *et al.* The calcium-binding protein complex S100A8/A9 has a crucial role in controlling macrophage-mediated renal repair following ischemia/reperfusion. *Kidney Int.* **87,** 85–94 (2015).
27. Stroo, I. *et al.* Chemokine expression in renal ischemia/reperfusion injury is most profound during the reparative phase. *Int. Immunol.* **22,** 433–42 (2010).
28. Gómez-Piña, V. *et al.* Role of MMPs in orchestrating inflammatory response in human monocytes via a TREM-1-PI3K-NF-κB pathway. *J. Leukoc. Biol.* **91,** 933–45 (2012).
29. Baruah, S. *et al.* Identification of a Novel Splice Variant Isoform of TREM-1 in Human Neutrophil Granules. *J. Immunol.* **195,** 5725–31 (2015).
30. Gibot, S. *et al.* Soluble triggering receptor expressed on myeloid cells and the diagnosis of pneumonia. *N. Engl. J. Med.* **350,** 451–8 (2004).
31. Gibot, S. Plasma Level of a Triggering Receptor Expressed on Myeloid Cells-1: Its Diagnostic Accuracy in Patients with Suspected Sepsis. *Ann. Intern. Med.* **141,** 9 (2004).
32. Su, L. *et al.* Diagnostic value of urine sTREM-1 for sepsis and relevant acute kidney injuries: a prospective study. *Crit. Care* **15,** R250 (2011).
33. Tzivras, M. *et al.* Role of soluble triggering receptor expressed on myeloid cells in inflammatory bowel disease. *World J. Gastroenterol.* **12,** 3416–9 (2006).
34. Kamei, K. *et al.* Role of triggering receptor expressed on myeloid cells-1 in experimental severe acute pancreatitis. *J. Hepatobiliary. Pancreat. Sci.* **17,** 305–12 (2010).
35. Gibot, S. *et al.* Modulation of the triggering receptor expressed on myeloid cells-1 pathway during pneumonia in rats. *J. Infect. Dis.* **194,** 975–83 (2006).
36. Wiersinga, W. J. *et al.* Expression profile and function of triggering receptor expressed on myeloid cells-1 during melioidosis. *J. Infect. Dis.* **196,** 1707–16 (2007).
37. Gibot, S. *et al.* Effects of the TREM 1 pathway modulation during hemorrhagic shock in rats. *Shock* **32,** 633–7 (2009).
38. Schenk, M., Bouchon, A., Seibold, F. & Mueller, C. TREM-1–expressing intestinal macrophages crucially amplify chronic inflammation in experimental colitis and inflammatory bowel diseases. *J. Clin. Invest.* **117,** 3097–106 (2007).
39. Murakami, Y. *et al.* Intervention of an inflammation amplifier, triggering receptor expressed on myeloid cells **1**, for treatment of autoimmune arthritis. *Arthritis Rheum.* **60,** 1615–23 (2009).
40. Bouchon, A., Facchetti, F., Weigand, M. A. & Colonna, M. TREM-1 amplifies inflammation and is a crucial mediator of septic shock. *Nature* **410,** 1103–7 (2001).
41. Wong-Baeza, I. *et al.* Triggering receptor expressed on myeloid cells (TREM-1) is regulated post-transcriptionally and its ligand is present in the sera of some septic patients. *Clin. Exp. Immunol.* **145,** 448–55 (2006).
42. Chen, L. C., Laskin, J. D., Gordon, M. K. & Laskin, D. L. Regulation of TREM expression in hepatic macrophages and endothelial cells during acute endotoxemia. *Exp. Mol. Pathol.* **84,** 145–55 (2008).
43. Wu, H. *et al.* TLR4 activation mediates kidney ischemia/reperfusion injury. *J. Clin. Invest.* **117,** 2847–59 (2007).
44. Hirayama, K. *et al.* Serum ratio of soluble triggering receptor expressed on myeloid cells-1 to creatinine is a useful marker of infectious complications in myeloperoxidase-antineutrophil cytoplasmic antibody-associated renal vasculitis. *Nephrol. Dial. Transplant* **26,** 868–74 (2011).
45. Essa, E. S. & Elzorkany, K. M. A. sTREM-1 in patients with chronic kidney disease on hemodialysis. *APMIS* **123,** 969–74 (2015).
46. Jung, E. S. *et al.* Relationships between genetic polymorphisms of triggering receptor expressed on myeloid cells-1 and inflammatory bowel diseases in the Korean population. *Life Sci.* **89,** 289–94 (2011).
47. Rivera-Chávez, F. A. *et al.* A TREM-1 Polymorphism A/T within the Exon 2 Is Associated with Pneumonia in Burn-Injured Patients. *ISRN Inflamm.* **2013,** 431739 (2013).
48. Su, L. *et al.* Dynamic changes in serum soluble triggering receptor expressed on myeloid cells-1 (sTREM-1) and its gene polymorphisms are associated with sepsis prognosis. *Inflammation* **35,** 1833–43 (2012).
49. Golovkin, A. S. *et al.* Association of TLR and TREM-1 gene polymorphisms with risk of coronary artery disease in a Russian population. *Gene* **550,** 101–9 (2014).
50. Golovkin, A. S. *et al.* An association between single nucleotide polymorphisms within TLR and TREM-1 genes and infective endocarditis. *Cytokine* **71,** 16–21 (2015).

51. Chen, Q. *et al.* Lack of association between TREM-1 gene polymorphisms and severe sepsis in a Chinese Han population. *Hum. Immunol.* **69,** 220–6 (2008).
52. Liu, J. *et al.* Cell-specific translational profiling in acute kidney injury. *J. Clin. Invest.* **124,** 1242–54 (2014).
53. Damman, J. *et al.* Crosstalk between complement and Toll-like receptor activation in relation to donor brain death and renal ischemia-reperfusion injury. *Am. J. Transplant* **11,** 660–9 (2011).
54. Purcell, S. *et al.* PLINK: a tool set for whole-genome association and population-based linkage analyses. *Am. J. Hum. Genet.* **81,** 559–75 (2007).

Acknowledgements
This work was supported by The Netherlands Organization for Health Research and Development (ZonMw, Meer Kennis met Minder Dieren; grant no. 40-42600-98-096). J.C.L., L.B. and M.C.D. have received support from the Netherlands Organization for Scientific Research (grant no. 016.126.386) and the Dutch Kidney Foundation (grant no. C06.6023 and C08.2274). Funders had no role in study design, data collection, analysis, writing the manuscript or decision to publish. The authors would like to thank the members of the REGaTTA cohort (REnal GeneTics TrAnsplantation; University Medical Center Groningen, University of Groningen, Groningen, the Netherlands): H.G.D. Leuvink, H. van Goor, J.L. Hillebrands, B.G. Hepkema, H. Snieder, J. van den Born, M.H. de Borst, S.J.L. Bakker, G.J. Navis and M. Seelen.

Author Contributions
A.T., J.K. and M.C.D. conceived and designed the experiments. A.T. and G.T. performed the experiments. D.E., I.S., N.C. and L.B. helped with laboratory techniques. J.D., G.N. and M.D. provided samples/tools. S.F. and J.C.L. were involved in interpretation of data. A.T., J.K. and M.C.D. wrote the manuscript. All the authors revised the manuscript and had final approval of the submitted version.

Additional Information
Supplementary information accompanies this paper at http://www.nature.com/srep

Competing financial interests: The authors declare no competing financial interests.

How to cite this article: Tammaro, A. *et al.* Effect of TREM-1 blockade and single nucleotide variants in experimental renal injury and kidney transplantation. *Sci. Rep.* **6**, 38275; doi: 10.1038/srep38275 (2016).

Publisher's note: Springer Nature remains neutral with regard to jurisdictional claims in published maps and institutional affiliations.

Supplementary Information

Effect of TREM-1 blockade and single nucleotide variants in experimental renal injury and kidney transplantation

Alessandra Tammaro[1,ζ]*, Jesper Kers[1 ζ], Diba Emal[1], Ingrid Stroo[1], Gwen J. D. Teske[1], Loes M. Butter[1], Nike Claessen[1], Jeffrey Damman[1], Marc Derive[2], Gerjan J. Navis[3,5], Sandrine Florquin[1,4], Jaklien C. Leemans[1], Mark C. Dessing[1]

[1]Department of Pathology, Academic Medical Center, University of Amsterdam, Amsterdam, The Netherlands. [2]INSERM UMR_S1116, Faculté de Médecine de Nancy, Université de Lorraine, Vandœuvre-les-Nancy, France. [3]Department of Internal Medicine, Division of Nephrology, University Medical Center Groningen, University of Groningen, Groningen, The Netherlands. [4]Department of Pathology, Radboud University Nijmegen Medical Center, Nijmegen, The Netherlands. [5]On behalf of the REGaTTA (REnal GeneTics TrAnsplantation) Groningen group. [ζ] These authors contributed equally to this work. *Correspondence and requests for materials should be addressed to A.T. (email: a.tammaro@amc.uva.nl)

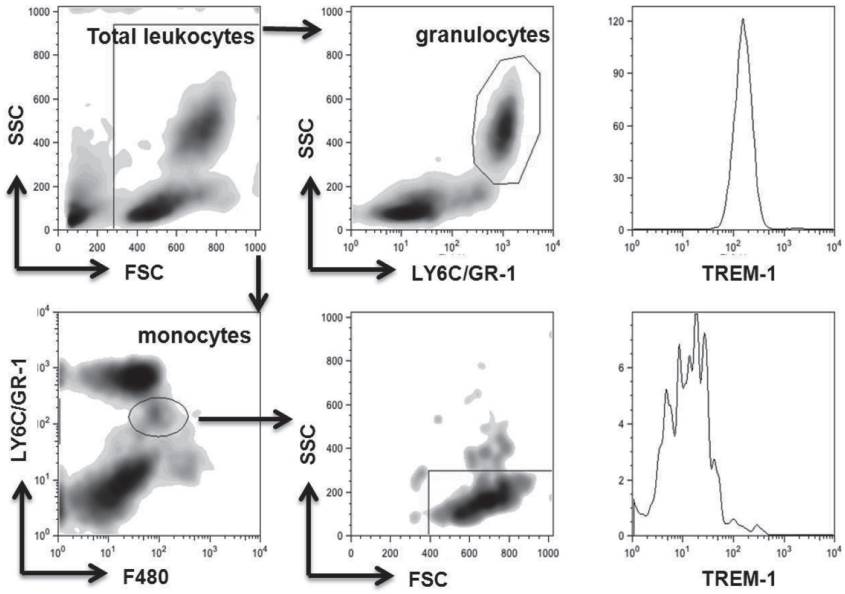

Supplementary Figure S1: Gating strategy of circulating leukocytes. Granulocytes are shown as percentage of LY6C/Gr-1 high by SSC of total leukocytes. Cells in the monocytes gate were identified as Ly6C/Gr-1positive and F4-80-negative (excluding granulocyte population by forward and side scatter). TREM-1 staining on each population is shown by histograms.

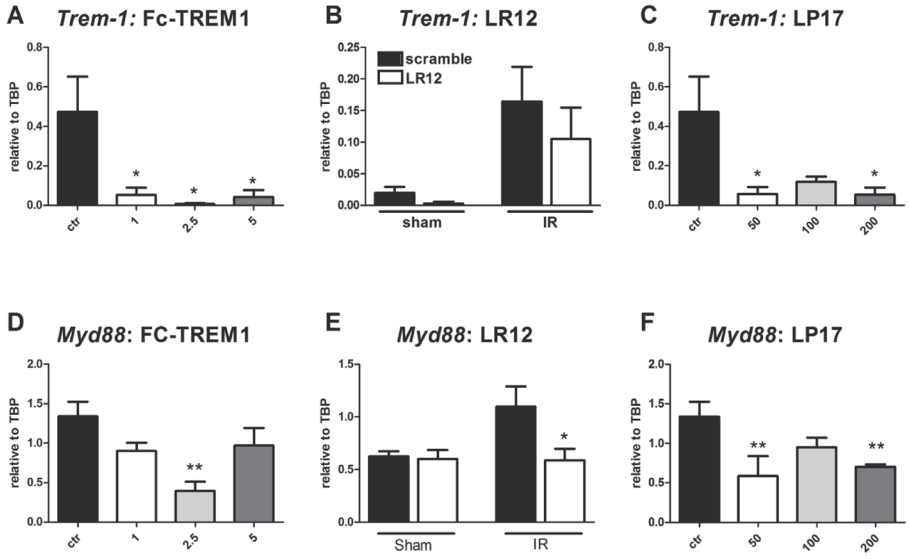

Supplementary Figure S2. TREM-1 expression and pathway are down-regulated by different inhibitors. Trem1 and Myd88 mRNA expression as measured by RT-PCR in the groups treated with Fc-TREM-1 (**A,D**) (n = 4/group), LR12 (**B,E**) (n = 6-8/group) and LP17 (**C,F**) (n = 4/group). Data are normalized to Tbp expression. Values are expressed as mean ± SEM. *P < 0.05 vs control. **P < 0.005 versus control.

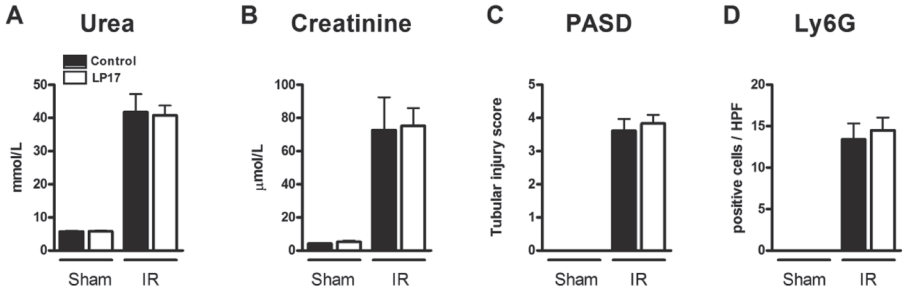

Supplementary Figure S3. LP17 pre-treatment does not prevent IR-induced injury in bilateral renal IR experiment. Plasma urea (**A**), creatinine (**B**), renal damage (**C**) and granulocyte influx (**D**) in mice pre-treated with 200 µg of LP17 or control protein in bilateral ischemia model. Treatment was performed 1 hour before surgery. Mice received 100 µl of LP17/control protein dissolved in sterile NaCl by intra-peritoneal injection. Sham mice received the same treatment (n =8-10/group).

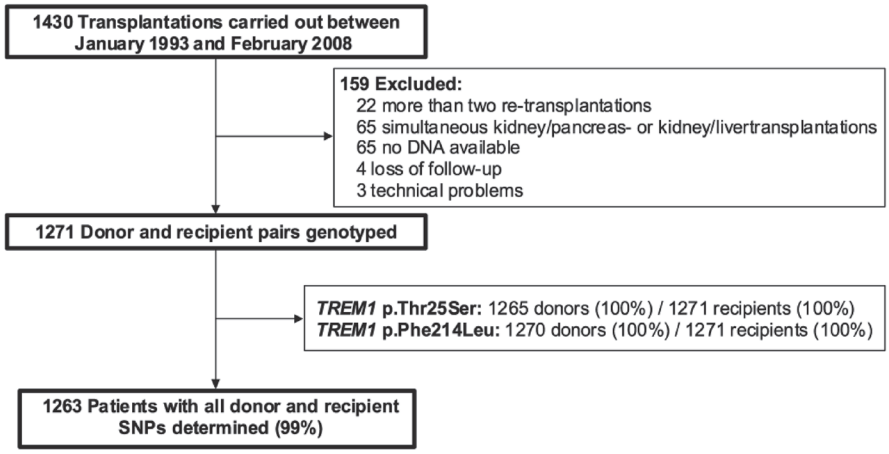

Supplementary Figure S4. Flow diagram of the in- and excluded patients with the amount of missing data on the three single nucleotide variants in donors and recipients.

Supplementary Table S1. Characteristics of the 5 renal transplant recipients with a homozygous recessive variant of TREM1 p.Thr25Ser. Pt, patient; CIT, cold ischemia time; WIT2, anastomosis time; DGF, delayed graft function; DCGF, death-censored graft failure.

Pt	Age (yr)	Donor type	CIT (min)	WIT2 (min)	DGF	Rejection	Time to rejection (months)	DCGF	Time to DCGF (years)
1	64	Deceased	1800	30	No	No	-	No	-
2	36	Deceased	720	17	No	Yes	1	No	-
3	59	Deceased	1560	35	No	Yes	1	Yes	7
4	35	Deceased	115	37	No	Yes	1	No	-
5	24	Deceased	152	41	No	Yes	5	Yes	2

Chapter 6

TREM-1 limits the maladaptive repair following renal ischemia/reperfusion by preserving mitochondrial function and proliferative capacity of tubular epithelial cells

A. Tammaro, A.M.L. Scantlebery, C. Borrelli, E. Rampanelli, N. Claessen, L.M. Butter, G.J.D. Teske, A. Soriani, M. Colonna, J. C. Leemans, M. C. Dessing and S. Florquin

Manuscript in preparation

Abstract

The long-term sequelae of acute kidney injury (AKI) include the loss of tubular epithelial cells (TECs) function, which constitutes a major clinical problem that is associated with a high risk for the development of chronic kidney disease (CKD). Infiltrating inflammatory cells and TECs play a pivotal role in the development of, and recovery from, AKI. TREM-1 is expressed on inflammatory cells but also on epithelial cells, and it enhances the inflammatory response elicited by Pattern Recognition Receptors. Fine tuning of the immune response is critical in preventing excessive inflammation and promoting tubular regeneration. Here we investigated whether TREM-1 plays a role in the recovery from renal ischemia/reperfusion (IR) injury. WT and TREM1/3 KO mice were subjected to renal IR and sacrificed 1, 5 and 10 days later. TREM1/3 KO mice displayed no major differences during the acute phase of injury, however, they showed significantly increased mortality. This detrimental effect was associated with a maladaptive repair response, characterized by persistent tubular damage, inflammation, fibrosis and tubular senescence. Interestingly, we found that TREM1/3- deficient TECs displayed an altered mitochondrial homeostasis and cellular metabolism, which resulted in increased senescence, following in vitro-simulated IR.

In summary, we have unraveled a novel mechanism that takes place in senescent TECs that involves metabolic reprogramming, regulated by the innate immune receptor TREM-1. This suggests that targeting TREM-1 may improve tubular regeneration and prevent the risk of AKI-CKD progression, by controling mitochondrial energy metabolism.

Introduction

Acute kidney injury (AKI) is still associated with high morbidity and mortality and represents a financial burden for society. Recent epidemiological and clinical studies have linked AKI to an increased risk of developing progressive chronic kidney disease (CKD)[1]. One of the most common causes of AKI is ischemic damage. Of all the cellular components within the nephron, the renal tubular epithelial cells (TECs) are the most sensitive to ischemic injuries, due to their high metabolic rate. These cells, however, are not merely silent victims of the injury, but they are a driving force in promoting detrimental interstitial inflammation, resulting in renal fibrosis[2]. Following ischemic damage, TECs start to release various kinds of danger molecules, eliciting the activation of the innate immune system through pattern recognition receptors (PRRs), incuding Toll Like Receptors. This results in the production of pro-inflammatory mediators, which act in an autocrine or paracrine manner, to stimulate leukocytic infiltration in the kidney and amplify tubulointerstitial inflammation, which further fuels cell death in TECs[3].

The renal epithelium has regenerative capacities; surviving TECs enter the cell cycle within a few hours after AKI, in order to promote renal repair[4,5,6]. This is the so-called "adaptive repair" post-AKI, which results in the recovery of renal function. However, maladaptive repair might also occur, as a consequence of cell cycle arrest or senescence in TECs. Subsequent release of pro-fibrotic factors from G2/M-arretsed TECs results in renal fibrosis, loss of renal function and CKD[7,8]. Cellular senescence can be triggered by DNA damage, oxidative stress or mitochondrial injury[9]. TECs are densely packed with mitochondria, because of their high metabolic functions. Thus, it is not surprising that mitochondrial dysfunction in TECs is thought to be a pathogenic mechanism underlying the transition from AKI to CKD[8,10].

Triggering Receptor Expressed on Myeloid cells-1 (TREM-1) is known as an amplifier of the inflammatory response elicited by TLR4, and we have previously published that following renal Ischemia Reperfusion (IR), TREM-1 is upregulated in the kidney, due to the infiltration of granulocytes, expressing high levels of TREM-1[11,12]. However, TREM-1-induced inflammation appears to be dispensable during IR, because TREM-1 blockers did not protect the kidney from damage and inflammation after the acute phase of injury, suggesting that other immune pathways are more relevant in this context[11]. During sterile inflammation the expression of TLR4 and TREM-1 is not restricted to cells of the myeloid lineage but is also detectable on epithelial cells[13,12]. TLR4-mediated inflammation appears detrimental during the acute phase of injury after IR but essential for tubular recovery[14,15,16,17]. Besides its role in immune regulation, TREM-1 has also been linked to cell survival and mitochondrial integrity[18]. Given the results of these studies, we hypothesized that TREM-1 could play a role in renal repair post-AKI.

Despite the fact that TREM-1 blockers did not result in renoprotection during the acute phase of injury, as we recently described, here we report a mechanism through which TREM-1 limits the maladaptive repair following IR, by preventing tubular senescence[11]. TREM-1 preserves the mitochondrial homeostasis and energy metabolism necessary for tubular proliferation, which favors renal regeneration after IR.

Materials and methods

Reagents and antibodies

Rat-anti-mouse F4/80 (BD pharmigen), mouse-anti-mouse αSMA (clone 1A4, DAKO), rabbit-polyclonal collagen type 1 (Genetex), rabbit-anti-Ki67 (Sp6, Neomarkers), goat polyclonal-anti TREM-1 (Santa Cruz), rabbit polyclonal-anti TREM-1 (Abcam), mouse-anti phosphorylated histone H3 (Phospho S10) (Abcam), anti Tom20 (Clone 2Fb.1) (Millipore) and anti p21/WAF/Cip1 (Millipore), rabbit-anti biotinylated TREM-1 antibody (50D1 clone; gift from Colonna Lab), rabbit-anti Mitofusin2 (D2D10) (Cell signaling), Rabbit-anti AMPKα and Phospho-AMPK α (Cell signaling), streptavidine-APC (BD).

Murine models of renal IR

All animal experiments were approved by the Institutional Animal Care and Use committee of University of Amsterdam, and were in compliance with the ARRIVE guidelines (NC3Rs). Eight-week-old male C57Bl/6J (B6J) mice were purchased by Charles River. TREM1/3 double KO mice were generated, as previously described[19], backcrossed to a C57Bl6 background and bred in the animal facility of the Academic Medical Center in Amsterdam, The Netherlands. Age- and sex-matched mice were used. Animals were kept under standard environmental conditions (temperature, humidity, ventilation, light/dark cycle), housed in specific pathogen-free conditions (SPF) with *ad libitum* access to water and food.

WT C57BL/6 and TREM1/3 KO mice (n=8) were subjected to severe AKI (bilateral renal IR, 25 minutes clamping time) or mild AKI (unilateral renal IR, 20 minutes clamping time), as previously described[11]. Under 2.5% isoflurane-induced anaesthesia, mice underwent clamping of the renal artery for the previously mentioned time periods. After clamp removal, kidneys were inspected for restoration of blood flow. Upon completing surgery, muscle and skin layers were closed with surgical sutures (6-0, Tyco). Fifty μg/kg buprenorphine was administered through a subcutaneous injection, for analgesic purposes (Temgesic Shering-Plough). Animals were sacrificed via cardiac exsanguination followed by cervical dislocation, at day 1, 5 and 10 post-surgery. Blood and kidneys were

harvested for further analysis. Sham mice were sacrificed at day one. Contralateral/ unobstructed left kidneys, were also used as controls for the mild AKI experiments.
For the isolation of primary TECs, we used a well-established protocol from our department[20]. Briefly, kidneys were removed and stored on ice in Hank's Balanced Salt Solution (HBSS), supplemented with 50 U penicillin and 50 µg/ml streptomycin. After removal of the renal capsule, tissue was minced with scalpels. A single-cell suspension was obtained by means of collagenase digestion. Cells were strained over a 70- and 40-µm filter mesh and cultured in HK-2 medium (see below) under normal culture conditions.

ELISA

The levels of KC, MCP-1 and soluble TREM-1 protein (sTREM-1) were measured by ELISA in kidney homogenates. Plasma levels of sTREM-1 were also measured. Frozen renal tissues were processed in Greenberger lysis buffer (150mM NaCl, 15mM Tris, 1mM $MgCl_2$ pH 7.4, 1mM $CaCl_2$, 1% Triton x-100), supplemented with 1% protease inhibitor cocktail (Sigma-Aldrich, Zwijndrecht, The Netherlands). sTREM-1 duo set Elisa (R&D) was used according to the manufacturer's protocol. Renal TREM-1 levels were adjusted for total protein concentration, as measured by BCA (Thermo Fischer).

Western blot

For tissue protein isolation, 30µM –thick, frozen kidney slices were used. Tissue and cells were lysed in RIPA buffer (50 mM Tris pH7.5, 0.15 M NaCl, 2 mM EDTA, 1% deoxycholic acid, 1% NP-40, 4 mM sodium orthovanadate, 10 mM sodium fluoride), supplemented with 1% protease inhibitor cocktail (Sigma-Aldrich). Lysates were loaded onto a 4-12% Nupage gel and blotted onto a PVDF membrane. After blocking aspecific signal, blots were incubated overnight with primary antibodies. Blots were incubated with horseradish-peroxidase-conjugated secondary antibodies and detected with ECL (Pierce).

Tissue staining

Paraffin-embedded kidney tissue, was fixed in 4% formalin for 24 hours before processing. For (immuno) histological examination, 4µM-thick paraffin sections were used. The tubular injury score was determined in PAS-D-stained sections, by a pathologist, in a blinded manner, using a 5-point scale that is based on the presence of necrosis, as previously described[21] . Immunohistochemical staining was performed for the detection of macrophages, myofibroblasts, collagen deposits and proliferating TECs. Sections were processed for antigen retrieval followed by overnight incubation with primary antibodies, at 4°C. Sections were then incubated with peroxidase-conjugated secondary antibodies for 30 minutes and stained with 3,3-diaminobenzidine (DAB). The amount of

positive staining for F4/80, αSMA and collagen I was quantified with ImageJ software, Fiji (NIH), a computer-based imaging analysis for reliable biomarker quantitation. Proliferating TECs were counted in the cortico-medullary region in 10 randomly chosen non-overlapping HPFs (magnification 40X).

RT-PCR

Total RNA was extracted from frozen kidneys using Trizol-reagent (Sigma-Aldrich). cDNA was synthesized using M-MLV reverse transcriptase and oligo-dT primers. Transcript analysis was performed by real-time quantitative PCR on the Roche Light Cycler 480 using SYBR green master mix (Bioline). Relative expression was analysed using LinRegPCR (developed by Hearth failure research center, University of Amsterdam, the Netherlands). Gene expression was normalized to murine Peptidylprolyl Isomerase A (*Ppia*) and Tata Box binding Protein (*Tbp*) housekeeping genes. Murine primers sequences are: *Tbp* (for 5'-GGAGAATCATGGACCAGAAC; rev 5'-GATGGGAATTCCAGGAGTCA); *Ppia* (for 5'- ATGCCAGGGTGGTGACTTTAC; rev 5'-GATGCCAGGACCTGTATGCT); *Neutrophil gelatinase–associated lipocalin (Ngal)* (for 5'-GCCTCAAGGACGACAACATC; rev 5'-CTGAACCAATTGGGTCTCGC); *Kidney injury molecule*-1 (*Kim1*) (for 5'-TGGTTGCCTTCCGTGTCTCT; rev 5'-TCAGCTCGGGAATGCACAA); *Il1b* (for 5'-CTGCAGCTGGAGAGTGTGGAT; rev 5'-GCTTGTGCTCTGCTTGTGAG); *Il6* (for 5'-GCTACCAAACTGGATATAATGGA; rev 5'-CCAGGTAGCTATGGTACT6CCAGAA); *Il1a* (for 5'- CGCTTGAGTCGGCAAAGAAAT; rev 5'- TGATACTGTCACCCGGCTCT) *Vascular endothelial growth factor (Vegf)* (for 5' -GCCCGGGCCTCGGTT; rev 5' -AACTTGATCACTTCATGGGACTTC); *Transforming growth factor β1 (Tgf)* (for 5'-GCAACATGTGGAACTCTACCAGAA; rev 5' –GACGTCAAAAGACAGCCACTCA); *Connective tissue growth factor (Ctgf)* (for 5- TGACCTGGAGGAAAACATTAAGA; rev 5'- AGCCCTGTATGTCTTCACACTG); *Mitochondrial transcription factor A (Tfam)* (for 5'-TCGCATCCCCTCGTCTATCA; rev 5'- CCACAGGGCTGCAATTTTCC); *Peroxisome proliferator-activated receptor gamma coactivator 1-α (Pgc1a)* (for 5'GAGCGAACCTTAAGTGTGGAA; rev 5'- TCTTGGTTGGCTTTATGAGGA).

Immunofluorescence

Cells cultured on coverslips were used for immunofluorescence staining. Primary and secondary antibody labelling was performed in 0.5% BSA and 0.1% Triton X-100. Secondary antibodies were detected with either Texas Red or Alexa fluor-labelled antibodies. Cells were counterstained with Hoechst 33342 for nuclear staining (Sigma). Fluorescence microscopy and image acquisition was performed on a Leica DM5000B using the LAS acquisition software (Leica).

Cell culture and in vitro-simulated IR

Cells were cultured in HK-2 medium (DMEM/F12 medium, supplemented with 10% FBS, 5 µg/ml insulin and transferrin, 5 ng/ml sodium selenite, 20 ng/ml triiodo-thyrionine, 50 ng/ml hydrocortisone, and 5 ng/ml prostaglandin E1 with l-glutamine and antibiotics). Conditionally immortalized TECs (IM-PTECs) were cultured at 33°C in the presence of 10 ng/ml IFN-γ (ProSpec) and kept at 37°C without IFN-γ for another week before the start of the experiment, resulting in loss of SV40 expression[22]. Primary TECs were isolated and cultured as described above[23].

Ischemia-reperfusion (IR) injury in primary or immortalized tubular epithelial cells was performed as follows. Cells were cultured until confluency, incubated in complete medium in the HypOxystation H35 (Don witley scientific) and cultured for 2 days in 1% Oxygen, 5% CO2 at 37°C, in order to mimic the hypoxic situation experienced *in vivo*, as previously described[24]. Cell viability was assessed with the MTT staining. Control (CTR) cells were kept in culture under standard conditions. After 2 days of hypoxia, both hypoxic and CTR cells received fresh medium and were cultured for an additional 24 hours under standard conditions.

Flow cytometry analysis (FACS)

To determine TREM-1 expression on proximal TECs, cells were detached by treatment with trypsin, washed and suspended in staining buffer (PBS without Ca2+ Mg2+, 0.5% BSA, 2 mM EDTA, 0.025% NaN3). Trypsin digestion did not affect TREM-1 surface expression, as observed in blood-derived granulocytes (data not shown). Anti-CD16/32 (clone 24G2) was added for 10 min to prevent non-specific Fc-mediated binding. Cells were then stained with anti-TREM-1 Ab in staining buffer for 20 min at 4°C. Propidium Iodide was added prior to acquisition for dead/live staining. Samples were analysed using the FACSCanto II flow cytometer (BD Biosciences) and data were analysed using FlowJo 7.6 software (TreeStar).

SA-β-Galactosidase staining

Frozen kidney tissue or cells cultured on coverslips were used for microscopic analysis. Fixation and staining was performed with the senescence-associated β-galactosidase (SA-β-Gal) staining kit (cell signaling), according to the manufacture's protocol. Senescent cells were identified as blue-stained cells by standard light microscopy. Quantification of positive staining was performed with Image Pro Premier (vs. 9.3; Media Cybernatics, Rockville, MD, USA). We used the smart segmentation approach to segment the immunopositive area, which is expressed as a percentage of the total tissue surface (area). The percentage of the immunopositive area was calculated in images of 10 non-overlapping HPFs, per slide (n=5).

SA-β-Gal activity was measured by means of a flow cytometric assay, using the fluorogenic substrate C_{12}FDG (Invitrogen), as previously described[25]. Cells were previously incubated with Fixable Viability Stain 780 (BD) in order to exclude dead cells.

In vitro assays

All *in vitro* assays were performed in primary TECs from WT and TREM1/3 KO mice (n=5-7) and 5-6 replicates were examined per animal.

Cellular oxygen consumption rate (OCR) was determined in primary cells plated on a PureCol coated XF 96well assay plate, one day prior to the assay. OCR data were determined with the XFe96 Extracellular flux analyzer (seahorse bioscience) using the XF Cell Mito Stress Test which was used according to the provided protocols[20]. Briefly, cells were incubated in assay medium (DMEM phenol red, 25mM D-glucose, 1mM Na pyruvate, 2mM glutamine, adjusted to pH 7.4) for 1 hour at 37°C in a non-CO_2 incubator, after subsequent injecting and mixing of the compounds (1.5μm oligomycin, 1μm FCCP or 1.25μm rotenone+ 2.5μm AntimycinA).

For ATP cell measurements, primary TECs were subjected to *in vitro* IR. ATP levels were detected with a kit, according to the manufacturer's protocol (Thermo Fischer) and adjusted for cell input by total protein concetration, as determined by BCA.

To examine the effect of *in vitro* IR on mitochondrial superoxide production, primary TECs were labeled with 5 μM MitoSOX Red (Thermo Fisher) in HBSS, supplemented with calcium and magnesium (Gibco), for 10 min in the dark at 37°C. Relative fluorescence was measured by FACS.

For the measurement of mitochondrial membrane polarity, primary TECs were plated in black 96-well Clear plates (Greiner) and subjected to *in vitro* IR, as described above. Mitochondrial polarity was determined using the MITO-ID Membrane potential cytotoxicity kit (Enzo Life Sciences). Dual fluorescence was measured using the CLARIOstar plate reader. Data are expressed as the ratio between the JC-1 red fluorescence (mitochondria) (514 nm Ex/590 nm Em) and green fluorescence (cytoplasm) (514 nm Ex/529 nm Em), as previously described[26].

Determination of intracellular metabolite abundance by LC-MS

Primary TECs, seeded at equal density and cultured for 48 hours, were used for metabolomics experiments which were performed at the Metabolomics Core Facility of the Academic Medical Center, University of Amsterdam. Procedure is explained below.

Cells were washed with ice-cold PBS and metabolism was quenched by adding 1 mL of ice-cold methanol followed by 1 mL of ice-cold water.Cells were collected by scraping. The samples were incubated in a sonication bath and sonicated for 15 minutes. The homogenate was transferred to a 2 mL tube and 1 mL of chloroform was added,

afterwhich the homogenate was vortexed and centrifuged for 5 minutes at 14,000 rpm at 4°C. The "polar" top layer was transferred to a new 1.5 mL tube and dried in a vacuum concentrator. Dried samples were dissolved in 100 µL methanol/water (6/4; v/v).
For the analysis, a Thermo Scientific ultra-high pressure liquid chromatography system (Waltman) coupled to Thermo Q Exactive (Plus) Orbitrap mass spectrometer (Waltman) was used. The autosampler was held at 10°C during the runs and 5 µL sample was injected onto the analytical column. The chromatographic separation was established using a SeQuant ZIC-cHILIC column (PEEK 100 x 2.1mm, 3.0µm particle size, Merck) and kept at 15°C. The flow rate was 0.250 mL/min. The mobile phase was composed of (A) 9/1 acetonitrile/water with 5 mM ammonium acetate; pH 6.8 and (B) 1/9 acetonitrile/water with 5 mM ammonium acetate; pH 6.8. The LC gradient program was as follows: beginning with 100% (A) hold 0-3 min; ramping 3-24 min to 20% (A); hold from 24-27 min at 20% (A); ramping from 27-28 min to 100% (A); and re-equilibrate from 28-35 min with 100% (A). The MS data were acquired in negative mode at full scan range at 140,000 resolution. Interpretation of the data was performed in the Xcalibur software (Thermo Fisher).

Wound healing assay

Primary TECs from WT and TREM1/3 KO animals (n=5) were isolated, cultured and subjected to *in vitro* IR, as described above. Subsequently, a scratch was made using a p100 pipette tip and cells were monitored for the following 24 hours, using a live cell phase-contrast microscope (Leica DMi8). Settings were adjusted with LasX software (Leica). Recovery was assessed by an in-house developed method (CiMicro software), which measures the surface of the wound area (in pixels).

Stable gene silencing by sgRNA

Stable knockout cells were generated by transduction with lentiviral particles harbouring single guide RNA (sgRNA) for 24h, in the presence of 8µg/ml polybrene (Sigma Aldrich) and puromycin (Sigma Aldrich). Selection was initiated 48h after transduction.
Lentiviral particles were produced by transfecting HEK293T cells, using GENIUS DNA Transfection Reagent (Westburg), with the following vectors: pMD2.G/VSVG (Addgene 12259), pPAX2 (Addgene 12260) and pLentiCRISPRv2 (Addgene 52961) at a DNA ratio of 6:15:20 µg DNA ratio, respectively. Single guide RNA (sequence: CTTCCATCCTGTCCGCCTGG) targeting murine TREM-1 was inserted into the lentiviral vector pLentiCRISPRv2, according to the protocol described by Sanjana et *al.*[27]

BrDU incorporation assay

For Cell-cycle analysis, cells were incubated for 1 hour with 20 µM BrdU (Sigma Aldrich) and subsequently fixed in 70% ice-cold ethanol. Cells were processed as described previously

in our department[28]. Staining with anti-BrdU FITC (clone B44; BD) was performed in buffer, containing 0.05% Tween-20/0.5% BSA in PBS. After washing, cells were stained with 0.1 µM TO-PRO-3-iodide (Invitrogen Life Technologies) in PBS/0.5% BSA, containing 500 µg/mL of RNAse-A (Bioke), for 15 minutes at 37°C. Cell-cycle distribution was analysed by flow cytometry.

Statistics

For in vivo experiments, comparisons between 2 groups were analyzed using Mann-Whitney U-test or between more than 2 groups with the Kruskal-Wallis test. For in vitro experiments comparison between two groups was analyzed using the two-tailed student t-test. Values are expressed as mean ± standard error of the mean (S.E.M). P values <0.05 were considered statistically significant.

Results

TREM-1 limits maladaptive repair following renal ischemia/reperfusion injury

We have previously described that 1 day post bilateral IR, TREM-1 is expressed in the kidney and plasma of WT mice[11]. Here, we show that TREM-1 protein level is also significantly increased during the recovery (*t=5*) and resolutive phase (*t=10*) in renal tissue, when compared to sham kidneys (Figure 1A). However, in circulation, TREM-1 protein levels increased only at day 1 and 5 post-IR (Figure 1B). Once it had been established that TREM-1 was indeed expressed in both the acute and recovery phases of IR, we speculated as to whether TREM-1 might play a role in renal tissue repair. Therefore, we subjected WT and TREM1/3 KO mice to bilateral IR. The survival graph (Figure 1C) shows significantly increased mortality in mice lacking TREM1/3, starting at 2 days post-IR. Suprisingly, renal inflammatory cytokines, including KC and MCP-1 did not show any differences between WT and TREM1/3 KO mice, in neither sham nor day 1 and 5 post-IR groups (Table 1). We did not include the *t=10* time point as the number of surviving KO animals was significantly decreased compared to that of WT mice (WT: n=8 vs TREM1/3 KO: n=3).

In order to investigate the role of TREM-1 during recovery from AKI, we switched to a milder model of AKI to avoid mortality (unilateral IR with 20 minutes clamping time). We observed that, compared to WT animals, mice lacking TREM1/3 displayed significantly more tubular damage 10 days post-AKI, as analysed by the PAS-D score (Figure 1D) and increased expression of tubular injury markers, such as *Kim-1* and *Ngal* (Figure 1E-F). This increased tubular damage suggested impaired repair, which could eventually lead to renal fibrosis[7]. Therefore, we looked at the infiltration of macrophages, which are well-

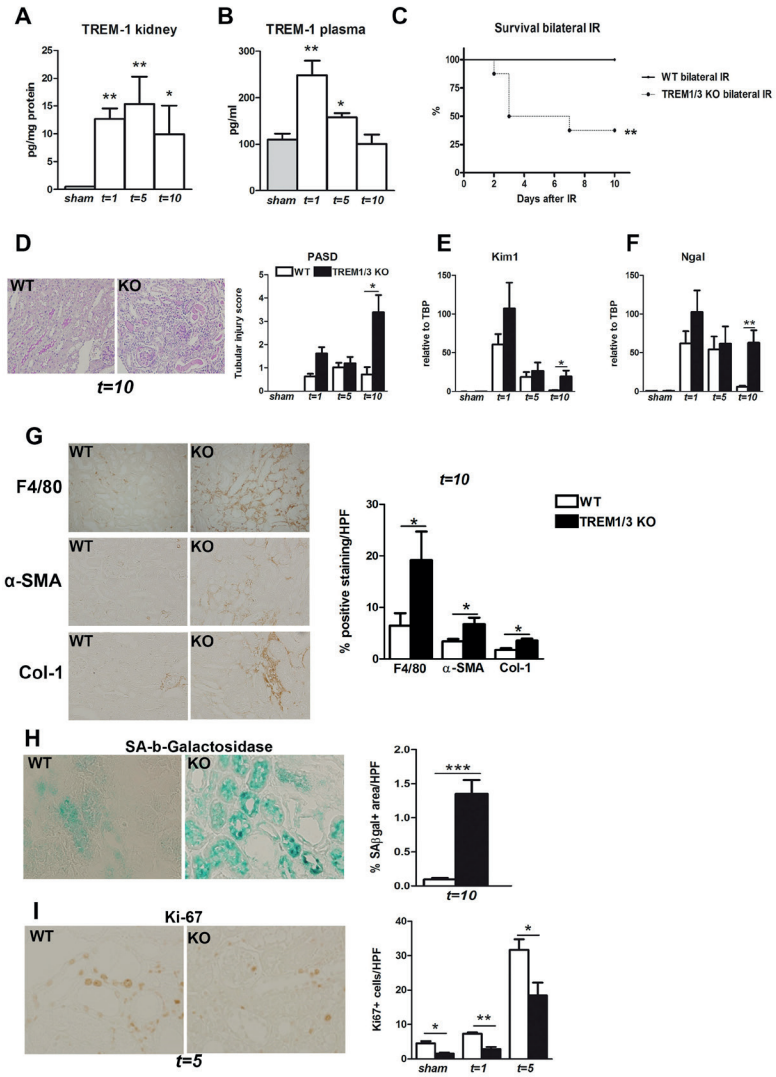

Figure 1: TREM-1 limits the maladaptive repair following renal IR injury.
(**A**) TREM-1 protein levels in kidney lysates and (**B**) plasma from sham-operated mice and WT mice subjected to bilateral IR (25 minutes clamping) and sacrificed at day 1, 5 and 10 post-surgery. (**C**) Survival graph of WT and TREM1/3 KO mice subjected to bilateral IR for 25 minutes (=severe AKI). (**D**) Quantification of tubular injury score obtained by PAS-D staining in kidney tissue from WT and TREM1/3 KO animals sacrificed at day 1, 5 and 10 post-unilateral IR (=mild AKI). Representative pictures of WT and TREM1/3 KO animals at day 10 post-IR. (**E-F**) Renal expression of tubular injury markers Kim-1 and Ngal measured by RT-PCR in tissue isolated from sham WT, WT and TREM1/3 KO mice sacrificed 1, 5 and 10 days post-IR. (**G**) Quantification of immunohistochemical staining and representative pictures for macrophages (F4/80), myofibroblasts (α-SMA) and collagen type-1 deposits in WT and TREM1/3 KO mice 10 days post-surgery (magnification 40X). (**H**) Quantification and representative pictures of SA-β-Gal staining in WT and TREM1/3 KO mice 10 days post-surgery (magnification 40X). (**I**) Quantification of tubular proliferation detected by Ki67 immunohistochemistry staining in WT and TREM1/3 KO mice in sham conditions and 1 and 5 days post-surgery. Representative pictures of WT and TREM1/3 KO kidneys at day 5 (magnification 40X). Data are expressed as mean ± SEM. One way Anova followed by Mann Whitney test was used to determine statistical differences. *P<0.05, **P<0.01, ***P<0.001

known to facilitate tubular repair but, if persistent, may further boost inflammation and drive fibrosis[29]. Renal tissue from TREM1/3 KO mice displayed increased infiltration of F4/80 positive macrophages, compared to WT animals at *t=10* time point. This excessive macrophage infiltrate was associated with the development of renal fibrosis, as reflected by an increase in α-SMA positive myofibroblasts and collagen type-1 deposits, in mice lacking TREM1/3, compared to WT animals (Figure 1G). Altogether, these data suggest the activation of a maladaptive repair process in TREM1/3 KO mice, which is often associated with tubular senescence and proliferation arrest in TECs. Therefore, we evaluated the presence of SA-β-Gal positive tubular cells in tissue from WT and TREM1/3 KO mice, 10 days after IR. As shown in Figure 1H, TREM1/3 KO mice displayed significantly increased tubular senescence, compared to WT animals. This is possibly linked to the decreased tubular proliferation observed in KO animals, both at steady state and after IR, as shown by the Ki67 staining (figure 1I). Taken together, these *in vivo* data suggest that the TREM-1 receptor plays a role in renal tissue repair after AKI, possibly by preventing tubular senescence and promoting regeneration.

TREM1/3-deficient TECs display cell cycle arrest and impaired energy metabolism at steady state

Tubular proliferation is essential for renal repair post-IR. In order to determine whether TREM-1 plays any role in this process, we first checked for TREM-1 expression in TECs following *in vitro*-simulated IR. With the use of different techniques, we detected an increased expression of TREM-1 in IR TECs, compared to CTR cells (Figure 2A-C), suggesting a role for TREM-1 in tubular regeneration. Since we observed a decrease in tubular proliferation *in vivo* in the absence of TREM1/3, we further explored the phenotype of steady state primary TECs, isolated from WT and KO animals. Consistent with the *in vivo* observation, we found an increased number of phosphorylated histone H3 Ser10 (p-H3ser10) positive nuclei in the absence of TREM1/3, indicative of a prolonged

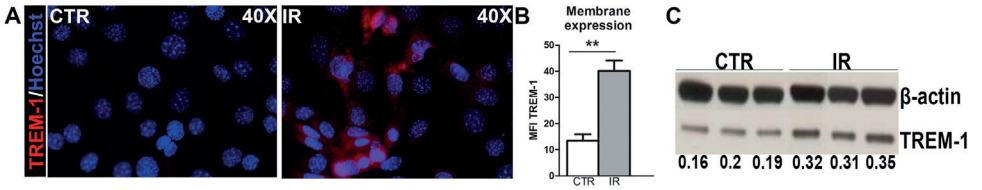

Figure 2: TREM-1 is expressed in TECs upon IR.
(**A**) Representative immunofluorescence images of IM-TECs cultured on coverslips in CTR conditions and after in vitro-simulated IR. Cells were stained with TREM-1 (red) and Hoechst (nuclei). (**B**) Mean Fluorescence intensity of TREM-1 membrane expression measured by flow cytometry. (**C**)Protein lysates of IM-TECs in CTR and IR conditions blotted for anti-TREM-1 Ab and β-actin. All data are expressed as mean ± SEM and the unpaired t-test was used to determine statistical differences. **P<0.01

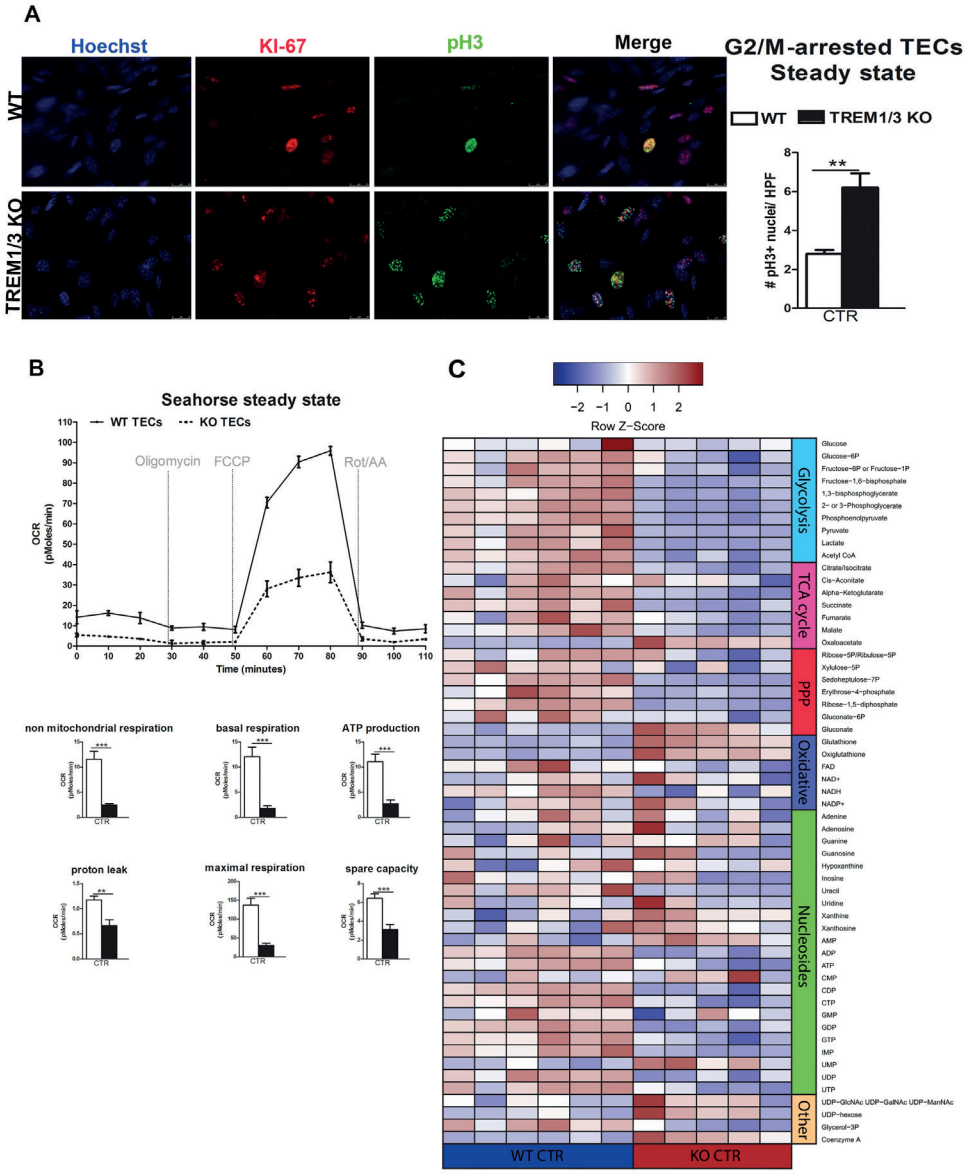

Figure 3: TREM-1 KO primary TECs display arrest in G2/M and reduced mitochondrial metabolism at steady state. (**A**) Representative immunofluorescence images of primary TECs isolated from WT and TREM1/3 KO animals (n=5) (magnification 40X). Cells were stained with Hoechst (nuclei), anti-Ki67 (proliferating cells; Texas Red) and anti-phosphorylated histone H3 (to identify cells in G2/M; FITC). Quantification of phosphorylated histone H3 positive nuclei per HPF. (**B**) Seahorse Bioanalyzer OCR readout of a typical mitochondrial function assay using WT and TREM1/3 KO primary TECs without adjustment for cell number. AA, antimycin A; rot, rotenone. Conditions were determined in triplicate. The bar graphs represent data adjusted for cell input for WT and TREM1/3 KO primary TECs. (**C**) Differences in cellular metabolites displayed is based on the metabolic pathways from WT amd TREM1/3 KO TECs at steady state. All data are expressed as mean ± SEM and the unpaired t-test was used to determine statistical differences. **P<0.01, ***P<0.001

arrest in the G2/M phase of the cell cycle (Figure 3A)[30]. Metabolically, to enter into mitosis, cells rely more on oxidative phosphorylation (OXPHOS) than glycolysis[31]. We examined the oxygen consumption rate (OCR) of steady state WT and TREM1/3 KO primary TECs using the Seahorse XF96respirometer. Our results show that TECs lacking TREM1/3 showed a significant down-regulation in oxidative metabolism, compared to WT cells, demonstrated by decreased non-mitochondrial respiration, basal respiration, ATP-linked respiration, proton leak, maximal respiration and spare capacity (Figure 3B). Similar results were obtained in a TEC cell line where only TREM-1 was silenced by CRISPR/CAS9 technology. In the absence of TREM-1, we observed delayed G2/M progression, which was associated with a reduction in several parameters of mitochondrial respriration (Supplementary Figure 1A-B). These results may exclude a role for TREM-3 in tubular proliferation *in vivo*.

To directly demonstrate the impact of TREM1/3 deficiency on TEC metabolism, we performed a mass spectrometry analysis of cellular metabolites. TREM1/3 absence has an important effect on tubular energy metabolism in general, as observed by a marked reduction in key intermediates of the glycolytic, tricarboxylic acid (TCA) and pentose phosphate pathway (PPP), and is evidently not restricted to OXPHOS. Interestingly, the levels of the antioxidants glutathione and oxiglutathione, were significantly upregulated in TREM1/3 KO TECs, compared to WT, suggesting an enhanced activity of mitochondrial defense systems against Reactive Oxigen Species (ROS) accumulation (Figure 3C).

Hence, these data suggest that TREM-1 may control energy metabolism to promote TEC proliferation.

TREM-1 fosters tubular repair after IR by preserving mitochondrial homeostasis.

From previous evidences obtained in bone marrow-derived macrophages, we know that TREM-1 plays a role in mitochondrial integrity[18]. Additionally, the increased levels of the anti-oxidants detected in TREM1/3 KO TECs, suggest an impaired control of antioxidants to control ROS levels, which could eventually impact mitochondrial energy metabolism. Therefore, we examined the functional and structural integrity of mitochondria after *in vitro*-simulated IR. To gain more insight into the mitochondrial morphology, we first looked at the expression of the mitochondrial protein TOM20. In TECs lacking TREM1/3, TOM20 staining clearly showed rounded and fragmented mitochondria, as compared to the typical filamentous network of mitochondria observed in WT cells. This altered morphology worsened when TREM1/3 KO TECs were exposed to IR (Figure 4A). In line with these findings, TOM20 protein levels, measured by WB, were significantly decreased in TREM1/3 KO TECs after IR, compared to WT cells (Figure 4B).

TREM1/3 deficiency was also associated with increased mitochondrial ROS production, as detected by the Mitosox probe, both in CTR and after *in vitro*-simulated IR (figure 4C). Futher analysis of mitochondrial function revealed an impressive mitochondrial depolarization, detected with the JC-1 potential-sensor (Figure 4D). Consequently, the mitochondrial dysfunction was associated with a decrease in ATP production in TREM1/3 KO TECs, compared to WT cells, under both CTR and IR conditions (Figure 4E). *Pgc1a*, *Tfam*, phospho-AMPK and Mitofusin-2 expression was found to be similar in WT and TREM1/3 KO TECs, indicating that the impaired mitochondrial homeostasis was not associated with any differences in mitochondrial biogenesis or dynamics (Supplementary Figure 2 A-C).

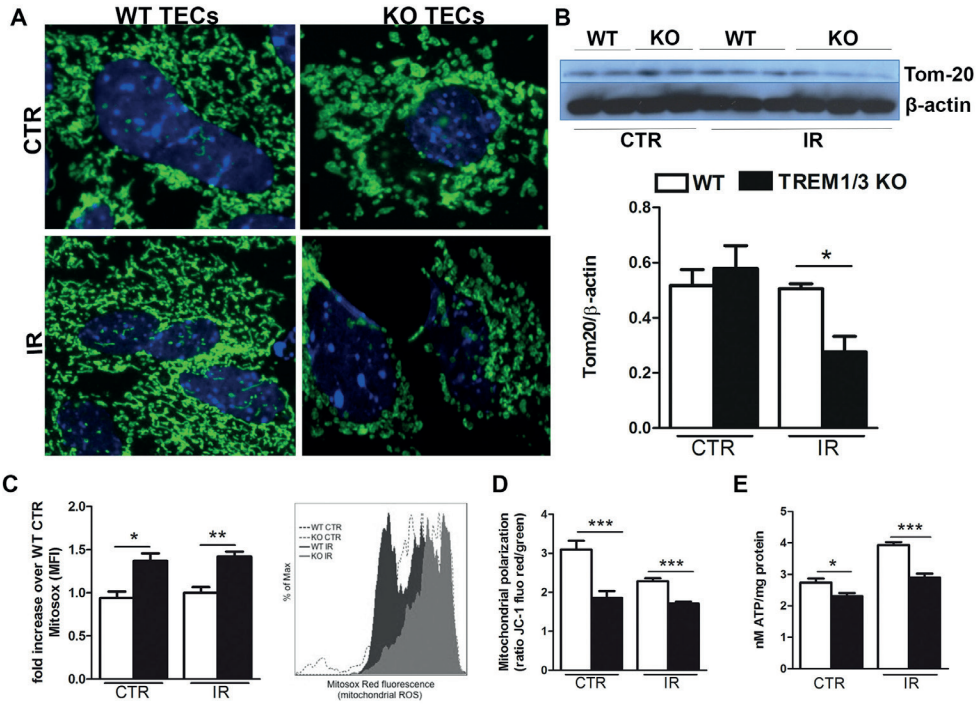

Figure 4: TREM-1 deficient TECs display altered mitochondrial homeostasis.
(**A**) Representative immunofluorescence images of primary TECs stained for mitochondrial protein TOM20 (FITC) and Hoechst (nuclear staining), under CTR conditions and 24 hours after IR (magnification 100X)(N=3 animals per conditions). (**B**) Western blot of WT and TREM1/3 KO primary TECs blotted for TOM20 and β-actin. (**C**) Mitochondrial ROS production measured by FACS analysis through MitoSox probe. Results are expressed as fold increase over CTR WT TECs of Mitosox Mean Fluorescence Intensity. Histogram representation of Mitosox events expressed as % of max. (N=5 animals per group). (**D**) Mitochondrial polarization measured by JC-1 fluorescent probe, expressed as a ratio between decrease in the red(mitochondria)/green(cytoplasm) fluorescence intensity. Results are expressed as a ratio of red/green fluorescent emission. (N=5 animals per group). (**E**) ATP production in protein lysates of WT and TREM1/3 KO primary TECs, corrected for the total protein measured by BCA (N=5 animals per group). All data are expressed as mean ± SEM and the unpaired t-test was used to determine statistical differences. *P<0.05, **P<0.01, ***P<0.001

Altogether, these data suggest that TREM-1 preserves mitochondrial homeostasis in TECs, possibly by limiting ROS production.

In vitro-simulated IR induces a senescent phenotype in TREM1/3 KO TECs

ROS-induced mitochondrial dysfunction can contribute to the development of senescence[32]. Considering that we observed tubular senescence *in vivo* after IR, we checked whether TREM1/3 KO TECs subjected to *in vitro*-stimulated IR could become senescent. By FACS analysis, we looked at C_{12}FDG positive cells (a fluorescente substrate for β-galactosidase, only retained in senescent cells). In WT cells, similar levels of C_{12}FDG incorporation were observed under CTR conditions and after IR. In contrast, TREM1/3 KO TECs show clear signs of senescence after *in vitro*-stimulated IR, as shown by FACS and microscopy (Figure 5A-B). Both cell cycle arrest and senescence have been shown to involve activation of the p21 $^{WAF1/CIP1}$ protein. TREM1/3 KO TECs displayed higher expression of p21, under CTR and IR conditions, as compared to WT TECs (Figure 5C), suggesting that TREM-1 may reduce the risk of cell cycle arrest and senescence in TECs.

TECs that are arrested in the G2/M phase, as well as those manifesting a senescent phenotype, release inflammatory and pro-fibrotic mediators to further exacerbate renal

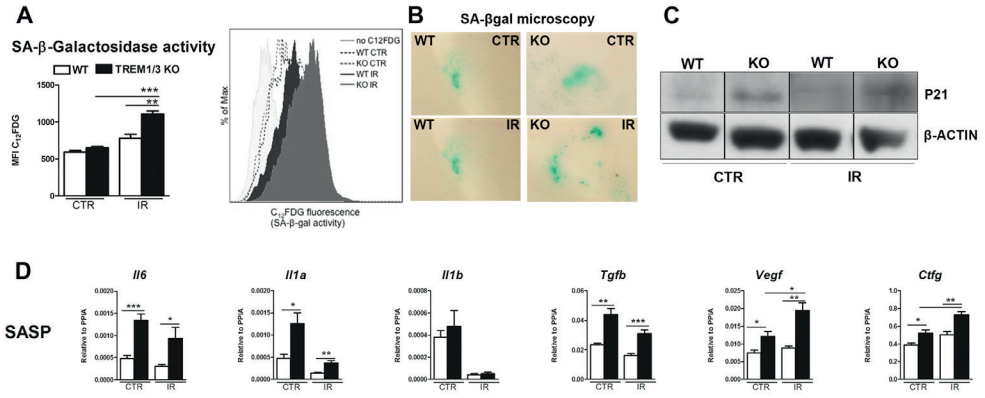

Figure 5: TREM1/3 KO TECs display senescence upon IR.
(**A**) FACS analysis of senescence- associated β-galactosidase (SA-βgal) assay by C_{12}FDG incorporation in WT and TREM1/3 KO primary TECs in CTR conditions and upon in vitro-IR (N=7). (**B**) (SA-βgal) staining obtained in primary WT and TREM1/3 KO TECs in CTR and IR conditions, cultured on coverslips (N=5). Blue/green cells represent senescent cells. (**C**) p21 protein expression showed by western blot in primary TEC lysates isolated from WT and TREM1/3 KO CTR animals and after 24 hours of IR. (**D**) Transcript expression of pro-inflammatory (Il6, Il1a, Il1b) and profibrotic genes (Tgfb, Vegf and Ctgf) in WT and TREM1/3 KO primary TECs under CTR conditions and after IR (N=5). All data are expressed as mean ± SEM and the unpaired ttest was used to determine statistical differences. *P<0.05, **P<0.01, ***P<0.001

inflammation and fibrosis[30,33]. Accordingly, under CTR conditions, TREM1/3 KO TECs displayed an increased secretory phenotype, characterized by higher transcription of pro-inflammatory genes, including *Il6* and *Il1,* compared to WT CTR TECs (Figure 5D). Furthermore, the expression of pro-fibrotic growth factors *Tgfb, Vegf* and *Ctgf* was significantly elevated in TREM1/3 KO CTR TECs, and increased even further when the cells became senescent upon *in vitro*-simulated IR (Figure 5D). In order to translate these findings into the functional settings of tissue repair, we subjected WT and TREM1/3 KO TECs to *in vitro*-simulated IR and then performed a wound healing assay. We measured the wound area (in pixels) at 8,16 and 24 hours after having scratched the monolayer with a pipette tip. In WT TECs the gap was completely closed after 24 hours, whereas TREM1/3 KO TECs showed a clear delay in wound healing. This suggests that senescence resulted in impaired wound healing (Figure 6A).

Taken together, these data suggest that TREM1/3 limits the development of tubular senescence by providing a bioenergetic balance necessary for renal repair after IR.

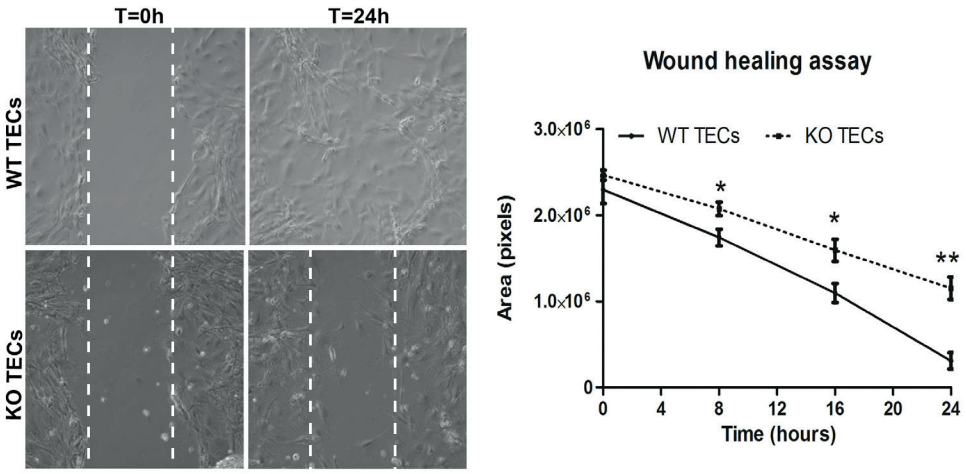

Figure 6: TREM1/3 KO TECs have impaired wound healing capacity after in vitro-IR.
Following in-vitro IR, the epithelial monolayer of WT and TREM1/3 KO TECs was damaged by a scratch with a p100 pipet tip. The damaged area is shown in the pictures taken with a contrast-phase microscope at T=0 and 24 hours later. Every 8 hours up to 24 hours the damaged area (shown in pixels) was measured with an in-house software (ci-Micro) developed by the department of cell biology and histology of our institution. All data are expressed as mean ± SEM (n=5) and the unpaired t-test was used to determine statistical differences. *P<0.05, **P<0.01

Discussion

Acute kidney injury (AKI) is a major clinical concern that is considered to be reversible, when not lethal in the acute phase. More recently, however, even mild episodes of AKI have been linked to subsequent development of CKD. One of the mechanisms underlying the detrimental progression to CKD is the maladaptive repair following AKI[34,8]. Thus, new avenues need to be explored to offer a therapeutic opportunity to reduce the risk of maladaptive repair and, hence, the development of CKD following AKI.

The innate immune receptor TREM-1 is involved in renal inflammation and fibrosis[12], however, its role in renal repair following AKI is still unknown. Herein, we provide evidences that TREM-1 preserves the functional integrity of mitochondria, which is crucial for an adequate energy supply and necessary for tubular proliferation. Thus, we are the first to establish a link between an innate immune receptor, mitochondrial energy metabolism and tubular senescence. We propose TREM-1 as a promising candidate for the improvement of renal repair after AKI and the prevention of CKD development.

We have previously described that TREM-1 does not play a crucial role in AKI. Indeed, TREM-1 blockers, namely LR12, LP17 and TREM-1 fusion protein, did not prevent renal damage and inflammation[11]. In contrast, in a model of renal fibrosis, TREM-1 had a direct effect on renal inflammation and macrophage alternative activation[35]. The role of TREM-1 in renal repair following AKI has not yet been completely unraveled. Here, we found that renal TREM-1 protein is greatly increased during repair (day 5), when tubular proliferation is at its highest level. When subjected to a severe model of IR, TREM1/3 KO animals show increased mortality starting at day 2 post-injury, when the acute phase of damage has declined and the repair phase is arising. Accordingly, in a milder model of injury, TREM-1/3 KO animals show no differences in renal damage 24 hours after reperfusion, but do display maladaptive repair with persistent tubular damage, inflammation, fibrosis and tubular senescence. Survival and proliferation of TECs are crucial for tubular regeneration after AKI and cell cycle disruption in TECs is associated with CKD[36]. We found that TREM-1 is expressed on TECs following IR. Previously, TREM-1 has been described as a hypoxia-inducible gene and was found to be upregulated in the epithelia of different organs upon inflammation[37,38,39]. Our results appear to be in line with these findings and suggest a role for TREM-1 in TEC recovery after IR. When we set out to dissect the mechanism, we noticed that already at steady state, TREM1/3 deficient TECs showed an altered cell cycle profile, namely increased G2/M arrest. Bonventre's group was the first to show that increased phosphorylation of histone H3 is indicative of prolonged arrest in the G2/M phase of the cell cycle, which hinders renal regeneration and exacerbates fibrosis[30,40]. For G2/M transition, cells sense and respond to an increase in energy demand, by

upregulating mitochondrial respiration, necessary for successful cell cycle progression[31]. The fact that mitochondrial respiration is greatly decreased in the absence of TREM-1, may explain the failure to progress in the cell cycle. However, a comprehensive analysis of cellular metabolites in TECs, revealed an overall metabolic meltdown in the absence of TREM1/3. The metabolic state of G2/M-arrested TECs has not yet been described, hence, we cannot exclude that the differences in the metabolic pathways might be related to the decreased proliferation. In order to carry out many functional tasks, TECs need an adequate energy supply and, therefore, healthy mitochondria. TREM1/3-deficient TECs displayed an impaired mitochondrial homeostasis with mitochondria fragmentation, massive accumulation of reactive oxygen species (ROS), membrane depolarization and decreased ATP production. When exposed to IR, the decline of mitochondrial function was even more evident. We believe that the root of mitochondrial dysfunction could be related to an increased oxidative damage. Mitochondria generate ROS during oxidative metabolism[41]; however, ROS levels that exceed the local antioxidant capacity is a biomarker for mitochondrial dysfunction[42,43,44]. The mitochondrial antioxidant glutathione (mGSH) for instance, maintains appropriate ROS levels to minimize oxidative damage and prevent mitochondrial dysfunction[44]. The excessive levels of mitochondrial ROS in TREM-1 KO TECs were associated with increased levels of glutathione, possibly as an adaptive response to sustained ROS production. This increase in oxidative damage may explain the impaired ability of mitochondria to synthesize ATP and carry out many metabolic functions, as observed in the TREM1/3 KO TECs[41]. In bone marrow-derived macrophages, TREM-1 enhances mitochondrial integrity by inducing Mitofusin-2, promoting mitochondrial fusion and inhibiting apoptosis[18]. However, in our model using TECs, no differences in the expression of Mitofusin-2 were observed, suggesting that mitochondrial dynamics were not the cause of the mitochondrial defects described in TECs. We also excluded the involvement of mitochondrial biogenesis as a cause of decreased mitochondrial function[45].

Disturbed mitochondrial homeostasis can predispose cells to senescence[46,47,48]. Additionally, many studies show that ROS accumulation can induce mitochondrial dysfunction, resulting in the inductiont of cellular senescence. When TREM1/3 KO TECs were exposed to an extra ROS-generating trigger, such as hypoxia/reperfusion, this was sufficient to drive the cells into a senescent state. Cell cycle arrest and senescence involve activation of the DNA damage response (DDR) and cyclin-dependent kinases, in order to recognize and repair genetic defects[49]. p21 is involved in the G2 checkpoints and its activation is linked to cell cycle arrest and senescence[50]. In line with these studies, the cell cycle arrest and senescence observed in TREM1/3 KO TECs were associated with increased p21 activation. Interestingly, mice deficient for p21 are protected against renal

dysfunction and fibrosis after renal ablation[30]. This would further support the evidence that decreased tubular proliferation may be the root of maladaptive repair and fibrosis in TREM1/3 KO mice. Additionally, the G2/M arrested TREM 1/3 KO TECs, were also able to release pro-fibrotic factors, which could possibly influence the renal microenviroment and create a vicious fibrotic cycle. Altogether, these observations indicate that in the absence of TREM 1/3, TECs are arrested in G2/M and that IR leads to a permanent arrest, manifested as senescence, which results in impaired wound healing. It is conceivable that the cell cycle arrest observed in TREM1/3 KO TECs is linked to DDR activation. Du et *al*. recently descibed that by decreasing DDR activation, TREM-1 directly promotes pre-leukemic stem cell expansion and leukemia development[51]. Possibly, a persistent DDR activation is present in the absence of TREM-1, which could explain the cell cycle arrest and senescence, as previously described[52].

Although we have demonstrated a link between TREM-1 and mitochondria energy metabolism, we remain unaware of the exact trigger for TREM-1 activation in this model and how an innate immune receptor present in the plasma membrane can affect mitochondrial homeostasis. Surely, TREM-1 ligand identification would help to clarify the mechanism, but this still represents a limitation in TREM-1 research[12]. One evidence that may explain the effect of TREM-1 on mitochondrial homeostasis points towards a direct effect of TREM-1 on TGFβ and vice versa[53,54]. Recently, it has been described that TGFβ1 and TREM-1 are mutually synergistic and that a positive feedback can be formed that accelerates the development and progression of pulmonary fibrosis[53]. Furthermore, the conventional role of TGFβ on tubular apoptosis has been reconsidered. Indeed, it appears that a transient expression of TGFβ on TECs is necessary for proliferation after IR and this accelerates recovery[55]. We propose that during repair, TGFβ is transiently induced in TECs to promote tubular proliferation[56,57], possibly through interaction with TREM-1, which is also expressed on surviving TECs. This cooperation leads to increased mitochondrial respiration, necessary for cell cycle progression and the restoration of tubular homeostasis after injury. Possibly, in the absence of TREM-1, the synergy between TGFβ and TREM-1 is interrupted, and the stimulation of tubular proliferation is, therefore, also lost. Consequently, the loss of this interaction may result in a steady (permanent), rather than transient, TGFβ expression, which may have deleterious effects on mitochondrial metabolism and senescence (see supplementary Figure 3). Supporting this speculation, TGFβ has been shown to modulate energy metabolism through the reduction of mitochondrial respiration and decrease ATP synthesis. This was associated with increased ROS and decreased membrane potential, leading to senescence in lung epithelial cells[58,59]. However, more research should be conducted to clarify this.

Finally, this study is the first to present a novel link between innate immune signaling, metabolic reprogramming and senescence. Although it is evident that senescence delays tissue repair and increases the risk of AKI-CKD progression, studies focused on the metabolic reprogramming that occurs in tubular senescent cells are at a very early stage. Here, we propose that the innate immune receptor TREM-1, is able to affect mitochondrial function in TECs, which regulates energy metabolism. In this way, TREM-1 has the ability to promote proliferation and regeneration in the tubular epithelium after AKI.

Targeting TREM-1 during active repair post-AKI may represent a novel strategy to directly induce cell cycle progression in TECs, by inhibiting the metabolic reprogramming, which decreases the risk of maladaptive repair post-AKI.

References

1. Chawla, L. S., Eggers, P. W., Star, R. A. & Kimmel, P. L. Acute Kidney Injury and Chronic Kidney Disease as Interconnected Syndromes. N. Engl. J. Med. 371, 58–66 (2014).
2. Liu, B.-C., Tang, T.-T., Lv, L.-L. & Lan, H.-Y. Renal tubule injury: a driving force toward chronic kidney disease. Kidney Int. 93, 568–579 (2018).
3. Bonventre, J. & Yang, L. Cellular pathophysiology of ischemic acute kidney injury. J. Clin. Invest. 121, (2011).
4. Berger, K. et al. Origin of regenerating tubular cells after acute kidney injury. Proc. Natl. Acad. Sci. U. S. A. 111, 1533–8 (2014).
5. Kusaba, T., Lalli, M., Kramann, R., Kobayashi, A. & Humphreys, B. D. Differentiated kidney epithelial cells repair injured proximal tubule. Proc. Natl. Acad. Sci. U. S. A. 111, 1527–32 (2014).
6. Lazzeri, E. et al. Endocycle-related tubular cell hypertrophy and progenitor proliferation recover renal function after acute kidney injury. Nat. Commun. 9, 1344 (2018).
7. Ferenbach, D. A. & Bonventre, J. V. Mechanisms of maladaptive repair after AKI leading to accelerated kidney ageing and CKD. Nat. Publ. Gr. 11, 264–276 (2015).
8. Basile, D. P. et al. Progression after AKI: Understanding Maladaptive Repair Processes to Predict and Identify Therapeutic Treatments. J. Am. Soc. Nephrol. 27, 687–97 (2016).
9. Ziegler, D. V., Wiley, C. D. & Velarde, M. C. Mitochondrial effectors of cellular senescence: Beyond the free radical theory of aging. Aging Cell 14, 1–7 (2015).
10. Ralto, K. M. & Parikh, S. M. Mitochondria in Acute Kidney Injury. Semin. Nephrol. 36, 8–16 (2016).
11. Tammaro, A. et al. Effect of TREM-1 blockade and single nucleotide variants in experimental renal injury and kidney transplantation. Sci. Rep. 6, 38275 (2016).
12. Tammaro, A. et al. TREM-1 and its potential ligands in non-infectious diseases: from biology to clinical perspectives. Pharmacol. Ther. 177, (2017).
13. Leemans, J. C., Kors, L., Anders, H.-J. & Florquin, S. Pattern recognition receptors and the inflammasome in kidney disease. Nat. Rev. Nephrol. 10, 398–414 (2014).
14. Wu, H. et al. TLR4 activation mediates kidney ischemia/reperfusion injury. J. Clin. Invest. 117, 2847–59 (2007).
15. Pulskens, W. P. et al. TLR4 promotes fibrosis but attenuates tubular damage in progressive renal injury. J. Am. Soc. Nephrol. 21, 1299–1308 (2010).
16. Dapito, D. H. et al. Promotion of hepatocellular carcinoma by the intestinal microbiota and TLR4. Cancer Cell 21, 504–516 (2012).
17. Kulkarni, O. P. et al. Toll-like receptor 4-induced IL-22 accelerates kidney regeneration. J Am. Soc. Nephrol 25, 978–989 (2014).
18. Yuan, Z. et al. Triggering receptor expressed on myeloid cells 1 (TREM-1)-mediated Bcl-2 induction prolongs macrophage survival. J Biol. Chem 289, 15118–15129 (2014).
19. Klesney-Tait, J. et al. Transepithelial migration of neutrophils into the lung requires TREM-1. J. Clin. Invest. 123, 138–49 (2013).

20. Stokman, G. et al. NLRX1 dampens oxidative stress and apoptosis in tissue injury via control of mitochondrial activity. J. Exp. Med. 214, 2405–2420 (2017).
21. Leemans, J. C. et al. Renal-associated TLR2 mediates ischemia/reperfusion injury in the kidney. J. Clin. Invest. 115, 2894–903 (2005).
22. Stokman, G. et al. Epac-Rap Signaling Reduces Cellular Stress and Ischemia-induced Kidney Failure. J. Am. Soc. Nephrol. 22, 859–872 (2011).
23. Pulskens, W. P. et al. Toll-like receptor-4 coordinates the innate immune response of the kidney to renal ischemia/reperfusion injury. PLoS One 3, e3596 (2008).
24. Zell, S. et al. Hypoxia Induces Mesenchymal Gene Expression in Renal Tubular Epithelial Cells: An in vitro Model of Kidney Transplant Fibrosis. Nephron Extra 3, 50–8 (2013).
25. Debacq-Chainiaux, F., Erusalimsky, J. D., Campisi, J. & Toussaint, O. Protocols to detect senescence-associated beta-galactosidase (SA-betagal) activity, a biomarker of senescent cells in culture and in vivo. Nat. Protoc. 4, 1798–806 (2009).
26. Perico, L. et al. Human mesenchymal stromal cells transplanted into mice stimulate renal tubular cells and enhance mitochondrial function. Nat. Commun. 8, 983 (2017).
27. Sanjana, N. E., Shalem, O. & Zhang, F. Improved vectors and genome-wide libraries for CRISPR screening. Nat. Methods 11, 783–784 (2014).
28. Ren, Z. et al. Syndecan-1 promotes Wnt/β-catenin signaling in multiple myeloma by presenting Wnts and R-spondins. Blood 131, 982–994 (2018).
29. Huen, S. C. & Cantley, L. G. Macrophages in Renal Injury and Repair. Annu. Rev. Physiol. 79, 449–469 (2017).
30. Yang, L., Besschetnova, T. Y., Brooks, C. R., Shah, J. V & Bonventre, J. V. Epithelial cell cycle arrest in G2/M mediates kidney fibrosis after injury. Nat. Med. 16, 535–543 (2010).
31. Wang, Z. et al. Cyclin B1/Cdk1 Coordinates Mitochondrial Respiration for Cell-Cycle G2/M Progression. Dev. Cell 29, 217–232 (2014).
32. Ziegler, D. V, Wiley, C. D. & Velarde, M. C. Mitochondrial effectors of cellular senescence: beyond the free radical theory of aging. Aging Cell 14, 1–7 (2015).
33. Sturmlechner, I., Durik, M., Sieben, C. J., Baker, D. J. & van Deursen, J. M. Cellular senescence in renal ageing and disease. Nat. Rev. Nephrol. 13, 77–89 (2017).
34. Chawla, L. S. & Kimmel, P. L. Acute kidney injury and chronic kidney disease: an integrated clinical syndrome. Kidney Int. 82, 516–524 (2012).
35. Lo, T.-H. et al. TREM-1 regulates macrophage polarization in ureteral obstruction. Kidney Int. 86, 1174–86 (2014).
36. Lovisa, S. et al. Epithelial-to-mesenchymal transition induces cell cycle arrest and parenchymal damage in renal fibrosis. Nat. Med. 21, 998–1009 (2015).
37. Bosco, M. C. et al. Hypoxia modulates the gene expression profile of immunoregulatory receptors in human mature dendritic cells: identification of TREM-1 as a novel hypoxic marker in vitro and in vivo. Blood 117, 2625–2639 (2011).

38. Chen, S. S. et al. Increased expression of triggering receptor expressed on myeloid cells 1 and 2 in inflamed human gingiva. J. Periodontal Res. 52, 512–521 (2017).
39. Rigo, I. et al. Induction of triggering receptor expressed on myeloid cells (TREM-1) in airway epithelial cells by 1,25(OH)(2) vitamin D(3). Innate Immun 18, 250–257 (2012).
40. Lovisa, S., Zeisberg, M. & Kalluri, R. Partial Epithelial-to-Mesenchymal Transition and Other New Mechanisms of Kidney Fibrosis. Trends Endocrinol. Metab. 27, 681–695 (2016).
41. Murphy, M. P. How mitochondria produce reactive oxygen species. Biochem. J. 417, 1–13 (2009).
42. Ježek, J., Cooper, K. F. & Strich, R. Reactive Oxygen Species and Mitochondrial Dynamics: The Yin and Yang of Mitochondrial Dysfunction and Cancer Progression. Antioxidants (Basel, Switzerland) 7, (2018).
43. Miyamoto, Y. et al. Oxidative Stress Caused by Inactivation of Glutathione Peroxidase and Adaptive Responses. Biol. Chem. 384, 567–74 (2003).
44. Traverso, N. et al. Role of Glutathione in Cancer Progression and Chemoresistance. Oxid. Med. Cell. Longev. 2013, 1–10 (2013).
45. Jornayvaz, F. R. & Shulman, G. I. Regulation of mitochondrial biogenesis. Essays Biochem. 47, 69–84 (2010).
46. Colavitti, R. & Finkel, T. Reactive Oxygen Species as Mediators of Cellular Senescence. IUBMB Life (International Union Biochem. Mol. Biol. Life) 57, 277–281 (2005).
47. Passos, J. F. et al. Mitochondrial Dysfunction Accounts for the Stochastic Heterogeneity in Telomere-Dependent Senescence. PLoS Biol. 5, e110 (2007).
48. Moiseeva, O., Bourdeau, V., Roux, A., Deschênes-Simard, X. & Ferbeyre, G. Mitochondrial dysfunction contributes to oncogene-induced senescence. Mol. Cell. Biol. 29, 4495–507 (2009).
49. Jackson, S. P. & Bartek, J. The DNA-damage response in human biology and disease. Nature 461, 1071–8 (2009).
50. Georgakilas, A. G., Martin, O. A. & Bonner, W. M. p21: A Two-Faced Genome Guardian. Trends Mol. Med. 23, 310–319 (2017).
51. Du, W., Amarachintha, S., Wilson, A. & Pang, Q. The immune receptor Trem1 cooperates with diminished DNA damage response to induce preleukemic stem cell expansion. Leukemia 31, 423–433 (2017).
52. Fumagalli, M., Rossiello, F., Mondello, C. & d'Adda di Fagagna, F. Stable Cellular Senescence Is Associated with Persistent DDR Activation. PLoS One 9, e110969 (2014).
53. Peng, L. et al. TGF-β1 Upregulates the Expression of Triggering Receptor Expressed on Myeloid Cells 1 in Murine Lungs. Sci. Rep. 6, 18946 (2016).
54. Dower, K., Ellis, D. K., Saraf, K., Jelinsky, S. A. & Lin, L. L. Innate Immune Responses to TREM-1 Activation: Overlap, Divergence, and Positive and Negative Cross-Talk with Bacterial Lipopolysaccharide. J Immunol 180, 3520–3534 (2008).

55. Guan, Q., Nguan, C. Y. C. & Du, C. Expression of Transforming Growth Factor-β1 Limits Renal Ischemia-Reperfusion Injury. Transplantation 89, 1320–1327 (2010).
56. Basile, D. P., Rovak, J. M., Martin, D. R. & Hammerman, M. R. Increased transforming growth factor-beta 1 expression in regenerating rat renal tubules following ischemic injury. Am. J. Physiol. Physiol. 270, F500–F509 (1996).
57. He, L. et al. AKI on CKD: heightened injury, suppressed repair, and the underlying mechanisms. Kidney Int. 92, 1071–1083 (2017).
58. Casalena, G., Daehn, I. & Bottinger, E. Transforming Growth Factor-β, Bioenergetics, and Mitochondria in Renal Disease. Semin. Nephrol. 32, 295–303 (2012).
59. Yoon, Y.-S., Lee, J.-H., Hwang, S.-C., Choi, K. S. & Yoon, G. TGF β1 induces prolonged mitochondrial ROS generation through decreased complex IV activity with senescent arrest in Mv1Lu cells. Oncogene 24, 1895–1903 (2005).

Supplementary informations

TREM-1 limits the maladaptive repair following renal ischemia/reperfusion by preserving mitochondrial function and proliferative capacity of tubular epithelial cells.

Alessandra Tammaro[1], Angelique Scantlebery[1], Cristiana Borrelli[2], Elena Rampanelli[1], Nike Claessen[1], Loes M. Butter[1], Gwendoline J.D. Teske[1], Alessandra Soriani[2], Marco Colonna[3], Jaklien C. Leemans[1], Mark C. Dessing[1] and Sandrine Florquin[1]

[1]Department of Pathology, Academic Medical Center, University of Amsterdam, The Netherlands; [2]Department of Molecular Medicine, Sapienza University of Rome, Laboratory Affiliated with Istituto Pasteur Italia - Fondazione Cenci Bolognetti, Rome, Italy; [3]Department of Pathology and Immunology, Washington University School of Medicine, St Louis, Missouri, USA.

Supplementary figures

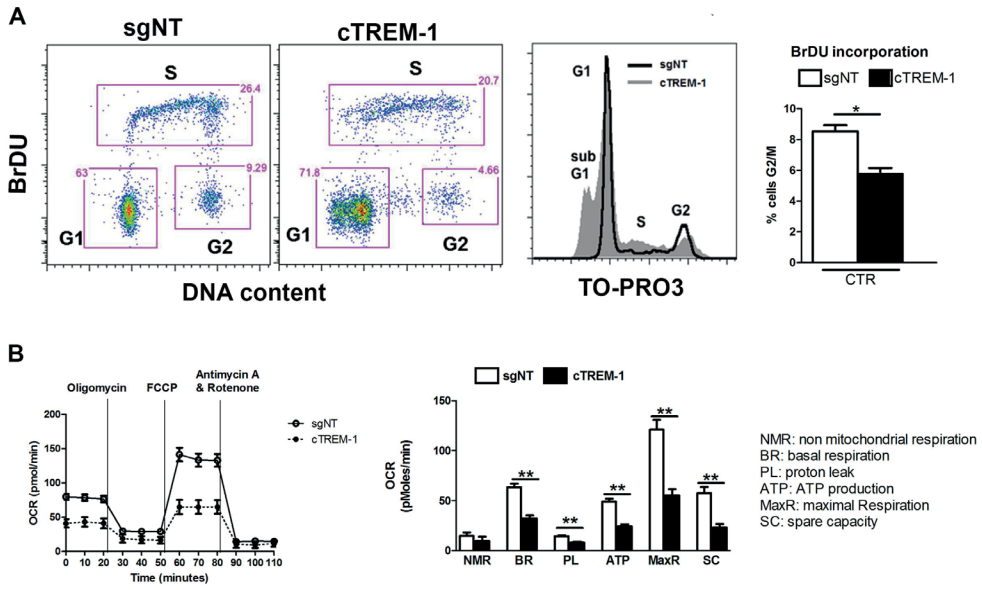

SF1: Tubular epithelial cell line (IM-TECs) with silenced TREM-1 has impaired cell proliferation and mitochondrial respiration.
TREM-1 was silenced in IM-TECs by CRISPR-Cas9 technology. (**A**) TREM-1 deficient TECs were cultured for 24 hours and subjected to a BrDU incorporation assay for cell cycle analysis. Histograms and polychromatic plots are shown for the 3 cell-cycle phases. Graphical visualization of the percentage of cells in G2/M. (**B**) Mitochondrial respiration measured with a standard protocol (Mitostress test) by Seahorse. TECs were analysed in replicates of 6. All data are expressed as mean ± SEM and the unpaired t test was used to determine statistical differences. *P<0.05, **P<0.01

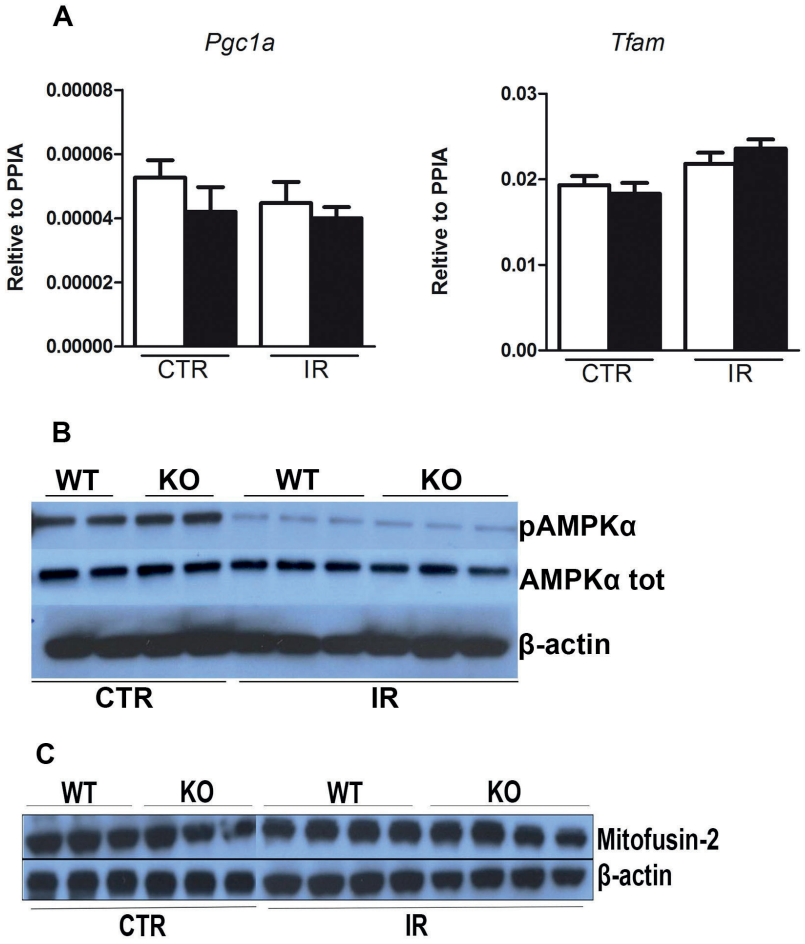

SF2: TREM1/3 does not effect mitochondrial biogenesis or dynamics. (**A**) Expression of genes involved in mitochondrial biogenesis (Tfam and Pgc1a) measured by RT-PCR. (N=5 animals per group). (**B**) Western blot for total and phosphorylated AMPK. (**C**) Western blot for Mitofusin-2 in WT and KO primary TECs under CTR conditions and after IR . All data are expressed as mean ± SEM.

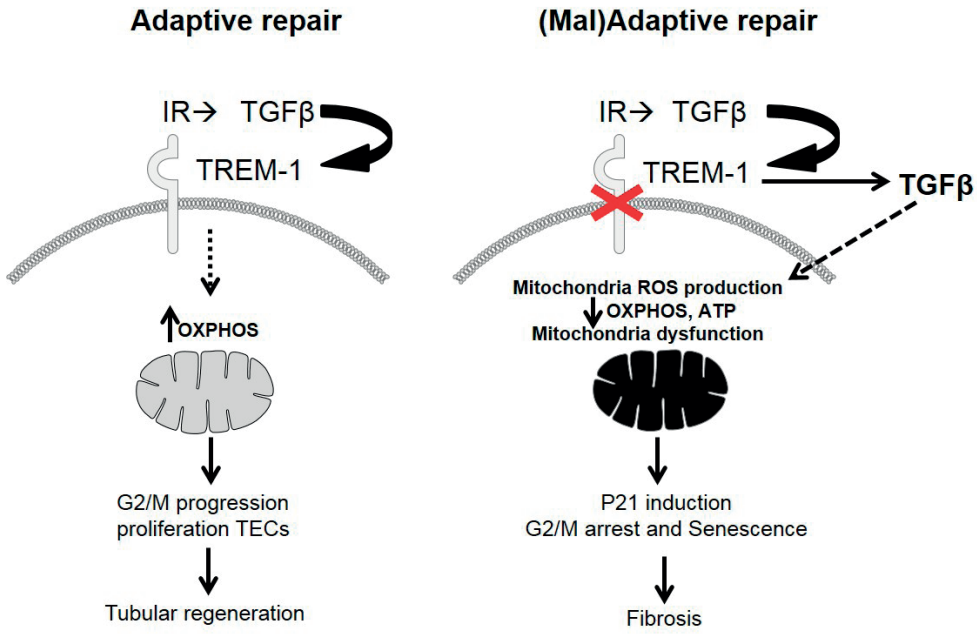

SF3: Proposed mechanism of TREM1-induced adaptive renal repair.
Following IR, TGFβ is transiently upregulated in TECs to promote tubular proliferation. Through synergism with the TREM-1 receptor, together may promote cell cycle progression by controlling mitochondrial oxidative phosphorylation (OXPHOS), which is necessary for G2/M progression. Possibly, in the absence of TREM-1, this synergy is interrupted and this may result in a steady (permanent), rather than transient, TGFβ expression, which many have deleterious effects on mitochondrial metabolism and senescence.

Supplementary Table 1: Renal Inflammation in WT and TREM1/3 KO mice upon severe AKI .
(N=8 mice per group). KC and MCP-1 levels were measured by ELISA.Values are expressed as average ± SEM.
* N=5 mice/group

	KC (pg/mg protein)		MCP1 (pg/mg protein)	
	WT	*TREM1/3 KO*	*WT*	*TREM1/3 KO*
Sham	756±104	659±89	22±3	18±2
t=1	1318±153	1635±90	27±2	34±4
t=5	831±174	1432±379	54±12	71±21*

Chapter 7

Role of TREM1-DAP12 in Renal Inflammation during Obstructive Nephropathy

PLoS One. 2013 Dec 16;8(12):e82498

OPEN ACCESS Freely available online

PLOS ONE

Role of TREM1-DAP12 in Renal Inflammation during Obstructive Nephropathy

Alessandra Tammaro[1◔], Ingrid Stroo[1◔], Elena Rampanelli[1], Froilan Blank[1], Loes M. Butter[1], Nike Claessen[1], Toshiyuki Takai[2], Marco Colonna[3], Jaklien C. Leemans[1], Sandrine Florquin[1,4], Mark C. Dessing[1]*

1 Department of Pathology, Academic Medical Center, University of Amsterdam, Amsterdam, The Netherlands, **2** Department of Experimental Immunology, Institute of Development, Aging and Cancer, Tohoku University, Sendai, Japan, **3** Department of Pathology and Immunology, Washington University School of Medicine, St. Louis, Missouri, United States of America, **4** Department of Pathology, Radboud University Nijmegen Medical Center, Nijmegen, The Netherlands

Abstract

Tubulo-interstitial damage is a common finding in the chronically diseased kidney and is characterized by ongoing inflammation and fibrosis leading to renal dysfunction and end-stage renal disease. Upon kidney injury, endogenous ligands can be released which are recognized by innate immune sensors to alarm innate immune system. A new family of innate sensors is the family of TREM (triggering receptor expressed on myeloid cell). TREM1 is an activating receptor and requires association with transmembrane adapter molecule DAP12 (DNAX-associated protein 12) for cell signaling. TREM1-DAP12 pathway has a cross-talk with intracellular signaling pathways of several Toll-like receptors (TLRs) and is able to amplify TLR signaling and thereby contributes to the magnitude of inflammation. So far, several studies have shown that TLRs play a role in obstructive nephropathy but the contribution of TREM1-DAP12 herein is unknown. Therefore, we studied TREM1 expression in human and murine progressive renal diseases and further investigated the role for TREM1-DAP12 by subjecting wild-type (WT), TREM1/3 double KO and DAP12 KO mice to murine unilateral ureter obstruction (UUO) model. In patients with hydronephrosis, TREM1 positive cells were observed in renal tissue. We showed that in kidneys from WT mice, DAP12 mRNA and TREM1 mRNA and protein levels were elevated upon UUO. Compared to WT mice, DAP12 KO mice displayed less renal MCP-1, KC and TGF-β1 levels and less influx of macrophages during progression of UUO, whereas TREM1/3 double KO mice displayed less renal MCP-1 level. Renal fibrosis was comparable in WT, TREM1/3 double KO and DAP12 KO mice. We conclude that DAP12, partly through TREM1/3, is involved in renal inflammation during progression of UUO.

Citation: Tammaro A, Stroo I, Rampanelli E, Blank F, Butter LM, et al. (2013) Role of TREM1-DAP12 in Renal Inflammation during Obstructive Nephropathy. PLoS ONE 8(12): e82498. doi:10.1371/journal.pone.0082498

Editor: Ines Armando, Universtiy of Maryland Schoool of Medicine, United States of America

Received May 17, 2013; **Accepted** October 24, 2013; **Published** December 16, 2013

Funding: The Dutch Kidney Foundation funded the study (C08.2274). The funders had no role in study design, data collection and analysis, decision to publish, or preparation of the manuscript.

Competing Interests: The authors have declared that no competing interests exist.

* E-mail: m.c.dessing@amc.uva.nl

◔ These authors contributed equally to this work.

Introduction

Fibroproliferative diseases, including chronically kidney disease, are a leading cause of morbidity and mortality and can affect all tissues and organ systems [1]. Tubulo-interstitial damage is a common finding in the chronically diseased kidney whereby the degree of tubulo-interstitial damage is a major determinant of renal function and outcome. Tubulo-interstitial injury is characterized by infiltration of leukocytes and myofibroblast accumulation with excessive deposition of extracellular matrix (ECM) [2–5]. As inflammation and interstitial fibrosis progress, tubular atrophy occurs which leads to renal dysfunction and finally to end-stage renal disease. Because the extent of fibrosis is an important predictor for outcome, much research has been put into the mechanisms behind this phenomenon. Unilateral ureteral obstruction (UUO) is a model frequently used in mice that mimics features observed in tubulo-interstitial injury including influx of leukocytes and accumulation of (myo)fibroblast followed by ECM deposition and tissue loss [2–5]. During tissue injury, like in UUO, damaged cells are able to elicit danger signals so called 'danger-associated molecular patterns' (DAMPs). These DAMPs are endogenous ligands which are able to alert the innate immune system through recognition by pattern-recognition receptors (PRR) including Toll-like receptors (TLRs) [6,7]. Recently, a new family of receptors were discovered which share intracellular signaling cascade of TLRs called TREM (triggering receptor expressed on myeloid cell). TREM1 is an activating receptor expressed on neutrophils, monocytes and some types of macrophages [8,9]. TREM1 lacks an intracellular signaling motif and associates with its adaptor molecule TYROBP (commonly called DAP12; DNAX-activating protein-12) to induce cytokine production. No specific ligand for TREM1 has been found so far but HMGB1, known to be increased following UUO, is a potential candidate [10–13]. Besides its own direct intracellular signaling cascade pathway, TREM1-DAP12 activation has a cross-talk with intracellular signaling pathways of several TLRs and is able to amplify TLR signaling and can thereby contribute to the magnitude of inflammation. So far, several studies have shown

that TLR2, TLR4 and their intracellular adopter molecule MyD88 play part in mechanisms of renal fibrosis [11,12,14–16]. We hypothesis that TREM1-DAP12 signaling contributes to the magnitude of inflammation during UUO. To our knowledge, no studies about TREM1-DAP12 in renal injury or fibrosis are known. We investigated localization of TREM1 in human kidneys suffering from obstructive nephropathy. Subsequently, we investigated the contribution of TREM1-DAP12 in renal fibrosis by subjecting wild-type, TREM1/3 KO and DAP12 KO mice to UUO model.

Materials and Methods

Patients

Kidney samples were obtained from patients diagnosed with terminal hydronephrosis characterized by extensive fibrosis and tubular atrophy at the Academic Medical Center as described before [11]. As control, we used a protocolar biopsy from a renal transplant patient with stable graft function, obtained 6 months after transplantation obtained from a cohort study at Academic Medical Center as described [17]. All renal biopsies were taken for diagnostic purposes only. This research project used only left-over biological material, anonyms and delinked from patient records, and as such was not subjected to any requirement for ethical review or approval.

Mice

Pathogen-free 9 to 12-week old female WT C57Bl/6 mice were purchased from Charles River Laboratories. TREM1/3 double KO mice were generated as recently described before [18]. TREM1/3 double KO mice were generated because TREM1 and TREM3 are highly homologous and likely to be redundant. Because TREM3 is a pseudogene in humans, TREM1/3 double KO mouse would more closely mimic human TREM1 deficiency. TREM1/3 double KO mice (further referred to as TREM1/3 KO mice) were fully backcrossed to a C57Bl/6 background. DAP12 KO mice backcrossed to C57bl/6 background were generated as before [19]. TREM1/3 KO and DAP12 KO mice were bred in the animal facility of the Academic Medical Center in Amsterdam, the Netherlands. Sex and age matched mice were used. The Animal Care and Use Committee of the University of Amsterdam approved all experiments.

Unilateral Ureteral Obstruction

Progressive renal injury was induced by unilateral ureteral obstruction (UUO) as described before [11,12,20–22]. Briefly, the right ureter was ligated under 2% isoflurane-induced anesthesia. After abdomen was closed, mice received a subcutaneous injection of 50 µg/kg buprenorphin (Temgesic, Shering-Plough). Mice were sacrificed 1, 3, 7 or 14 days after surgery. (Un)obstructed kidney was divided for immunohistochemistry (paraffin) or snap-frozen in liquid nitrogen for RNA and protein determination.

Immunohistochemistry

Human and murine renal tissue was fixed in 10% formalin and embedded in paraffin. Tissue sections of kidney (4 µm) were dried overnight and deparaffinized. Antigen retrieval, blocking of non-specific binding, incubation with primary and secondary antibody and development were performed as described before [11,12,20–22]. For TREM1 immunohistochemistry, human renal tissue section were pretreated with citrate buffer (10 mM Sodium Citrate, pH 6.0), incubated with TREM1 antibody (Rabbit-anti Human; Sigma HPA005563), followed by BrightVision Poly-HRP-Anti Rabbit (Immunoligic) and developed using 1% H_2O_2 and DAB (Sigma) in 0.05 M Tris-HCl (pH 7.9). On mouse renal sections, detection of macrophages (rat anti-mouse F4/80; Serotec), granulocytes (rat anti-mouse Ly6/G-Fitc; Pharmingen), α-smooth muscle actine (mouse-anti-human αSMA-IgG2a; Dako), collagen type I (rabbit polyclonal to collagen type I; Genetek) and apoptotic cells (rabbit anti-human active caspase-3; Cell Signalling Technology) was performed with appropriate secondary antibody and developed using 1% H_2O_2 and DAB (Sigma) in 0.05 M Tris-HCl (pH 7.9). For the quantification of macrophages, αSMA and collagen type I staining, photos of kidney tissue slides (magnification x20) were taken and analyzed using ImageJ v1.47. Percentage of positive DAP staining was related to total tissue area. Granulocytes and apoptotic cells were counted in 10 high power field (HPF, magnification x40). Histopathological scoring for Periodic Acid-Schiff Diastase (PASD) stained renal tissue sections were performed in the cortex. Criteria for measuring tubular damage were epithelial flattening, tubular dilatation and brush border loss. Sections were graded from 0 = 0%, 1 = 0–10%, 2 = 10–25%, 3 = 25–50%, 4 = 50–75% and 5 = more than 75% damaged tubules in the cortex. Interstitial edema was estimated using a 4-point scale: 0 = normal; 1 = mild; 2 = moderate; 3 = severe and 4 = extensive edema. Tubular injury and edema scoring was performed in 10 randomly chosen, non-overlapping fields (magnification x400).

In Situ Hybridization

Fragments of the Trem1 and Tyrobp cDNAs were obtained by PCR using specific primers Trem1 F: 5′-CACAGAGGCAGTCGTTGGAG, R: 5′- ACATCTGAAGAACCCTTGGTCA; Tyrobp F: 5′- GTGGGAGGATTAAGTCCCGTA, R: 5′- CAGGGAGGTACCCTGTGGAT. The PCR product was cloned into pGEM-T-easy vector (Promega Benelux BV; Leiden, The Netherlands) and verified by sequence analysis. Digoxigenin-11-UTP-labeled riboprobes were synthesized from SphI or PstI linearized plasmids by in vitro transcription reaction with T7 or Sp6 polymerase (Roche Applied Science). After the labeling reaction, the template DNA was digested using RQ-DNase (Promega), and the labeled RNA probe was precipitated. The probe was dissolved in 10 mM Tris-HCl,1 mM EDTA pH 8 and 1U RNAsin/ul and its concentration measured by Nanodrop. The non-radioactive in situ hybridization procedure was performed, in general, as partly described before [23]. Ten-µm-thick sections were prepared and mounted onto coated slides. After deparaffinization and hydration, sections were incubated with 20 µg/ml proteinase K dissolved in PBS for 15 min at 37C. The proteinase K activity was blocked by rinsing the sections in 0.2% glycine in PBS for 5 min. After two washes in PBS for 5 min, the sections were postfixed for 10 min in 4% PFA and 0.2% glutaraldehyde in PBS, followed by two washes in PBS for 5 min. Before prehybridization, a hydrophobic barrier was drawn around each individual section using an ImmEdge pen (Vector Laboratories; Burlingame, CA). This barrier allows treatment of each individual section with a different RNA probe. After prehybridization for at least 1 hr at 70C in hybridization mix (50% formamide, 5X SSC (20X SSC; 3 M NaCl, 0.3 M tri-sodium citrate, pH 4.5), 1% blocking solution (Roche), 5 mM EDTA, 0.1% 3–[(3-Cholamidopropyl) dimethylammonio]-1-propanesulfonate (Sigma; Steinheim, Germany), 0.1 mg/ml heparin (BD Biosciences; Erembodegem, Belgium), and 1 mg/ml yeast total RNA (Roche), a digoxigenin (DIG)-labeled probe was added to the hybridization mix in a final concentration of 3 ng/µl. After overnight hybridization, the sections were rinsed with 2X SSC, followed by 2 washes with 50% formamide, 2X SSC, pH 4.5, at 65C for 30 min and 1 hour, and finally, three washes in TBS tween 0.05%

at room temperature. Subsequently, the sections were incubated for 30 minutes with 2% blocking solution in PBS-T, followed by overnight incubation with 2% blocking solution in PBS-T containing 100 mU/ml anti-DIG Fab fragment covalently coupled to alkaline phosphatase (AP) (Roche). Probe binding was visualized using nitro blue tetrazolium chloride and 5-bromo-4-chloro-3-indolyl-phosphate, toluidine-salt as the chromogenic substrate for anti-DIG-AP, according to the manufacturer's protocol (Roche). After staining times of 4–6 hr at room temperature, the color development was stopped by rinsing in double-distilled water. The sections were dehydrated in a graded ethanol series, rinsed in xylene, and embedded in Pertex. DAP12 and TREM1- in situ hybridization was not observed using sense strains (data not shown).

Isolation and stimulation of primary renal tubular epithelial cells

Primary renal tubular epithelial cells (TECs) from WT mice were cultured as described before [11,12,20–22] and cultured in HK2 medium in 6-wells plate until monolayer (DMEM/F12 supplemented with 10% FCS, Penicillin/streptomycin, L-glutamine (all Invitrogen), 1% ITS and 1% S1 hormone mixture (Sigma)). TECs were stimulated with 1 or 5 ng/ml recombinant human TGF-β1(R&D systems) for 1 or 3 days.

RNA purification and rtPCR

Total RNA was isolated from 10–15 renal frozen tissue slides (20 μM) and *in vitro* cell culture using Trizol reagent (Invitrogen) according to manufacturer's protocol. RNA samples were quantified by spectrophotometry (Nanodrop) and converted to cDNA using oligo-dT. mRNA expression was analyzed by RT-PCR with SYBR green PCR master mix on a Roche LC480 lightcycler. Relative expression was analyzed using LinRegPCR v12.4. Gene expression was correlated to housekeeping gene (TATA-binding protein; TBP). Primer sequences: Sirpb1 forward (F): 5′-GGTGGCACTGAGTTGTTAGTCC, reverse (R): 5′-AAAGGTCACTGTCTGCTGAGG; Pilrb1 F: 5′-TGGAACCCAACTCAACGTG, R: 5′-GGATTCCTCTGGTCGCTTG; Pilrb2 F: 5′-GCACACAAGGGACAAGAGGAA, R: 5′-TGCTGGTTCTCCATCCTGACT; Cd200r3 F: 5′-TACAACCAGCATCCTGCCTTC, R: 5′-TGCTTCTCGGAATCTCAGCAC; Cd200r4 F: 5′-CACTGTGACTGTCAGGAGCAC, R: 5′-GGGGGTGGTCATTGTACCTT; Clec5a F: 5′-TGGAGAGAAAAAGTGGCGCT R: 5′-CTGGGCTGGTTTCAGTCACA; Trem1 F: 5′-GCGTCCCATCCTTATTACCA, R: 5′-AAACCAGGGCTCTTGCTGAGA; Trem2 F: 5′-ACCCACCTCCATTCTTCTCC, R: 5′-GGGTCCAGTGAGGATCTGAA; Trem3 F: 5′-AAAGCTGGGCCTAAGGTGTT, R: 5′-CCCAGATTGTCCCCAATACA; Cd300lb F: 5′-GACACGGACACTTACTGGTGT, R: 5′-GCACCAACCAAGATGAGCAA; AF251705 F: 5′-GACCCAGTCACAGGTTCGAG, R: 5′-AGAAGTAGAGGCTGCTCCGA; Siglech F: 5′-CCATGTCTCTGGAAGAGTTGGT, R: 5′-GTATGGGATCTCTTGCTGAGGA; Siglec15 F: 5′-AGGCCAGCGTCTACCTGTTC, R: 5′-TGGTGATGGCTGAGGAGTTC; Tyrobp F: 5′-CGAAAACAACACATTGCTGA, R: 5′-GGGCATAGAGTGGGCTCAT; Treml-1 F: 5′ -AGAATCGGAACCGGAAGTCT, R: 5′ -GGCCATCACAGCAAATATCA; Treml-2 F: 5′-CACCTGTGGTGTTGGTCGTA, R: 5′-CCTTCTGAACCCACTGGAAA; Treml-4 F: 5′-ATGGACTCCTCCTGCTCAAG, R: 5′-AGATGTGGCTAACCGTGTCC, Tlr2 F: 5′-GGGGCTTCACTTCTCTGCTT, R: 5′-AGCATCCTCTGAGATTTGACG, Tlr4 F: 5′ -GGACTCTGATCATGGCACTG, R: 5′-CTGATCCATGCATTGGTAGGT and TBP F: 5′-GGAGAATCATGGACCAGAACA, R: 5′-GATGGGAATTCCAGGAGTCA.

ELISA and Western Blot

For ELISA, snap-frozen kidney part was homogenized in Greenberger Lysis buffer (300 mM NaCl, 15 mM Tris, 2 mM MgCl, 1 mM $CaCl_2$ and 1% Triton X100, pH 7.4 with 100 μg/ml pepstatin A, leupeptin and aprotinin mix), incubated for 30 minutes at 4°C, centrifuged at 1500 g and stored in −80°C. Levels of keratineocyte-derived cytokine (KC), monocyte chemotactic protein (MCP)-1 and transforming growth factor (TGF)-β1 (all R&D Systems) were measured in kidney homogenate according to manufacturer's instructions. Protein levels were corrected for total protein level present in sample using BioRad protein assay (BioRad Laboratories) with IgG as standard. For western blot, kidney lysates were prepared from 15 frozen sections (30 μm thick) or from primary TEC in culture, incubated at 4°C for 30 min in RIPA buffer containing 50 mM Tris pH7.5, 0.15 M NaCl, 2 mM EDTA, 1% deoxycholic acid, 1% NP-40, 4 mM sodium orthovanadate, 10 mM sodium fluoride, 1% protease inhibitor cocktail (P8340, Sigma). The lysates were then centrifuged at 12000 rpm for 15 minutes and the supernatants were collected and stored at −20°C. SDS-polyacrylamide gel electrophoresis was carried out in 10% gradient slab gels and proteins were electrophoretically transferred onto methanol-activated polyvinylidene fluoride (PVDF) microporous membranes (Millipore, Etten Leur, The Netherlands). Membranes were blocked for one hour with 5% bovine serum albumin (Sigma) in Tris-buffered saline containing 0.1% Tween 20 (TBS-T), followed by overnight incubation at 4°C with primary rabbit anti-mouse/human TREM1 (Abcam ab104413, Cambridge, UK). HRP-conjugated secondary antibodies (DAKO, Glostrup, Denmark) were incubated for one hour at room temperature, and HRP activity was visualized with ECL-reagent (Amersham Pharmacia Biotech, Roosendaal, The Netherlands. β-actin was used as loading control and detected by mouse IgG1 anti-β-actin (Abcam, Cambridge, UK). Densitometric quantification analysis was performed on imagines of scanned films using the image processing program ImageJ (National Institute of Health, US).

Statistical analysis

Comparison between >2 groups was analyzed using Kruskal-Wallis test followed by Dunn's Multiple Comparison test. Level of significance between 2 groups was determined by Mann-Whitney. Data are expressed as mean ± standard deviation (SD). Eight mice per group were analyzed at every time point. $P<0.05$ was considered statistically significant.

Results

TREM1 expressing cells in hydronephrosis

Renal fibrosis is characterized by accumulation of interstitial leukocytes and myofibroblasts, induction of inflammation with eventual tubular atrophy and loss of renal function. Fibrosis and tubular atrophy are characteristic features of hydronephrosis. TREM1 expression has never been reported in human kidney disease and could contribute in inflammatory processes during hydronephrosis. In renal tissue from patients with hydronephrosis, TREM1 was expressed on tubulointerstitial cells (figure 1) which was not detectable in renal biopsies from renal transplant patients with stable graft.

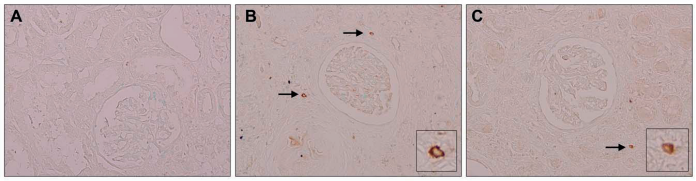

Figure 1. TREM1 expression and localization during hydronephrosis. TREM1 expression on renal biopsies from renal transplant patients with stable graft function (A) and from patients with obstructive hydronephrosis (B+C). Arrow indicates examples of TREM1-positive cells. Inserts display enlargement of TREM1-positive cells. Magnification x20.
doi:10.1371/journal.pone.0082498.g001

TREM1-DAP12 expression upon murine UUO

Murine UUO is a frequently used model which represents progressive renal injury and fibrosis and has the same pathology as hydronephrosis. We screened for DAP12 and TREM1 mRNA levels in kidneys from WT mice following UUO. DAP12 and especially TREM1 mRNA levels significantly increased following UUO with highest expression at day 14 (DAP12: 18-fold and TREM1: 800-fold compared to control; figure 2). In situ hybridization showed that DAP12- and TREM1-mRNA positive tubulointerstitial cells are present upon UUO which was not present in control kidneys. Following UUO, TREM1 expression also increased on protein level, especially 14 days after UUO (figure 2C). TREM1 expression was not observed in kidneys from TREM1/3 KO mice (data not shown). Increased renal TREM1 expression could originate from infiltrating TREM1-expressing myeloid cells or, although yet unknown, upregulation of TREM1 on renal cells like TECs. *In vitro* studies showed that DAP12 and TREM1 mRNA level in TECs were low and remained similar upon stimulation with 1 or 5 ng/ml TGF-β1for 1 or 3 days (data not shown). In addition, we showed TREM1 expression on protein level on TECs which remained similar upon stimulation with 1 or 5 ng/ml TGF-β1for 3 days (figure S1).

TREM (like) family and TLR expression in WT, TREM1/3 KO and DAP12 KO mice

The murine family of TREM receptors includes Trem1, Trem2, Trem3 and Trem-like transcript (Treml) -1, -2 and -4. We screened these genes in TREM1/3 KO mice (and DAP12 KO mice) to exclude any potential compensation of these genes due to mutation in KO mice. Renal mRNA levels of TREM2, Trem-like transcript (Treml) -1, -2 and -4 were similar between WT, TREM1/3 KO and DAP12 KO mice in control kidneys (data not shown). TREM1-DAP12 pathway is involved in modulating the TLR-signaling cascade, most likely TLR2 and TLR4 [24]. We next investigated TLR2 and TLR4 expression in WT, TREM1/3

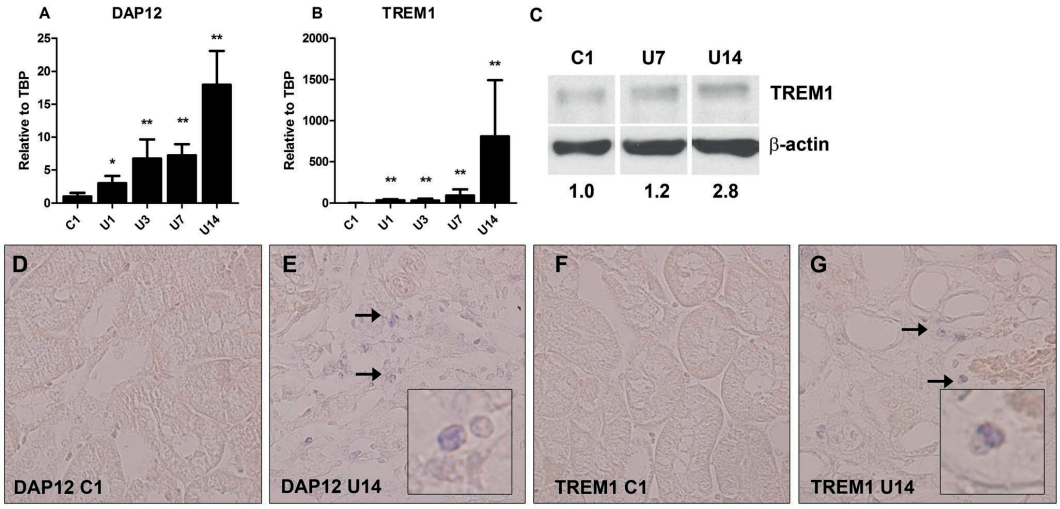

Figure 2. Renal levels of DAP12 and TREM1 upon UUO. Frozen kidney sections were cut and dissolved in TRIzol (A+B) or RIPA buffer (C) to isolate RNA and protein respectively. Renal mRNA levels of DAP12 (A) and TREM1 (B) were determined in WT mice, 1, 3, 7 and 14 days following UUO. Contralateral unobstructed kidney 1 day after UUO was used as control (C1). Gene expression is relatively expressed to housekeeping gene TBP and control is adjusted to relative expression of 1. (C): representative TREM1 western blot (WB) of kidney tissue in control WT mice (C1), 7 (U7) and 14 (U14) days after UUO. Ten μg of total protein was loaded in each lane. Values below WB indicate TREM1 protein densitometric quantification normalized to loading control β-actin and control (C1) was set to 1. *P<0.001, **P<0.0005 vs. control. DAP12 (D+E) and TREM1 (F+G) in situ hybridization was performed on renal paraffin section from WT mice 14 days following UUO. Contralateral unobstructed kidney 1 day after UUO was used as control. Arrows indicate example of positive cells. Inserts display enlargement of positive cells. Magnification x40.
doi:10.1371/journal.pone.0082498.g002

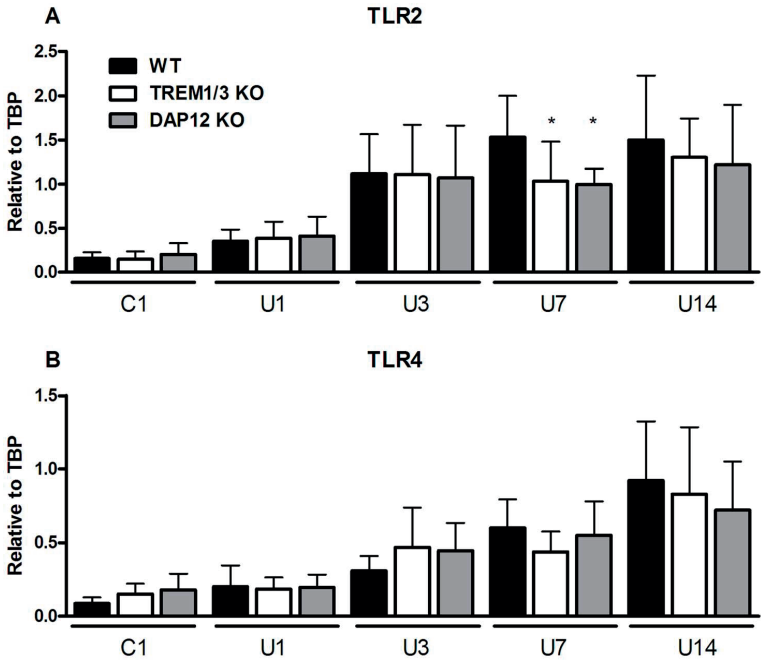

Figure 3. TLR2 and TLR4 expression upon UUO in WT, TREM1/3 KO and DAP12 KO mice. Frozen kidney sections were cut and dissolved in TRIzol to isolate RNA. Renal mRNA levels of TLR2 (A) and TLR4 (B) were determined in WT (black bars), TREM1/3 KO (white bars) and DAP12 KO (grey bars) 1, 3, 7 and 14 days following UUO. Contralateral unobstructed kidney 1 day after UUO was used as control (C1). Gene expression is relatively expressed to housekeeping gene TBP and control is adjusted to relative expression of 1. *P<0.05, **P<0.01 versus WT at indicated time point.
doi:10.1371/journal.pone.0082498.g003

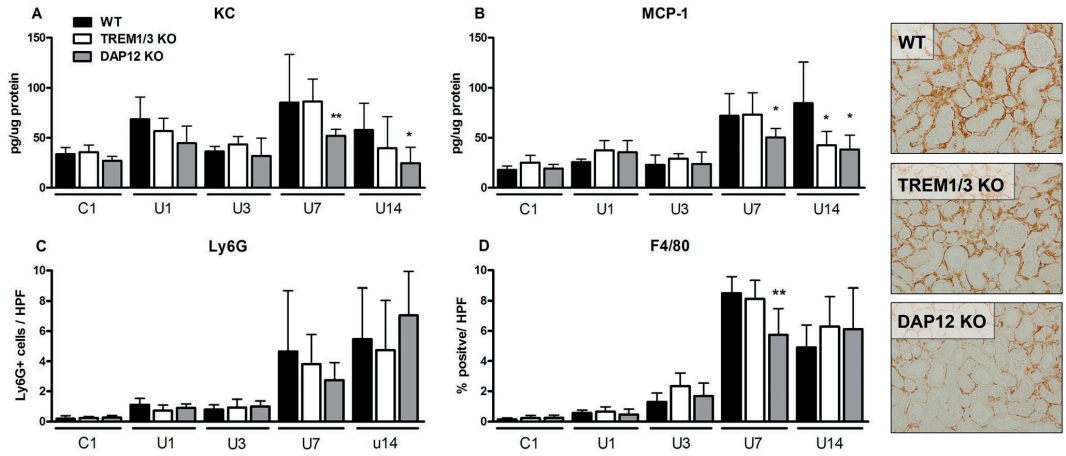

Figure 4. Inflammation upon UUO in WT, TREM1/3 KO and DAP12 KO mice. Renal tissue was processed to determine KC (A) and MCP1 (B) expression, granulocyte (C) and macrophage (D) influx in WT (black bars), TREM1/3 KO (white bars) and DAP12 KO (grey bars) mice 1, 3, 7 and 14 days following UUO. Contralateral unobstructed kidney 1 day after UUO was used as control (C1). Ly6G cells were counted per high power field (HPF, magnification x400). F4/80 staining is expressed as % positive staining per HPF, magnification x20. *P<0.05, **P<0.01 versus WT at indicated time point. Pictures are representative photographs of F4/80 IHC staining of kidney tissue slides from WT, TREM1/3 KO and DAP12 KO mice, 7 days following UUO (magnification x20).
doi:10.1371/journal.pone.0082498.g004

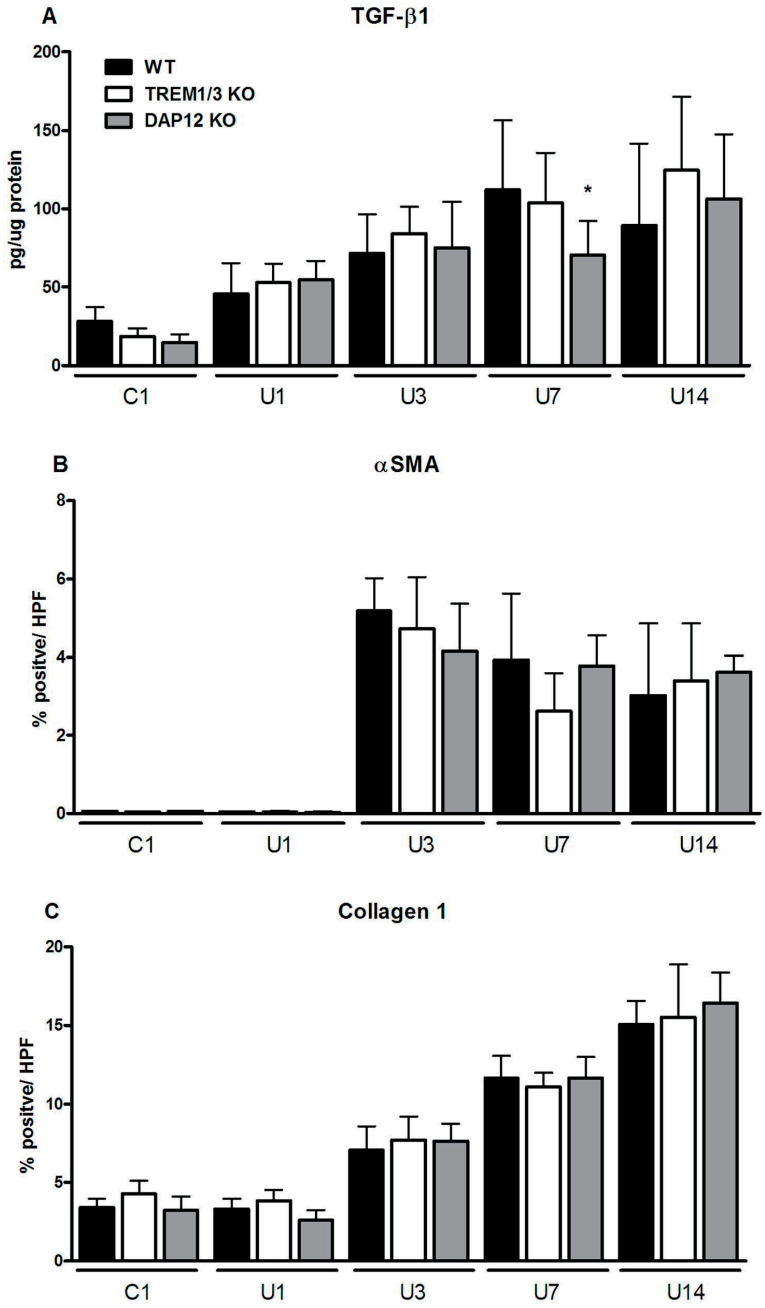

Figure 5. Renal fibrosis markers upon UUO. Renal tissue was processed to determine TGF-β1expression in kidney homogenate (A) and αSMA (B) and collagen type I (B) staining on kidney tissue slides in WT (black bars), TREM1/3 KO (white bars) and DAP12 KO (grey bars) 1, 3, 7 and 14 days following UUO. TGF-β1is corrected for total protein level per sample. αSMA and collagen type I staining is expressed as % positive staining per high power field. Contralateral unobstructed kidney 1 day after UUO was used as control (C1). *P<0.05 versus WT at indicated time point.
doi:10.1371/journal.pone.0082498.g005

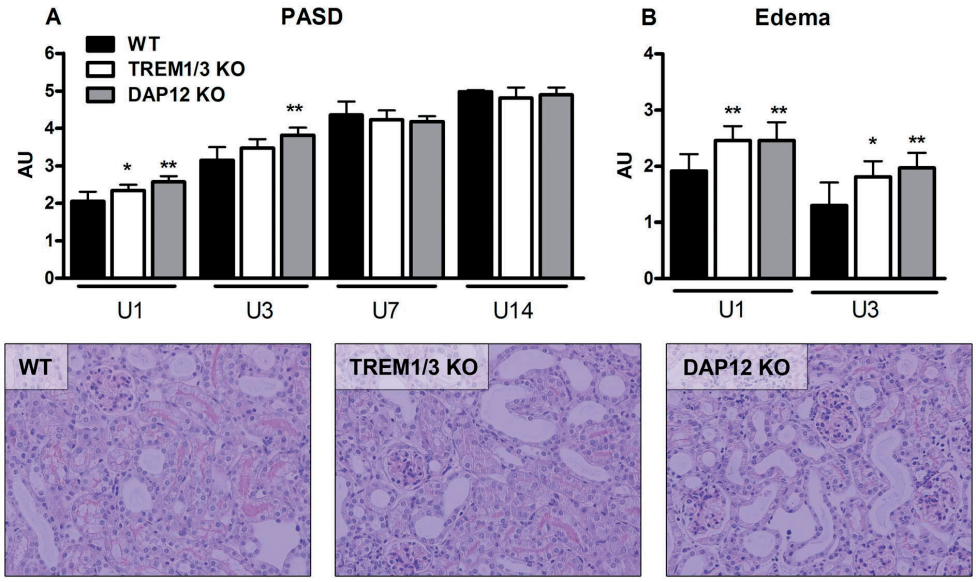

Figure 6. Tubular injury and edema upon UUO. Kidney tissue slides were cut and quantified for PASD (A) and edema score (B) in WT (black bars), TREM1/3 KO (white bars) and DAP12 KO (grey bars) mice following UUO. PASD score was graded according to % of damaged tubuli on an increasing 5-point scale (see methods section). Interstitial edema score was graded according to severity on an increasing 4-point scale (see methods section). *P<0.05, **P<0.01 versus WT at indicated time point. Pictures are representative photographs of PASD staining of kidney tissue slides from WT, TREM1/3 KO and DAP12 KO mice, 3 days following UUO (magnification x20).
doi:10.1371/journal.pone.0082498.g006

KO and DAP12 KO mice following UUO. In WT mice following UUO, renal TLR2 mRNA (day 3, 7 and 14) and TLR4 mRNA (day 7 and 14) increased significantly compared to control as described earlier [11][12], (figure 3, statistics not displayed). Renal TLR2 and TLR4 mRNA increased similar in all three groups following UUO except for reduced TLR2 mRNA levels in TREM1/3KO and DAP12 KO mice, 7 days after UUO (figure 3).

Inflammation in WT, TREM1/3 KO and DAP12 KO mice upon UUO

Typically, progressive renal injury is characterized by production of chemokines and recruitment of inflammatory cells including macrophages and granulocytes [11][12]. In WT mice following UUO renal KC (day 1 and 3) and MCP1, Ly6G staining and F4/80 staining (all day 7 and 14) increased significantly compared to their control (figure 4; statistics not displayed). Compared to WT mice, DAP12 KO mice displayed less renal KC and MCP-1 levels (figure 4A+B, day 7 and 14) and reduced level of macrophages 7 days after UUO (figure 4D). TREM1/3 KO mice displayed less renal MCP-1 levels 14 days after UUO (figure 4B). The number of infiltrating granulocytes progressively increased upon UUO over time and displayed similar pattern in WT, TREM1/3 and DAP12 KO mice (figure 4C).

Fibrosis marker upon UUO

To establish the effect of TREM1/3 and DAP12 deficiency on the development of fibrosis we measured renal TGFβ, accumulation of αSMA expressing cells and collagen type I deposition. In WT mice following UUO renal TGF-β1, αSMA staining and Collagen 1 staining (all day 3, 7 and 14) increased significantly compared to control (figure 5; statistics not displayed). Compared to WT mice, DAP12 KO mice displayed less renal TGF-β1 levels, 7 days after UUO (figure 5A). The accumulation of αSMA expressing cells and collagen type I deposition increased similar in WT, TREM1/3 KO and DAP12 KO mice (figure 5B+C).

Tubular injury and interstitial edema upon UUO

We counted apoptotic TECs and scored tubular damage and edema on renal tissue sections. Presence of caspase3+ TECs was observed especially 7 and 14 days after UUO and numbers were not significantly different between groups (data not shown). In WT mice, tubular injury (as depicted by PASD score) significantly increased 3, 7 and 14 days after UUO compared to day 1 (figure 6; statistics not displayed). A small but significant increase in tubular damage was observed in TREM1/3 KO (day 1) and DAP12 KO mice (day 1+3) compared to WT mice which was in line with enhanced interstitial edema in these mice (figure 6).

Other DAP12-associated receptors

TREM1/3 KO mice displayed only partly similar phenotype compared to DAP12 KO mice. Possibly, also other DAP12-associated receptors contribute to the induction of inflammation upon UUO. We screened for other DAP12-associated myeloid receptors including Sirpb1 (signal-regulatory protein beta 1A), Pilrb1+2 (paired immunoglobin-like type 2 receptor beta), Cd200r3, CD200r4, Clec5a (C-type lectin domain family 5, member a), Trem2, Trem3, Cd300lb (CD300 antigen like family member B), AF251705 (cDNA sequence AF251705 known as MAIR-II), Siglech (sialic acid binding Ig-like lectin H) and Siglec15[25]. Renal mRNA levels of mentioned DAP12-associated myeloid receptors all gradually increased upon UUO with highest expression at day 14 (figure 7). In order of magnitude, 14 days

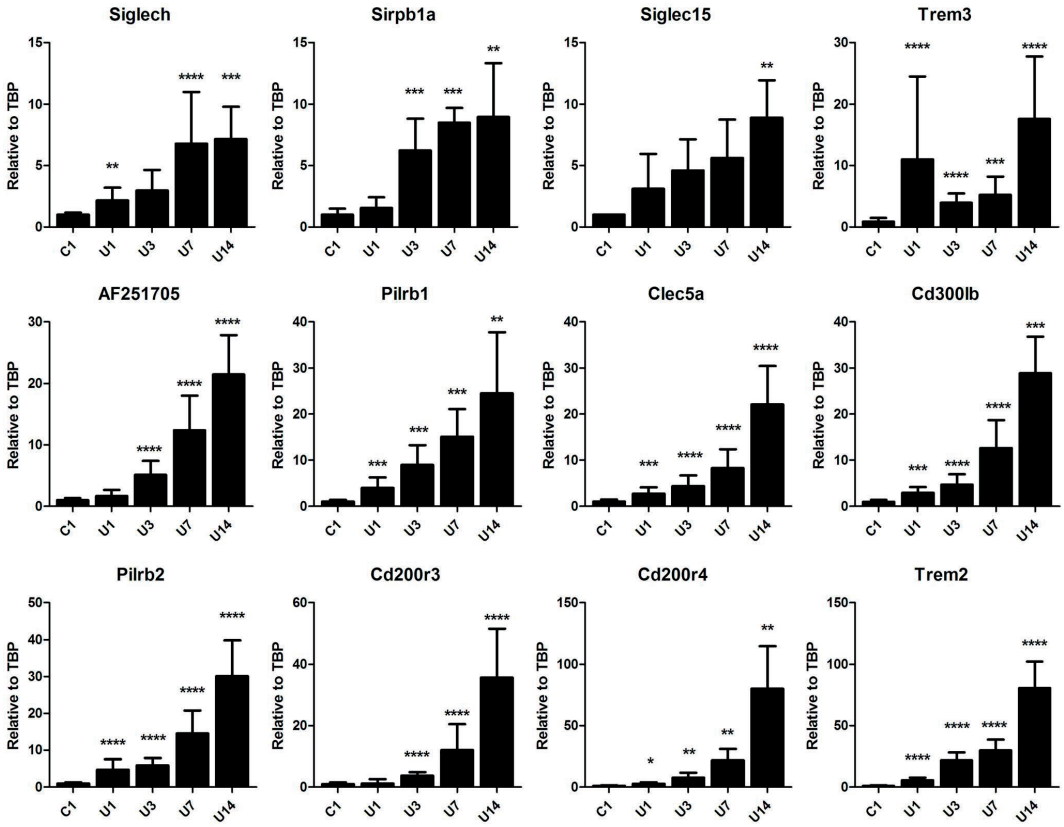

Figure 7. Renal mRNA levels of DAP12-associated myeloid receptors upon UUO. Frozen kidney sections were cut and dissolved in TRIzol to isolate RNA. Renal mRNA levels of Siglech, Sirpb, Siglec15, Trem3, AF251705, Pilrb1, Clec5a, Cd300lb, Pilrb2, Cd200r3, Cd200r4 and Trem2 were determined in WT mice, 1, 3, 7 and 14 days following UUO. Contralateral unobstructed kidney 1 day after UUO was used as control (C1). Genes are presented top-left to bottom-right in order of magnitude (expression on day 14 compared to control). Gene expression is relatively expressed to housekeeping gene TBP and group C1 is adjusted to relative value of 1. *P<0.01, **P<0.005, ***P<0.001, ****P<0.0005 vs. control.
doi:10.1371/journal.pone.0082498.g007

after UUO renal mRNA levels of Siglech (7.2-fold), Sirpb (8,1-fold), Siglec15 (8,9-fold), Trem3 (16,1-fold), AF251705 (21,5-fold), Pilrb1 (21,6-fold), Clec5a (22,2-fold), Cd300lb (28,9-fold), Pilrb2 (30,1-fold), Cd200r3 (35,7-fold), Cd200r4 (80,1-fold) and Trem2 (80,6-fold) were significantly increased compared to control (P<0.005 to P<0.0005 vs. control). It remains to be investigated which, next to TREM1, DAP12-associated receptors contributes to inflammation upon UUO.

Discussion

Tubulo-interstitial damage is characterized by inflammation and myofibroblast accumulation with excessive deposition of extracellular matrix (ECM) [2–5]. Inflammatory response can be triggered by TREM1-DAP12 pathway activation through amplification of TLR-signaling. Whereas the contribution of TLRs in obstructive nephropathy is known, the contribution of TREM1-DAP12 herein is not. We showed that TREM1-expressing cells infiltrate kidney tissue from patients suffering obstructive nephropathy. In mice, DAP12 and especially TREM1 expression increased during progression of UUO. DAP12, partly through TREM1/3, contributes to inflammation during progression of UUO but does not affect fibrosis.

TREM1 expression has been reported in several human myeloid and non-myeloid cells and in inflamed human lung, skin and intestinal tissue [26–30] and is expressed to a lesser extend on lymphocytes [28]. To our knowledge we are the first to report TREM1 expression in kidney disease. These TREM1 positive cells could contribute to the magnitude of inflammation and TREM1-DAP12 signaling and was therefore further investigated using TREM1/3 KO and DAP12 KO mice. TREM1 KO and TREM1/3 KO mice were described only very recently [18] and so far, studies on TREM1 signaling were generally performed using agonistic or inhibitory antibodies and/or peptides. TREM1-DAP12 signaling was shown to be important in modulating the innate immune response, most likely by amplifying TLR-induced inflammation. TREM1-DAP12 is known to be involved in magnitude of inflammation during sepsis and bacterial infections [9][31]. However, the contribution of TREM1-DAP12 during tissue injury is limited. Inhibition of TREM1 reduced

inflammatory symptoms and improved survival during mesenteric ischemia-reperfusion injury and hemorrhagic shock [32][33]. Similar, pretreatment with TREM1 inhibitor improved the hepatic and renal dysfunction in experimental model of severe acute pancreatitis [34]. A study by Lech *et al.* reported enhanced TREM1 and DAP12 mRNA levels following renal IR and UUO but so far, no studies about the contribution of TREM1-DAP12 signaling in kidney diseases are known [35]. We showed that DAP12 mRNA and TREM1 mRNA/protein levels are elevated 14 days after induction of UUO (figure 2). We believe that increased levels most likely originate from infiltration and activation of TREM1-DAP12 expressing cells like granulocytes and macrophages [36] and not from increased expression on renal cells like TECs. So far, we were unsuccessful in localizing TREM1 or DAP12 positive cells on murine renal tissue sections using immunohistochemistry with commercially available antibodies (data not shown). Although a specific ligand for TREM1 is unknown, endogenous DAMPs like HSP70 and HMGB1 have been suggested [10]. Of these two candidates, HMGB1, but not HSP70, is known to be upregulated during progression of UUO [11,12,37]. HMGB1 is also a well known TLR ligand and it remains to be investigated if HMGB1 signals through TREM1/3 and/or TLR during UUO.

During later phase of UUO, TREM1/3 KO and especially DAP12 KO mice displayed reduced levels of renal chemokines compared to WT mice showing that DAP12 signaling, partly through TREM1/3, contributes to renal inflammation upon progression of UUO (figure 4). The delayed macrophage influx in DAP12 KO mice could be related to lower renal levels of MCP1. Otherwise, delayed macrophage influx could be related to intrinsic feature of DAP12 deficient macrophages; DAP12-deficient macrophages are known to have a reduced migration capacity towards MCP1 [38]. But at day 14, macrophage influx was similar between WT and DAP12 KO mice, despite differences in renal MCP1 level making the latter hypothesis less likely. The exact reason for the delayed macrophage influx remains speculative. The alterations in inflammation in TREM1/3 KO and DAP12 KO mice did not affect development of fibrosis given that myofibroblast accumulation and collagen deposition increased similarly in all three groups (figure 5). In addition, tubular apoptosis and renal damage increased similarly in all three groups during progression of UUO. However, early after UUO, tubular damage was slightly higher in TREM1/3 KO mice (day 1) and DAP12 KO mice (day 1+3) which was in line with more edema in these mice (figure 6). Enhanced tubular damage upon UUO was also observed in TLR4 KO mice [12], possibly because of TLR4 involvement in regulation of adhesion molecules by fibroblasts, epi- and endothelial cells and its role in tubular architecture and integrity [39–41]. TREM1 has been described to interact with TLR4 [42][24] and we showed TREM1 expression on murine TECs. Possibly, similar mechanisms may play part in enhanced tubular damage in TREM1/3 KO mice as seen in TLR4 KO mice but this remains to be investigated in future.

During UUO, TREM1/3 KO mice displayed only partial similar phenotype compared to DAP12 KO mice. This implicates that other DAP12-related receptors might be involved, for instance Sirpb1, Pilrb, Cd200r3+4, Clec5a, TREM2, Cd300lb, AF251705 (MAIR-II), Siglec-h, and Siglec15 (reviewed in [25]). In a screening for these DAP12 associated myeloid receptors upon UUO, we observed increased mRNA levels of all mentioned genes (figure 7). Earlier studies have shown that Cd300lb[43], Pilrb[44], Clec5a[45][46], MAIR-II[47], Siglec-h[48], Siglec-15[49] are involved in induction of inflammation. So far, only the contribution of DAP12-associated myeloid receptors Cd300lb (commonly described as LMIR5) has been investigated in renal diseases showing that LMIR5 deficiency ameliorates mouse kidney IRI [50]. LMIR5 deficient mice displayed less renal inflammatory mediators, including MCP1, neutrophil influx and renal damage following IR [50]. If LMIR-5, or other DAP12-associted receptors except for TREM1/3, play part in UUO remains to be investigated and is beyond the scope of this paper. In conclusion, our results show that DAP12, partly through TREM1/3, is involved in renal inflammation during progression of UUO whereas TREM1-DAP12 does not play part in renal fibrosis.

Supporting Information

Figure S1 TREM1 protein expression on TEC. Primary TECs were isolated, cultured and TREM1 protein expression was determined by western blot. TECs from WT mice were stimulated with 1 or 5 ng TGF-β1/ml medium for 3 days. Cell lysates were obtained and quantified for TREM1 protein expression (A). Densometric quantification analysis of western blot is displayed in B, control was set to 1. Data are mean ± SD, N = 2 per group. AU = arbitrary units.
(TIF)

Acknowledgments

We would like to thank Quinn D. Gunst (Heart Failure Research Center, Academic Medical Center, Amsterdam, The Netherlands) for technical assistance with in situ hybridization.

Author Contributions

Conceived and designed the experiments: MD JL SF. Performed the experiments: IS AT ER FB LB NC. Analyzed the data: MD AT ER FB. Contributed reagents/materials/analysis tools: TT MC. Wrote the paper: IS AT MD JL SF.

References

1. Wynn TA (2007) Common and unique mechanisms regulate fibrosis in various fibroproliferative diseases. The Journal of clinical investigation 117: 524–529.
2. Chevalier RL, Forbes MS, Thornhill BA (2009) Ureteral obstruction as a model of renal interstitial fibrosis and obstructive nephropathy. Kidney international 75: 1145–1152.
3. Boor P, Ostendorf T, Floege J (2010) Renal fibrosis: novel insights into mechanisms and therapeutic targets. Nature reviews 6: 643–656.
4. Chevalier RL, Thornhill BA, Forbes MS, Kiley SC (2010) Mechanisms of renal injury and progression of renal disease in congenital obstructive nephropathy. Pediatric nephrology. Pediatr Nephrol 4: 687–697.
5. Zeisberg M, Neilson EG (2010) Mechanisms of tubulointerstitial fibrosis. J Am Soc Nephrol 21: 1819–1834.
6. Anders HJ, Banas B, Schlondorff D (2004) Signaling danger: toll-like receptors and their potential roles in kidney disease. J Am Soc Nephrol 15: 854–867.
7. Gluba A, Banach M, Hannam S, Mikhailidis DP, Sakowicz A, *et al.* (2010) The role of Toll-like receptors in renal diseases. Nature reviews 6: 224–235.
8. Colonna M (2003) TREMs in the immune system and beyond. Nat Rev Immunol 3: 445–453.
9. Sharif O, Knapp S (2008) From expression to signaling: roles of TREM-1 and TREM-2 in innate immunity and bacterial infection. Immunobiology 213: 701–713.
10. El Mezayen R, El Gazzar M, Seeds MC, McCall CE, Dreskin SC, *et al.* (2007) Endogenous signals released from necrotic cells augment inflammatory responses to bacterial endotoxin. Immunol Lett 111: 36–44.
11. Leemans JC, Butter LM, Pulskens WP, Teske GJ, Claessen N, *et al.* (2009) The role of Toll-like receptor 2 in inflammation and fibrosis during progressive renal injury. PLoS One 4: e5704.
12. Pulskens WP, Rampanelli E, Teske GJ, Butter LM, Claessen N, *et al.* (2010) TLR4 promotes fibrosis but attenuates tubular damage in progressive renal injury. J Am Soc Nephrol 21: 1299–1308.

13. Wu J, Li J, Salcedo R, Mivechi NF, Trinchieri G, *et al.* (2012) The proinflammatory myeloid cell receptor TREM-1 controls Kupffer cell activation and development of hepatocellular carcinoma. Cancer research 72: 3977–3986.
14. Wang S, Schmaderer C, Kiss E, Schmidt C, Bonrouhi M, *et al.* (2010) Recipient Toll-like receptors contribute to chronic graft dysfunction by both MyD88- and TRIF-dependent signaling. Disease models & mechanisms 3: 92–103.
15. Correa-Costa M, Braga TT, Semedo P, Hayashida CY, Bechara LR, *et al.* (2011) Pivotal role of Toll-like receptors 2 and 4, its adaptor molecule MyD88, and inflammasome complex in experimental tubule-interstitial nephritis. PLoS One 6: e29004.
16. Braga TT, Correa-Costa M, Guise YF, Castoldi A, De Oliveira CD, *et al.* (2012) MyD88 Signaling Pathway is Involved in Renal Fibrosis by favoring a TH2 Immune Response and Activating Alternative M2 Macrophages. Molecular medicine 18:1231–9.
17. Scholten EM, Rowshani AT, Cremers S, Bemelman FJ, Eikmans M, *et al.* (2006) Untreated rejection in 6-month protocol biopsies is not associated with fibrosis in serial biopsies or with loss of graft function. J Am Soc Nephrol 17: 2622–2632.
18. Klesney-Tait J, Keck K, Li X, Gilfillan S, Otero K, *et al.* (2012) Transepithelial migration of neutrophils into the lung requires TREM-1. The Journal of clinical investigation 123(1):138–49.
19. Kaifu T, Nakahara J, Inui M, Mishima K, Momiyama T, *et al.* (2003) Osteopetrosis and thalamic hypomyelinosis with synaptic degeneration in DAP12-deficient mice. The Journal of clinical investigation 111: 323–332.
20. Rouschop KM, Sewnath ME, Claessen N, Roelofs JJ, Hoedemaeker I, *et al.* (2004) CD44 deficiency increases tubular damage but reduces renal fibrosis in obstructive nephropathy. J Am Soc Nephrol 15: 674–686.
21. Rouschop KM, Claessen N, Pals ST, Weening JJ, Florquin S (2006) CD44 disruption prevents degeneration of the capillary network in obstructive nephropathy via reduction of TGF-beta1-induced apoptosis. J Am Soc Nephrol 17: 746–753.
22. Stokman G, Leemans JC, Stroo I, Hoedemaeker I, Claessen N, *et al.* (2008) Enhanced mobilization of bone marrow cells does not ameliorate renal fibrosis. Nephrol Dial Transplant 23: 483–491.
23. Moorman AF, Houweling AC, de Boer PA, Christoffels VM (2001) Sensitive nonradioactive detection of mRNA in tissue sections: novel application of the whole-mount in situ hybridization protocol. J Histochem Cytochem 49: 1–8.
24. Arts RJ, Joosten LA, Dinarello CA, Kullberg BJ, van der Meer JW, *et al.* (2011) TREM-1 interaction with the LPS/TLR4 receptor complex. European cytokine network 22: 11–14.
25. Lanier LL (2009) DAP10- and DAP12-associated receptors in innate immunity. Immunological reviews 227: 150–160.
26. Colonna M, Facchetti F (2003) TREM-1 (triggering receptor expressed on myeloid cells): a new player in acute inflammatory responses. The Journal of infectious diseases 187 Suppl 2: S397–S401.
27. Chen LC, Laskin JD, Gordon MK, Laskin DL (2008) Regulation of TREM expression in hepatic macrophages and endothelial cells during acute endotoxemia. Exp Mol Pathol 84: 145–155.
28. Matesanz-Isabel J, Sintes J, Llinas L, de Salort J, Lazaro A, *et al.* (2011) New B-cell CD molecules. Immunol Lett 134: 104–112.
29. Rigo I, McMahon L, Dhawan P, Christakos S, Yim S, *et al.* (2012) Induction of triggering receptor expressed on myeloid cells (TREM-1) in airway epithelial cells by 1,25(OH)(2) vitamin D(3). Innate immunity 18: 250–257.
30. Hyder LA, Gonzalez J, Harden JL, Johnson-Huang LM, Zaba LC, *et al.* (2013) TREM-1 as a potential therapeutic target in psoriasis. J Invest Dermatol 133: 1742–1751.
31. Ford JW, McVicar DW (2009) TREM and TREM-like receptors in inflammation and disease. Current opinion in immunology 21: 38–46.
32. Gibot S, Massin F, Alauzet C, Montemont C, Lozniewski A, *et al.* (2008) Effects of the TREM-1 pathway modulation during mesenteric ischemia-reperfusion in rats. Critical care medicine 36: 504–510.
33. Gibot S, Massin F, Alauzet C, Derive M, Montemont C, *et al.* (2009) Effects of the Trem-1 Pathway Modulation During Hemorrhagic Shock in Rats. Shock 32(6):633–7.
34. Kamei K, Yasuda T, Ueda T, Qiang F, Takeyama Y, *et al.* (2010) Role of triggering receptor expressed on myeloid cells-1 in experimental severe acute pancreatitis. Journal of hepato-biliary-pancreatic sciences 17: 305–312.
35. Lech M, Susanti HE, Rommele C, Grobmayr R, Gunthner R, *et al.* (2012) Quantitative expression of C-type lectin receptors in humans and mice. International journal of molecular sciences 13: 10113–10131.
36. Bouchon A, Dietrich J, Colonna M (2000) Cutting edge: inflammatory responses can be triggered by TREM-1, a novel receptor expressed on neutrophils and monocytes. J Immunol 164: 4991–4995.
37. Ramaiah SK, Gunthner R, Lech M, Anders HJ (2013) Toll-like receptor and accessory molecule mRNA expression in humans and mice as well as in murine autoimmunity, transient inflammation, and progressive fibrosis. International journal of molecular sciences 14: 13213–13230.
38. Koth LL, Cambier CJ, Ellwanger A, Solon M, Hou L, *et al.* (2010) DAP12 is required for macrophage recruitment to the lung in response to cigarette smoke and chemotaxis toward CCL2. J Immunol 184: 6522–6528.
39. Cetin S, Ford HR, Sysko LR, Agarwal C, Wang J, *et al.* (2004) Endotoxin inhibits intestinal epithelial restitution through activation of Rho-GTPase and increased focal adhesions. The Journal of biological chemistry 279: 24592–24600.
40. Kumagai N, Fukuda K, Fujitsu Y, Lu Y, Chikamoto N, *et al.* (2005) Lipopolysaccharide-induced expression of intercellular adhesion molecule-1 and chemokines in cultured human corneal fibroblasts. Investigative ophthalmology & visual science 46: 114–120.
41. Sawa Y, Ueki T, Hata M, Iwasawa K, Tsuruga E, *et al.* (2008) LPS-induced IL-6, IL-8, VCAM-1, and ICAM-1 expression in human lymphatic endothelium. J Histochem Cytochem 56: 97–109.
42. Ornatowska M, Azim AC, Wang X, Christman JW, Xiao L, *et al.* (2007) Functional genomics of silencing TREM-1 on TLR4 signaling in macrophages. Am J Physiol Lung Cell Mol Physiol 293: L1377–L1384.
43. Yamanishi Y, Takahashi M, Izawa K, Isobe M, Ito S, *et al.* (2012) A soluble form of LMIR5/CD300b amplifies lipopolysaccharide-induced lethal inflammation in sepsis. J Immunol 189: 1773–1779.
44. Banerjee A, Stevenaert F, Pande K, Haghjoo E, Antonenko S, *et al.* (2010) Modulation of paired immunoglobulin-like type 2 receptor signaling alters the host response to Staphylococcus aureus-induced pneumonia. Infection and immunity 78: 1353–1363.
45. Chen ST, Lin YL, Huang MT, Wu MF, Cheng SC, *et al.* (2008) CLEC5A is critical for dengue-virus-induced lethal disease. Nature 453: 672–676.
46. Cheung R, Shen F, Phillips JH, McGeachy MJ, Cua DJ, *et al.* (2010) Activation of MDL-1 (CLEC5A) on immature myeloid cells triggers lethal shock in mice. The Journal of clinical investigation 121: 4446–4461.
47. Yotsumoto K, Okoshi Y, Shibuya K, Yamazaki S, Tahara-Hanaoka S, *et al.* (2003) Paired activating and inhibitory immunoglobulin-like receptors, MAIR-I and MAIR-II, regulate mast cell and macrophage activation. The Journal of experimental medicine 198: 223–233.
48. Zhang J, Raper A, Sugita N, Hingorani R, Salio M, *et al.* (2006) Characterization of Siglec-H as a novel endocytic receptor expressed on murine plasmacytoid dendritic cell precursors. Blood 107: 3600–3608.
49. Takamiya R, Ohtsubo K, Takamatsu S, Taniguchi N, Angata T (2013) The interaction between Siglec-15 and tumor-associated sialyl-Tn antigen enhances TGF-beta secretion from monocytes/macrophages through the DAP12-Syk pathway. Glycobiology 23: 178–187.
50. Yamanishi Y, Kitaura J, Izawa K, Kaitani A, Komeno Y, *et al.* (2010) TIM1 is an endogenous ligand for LMIR5/CD300b: LMIR5 deficiency ameliorates mouse kidney ischemia/reperfusion injury. The Journal of experimental medicine 207: 1501–1511.

Supplementary Information

Role of TREM1-DAP12 in renal inflammation during obstructive nephropathy

Alessandra Tammaro[1]* , Ingrid Stroo[1]*, Elena Rampanelli[1] , Froilan Blank[1], Loes Butter[1], Nike Claessen[1], Toshiyuki Takai[2], Marco Colonna[3], Jaklien C. Leemans[1], Sandrine Florquin[1,4] and Mark C. Dessing[1]

1 Department of Pathology, Academic Medical Center, University of Amsterdam, Amsterdam, the Netherlands, 2 Department of Experimental Immunology, Institute of Development, Aging and Cancer, Tohoku University, Sendai, Japan, 3 Department of Pathology & Immunology, Washington University School of Medicine, St. Louis, USA, 4 Department of Pathology, Radboud University Nijmegen Medical Center, Nijmegen, the Netherlands. * Contributed equally to manuscript

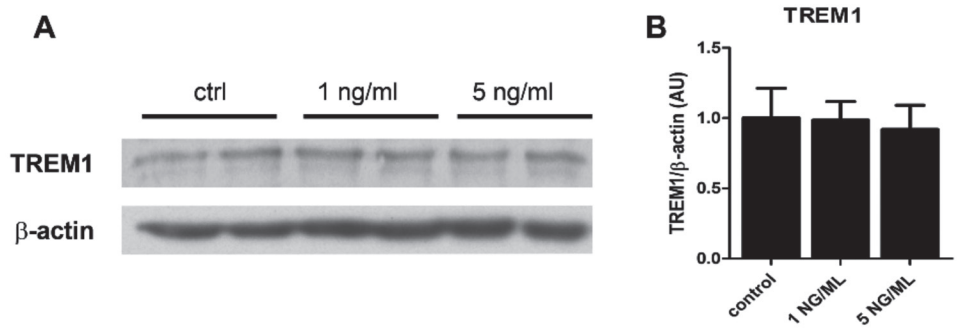

Supplementary figure 1: TREM1 protein expression on TEC. Primary TECs were isolated, cultured and TREM1 protein expression was determined by western blot. TECs from WT mice were stimulated with 1 or 5 ng TGF-β1/ ml medium for 3 days. Cell lysates were obtained and quantified for TREM1 protein expression (A). Densometric quantification analysis of western blot is displayed in B, control was set to 1. Data are mean ± SD, N=2 per group. AU= arbitrary units.

Chapter 8

General discussion

General discussion

With the studies presented in this thesis, we intended to provide novel insights into the pathogenesis of acute injury and progression to chronic kidney disease. Specifically, we sought to identify novel targets amongst the plethora of innate immune response activators, which could lay the basis for effective treatment regimes in patients with kidney diseases.

Key findings of this thesis:

1. The damage-associated protein S100A8/A9 is a pivotal player in renal repair following hypoxic damage, through an immune-regulatory role resulting in the alternative activation of macrophages. By controlling excessive M2 polarization, S100A8/A9 fine-tunes the adaptive response of the kidney to IR-induced AKI (**Chapter 2**).

2. In chronically inflamed kidneys, S100A8/A9 contributes to the development of fibrosis possibly through a direct effect on dedifferentiation and apoptosis in tubular epithelial cells. This effect was independent of S100A8/A9-induced inflammation and recruitment of leukocytes into the kidney (**Chapter 3**).

3. The innate immune receptor Triggering receptor expressed on myeloid cells-1 (TREM-1) is not involved in the amplification of acute renal damage and inflammation in preclinical model of acute kidney injury. Additionally, renal transplanted patients carrying the TREM1 gene variant p.Thr25Ser do not show any association with pathological consequences after transplantation (**Chapter 5**).

4. The activating receptor TREM-1 limits the maladaptive repair post IR-induced AKI, through a direct effect on tubular epithelial mitochondrial homeostasis and energy production, empowering cell cycle progression. The metabolic advantage provided by TREM-1 is indispensable for tubular proliferation, which sustains renal repair and accelerates the recovery from IR (**Chapter 6**).

5. TREM-1 and its adapter molecule DAP12 are not involved in the development of renal fibrosis in the preclinical model of chronic kidney disease. DAP12, partly through TREM-1, modulates the renal inflammatory response following unilateral ureteral obstruction (**Chapter 7**).

The complex nature of innate immunity in renal diseases: the fine line between healing and tissue degeneration.

The incidence of renal diseases is dramatically rising in the western world, causing high rates of morbidity and mortality. More specifically, the incidence of Acute Kidney Injury (AKI) is increasing as populations continue to age[1]. AKI accounts for 25% of hospitalized patients and can reach as high as 70% of patients in the intensive care unit. Despite advances in basic research, management of AKI is still supportive and associated with an unacceptably high mortality rate, prolonged hospitalization and dialysis dependence. Renal replacement therapies have extended life expectancy for patients with AKI and terminal CKD, but in general represents only a supportive measure, rather than a curative therapy. Given the kidney's high regenerative capacity, loss of nephrons that fail to regenerate after an episode of AKI, determines the progression to CKD[2]. Research that describes the molecular mechanism underlying this failed regeneration, has high potential for identifying effective therapies for patients at high risk of developing renal failure.

During the last decades, an increased body of evidence suggests that the activation of the inflammatory response is necessary to orchestrate adaptive repair of the kidney, however when the inflammatory response is unbalanced chronic complications can develop[3]. The primary mechanism by which the kidney responds to damage involves the activation of pattern recognition receptors (PRRs), including Toll like receptors (TLRs). During a state of homeostasis TLRs are expressed in resident immune cells and parenchymal cells which when alerted by damage associated molecular patterns (DAMPs) become activated and shape the adaptive immune response. However, a maladaptive inflammatory response is often the cause of a vicious cycle which perpetuates inflammation leading to tissue fibrosis and dysfunction[3,4]. Therefore, the immune system is an integral part of kidney homeostasis, injury and controls the regenerative capacity of the tissue. Danger molecules can be released from any intracellular compartment into the extracellular space, bind to specific PRRs and promote the recruitment and activation of various immune cells, including neutrophils and monocyte/macrophages, that remove cellular debris and secrete many inflammatory factors necessary for tissue repair[5]. Both PRRs as well as DAMPs were described to play a pivotal role in renal inflammation as well as repair in preclinical models of AKI and CKD. However, many PRRs and DAMPs have not yet been studied in the context of acute and chronic kidney diseases. In this thesis we focused on the individual role of the danger protein S100A8/A9 and the activating receptor TREM-1 in the experimental models of ischemia/reperfusion (IR)-induced acute kidney injury (AKI) and unilateral ureteral obstruction (UUO)-induced chronic kidney disease (CKD).

S100A8/A9 is recognized as a DAMP but besides its role in inflammation it is also involved in other biological processes such as development and wound healing[6,7]. In **Chapter 2 and 3** we describe that the danger programs activated by S100A8/A9 drive renal regeneration and fibrosis. We found that long-term inhibition of this inflammatory signal affects renal repair in the preclinical model of AKI, but it is beneficial in the preclinical model of CKD. Therefore, a therapeutic approach that leaves the S1000A8/A9-induced inflammatory response intact during the phase of active repair after AKI is preferable, whereas, in chronically inflamed kidney, S100A8/A9 blockade would preserve the tissue from parenchymal destruction and loss of function.

TLR4 represents one of the best characterized PRRs in the pathophysiology of renal diseases[3]. Functional TLR4 on the renal tubule is required to activate an adaptive immune response during the acute phase of AKI and interfering with its signal dampens the excessive inflammatory response and collateral tissue damage. The double edge sword of blocking TLR4 activation, is the eventual impairment of host defense against pathogens. To overcome this, we investigated the effect of the TLR4 endogenous ligand, S100A8/A9 in the pathogenesis of AKI, expecting a similar role to TLR4 . Our hypothesis was further supported by an early report that showed a detrimental effect of S100A8/A9 in cerebral IR-induced damage, possibly through activation of TLR4-mediated inflammatory response[8].

In sharp contrast **(Chapter 2)** we found that S100A8/A9 is crucially involved in renal adaptive repair after ischemia, by controlling excessive M2 macrophage polarization and preventing renal fibrosis. During the acute phase of injury, an increase in S100A8/A9 protein expression was detected in the kidney, most likely due to the infiltration of granulocytes, which contain S100A8/A9. Unexpectedly, in the absence of S100A8/A9, no differences in the inflammatory cell infiltration nor in renal damage parameters were observed during the acute phase of IR, compared to WT mice. During the early phase of renal IR injury, leukocytes populations have a detrimental role because they promote cell death by releasing reactive oxygen species and activating apoptotic programs. Therefore, the comparable levels of inflammation and renal damage between the two mice strains might be related to the similar influx of leukocytes. Despite this similar phenotype detected in the acute phase, sustained activation of inflammation together with development of fibrosis were observed later during the repair phase in the absence of S100A8/A9. We discovered that the maladaptive repair was elicited by the excessive M2 macrophage polarization in the S100A9 KO animals. Macrophages have an important role in the maintenance of tissue integrity. Depending on the renal inflammatory milieu, macrophage skewing occurs in order to contribute to inflammation

or tissue repair[9]. Specifically, M1 polarization contributes to renal damage[10,11], whereas during renal repair M2 polarization ensures proper tissue healing[12]. Aberrant alternative activation of M2, observed in absence of S100A8/A9 may account for the persistent activation of inflammation and increased renal fibrosis. Although it appears incongruent that the excessive M2 polarization observed in the S100A9 KO animals associates with an M1 signaling activation (namely increased TNFα and IL1β cytokines expression), we believe that this is a secondary response of the kidney which progresses into fibrosis and may activate other cell types with a pro-inflammatory activity, such as dendritic cells[13,14]. Supporting our speculation, Eikmans's group recently described that overexpression of S100A8/A9 in the human monocyte cell line THP-1 does not lead to any difference in TNFα or IL1β expression, when compared to cells transfected with an empty vector[15]. The same group provided the clinical translational potential of our study, by describing that patients with relatively high expression of myeloid-related S100A8 and S100A9 during acute rejection, had an improved long-term outcome. They demonstrated an immuno-regulatory role for S100A8/A9 in orchestrating allogenic T cell activity during rejection. Stimulation of dendritic cells with recombinant S100A8/A9 dampened their maturation and the ability of stimulating the T cell response. This is related to the enhanced ROS production elicited by S100A8/A9, which dampens T cell activity. Apparently, macrophages with high levels of S100A9 have a beneficial immune effect through the activation of the adaptive immune response and anti-inflammatory effects, resulting in reduced tissue damage after transplantation[16]. This body of evidence appears to be in line with our findings, unfortunately, the levels of ROS and dendritic cells activation were not investigated in our study. However, we found that the maladaptive repair observed in absence of S100A8/A9 was associated with enhanced infiltration of CD11C+ cells. Despite being commonly seen as a marker for conventional dendritic cells activation, recent studies also describe CD11C expression in T cells. Additionally, a recent study identified a novel subset of cells in mouse and humans that contains properties of both DC and T cells, including CD11C expression[17,18]. Therefore, it is conceivable that in our preclinical AKI model a similar mechanism can take place.

Finally, we show that S100A8/A9 is crucial for shaping and promoting an adaptive immune response after IR. To conclude, the main message of this study is that some degree of inflammation during the acute phase is crucial for renal tissue repair, as previously described for other PRRs and DAMPs in renal repair.

Given the immune-regulatory effect of S100A8/A9 in macrophages, which are well known to mediate the development of progressive renal fibrosis, we sought to unravel whether this danger protein plays a role in the preclinical model of renal fibrosis: the unilateral ureteric obstruction model (UUO). Interestingly, macrophage infiltration in

this model show predominantly an M2-like phenotype[19] , therefore, we hypothesized a beneficial role for S100A8/A9. In contrast to our finding obtained in the preclinical model of AKI, in **Chapter 3** we demonstrated that S100A8/A9 promotes renal fibrosis by inducing permanent loss of integrity and apoptosis in tubular epithelial cells. We found that S100A8/A9 is expressed in patients with obstructive nephropathy and in the experimental model of UUO. The majority of S100A8/A9 positive cells appear to be granulocytes, as previously described in the preclinical model of AKI[20]. In the absence of S100A9, mice were protected against UUO-induced renal fibrosis, especially during the late stages of damage, which was associated with a decrease in TGFβ activation and plasma creatinine levels. Surprisingly, macrophage infiltration and polarization, as well as the renal inflammatory milieu were unchanged between the two mice strains, contrary to what is described in the study from Fuji et *al*. in the same experimental model[21]. This study suggests that the transcriptional regulator of S100A8/A9, Krüppel-like factor–5 (KLF5), controls S100A8/A9 release from collecting duct cells, resulting in recruitment of inflammatory monocytes to the kidney and promoting their polarization into the M1 inflammatory phenotype. They conclude that KLF5-mediated S100A8/A9 release promotes renal inflammation and tissue remodeling, limiting fibrosis in the UUO model. We believe that the discrepancy with our study is related to the genetic model used in their experiment, which does not entail an endogenous disturbance of S100A8/A9 induction. Additionally, KLF5 has been shown to promote inflammation and cell differentiation, also independently of S100A8/A9. Besides the activation of the inflammatory response, S100A8/A9 can affect endothelial integrity and cell death[22]. In the experimental model of UUO, we excluded a role in renal inflammation, instead, we found that TECs from S100A9 KO mice displayed decreased apoptosis and increased morphological and functional signs of preserved integrity, resulting in decreased fibrosis and TGFβ activation. The functional relationship between S100A8/A9 and TGFβ have been described earlier in relation to proliferation inhibition[23]. Additionally, in renal biopsies of patients with acute rejection not progressing into chronic allograft nephropathy, Eikmans et *al*. described a significant correlation between S100A8/A9 and TGFβ. The transcript levels of both mediators displayed a significant increase, suggesting indeed that during acute rejection they play a beneficial action for long term outcomes[23]. Given the pattern of expression of S100A8/A9 and TGFβ in the experimental model of UUO, it is conceivable that this correlation is also present in our study. Nonetheless, it appears that in chronically damaged kidney the correlation with TGFβ has a different purpose from the aforementioned study. Indeed, we found that extracellular S100A8/A9 has an effect on tubular epithelial cells dedifferentiation and when S100A8/A9 is combined with TGFβ, the synergy results in enhanced apoptosis. S100A8/A9 has already been described to induce apoptosis in several cancer cell lines, but we were the first to demonstrate

it in TECs[24,25]. This effect may be mediated by RAGE, known to be expressed on TECs upon UUO. Supporting our speculation, S100B, another member of the S100 family, mediates myoblast apoptosis in a RAGE- dependent manner[26]. Whether this occurs as well in tubular epithelial cells, remains to be determined. Taken together, this body of evidences suggests that the endogenous S100A8/A9 signaling in macrophages plays a dispensable role in inflammation-driven renal fibrosis, possibly due to redundancy or compensatory pathways activated in immune cells. The two activating receptors that recognize S100A8/A9, namely TLR4 and RAGE, drive the development of renal fibrosis via a direct effect on epithelial cells integrity and function[27,28], but have a mild effect on renal inflammation. The results shown in this study strengthen the theory that the magnitude of inflammation is not correlated with the extend of fibrosis, as described earlier for TLR4 and that TECs contribute to the development of renal fibrosis.

The sharp contrast of roles for S100A8/A9 described in chapter 2 and 3 might be explained by the different primary insult that led to fibrosis in ischemic damage and obstructive nephropathy. For instance, the timing and the activation of the immunological response differ in IR-induced AKI and UUO-induced CKD. Leukocytes that abundantly express S100A8/A9, are recruited and activated in the kidney much earlier upon IR as compared to the UUO model. Therefore, it is not surprising that the S100A8/A9-mediated immune cells play such an important role in the acute model of renal injury. During chronic renal inflammation many other inflammatory pathways can be activated that overrule S100A8/A9's action. Finally, we provide strong evidences that S100A8/A9 mediates renal repair and fibrosis through the regulation of macrophage function and parenchymal damage. What remains to be studied is the relevance of S100A8/A9 as a biomarker for the development of end stage renal disease of the native kidney and whether S100A8/A9 neutralizing antibody can be a potential therapeutic strategy used to hamper tissue deterioration in fibrotic kidney.

In the second part of this thesis we describe the role of an activating PRRs, the Triggering receptor expressed on myeloid cells-1 (TREM-1) in the pathogenesis of sterile inflammatory disorders. Since its discovery in the early 2000's by Colonna and colleagues, TREM-1 has been implicated in the innate immune response activation primarily in infectious disease and considered as a potential target for treatments[29]. TREM-1 works in concert with other PRRs and causes an excessive inflammatory response activation, particularly potentiating TLR-elicited inflammation[30]. Therefore, many TREM-1 inhibiting strategies have been developed to fine tune the immune response as treatment for infectious diseases[31]. However, as we extensively described in **Chapter 4,** the emerging role of TREM1-mediated inflammatory response in non-infectious diseases is

accumulating. Indeed, the same TREM-1 blocking strategies used in infectious diseases, have been shown to dampen excessive inflammation and provide tissue protection in sterile inflammatory disorders such as atherosclerosis, myocardial ischemia, rheumatoid arthritis and many others. However, these studies do not provide any strong evidence for a specific TREM-1 ligand and the underlying mechanism. Elucidation of this mechanism represents an intriguing research line especially in the context of sterile inflammatory disorders.

In the work presented in **chapter 5, 6** of this thesis we found that TREM-1 actually improves tissue repair upon ischemic damage and that its activation is dispensable in the acute phase of renal injury, similarly to what we described earlier for S100A8/A9. Additionally in **Chapter 7** we describe that TREM-1, together with its adapter molecule DAP12, does not seem to play a role in the magnitude of inflammation during the development of renal fibrosis.

This body of evidence suggests that the inflammatory response elicited by PRRs is pivotal in shaping renal regeneration. Despite its well- established role in immune cells, in Chapter 6 we describe a novel role for TREM-1 in TECs proliferation empowering tubular repair.

Early pro-inflammatory signals generated in the kidney upon IR injury mediate the renal response to damage. Fine tuning the inflammatory response by containing excessive activation ensure that the renal microenviroment is primed for adaptive repair and optimal healing. TLR4- elicited inflammation has been shown to be deleterious in renal IR injury and mediates tubular damage[32]. In **chapter 5** we investigated whether the TLR4 synergistic receptor, TREM-1, could be involved in the induction of an exaggerated inflammatory response following IR. Despite the increased number of cells transcribing *Trem1* mRNA in the kidney upon IR, different attempts to modulate TREM-1 function *in vivo* did not result in renoprotection after reperfusion. Targeting TREM1-mediated immune response by short inhibitory peptides or fusion protein seems to be effective in downregulating downstream signaling activation, such as Myd88, but has no effect on the renal inflammatory response, nor renal damage, in the 24 hours following reperfusion. Our findings appear in contrast with studies showing that TREM-1 inhibition dampens inflammation and tissue damage upon ischemia in other organs, but is in line with a similar study conducted in the kidney. We considered that the absence of renoprotection in our model could have been related to the time of intervention, however, Duffield's group demonstrated that daily injection of TREM-1 fusion protein, following renal ischemia or ureteral obstruction, did not alter macrophage activation or renal injury and fibrosis[33]. Whether the inflammatory response elicited by myeloid cells- associated TREM-1 is

redundant during renal IR or plays a tissue specific role, remains to be determined. Our data would reinforce the concept that tubular-specific PRRs are the major determinant in driving the renal inflammatory response, instead of myeloid cells-associated PRRs. Among the different PRRs involved in renal dysfunction in the experimental model of renal IR, TLR4 is the most studied and characterized. Despite the many experimental studies suggesting an immune-regulatory role for TLR4 in allograft tolerance, in various human renal transplanted cohorts, TLR4 single nucleotide polymorphisms (SNPs) were not found to be associated with any pathological consequences after kidney transplantation. This suggests that in the complexity of the human allograft response, TLR4 may represent a minor determinant[34]. Hence, caution is warranted in extrapolating results from experimental studies to human diseases and alternative animal models that mimic different aspects of human AKI are necessary.
The findings that TREM-1 plays a limited role in the renal innate inflammatory response after IR, were corroborated by the results obtained in a human transplantation study. In a relatively large cohort of renal transplanted patients, neither donor or recipient carriers of the non-synonymous *TREM1* variant p.Thr25Ser, showed any association with post-transplant graft outcome. Interestingly, the 5 patients who were homozygous recessive for this variant did not develop delayed graft function, but due to the small number, statistical analysis could not be performed. Whether this variant is associated with a gain of function that could eventually explain the improved graft outcome, supported by the novel role of TREM-1 in tubular regeneration we described in **chapter 6,** warrants further investigation**.**

Herein, we provide an in depth study of the role of TREM-1 in injury and regeneration after IR-induced AKI, by using mice deficient for TREM1/3. In mild renal IR, TREM1/3 KO mice display a maladaptive repair with development of fibrosis and tubular senescence. Remarkably, sham-operated mice in absence of TREM1/3 showed a decreased tubular proliferation, suggesting that the tubular senescence was not a secondary effect, but probably the major cause of the maladaptive repair. The conventional expression of TREM-1 belongs to the innate immune cells, but TREM-1 expression is well described in several epithelia upon inflammation, conferring them a pro-inflammatory character[35,36]. Additionally, TREM-1 is an hypoxia-inducible gene in dendritic cells, empowering their pro-inflammatory activities[37]. Corroborating these findings, we describe an upregulation of TREM-1 protein on TECs after *in vitro*-simulated IR, suggesting indeed a role for TREM-1 in TEC's recovery after hypoxic damage. When we further characterized primary TECs, we found that the absence of TREM1/3 resulted in G2/M arrest, already at steady state. Bonventre's group described an innovative concept about TECs cell cycle and renal fibrosis. They demonstrated that G2/M-arrested TECs upregulate the production of pro-fibrotic

cytokines influencing the renal microenviroment[38]. Interestingly, the cell cycle arrest in TREM1/3 deficient TECs was associated with an upregulation of TGFβ and CTGF transcripts. In order to progress into the cell cycle, cells sense and respond to a bioenergetics demand. Activation of mitochondrial respiration is required for G2/M transition[39]. The cell cycle arrest in TREM1/3 KO TECs was associated with a decreased mitochondria metabolism. Since these cells carry out many tasks in a high energy dependent manner, mitochondrial homeostasis is crucial for their function. During oxidative phosphorylation, mitochondria generate ROS or electron transfer, but paradoxically, increased levels of ROS may attack the mitochondria machinery leading to increased oxidative damage, which is considered a cause of cell and organ dysfunction[40]. TREM1/3 KO TECs displayed increased levels of antioxidants, probably due to the extreme ROS levels we detected in mitochondria, which impaired their ability to carry out many metabolic functions. Supporting the beneficial role of TREM-1 in mitochondria homeostasis, Yang et *al.* described that in bone marrow derived macrophages, TREM-1 regulates mitochondria integrity favoring cell survival[41], through upregulation of Mitofusin-2 (involved in the mitochondria fusion process). However, in TECs this effect appears to be mitofusin-2 independent. When exposed to an extra ROS-generating trigger, such as the *in vitro*-simulated IR, TREM1/3 KO TECs displayed canonical markers of senescence activation, such as the senescence associated-β galactosidase, suggesting that IR was enough to cause a permanent cell cycle arrest. Cellular senescence is referred to as a permanent arrest of cell division, conventionally known as a safety mechanism to defeat cancer development[42]. In the context of tissue repair, senescent cells may be beneficial in the initial phase of injury and help regeneration, however prolonged accumulation of senescent cells delays tissue regeneration and establishment of homeostasis. Additionally, they can spread their senescent state through the senescent associated secretory phenotype (SASP), propagating a vicious inflammatory and pro-fibrotic cycle in the whole tissue. Thus, spreading of senescence can lead to a uniform tissue deterioration, because tubular regeneration cannot be compensated. In light of the aberrant effect of the secretory phenotype on neighbor's cells, senescent TREM 1/3 KO TECs displayed a potentiated pro-inflammatory and fibrotic secretome, which could contribute to the establishment of renal fibrosis. Therefore, we speculate that the prolonged senescence is the root of the maladaptive repair observed *in vivo* and leads to altered wound healing capacities. Additionally, it is conceivable that what was observed in TREM1/3 KO TECs belongs to the category of stress-induced senescence, caused by ROS and DNA damage. Indeed, we described a positive feedback between ROS accumulation, mitochondrial damage and p21 activation, leading to the establishment of senescence as described previously[43]. The increased ROS production observed in the KO animals could be the leading cause of the establishment of senescence. Possibly, as a consequence there is an ongoing DNA

damage response, resulting in cell cycle arrest. Recently, TREM-1 has been described to decrease the DNA damage response (DDR) and stimulate proliferation of leukemic stem cells[44]. Indeed, TREM-1 modulation has attracted attention as potential therapeutic target during cancer in order to prevent tumor progression[31]. Therefore, persistent DDR activation in absence of TREM1/3 may contribute to the cell cycle arrest and decreased proliferation. However we remain unaware of what triggers TREM-1 activation in TECs after IR and how an innate immune receptor localized on the plasma membrane can affect mitochondrial dysfunction and senescence in TECs. We speculate that this effect may be related to the synergistic relationship between TREM-1 and TGFβ[45]. Although TGFβ has been described as a potent inducer of epithelial apoptosis, some studies point to a beneficial role of this growth factor in tubular regeneration after ischemia, which accelerates renal recovery. TECs transiently express TGFβ during proliferation and we speculate that TGFβ may bind to TREM-1, acting as a positive feedback loop for proliferation. In absence of this synergy, TGFβ may become steadily expressed and have fatal consequences, especially for the mitochondrial function and ROS production, as already described[46].

In conclusion, this study highlights a novel role for TREM-1 beyond the innate immune cells. TREM-1 empowers successful proliferation of TECs, possibly by regulating mitochondrial homeostasis and therefore accelerates renal recovery after IR-induced AKI. Additionally, for the first time we show that PRRs are able to modulate tubular senescence, which highlights the power of TECs in dictating the maladaptive repair post-AKI. Again, these basic research findings about TREM-1 in AKI emphasize that a low degree of TREM-1 activation is necessary to orchestrate an adaptive repair. Targeting TREM-1 during active repair may preserve mitochondrial homeostasis and supply the TECs with the energy necessary to proliferate.

In the last chapter (**Chapter 7**) of this thesis, we rule out a role for TREM-1 and its adapter molecule DAP12, in mediating inflammation-driven renal fibrosis, in the UUO model. TREM-1 seems to be implicated in the inflammatory response in many chronic diseases. Although interstitial cells, most likely granulocytes, infiltrating the renal parenchyma following UUO transcribe *Trem1* and *Dap12*, no considerable differences in the inflammatory response or renal fibrosis were found to be mediated by TREM-1. Corroborating our findings, Duffield's group described that daily treatment with TREM-1 fusion protein after UUO, does not result in renoprotection[33]. DAP12 instead (partly through TREM-1), mediates renal inflammation during UUO. Specifically, the reduced infiltration of macrophages observed in theDAP12 KO animals in the advanced stages of renal fibrosis, could be related to the decreased production of macrophage chemoattractant protein-1 or simply to a defect in migration, intrinsic to DAP12 KO

macrophages[47]. It is possible that the effect mediated by DAP12 in renal inflammation entails the activation of other DAP12-associated receptors, which were upregulated in WT mice following obstructive nephropathy. Noticeably, TREM1/3 and DAP12 KO animals displayed increased tubular injury and edema in the early days upon obstruction, a phenotype similar to the TLR4 KO mice, which displayed enhanced renal damage following UUO, as a consequence of decreased tubular integrity but without any effect on interstitial inflammation[27]. Whether this mechanism is also taking place in TREM1/3 or DAP12 KO mice, is still unknown. Unfortunately, tubular integrity or proliferation were not measured in the two animal strains upon UUO. Since impaired mitochondrial homeostasis in TECs can ultimately result in ATP depletion, cytoskeletal changes, loss of the brush border and tubular epithelial cell detachment[48]. Given the protective role of TREM-1 in TEC's mitochondrial energy metabolism described in chapter 6, we speculate that the increased tubular damage and edema observed in the early days upon obstruction, may be a consequence of the mitochondrial dysfunction-driven tubular damage. Our evidence, however, appears to be in contrast with the study from Lo et *al*., which demonstrated that TREM-1 deletion ameliorated renal pathology after UUO by modulating M1 polarization[49]. Their findings were obtained with TREM-1 only KO mice, whereas in our studies we used mice deficient for both TREM-1 and TREM-3, as a model for TREM-1 deficiency[50]. If phenotypes are different in the two murine strains and if TREM-3 plays any role in inflammation and fibrosis, remains to be determined.

In summary, this evidence suggest that TREM-1 activation is dispensable in renal fibrosis, possibly because during the extensive and prolonged renal damage, other PRRs may overrule its function.

Concluding remarks and future perspectives

In this thesis we have described different aspects of S100A8/A9 and TREM-1 functions in the pathology of kidney diseases: from inflammation, fibrosis, wound healing and parenchymal integrity to metabolism and senescence. From the evidence obtained in these 5 years of research it appears clear that both immune cells and TECs are essential in shaping renal immunity and drive regeneration. The recurring theme we found is that constant inhibition of inflammation has the side effect of reduced wound healing and for a high risk of infections. We show that the inflammatory signaling elicited by S100A8/A9 or TREM-1 enhance renal repair; this makes them an attractive novel therapeutic target. Fine tuning the inflammatory response by timing and dosing S100A8/A9 or TREM-1 modulators, appears to be the desirable approach, yet very challenging to accomplish. Defining the timing and the extend of the therapeutic window of opportunity to regulate renal homeostasis, should be the goal of future research.

Interestingly, we unraveled a novel role for the innate immune receptor TREM-1 in preserving mitochondrial homeostasis and proliferative capacities of tubular epithelial cells, which could be targeted to enhance the reparative process. The absence of TREM-1 induces a metabolic reprogramming that predisposes the tubular cells to stress-induced premature senescence.

For the time being where population longevity is increasing, research on senescence has gained more attention. Renal transplant patients that receive a kidney from elderly people, may also inherit an increased risk of age-related disorders and decreased regenerative capacity of the kidney. In the last few years many attempts to target senescent cells in renal diseases have shown contrasting results. Apparently, senescence is important in the acute phase of damage and would support regeneration, whereas chronic senescence appears to be detrimental. Unravelling the pathological mechanisms taking place in senescent tubular cells, such as changes in their metabolism or their secretome, may overcome the issue of "rejuvenate" by elimination. Understanding changes in mitochondria homeostatic processes and the metabolism of senescent TECs may bring to light novel mechanisms that can be targeted to release the brake and supply the energy necessary for cell cycle progression.

As the aging of the immune system matters and immunosenescence represent fertile ground for treatment of acute and chronic disorders, we would not be surprised whether these age-related changes will be displayed by TECs as well, as they fulfil the task of an inflammatory cell, by expressing PRRs and undergoing senescence with ageing. Surely, a more detailed analysis on the role of tubular-associated PRRs and senescence deserves more consideration.

References

1. Negi, S. et al. Acute kidney injury: Epidemiology, outcomes, complications, and therapeutic strategies. Semin. Dial. (2018). doi:10.1111/sdi.12705
2. Basile, D. P. et al. Progression after AKI: Understanding Maladaptive Repair Processes to Predict and Identify Therapeutic Treatments. J. Am. Soc. Nephrol. 27, 687–97 (2016).
3. Leemans, J. C., Kors, L., Anders, H.-J. & Florquin, S. Pattern recognition receptors and the inflammasome in kidney disease. Nat. Rev. Nephrol. 10, 398–414 (2014).
4. Anders, H.-J. & Schaefer, L. Beyond Tissue Injury--Damage-Associated Molecular Patterns, Toll-Like Receptors, and Inflammasomes Also Drive Regeneration and Fibrosis. J. Am. Soc. Nephrol. 25, 1387–1400 (2014).
5. Jang, H. R. & Rabb, H. Immune cells in experimental acute kidney injury. Nat. Rev. Nephrol. 11, 88–101 (2015).
6. Baker, J. R. et al. Distinct roles for S100a8 in early embryo development and in the maternal deciduum. Dev. Dyn. 240, 2194–2203 (2011).
7. Kerkhoff, C. et al. Novel insights into the role of S100A8/A9 in skin biology. Exp. Dermatol. 21, 822–826 (2012).
8. Ziegler, G. et al. Mrp-8 and -14 mediate CNS injury in focal cerebral ischemia. Biochim Biophys Acta 1792, 1198–1204 (2009).
9. Lee, S. et al. Distinct macrophage phenotypes contribute to kidney injury and repair. J. Am. Soc. Nephrol. 22, 317–26 (2011).
10. Jo, S.-K., Sung, S.-A., Cho, W.-Y., Go, K.-J. & Kim, H.-K. Macrophages contribute to the initiation of ischaemic acute renal failure in rats. Nephrol. Dial. Transplant 21, 1231–9 (2006).
11. Tian, S. & Chen, S.-Y. Macrophage polarization in kidney diseases. Macrophage 2, (2015).
12. Lee, S. et al. Distinct macrophage phenotypes contribute to kidney injury and repair. J Am Soc Nephrol 22, 317–326 (2011).
13. Weisheit, C. K., Engel, D. R. & Kurts, C. Dendritic Cells and Macrophages: Sentinels in the Kidney. Clin. J. Am. Soc. Nephrol. 10, 1841–1851 (2015).
14. Kezić, A., Stajic, N. & Thaiss, F. Innate Immune Response in Kidney Ischemia/Reperfusion Injury: Potential Target for Therapy. J. Immunol. Res. 2017, 6305439 (2017).
15. Yang, J. et al. Calcium-Binding Proteins S100A8 and S100A9: Investigation of Their Immune Regulatory Effect in Myeloid Cells. Int. J. Mol. Sci. 19, 1833 (2018).
16. Rekers, N. V et al. Beneficial Immune Effects of Myeloid-Related Proteins in Kidney Transplant Rejection. Am. J. Transplant 16, 1441–55 (2016).
17. Kuka, M., Munitic, I. & Ashwell, J. D. Identification and characterization of polyclonal αβ-T cells with dendritic cell properties. Nat. Commun. 3, 1223 (2012).
18. Ganguly, D., Haak, S., Sisirak, V. & Reizis, B. The role of dendritic cells in autoimmunity. Nat. Rev. Immunol. 13, 566–577 (2013).

19. Nikolic-Paterson, D. J., Wang, S. & Lan, H. Y. Macrophages promote renal fibrosis through direct and indirect mechanisms. Kidney Int. Suppl. 4, 34–38 (2014).
20. Dessing, M. C. et al. The calcium-binding protein complex S100A8/A9 has a crucial role in controlling macrophage-mediated renal repair following ischemia/reperfusion. Kidney Int. 87, 85–94 (2015).
21. Fujiu, K., Manabe, I. & Nagai, R. Renal collecting duct epithelial cells regulate inflammation in tubulointerstitial damage in mice. J. Clin. Invest. 121, 3425–41 (2011).
22. Pruenster, M., Vogl, T., Roth, J. & Sperandio, M. S100A8/A9: From basic science to clinical application. Pharmacol. Ther. 167, 120–131 (2016).
23. Eikmans, M. et al. Expression of surfactant protein-C, S100A8, S100A9, and B cell markers in renal allografts: investigation of the prognostic value. J Am Soc Nephrol 16, 3771–3786 (2005).
24. Ghavami, S. et al. S100A8/9 induces cell death via a novel, RAGE-independent pathway that involves selective release of Smac/DIABLO and Omi/HtrA2. Biochim. Biophys. Acta - Mol. Cell Res. 1783, 297–311 (2008).
25. Ghavami, S. et al. S100A8/A9 at low concentration promotes tumor cell growth via RAGE ligation and MAP kinase-dependent pathway. J. Leukoc. Biol. 83, 1484–1492 (2008).
26. Sorci, G., Riuzzi, F., Agneletti, A. L., Marchetti, C. & Donato, R. S100B causes apoptosis in a myoblast cell line in a RAGE-independent manner. J. Cell. Physiol. 199, 274–283 (2004).
27. Pulskens, W. P. et al. TLR4 promotes fibrosis but attenuates tubular damage in progressive renal injury. J. Am. Soc. Nephrol. 21, 1299–1308 (2010).
28. Gasparitsch, M. et al. RAGE-mediated interstitial fibrosis in neonatal obstructive nephropathy is independent of NF-κB activation. Kidney Int. 84, 911–9 (2013).
29. Bouchon, A., Facchetti, F., Weigand, M. A. & Colonna, M. TREM-1 amplifies inflammation and is a crucial mediator of septic shock. Nature 410, 1103–7 (2001).
30. Klesney-Tait, J., Turnbull, I. R. & Colonna, M. The TREM receptor family and signal integration. Nat. Immunol. 7, 1266–73 (2006).
31. Tammaro, A. et al. TREM-1 and its potential ligands in non-infectious diseases: from biology to clinical perspectives. Pharmacol. Ther. 177, (2017).
32. Wu, H. et al. TLR4 activation mediates kidney ischemia/reperfusion injury. J. Clin. Invest. 117, 2847–59 (2007).
33. Campanholle, G. et al. TLR-2/TLR-4 TREM-1 signaling pathway is dispensable in inflammatory myeloid cells during sterile kidney injury. PLoS One 8, e68640 (2013).
34. Dessing, M. C. et al. Toll-Like Receptor Family Polymorphisms Are Associated with Primary Renal Diseases but Not with Renal Outcomes Following Kidney Transplantation. PLoS One 10, e0139769 (2015).
35. Schmausser, B. et al. Triggering receptor expressed on myeloid cells-1 (TREM-1) expression on gastric epithelium: implication for a role of TREM-1 in Helicobacter pylori infection. Clin. Exp. Immunol. 152, 88–94 (2008).

36. Rigo, I. et al. Induction of triggering receptor expressed on myeloid cells (TREM-1) in airway epithelial cells by 1,25(OH)(2) vitamin D(3). Innate Immun 18, 250–257 (2012).
37. Bosco, M. C. et al. Hypoxia modulates the gene expression profile of immunoregulatory receptors in human mature dendritic cells: identification of TREM-1 as a novel hypoxic marker in vitro and in vivo. Blood 117, 2625–2639 (2011).
38. Yang, L., Besschetnova, T. Y., Brooks, C. R., Shah, J. V & Bonventre, J. V. Epithelial cell cycle arrest in G2/M mediates kidney fibrosis after injury. Nat. Med. 16, 535–543 (2010).
39. Wang, Z. et al. Cyclin B1/Cdk1 Coordinates Mitochondrial Respiration for Cell-Cycle G2/M Progression. Dev. Cell 29, 217–232 (2014).
40. Murphy, M. P. How mitochondria produce reactive oxygen species. Biochem. J. 417, 1–13 (2009).
41. Yuan, Z. et al. Triggering receptor expressed on myeloid cells 1 (TREM-1)-mediated Bcl-2 induction prolongs macrophage survival. J Biol. Chem 289, 15118–15129 (2014).
42. Valentijn, F. A., Falke, L. L., Nguyen, T. Q. & Goldschmeding, R. Cellular senescence in the aging and diseased kidney. J. Cell Commun. Signal. 12, 69–82 (2018).
43. Ziegler, D. V., Wiley, C. D. & Velarde, M. C. Mitochondrial effectors of cellular senescence: Beyond the free radical theory of aging. Aging Cell 14, 1–7 (2015).
44. Du, W., Amarachintha, S., Wilson, A. & Pang, Q. The immune receptor Trem1 cooperates with diminished DNA damage response to induce preleukemic stem cell expansion. Leukemia 31, 423–433 (2017).
45. Peng, L. et al. TGF-β1 Upregulates the Expression of Triggering Receptor Expressed on Myeloid Cells 1 in Murine Lungs. Sci. Rep. 6, 18946 (2016).
46. Yoon, Y.-S., Lee, J.-H., Hwang, S.-C., Choi, K. S. & Yoon, G. TGF β1 induces prolonged mitochondrial ROS generation through decreased complex IV activity with senescent arrest in Mv1Lu cells. Oncogene 24, 1895–1903 (2005).
47. Koth, L. L. et al. DAP12 is required for macrophage recruitment to the lung in response to cigarette smoke and chemotaxis toward CCL2. J Immunol 184, 6522–6528 (2010).
48. Perico, L. et al. Human mesenchymal stromal cells transplanted into mice stimulate renal tubular cells and enhance mitochondrial function. Nat. Commun. 8, 983 (2017).
49. Lo, T.-H. et al. TREM-1 regulates macrophage polarization in ureteral obstruction. Kidney Int. 86, 1174–86 (2014).
50. Klesney-Tait, J. et al. Transepithelial migration of neutrophils into the lung requires TREM-1. J. Clin. Invest. 123, 138–49 (2013).

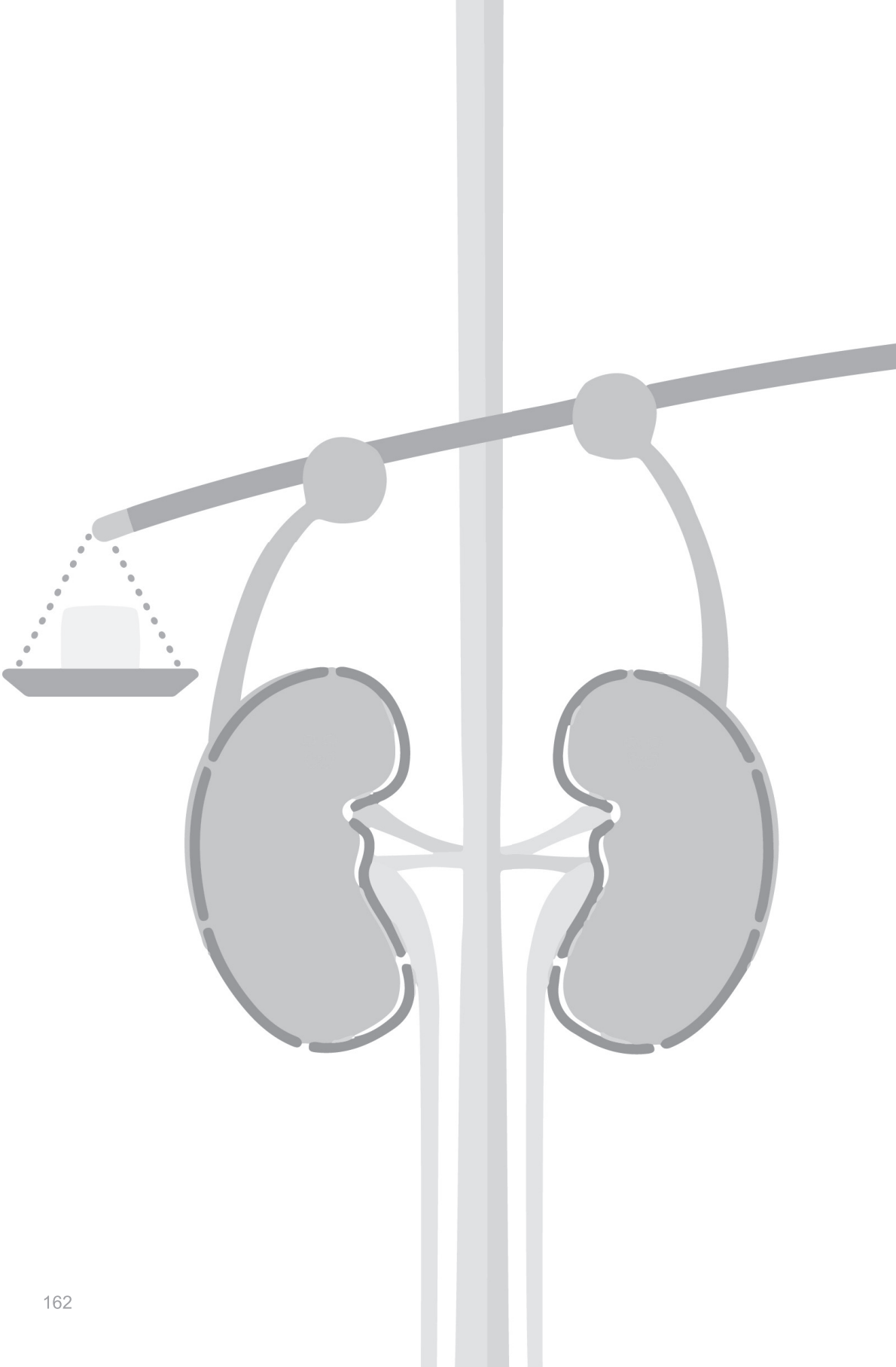

Appendix

English summary

The incidence of renal diseases has increased significantly and it is a chief cause of morbidity and mortality worldwide. Specific treatment for patients with kidney diseases remains unavailable and current therapies, which are only supportive, consist of dialysis and renal transplantation. A better understanding of the pathogenesis of kidney diseases is required to develop new treatment opportunities. The innate immune system represents the first line of defense against invading pathogens but also plays a crucial role in renal tissue damage by alarming the host. Danger proteins released by damaged or inflammatory cells, the so-called Damage Associated Molecular Patterns (DAMPs), act as a ligand for Pattern Recognition Receptors (PRRs) and initiate an inflammatory reaction. This results in a clearance of invading pathogens that segues into tissue repair. Inflammatory cells are the main players in most inflammatory processes.

The danger protein S100A8/A9 and the innate immune receptor TREM-1 are expressed by neutrophils and monocyte/macrophages; both are able to elicit or amplify inflammatory signals through other PRRs. This thesis focuses on the role of the danger protein S100A8/A9 and the activating immune receptor TREM-1 in preclinical models of acute kidney injury (AKI) and chronic kidney disease (CKD).

In **Chapter 1** we give a brief overview of renal homeostasis and disease, together with a detailed description of the factors involved in the innate immune response, which was the main focus for the research described in this thesis.

Chapter 2 describes the contribution of S100A8/A9 in renal Ischemia/Reperfusion (IR)-induced AKI and it explores the significant role that danger proteins play in renal repair post-AKI. We subjected both wild type and S100A9 KO animals to bilateral clamping of the renal artery, followed by reperfusion for several days, in order to study the different phases of renal injury. We observed that S100A8/A9 expression was increased in the kidney during IR injury, especially 24 hours post-ischemia. This can most-likely be attributed to the infiltration of granulocytes that express high levels of S100A8/A9. Despite the increased expression of the protein 1 day post-IR, S100A9 KO animals displayed no major changes in renal inflammation or damage marker expression at this time point. However, we found that S100A8/A9 is crucial in limiting maladaptive repair post-AKI. Indeed, during the repair phase, S100A9 KO mice displayed signs of renal dysfunction and increased expression of tubular damage markers, which was also associated with an increased production of renal chemokines and cytokines. Finally, we show that S100A9 KO animals developed renal fibrosis, as shown by increased collagen deposition and TGFβ production. We found that the maladaptive repair phenotype observed in the S100A9 KO

animals, could be ascribed to an altered macrophage function. This is highly conceivable, considering the role that macrophages play in tissue repair has been well established. S100A9 KO macrophages revealed an aberrant M2-like phenotype *in vivo*, as shown by increased transcription of alternative M2 macrophage activation markers, namely Arg1, MGL1 and IRF5. Through *in vitro* experiments, we confirmed that upon M2 skewing with IL4 and IL13 cytokines, S100A9 KO macrophages displayed a phenotype similar the one observed *in vivo*. Possibly, during the repair phase, excessive M2 polarization, which is often associated with the release of pro-fibrotic factors, may further fuel the improper wound healing response, thereby leading to scar formation. Thus, S100A8/A9 is crucially involved in renal adaptive repair after ischemia, by controlling excessive M2 macrophage polarization and preventing renal fibrosis.

Macrophages are known to accumulate in the kidney during renal fibrosis and may also play a role in tissue degeneration. As we observed that S100A9 KO animals display increased fibrosis upon AKI due to excessive M2 macrophage polarization, we further investigated the role of S100A8/A9 in the development of renal fibrosis in **Chapter 3**. In this chapter we used the unilateral ureteral obstruction (UUO) in WT and S100A9 KO animals as a chronic model of renal damage, which leads to the development of severe tubulointerstital fibrosis. During the course of UUO, intrarenal S100A8/A9 positive cells increased overtime and co-expressed the granulocyte activation marker Ly6G. However, the infiltration of these inflammatory cells did not differ between WT and S100A9 KO animals . The expression profile of S100A8/A9 in the preclinical model was analogous to the one observed in patients with obstructive hydronephrosis. In contrast with previous evidences, S100A9 KO animals were protected against renal fibrosis, as displayed by decreased infiltration of myofibroblasts and collagen deposition. We found that the reduction in fibrosis, observed in KO animals that had sustained chronic damage, was related to the preservation of tubular epithelial cells (TEC) integrity. S100A9 KO animals displayed decreased tubular apoptosis and activation of critical epithelial-mesenchymal transition steps. In line with these findings, we observed that stimulation of TECs with recombinant S100A8/A9 induced cell cycle arrest and signs of dedifferentiation, including decreased expression of cell junction and adhesion molecules that are essential in supporting tubular structure and function. When exposed to additional stimulation with the profibrotic factor TGFβ, S100A8/A9 led to irreversible damage and cell death. Therefore, our data suggest that S100A8/A9 mediates the development of renal fibrosis, possibly through a direct effect on dedifferentiation and apoptosis in TECs.

Chapter 4 introduces the reader to a different inflammatory mediator: Triggering Receptor expressed on myeloid cells-1 (TREM-1). Herein, we extensively reviewed

TREM-1 function, from biological relevance to therapeutic intervention, solely in sterile inflammatory disorders.

Our contribution in this field begins with **Chapter 5**, where we investigated the role of TREM-1 in an experimental model of IR-induced AKI and in human renal transplantation. WT mice were subjected to bilateral IR injury and sacrificed 24 hours later to study the acute inflammatory response. We found that during IR injury, there is an infiltration of cells transcribing TREM-1 in the renal interstitium. Moreover, both the TREM-1 receptor and its soluble protein are increased in tissue lysates and plasma. Monocytic TREM-1 expression was also found to be increased. Taken together, this suggests that TREM-1 may be involved in the amplification of the inflammatory signals driving the development of IR injury. To further evaluate this hypothesis, we treated the mice with different TREM-1 inhibitors, which were previously shown to modulate TREM-1-induced inflammation and prevented tissue dysfunction. Despite downregulation of the TREM-1 pathway, the approaches we used failed to protect the kidney from inflammation and damage. Additionally, we evaluated whether Single Nucleotide Variants (SNVs) in the TREM-1 gene were associated with any pathological outcomes after kidney transplantation. In line with the findings from the preclinical model, we observed that neither donor nor recipient carriers of the TREM-1 gene variant p.Thr25Ser (heterozygous and non synonymous) were associated with delayed graft function, rejection or graft failure. From this study, it appears that TREM-1 does not play a prominent role in the kidney's acute response to hypoxic damage.

Since PRRs may also be involved in kidney regeneration after damage, we sought to carry out an in depth study into the role of TREM-1 in the repair phase of IR injury. Therefore, in **Chapter 6,** we subjected WT and TREM1/3 KO animals to renal IR and monitored the mice to study the injury, repair and resolutive phase following hypoxic damage. Herein, we confirmed that TREM-1 pathway activation is dispensable during the acute phase of injury, as WT and TREM1/3 KO mice display similar degrees of renal inflammation and damage following 24 hours of reperfusion. To our surprise, we observed increased mortality in TREM1/3KO animals during the repair phase. By switching to a milder model of renal damage we were able to show that TREM1/3 KO mice suffer from maladaptive repair with progression to CKD. In the absence of TREM1/3, in particular, we observed persistent tubular damage and interstitial fibrosis, as shown by increased macrophage infiltration, accumulation of α-SMA+ cells and collagen deposition. Additionally, TREM1/3-deficient mice failed to regenerate TECs, due to the development of tubular senescence and the associated reduction in proliferation. By means of *in vitro*-simulated IR experiments, we were able to show that TREM-1 is expressed on TECs after hypoxic damage, suggesting a direct effect of TREM-1 in the tubular response to injury. A possible mechanism driving

the failed tubular regeneration after IR could be found in the fact that at steady state TREM1/3 KO TECs already experience a cell cycle blockade, specifically in the G2/M phase. This growth arrest was possibly related to major differences we detected in the anabolic and metabolic pathways between WT and TREM1/3 deficient TECs, particularly those related to mitochondrial antioxidant levels, suggesting an increase in oxidative stress in the absence of TREM1/3. Indeed, TREM1/3-deficient TECs display an altered mitochondrial homeostasis, with disrupted morphology, increased ROS accumulation, mitochondria depolarization and impaired capacity for energy production. Additionally, this resulted in an increased expression of pro-inflammatory and fibrotic mediators by TECs. This phenotype worsened when cells were exposed to *in vitro*-simulated ischemia. The increase in cellular senescence resulted in a permanent growth arrest in TECs , which led to an altered wound healing response. Thus, we identified a novel role for TREM-1 in tubular epithelial cells, which preserves mitochondrial integrity and confers a metabolic advantage for TECs to progress into the cell cycle and proliferate. In summary, TREM-1 fosters tubular regeneration and limits maladaptive repair post-AKI.

Since maladaptive repair led to fibrosis, in **Chapter 7,** we evaluated the specific role of TREM-1 and its adaptor molecule DAP12, in the chronic model of obstructive nephropathy, which is the classic model for renal fibrosis. Herein, we show that in patients with obstructive hydronephrosis, TREM-1 was detected in interstitial cells, but was absent in protocolar renal biopsies of transplanted patients with stable graft function. In the experimental model, we subjected WT, TREM1/3 KO and DAP12 KO animals to permanent UUO and analyzed the animals at different time points post-obstruction. Although UUO induces the transcription of TREM-1 and DAP12 by interstitial cells, it appears that DAP12, partly through TREM1/3, mediates renal inflammation after UUO, but that both play a dispensable role in the development of renal fibrosis. Indeed, myofibroblast accumulation and collagen deposition were similar between the experimental groups. However, in the absence of TREM1/3 and DAP12, we observed increased tubular damage and edema in the early stages after obstruction, suggesting a possible role for TREM1/3 and DAP12 in tubular integrity.

Nederlandse samenvatting

De incidentie van nierziekten is aanzienlijk toegenomen en is wereldwijd een belangrijke oorzaak van morbiditeit en mortaliteit. Gerichte behandelingen voor patiënten met nierziekten zijn nog steeds niet beschikbaar. De huidige therapieën, die alleen ondersteunend zijn, bestaan uit dialyse en niertransplantatie. Een beter begrip van de pathogenese van nierziekten is nodig voor de ontwikkeling van nieuwe behandelingsmogelijkheden. Het aangeboren immuunsysteem vertegenwoordigt de eerste verdedigingslinie tegen binnendringende pathogenen, maar speelt ook een cruciale rol bij renale beschadiging. Eiwitten die vrijkomen door beschadigde- of inflammatoire-cellen, de zogenaamde Damage Associated Molecular Patterns (DAMPs), werken als een ligand voor Pattern Recognition Receptors (PRRs) en initiëren een ontstekingsreactie. Dit resulteert in een klaring van binnenvallende pathogenen en weefselherstel. Ontstekingscellen zijn de belangrijkste spelers in de meeste inflammatoire processen.

Het gevaars-eiwit S100A8/A9 en de aangeboren immuun-receptor TREM-1 worden tot expressie gebracht door neutrofielen en monocyten/ macrofagen; beide kunnen ontstekingssignalen opwekken of versterken via PRRs. Dit proefschrift richt zich op de rol van het gevaars-eiwit S100A8/A9 en de activerende immuun-receptor TREM-1 in preklinische modellen van acute nierschade (AKI) en chronische nierziekte (CKD).
In **hoofdstuk 1** geven we een kort overzicht van de renale homeostase en ziekten, samen met een gedetailleerde beschrijving van factoren die betrokken zijn bij de aangeboren immuunrespons, dat de belangrijkste focus is voor het onderzoek beschreven in dit proefschrift.

Hoofdstuk 2 beschrijft de bijdrage van S100A8/A9 aan renale ischemie/reperfusie (IR)-geïnduceerde AKI, hierin wordt de rol die gevaars-eiwitten spelen bij renaal herstel na de AKI onderzocht. We onderwierpen zowel wildtype als S100A9 KO-dieren aan een bilaterale afklemming van de nierslagader, gevolgd door verschillende dagen van reperfusie om de verschillende fasen van renale beschadiging en herstel te bestuderen. We hebben waargenomen dat de expressie van S100A8/A9 in de nier was verhoogd tijdens IR-letsel, met name 24 uur na ischemie. Dit kan hoogstwaarschijnlijk worden toegeschreven aan de infiltratie van granulocyten die hoge levels van S100A8/A9 tot expressie brengen. Ondanks de verhoogde expressie van het eiwit 1 dag na IR, vertoonden S100A9 KO-dieren op dit tijdstip geen belangrijke veranderingen in renale inflammatie of veranderde expressie van renale schademarkers. We hebben echter vastgesteld dat S100A8/A9 cruciaal is in het beperken van de maladaptieve herstel na

AKI. Tijdens de regeneratieve-fase vertoonden S100A9 KO-muizen inderdaad tekenen van nier disfunctie in combinatie met verhoogde expressie van tubulaire schade markers, wat is geassocieerd met een verhoogde productie van chemokinen en cytokinen in de nier. Ten slotte laten we zien dat S100A9 KO-dieren nierfibrose ontwikkelen, zoals blijkt uit een verhoogde collageendepositie en TGFβ-productie. Het maladaptieve herstel-fenotype waargenomen in de S100A9 KO-dieren kan volgens ons worden toegeschreven aan een veranderde macrofaagfunctie. Gezien de rol die macrofagen spelen bij weefselherstel is dit inderdaad goed mogelijk,. S100A9 KO-macrofagen laten in vivo een afwijkend M2-achtig fenotype zien, door verhoogde transcriptie van alternatieve M2-macrofaagactiveringsmarkers, zoals Arg-l, MGL1 en IRF5. Door middel van in vitro experimenten bevestigden we dat na M2-skewing met IL4- en IL13-cytokines S100A9 KO-macrofagen een fenotype vertoonden dat vergelijkbaar is met het waargenomen in vivo fenotype. Mogelijk kan tijdens de reparatiefase buitensporige M2-polarisatie, welke vaak gepaard gaat met het vrijkomen van pro-fibrotische factoren, de onjuiste reactie op genezing verder ontwikkelen, wat leidt tot verlittekening van het weefsel. S100A8/A9 is door het beheersen van een overmatige M2-macrofaagpolarisatie en het voorkomen van nierfibrose dus van cruciaal belang bij het herstel van de nier na ischemie.

Het is bekend dat macrofagen zich ophopen in de nier tijdens nierfibrose en mogelijk ook een rol spelen bij weefselafbraak. Aangezien we hebben waargenomen dat S100A9 KO-dieren verhoogde fibrose vertonen bij AKI als gevolg van overmatige M2-macrofaagpolarisatie, onderzochten we in **hoofdstuk 3** de rol van S100A8/A9 tijdens de ontwikkeling van renale fibrose. In dit hoofdstuk gebruikten we het eenzijdige ureter obstructie (UUO) als chronisch model voor renale beschadiging, wat leidt tot de ontwikkeling van ernstige tubulo-interstitiële fibrose in WT en S100A9 KO dieren. Gedurende het UUO verloop in WT nieren werd een toename in de aanwezigheid van intra-renale S100A8/A9-positieve cellen die ook de granulocyt activatiemarker Ly6G tot expressie brengen waargenomen. De infiltratie van deze ontstekingscellen verschilde echter niet tussen WT en S100A9 KO-dieren. Het expressieprofiel van S100A8/A9 in het preklinische UUO model was overeenkomend met het profiel dat werd waargenomen bij patiënten met obstructieve hydronefrose. In tegenstelling tot wat eerder is aangetoond, vonden wij door verminderde infiltratie van myofibroblasten en collageenafzetting, dat S100A9 KO-dieren beschermd zijn tegen nierfibrose. We vonden dat de reductie in fibrose, waargenomen bij KO dieren die chronische schade hadden opgelopen, gerelateerd was aan het behoud van tubulaire epitheliale cel (TEC) integriteit. S100A9 KO-dieren vertoonden namelijk verminderde tubulaire apoptose en activering van belangrijke epitheliale-mesenchymale transitie parameters. In overeenstemming met deze bevindingen hebben we waargenomen dat stimulatie van TECs met recombinant

S100A8/A9 eiwit stopzetting van de celcyclus en tekenen van dedifferentiatie induceert, waaronder verminderde expressie van cel vermenigvuldiging en adhesiemoleculen die essentieel zijn bij het ondersteunen van de renale tubuli structuur en functie. Stimulatie met de pro-fibrotische factor TGFβ in aanwezigheid van recombinant S100A8/A9 eiwit leidde tot onomkeerbare schade en celdood van TECs. Daarom suggereert onze studie dat S100A8/A9 de ontwikkeling van renale fibrose medieert, mogelijk door een direct effect op TEC dedifferentiatie en apoptose.

Hoofdstuk 4 introduceert een andere inflammatoire mediator: Triggering Receptor expressed on myeloid cells-1 (TREM-1). In dit hoodstuk hebben we uitvoerig de functie van TREM-1 in uitsluitend steriele ontstekingsaandoeningen, van biologische relevantie tot therapeutische interventie, gereviewd.
Onze bijdrage op dit gebied begint met **hoofdstuk 5**, waarin we de rol van TREM-1 in een experimenteel model van IR-geïnduceerde AKI en bij menselijke niertransplantatie hebben onderzocht. WT muizen werden onderworpen aan bilaterale IR en 24 uur later opgeofferd om de acute ontstekingsreactie te bestuderen. We vonden dat er tijdens IR-letsel een infiltratie ontstaat van cellen die TREM-1 tot expressie brengen in het renale interstitium. Bovendien zijn zowel de TREM-1 receptor als het TREM-1 oplosbare eiwit verhoogd aanwezig in zowel nier weefsel lysaten als plasma. De TREM-1 expressie door monocyten bleek ook te zijn toegenomen. Dit suggereert dat TREM-1 mogelijk betrokken is bij de amplificatie van de ontstekingssignalen die de ontwikkeling van IR-letsel stimuleren. Om deze hypothese verder te evalueren, hebben we de muizen behandeld met verschillende TREM-1 remmers waarvan eerder is aangetoond dat ze TREM-1 geïnduceerde ontsteking moduleren en weefseldisfunctie voorkomen. Ondanks de downregulatie van de TREM-1 pathway, bleek deze interventie de nier niet te beschermen tegen ontsteking en schade. Bovendien onderzochten we of Single Nucleotide Variants (SNV's) in het TREM-1 gen geassocieerd zijn met pathologische ontwikkelingen na niertransplantatie. In overeenstemming met de bevindingen van het preklinische model, hebben we waargenomen dat noch donor noch ontvangende dragers van de TREM-1 genvariant p.Thr25Ser (heterozygoot en niet-synoniem) worden geassocieerd met een vertraagde niertransplantaat functie, afstoting of transplantaat falen. Uit deze studie blijkt dat TREM-1 geen prominente rol speelt in de reactie van de nieren op acute hypoxische schade.

Aangezien PRRs mogelijk ook betrokken zijn bij renale regeneratie na beschadiging, hebben we de rol van TREM-1 in de reparatiefase van IR-letsel te onderzoeken. Daarom hebben we in **hoofdstuk 6** WT en TREM1/3 KO dieren onderworpen aan renale IR en de muizen gevolgd om de letsel-, herstel- en resolutiefase na hypoxische schade te

bestuderen. Hiermee hebben we bevestigd dat activering van de TREM-1-pathway overbodig is tijdens de acute fase van de schade, aangezien WT en TREM1/3 KO muizen na 24 uur reperfusie een vergelijkbare graad van renale-ontsteking en -beschadiging vertonen. Tot onze verbazing constateerden we een verhoogde mortaliteit bij TREM1/3 KO dieren tijdens de herstelfase. Door over te schakelen op een milder model van acute renale beschadiging konden we aantonen dat TREM1/3 KO muizen een maladaptieve repair ondergaan met progressie naar CKD. In afwezigheid van met name TREM1/3, observeerden we aanhoudende tubulaire schade en interstitiële fibrose, zoals aangetoond door de verhoogde infiltratie van macrofagen, accumulatie van α-SMA positieve cellen en collageenafzetting. Bovendien werd er geen regeneratie gezien van TECs in TREM1/3 deficiënte muizen, vanwege de ontwikkeling van tubulaire senescence en de daarmee gepaard gaande vermindering in proliferatie. Door middel van in vitro gesimuleerde IR-experimenten konden we aantonen dat TREM-1 na hypoxische schade op TECs tot expressie wordt gebracht, wat duidt op een direct effect van TREM-1 in de tubulaire respons op letsel. Een mogelijk mechanisme dat de gefaalde tubulaire regeneratie na IR kan verklaren, kan worden gevonden in het feit dat TREM1/3 KO TECs op basaal niveau al een blokkade van de celcyclus ervaren, met name in de G2/M-fase. Deze groeistop is mogelijk gerelateerd aan de grote verschillen die we detecteerden in de anabole en metabole pathways tussen WT en TREM1/3 deficiënte TECs, met name de dominante aanwezigheid van pathways gerelateerd aan mitochondriale antioxidant niveaus in TREM1/3 deficiënte TECs duidt op een toename van oxidatieve stress in afwezigheid van TREM1/3. TREM1/3 deficiënte TECs vertoonden inderdaad een veranderde mitochondriale homeostase, met een verstoorde mitochondriale morfologie, verhoogde ROS-accumulatie, depolarisatie van mitochondria en een verminderde energie producerende capaciteit. Bovendien resulteerde dit in een verhoogde expressie van pro-inflammatoire en fibrotische mediatoren door TECs. Dit fenotype verslechterde toen cellen werden blootgesteld aan ischemie. De toename in cellulaire senescence resulteerde in een permanente groei-arrest van TECs, wat leidde tot een veranderde wondgenezing. We identificeerden hiermee een nieuwe rol voor TREM-1 in tubulaire epitheliale cellen, waarbij TREM-1 zorgt voor behoud van de mitochondriale integriteit en een metabool voordeel geeft aan TECs wat nodig is voor het verloop van de celcyclus en proliferatie. Samengevat, TREM-1 bevordert tubulaire regeneratie en beperkt maladaptief herstel na AKI.

Omdat maladaptief herstel leidde tot fibrosis, in **hoofdstuk 7**, we evalueerden de specifieke rol van TREM-1 en zijn adaptormolecuul DAP12, in het chronische model van obstructieve nefropathie en het klassieke model voor nierfibrose. Hierin laten we zien dat bij patiënten met obstructieve hydronefrose TREM-1 werd gedetecteerd in interstitiële

cellen, maar afwezig was in protocolaire nierbiopten van getransplanteerde patiënten met een stabiele niertransplantaat functie. In het experimentele model stelden we WT, TREM1/3 KO en DAP12 KO-dieren bloot aan UUO en analyseerden de nieren van deze dieren op verschillende tijdstippen na obstructie. Hoewel UUO de transcriptie van TREM-1 en DAP12 door interstitiële cellen induceert en DAP12, deels via TREM 1/3, invloed uitoefent op de renale inflammatierespons, vonden we dat zowel TREM-1 als DAP12 geen leidende rol spelen in de ontwikkeling van nierfibrose. De accumulatie van myofibroblasten en de collageenafzetting waren immers vergelijkbaar tussen de experimentele groepen. In de afwezigheid van TREM1/3 en DAP12 hebben we echter in de vroege stadia na obstructie wel verhoogde tubulaire schade en oedeem waargenomen, wat duidt op een mogelijke rol voor TREM1/3 en DAP12 in het behoudt van de tubulaire integriteit.

Riassunto

L'incidenza delle malattie renali è aumentata in modo significativo ed è una delle principali cause di morbidità e mortalità in tutto il mondo. Una specifica terapia per i pazienti affetti da malattie renali non è disponibile e le terapie attuali, che sono solo di supporto, consistono nella dialisi e nel trapianto renale. Per sviluppare nuove opportunità di trattamento e' necessaria una maggiore comprensione della patogenesi delle malattie renali. Il sistema immunitario innato che possediamo, rappresenta la prima linea di difesa contro i patogeni, ma svolge anche un ruolo cruciale nel danno tissutale renale. Le proteine associate al danno che vengono rilasciate da cellule danneggiate o infiammatorie, i cosiddetti Damaged associated molecular pattern (DAMP), agiscono da ligando per i Pattern Recognition receptor (PRR) dando inizio così a una reazione infiammatoria. Questo si traduce in una eliminazione dei patogeni e il conseguente riparo del danno tissutale causato da quest'ultimi.
Le cellule infiammatorie sono i principali protagonisti nella maggior parte in questo processo. La proteina S100A8/A9 e il recettore TREM-1 sono espressi da neutrofili e monociti/macrofagi; entrambi sono in grado di dare inizio o amplificare la risposta infiammatoria attraverso altri PRR. L'obiettivo di questa tesi è stato quello di studiare il ruolo di S100A8/A9 e TREM-1 in modelli preclinici di danno renale acuto (AKI) e malattia renale cronica (CKD).

Nel **Capitolo 1** viene fornita una breve panoramica della funzionalita' renale e delle varie malattie che sono state oggetto di questa tesi. Il **Capitolo 2** invece, descrive il contributo di S100A8/A9 nel modello di AKI indotto dall' ischemia/riperfusione (IR) renale ed esplora il ruolo significativo che questa proteina svolge nella rigenerazione renale dopo il danno causato da IR. Infatti abbiamo sottoposto sia topi Wild Type (WT) che animali senza S100A8/A9 (S100A9 KO) all'occlusione delle arterie renali per diversi minuti, che ha generato una carenza d'ossigeno al rene dovuta alla ridotta perfusione sanguigna (=ischemia). Dopodiche'abbiamo rilasciato l'occlusione in modo da ristabilire la perfusione (=riperfusione) e abbiamo monitarato i topi per diversi giorni per valutare l'effetto sul rene dettato dall'assenza di S100A8/A9. Nei topi WT e' stato osservato che l'espressione di S100A8/A9 aumenta nel rene durante IR, in particolare 24 ore dopo l'ischemia. Questo può essere attribuito molto probabilmente all'infiltrazione dei granulociti che esprimono alti livelli di S100A8/A9. Nonostante l'aumentata espressione della proteina un giorno dopo l'IR, gli animali S100A9 KO non hanno mostrato grossi cambiamenti nell'infiammazione renale ne' tantomeno hanno mostrato segni di danno. Tuttavia, abbiamo scoperto che S100A8/A9 è fondamentale nel riparo del danno renale dopo IR. Infatti, durante la fase di riparo, i topi S100A9 KO hanno mostrato segni di

disfunzione renale e un aumento d'espressione di segnali di danno provenienti dalle cellule tubulari renali, che era inoltre associato ad un aumento della produzione di chemochine e citochine, che richiamano cellule infiammatorie nel rene. Infine, abbiamo notato che gli animali S100A9 KO hanno sviluppato fibrosi renale, come evidenziato dall'aumento della deposizione di collagene e della produzione della proteina fibrotica TGFβ.
E' stato poi riscontrato che la fibrosi renale fosse dovuta a una funzione alterata dei macrofagi che avevano i topi S100A9 KO. Questo è plausibile, considerato che i macrofagi giocano un ruolo fondamentale nel riparo dei tessuti, specialmente dopo IR. I macrofagi S100A9 KO hanno un fenotipo M2 alterato, come è stato dimostrato dall'aumentata trascrizione di geni coinvolti nell'attivazione M2 dei macrofagi, ovvero Arg1, MGL1 e IRF5. Attraverso esperimenti *in vitro*, abbiamo confermato che dopo stimolazione con le citochine IL4 e IL13, i macrofagi S100A9 KO hanno mostrato un fenotipo simile a quello osservato *in vivo*, ovvero alterata attivazione M2. Probabilmente, durante la fase di riparo, un'eccessiva polarizzazione M2, che è spesso associata al rilascio di fattori pro-fibrotici, può ulteriormente alimentare il processo fibrotico, portando così alla formazione di cicatrici. Pertanto, S100A8/A9 è coinvolto in modo cruciale nel riparo renale dopo ischemia, controllando che la polarizzazione dei macrofagi M2 avvenga in maniera controllata, cosi' da prevenire la fibrosi renale.

E' risaputo che i macrofagi si accumulano nel rene durante la fibrosi renale e possono anche avere un ruolo nella degenerazione dei tessuti. Così, siccome abbiamo osservato che gli animali S100A9 KO mostrano una fibrosi nel modello di danno acuto (AKI) a causa dell'eccessiva polarizzazione dei macrofagi M2, nel **Capitolo 3** abbiamo ulteriormente analizzato il ruolo di S100A8/A9 nello sviluppo della fibrosi renale. In questo capitolo abbiamo usato l'ostruzione ureterale unilaterale (UUO) negli animali WT e S100A9 KO, come modello cronico di danno che conduce allo sviluppo di una grave fibrosi renale. Durante lo sviluppo della fibrosi renale, le cellule positive per S100A8/A9 si accumulano nel rene e co-esprimono il marcatore di attivazione dei granulociti Ly6G; quindi sembrano essere dei granulociti. Tuttavia, l'infiltrazione di queste cellule infiammatorie non differisce tra gli animali WT e S100A9 KO. Il profilo di espressione di S100A8/A9 nel modello preclinico era analogo a quello osservato nei pazienti con idronefrosi. In contrasto con cio'che abbiamo riscontrato nel modello di danno renale acuto, gli animali S100A9 KO hanno sviluppato un attenuata fibrosi renale, come dimostrato dalla diminuzione dell'infiltrazione di miofibroblasti e della deposizione di collagene. E' stato scoperto che la ridotta fibrosi, osservata negli animali KO che avevano subito un danno cronico, era correlata all'integrita' delle cellule epiteliali tubulari (TECs). Gli animali S100A9 KO hanno mostrato una diminuzione dell'apoptosi tubulare e dei processi di

transizione epiteliale-mesenchimale. In linea con questi risultati, è stato osservato che la stimolazione delle TECs con la proteina ricombinante S100A8/A9 induceva l'arresto del ciclo cellulare e portava a manifestare segni di dedifferenziazione epiteliale, inclusa la diminuita espressione delle proteine della giunzione cellulare e delle molecole di adesione, che sono essenziali nel mantenere la struttura e la funzione tubulare. Inoltre S100A8/A9, insieme al fattore profibrotico TGFβ, ha portato a un danno irreversibile e morte cellulare attraverso apoptosi nelle TECs. Pertanto, questi dati suggeriscono che S100A8/A9 e' coinvolto nello sviluppo della fibrosi renale, probabilmente attraverso un effetto diretto sulla dedifferenziazione e apoptosi delle TECs.

Il **capitolo 4** introduce al lettore un altro mediatore dell'infiammazione: il recettore di attivazione espresso su cellule mieloidi-1 (TREM-1). In questo capitolo viene ampiamente riassunta la funzione di TREM-1, a partire dalla rilevanza biologica fino all'intervento terapeutico, esclusivamente in malattie infiammatori che non coinvolgono patogeni.

Il nostro contributo in questo campo inizia con il **capitolo 5**, in cui abbiamo studiato il ruolo di TREM-1 nel modello sperimentale di AKI indotto da IR e nel trapianto renale umano. I topi WT sono stati sottoposti a IR e sacrificati 24 ore dopo, col fine di studiare la risposta infiammatoria acuta. Abbiamo scoperto che durante il danno da IR, si verifica un'infiltrazione di cellule che esprimono TREM-1 nell'interstizio renale. Inoltre, sia il recettore TREM-1 che la proteina solubile risultano aumentati nei rene e nel plasma dei topi. Anche l'espressione monocitica di TREM-1 è risultata aumentata. Ciò suggerisce che TREM-1 potrebbe essere coinvolto nell'amplificazione dei segnali infiammatori che guidano lo sviluppo del danno da IR. Per valutare ulteriormente questa ipotesi, abbiamo trattato i topi con diversi inibitori di TREM-1, che in precedenza si erano dimostrati efficaci nell'inibire l'azione dannosa legata all'eccessiva infiammazione da TREM-1 e di prevenire la disfunzione renale. Nonostante gli inibitori hanno ridotto l'espressione di TREM-1 e delle molecole associate ad esso, gli approcci usati non sono riusciti a proteggere il rene dall'infiammazione e dai danni legati all'IR. Inoltre, abbiamo valutato se le Varianti Nucleotidiche Singole (SNVs) nel gene di TREM-1 fossero associate ad eventuali esiti patologici dopo un trapianto di rene. In linea con i risultati del modello preclinico, abbiamo osservato che né i donatori né i trapiantati che possedevano la specifica variante genica p.Thr25Ser (eterozigote e non sinonimo) nel gene di TREM-1 mostravano alcun esito patologico a lungo termine dopo il trapianto. Da questo studio appare che TREM-1 non svolge un ruolo rilevante nella risposta acuta del rene al danno ipossico.

Ma poiché i PRR possono anche essere coinvolti nella rigenerazione dei reni dopo il danno, abbiamo cercato di effettuare uno studio approfondito sul ruolo di TREM-1 nella

fase di riparo dal danno causato da IR. Pertanto, nel **Capitolo 6**, abbiamo sottoposto gli animali WT e TREM1/3 KO a IR renale e in più i topi sono stati monitorati per studiare la fase del danno, del riparo e della rigenerazione renale dopo il danno ipossico. A questo punto, abbiamo confermato che l'attivazione di TREM-1 non ha alcun effetto durante la fase acuta dopo danno ischemico, in quanto i topi WT e TREM1/3 KO hanno mostrato gradi simili di infiammazione e di danno renale dopo 24 ore di riperfusione. Con sorpresa, abbiamo osservato un aumento della mortalità negli animali TREM1/3 KO durante la fase di riparo. Passando a un modello più lieve di danno siamo stati in grado di dimostrare che i topi TREM1/3 KO soffrono di un alterata fase di riparo che porta allo sviluppo del danno cronico, a partire da quello acuto. In assenza di TREM1/3, in particolare, abbiamo osservato un danno persistente alle cellule tubulari e una fibrosi interstiziale, come dimostrato da una maggiore infiltrazione dei macrofagi, da un accumulo di fibroblasti e dalla deposizione di collagene. Inoltre, i topi con deficit di TREM1/3 non sono riusciti a rigenerare le cellule tubulari, a causa dello sviluppo della senescenza tubulare e della ridotta proliferazione. Attraverso alcuni esperimenti di IR *in vitro*, siamo stati in grado di dimostrare che TREM-1 viene espresso su TECs dopo il danno ipossico, suggerendo un effetto diretto di TREM-1 nella rigenerazione tubulare. Un possibile meccanismo che potrebbe essere alla base della fallita rigenerazione tubulare dopo IR, può essere trovato nel fatto che allo stato stazionario le cellule tubulari che non possiedono TREM1/3 già sperimentano un blocco del ciclo cellulare, in particolare nella fase G2/M. Questo arresto della crescita e' probabilmente correlato al diminuito metabolismo riscontrato nelle TECs che non hanno TREM1/3, in particolare relativi ai livelli di antiossidanti, suggerendo un aumento di stress ossidativo in assenza di TREM1/3. Infatti, queste TECs senza TREM1/3 mostrano alterata omeostasi mitocondriale, con morfologia perturbata, un aumento dell'accumulo di ROS, depolarizzazione dei mitocondri e ridotta capacità di produrre energia. Inoltre, questo ha comportato una maggiore espressione di mediatori pro-infiammatori e fibrotici in queste TECs. Questo fenotipo risulta peggiorato quando le cellule vengono esposte all'IR *in vitro*. Infatti, dopo il danno ischemico queste cellule mostrano un arresto permanente della proliferazione cellulare, definito come senescenza, che ha portato ad una alterata risposta al riparo del danno. Pertanto, abbiamo identificato un nuovo ruolo per TREM-1 nelle cellule epiteliali tubulari, che preserva l'integrità mitocondriale e conferisce un vantaggio metabolico affinché le TEC progrediscano nel ciclo cellulare e proliferino. Per concludere: TREM-1 favorisce la rigenerazione tubulare e limita il danno maladattivo che porta alla progression verso la fibrosi renale.

Visto cio' nel **Capitolo 7** abbiamo valutato il ruolo specifico di TREM-1 e della sua molecola adattatrice DAP12, nel modello cronico di nefropatia ostruttiva unilaterale (UUO), che è il modello classico per la fibrosi renale. Qui, mostriamo che nei pazienti con idronefrosi,

TREM-1 è stato rilevato nelle cellule interstiziali, ma era assente nelle biopsie renali protocolari di pazienti trapiantati con stabile funzione renale. Nel modello sperimentale, abbiamo sottoposto gli animali WT, TREM1/3 KO e DAP12 KO a UUO permanente e abbiamo analizzato gli animali in diversi tempi in fase post-ostruzione. Sebbene UUO porta ad un aumento di espressione di TREM-1 e DAP12 da parte delle cellule interstiziali, sembra che DAP12, in parte attraverso TREM1/3, tende a mediare l'infiammazione renale dopo UUO, ma che entrambi non svolgano un ruolo decisivo nello sviluppo della fibrosi renale. Infatti, l'accumulo di miofibroblasti e i depositi di collagene risultavano simili tra i diversi gruppi di animali. Tuttavia, in assenza di TREM1/3 e DAP12, abbiamo osservato un aumento del danno tubulare e dell'edema nelle prime fasi dopo l'ostruzione, suggerendo un possibile ruolo per TREM1/3 e DAP12 nell'integrità tubulare.

PhD portfolio

Alessandra Tammaro

PhD period: November 2012-2017

PhD supervisor: Prof. dr. S. Florquin

Co-supervisors: dr. M.C. Dessing

dr. J.C. Leemans

	Year
Courses	
- Laboratory Animal Science (Art.9 certification)	2013
- Basic Laboratory safety	2013
- The AMC world of science	2013
- DNA technology	2013
- Scientific writing for publication	2013
- Advanced immunology	2015
Seminars, workshops and master classes	
- Masterclass by Prof. Roy Bloom	2017
- Weekly departments and journal club meetings	2012-17
- APROVE symposium "Sexy science"	2013
- APROVE symposium "Making money in science"	2014
Conferences and presentation	
- European Congress Immunology (ECI 2018), Amsterdam, The Netherlands (oral presentation)	2018
- Keystone symposia, Injury inflammation and fibrosis, Snow bird, Utah, USA (poster presentation)	2017
- Amsterdam infection and immunity retreat, Heemskerk, The Netherlands (oral presentation)	2017
- Dutch symposia of Nephrology, Veldhoven, the Netherlands (oral presentation)	2016
- ENII summer school in immunology, Porto Cervo, Italy (poster and oral presentation)	2016
- International retreat of PhD students in Immunology, Naples, Italy (poster and oral presentation)	2016
- Dutch fall symposia of Nephrology, Lunteren, the Netherlands (poster and oral presentation)	2016
- Toll 2015, Marbella, Spain	2015
- Dutch symposia of Nephrology, Veldhoven, the Netherlands (poster presentation)	2015
- American Association of immunological society 2015- New Orleans (LA) (poster presentation)	2015
- American Society of nephrology- Kidney week, Philadelphia, PA (USA)	2014
- Fall Symposia of Nephrology, Utrecht, the Netherlands	2013
- Dutch symposia of Nephrology, Veldhoven, the Netherlands (poster presentation)	2013
- Platform Aio Nephrology (PLAN) day, Rotterdam, the Netherlands	2013

Lecturing	
- Lecture on Innate immune signalling in acute and chronic renal injury	2017
Tutoring, Mentoring/Supervising	
- Research projects (student): Role of S100A8/A9 in obstructive nephropathy	2016
- Research projects (Erasmus student): Role of TREM-1 in IR-induced AKI	2016
- Research projects (research collaboration): Role of TREM-1 in tubular epithelial cell senescence.	2017
Parameters of Esteem	
- Amsterdam infection and immunity institute: travel award	2017
- Spinoza grant (University of Amsterdam): travel grant	2017
- European network of immunology society: travel grant	2016
- SIICA (italian society of immunology): travel grant	2016
- European Society for Organ Transplantation- Basic science travel grant	2015
- European Federation of Immunological Societies-IL world fellowship visiting grant	2014
- Dutch Kidney Foundation: Kolff PhD/Post doc fellowship visiting grant	2014
Peer reviews	
- 1 article for journal of Crohn's and colitis (impact factor 5.9)	2017
- 1 article for Pathology research and practice (Impact factor 1.54)	2017
Additional Activities	
- Co-organizer of the Promovendi Netwerk Nederland (PNN)'s "National PhD day"	2016

Publications

A. Tammaro, I. Stroo, E. Rampanelli, F. Blank, L. M. Butter, N. Claessen, T. Takai, M. Colonna, J. C. Leemans, S. Florquin, and M. C. Dessing, "Role of TREM1-DAP12 in Renal Inflammation during Obstructive Nephropathy." *PLoS One*. 2013 Dec 16;8(12):e82498

M. C. Dessing, **A. Tammaro**, W. P. Pulskens, G. J. Teske, L. M. Butter, N. Claessen, M. van Eijk, T. van der Poll, T. Vogl, J. Roth, S. Florquin, and J. C. Leemans, "The calcium-binding protein complex S100A8/A9 has a crucial role in controlling macrophage-mediated renal repair following ischemia/reperfusion." *Kidney Int*. 2015 Jan;87(1):85-94.

A. Tammaro, J. Kers, D. Emal, I. Stroo, G. J. D. Teske, L. M. Butter, N. Claessen, J. Damman, M. Derive, G. Navis, S. Florquin, J. C. Leemans, and M. C. Dessing, "Effect of TREM-1 blockade and single nucleotide variants in experimental renal injury and kidney transplantation." *Sci Rep*. 2016 Dec 8;6:38275

A. Tammaro, M. Derive, S. Gibot, J. C. Leemans, S. Florquin, and M. C. Dessing, "TREM-1 and its potential ligands in non-infectious diseases: from biology to clinical perspectives." *Pharmacol Ther.* 2017 Sep;177:81-95.

A. Tammaro, S. Florquin, M. Brok, N. Claessen, L. M. Butter, G. J. D. Teske, O. J. de Boer, T. Vogl, J. C. Leemans, and M. C. Dessing, "S100A8/A9 promotes parenchymal damage and renal fibrosis in obstructive nephropathy." *Clin. Exp. Immunol*., 2018.

About the author

Alessandra Tammaro, daughter of Stefania and Pietro, was born on April 27th 1987 in Naples, Italy. Since high school she manifested a passion for biology that brought her in march 2010 to receive the bachelor diploma in biotechnology, from the University of Naples. Afterwards, she moved to London for several months to improve the english language and obtained several certifications. She continued with master studies in medical biotechnology in Naples, where she carried out a scientific research at Francesco Beguinot's laboratory (National Research Council Institute, Naples). Here, she investigated vascular complications associated with type 2 diabetes. Meanwhile, having received an Erasmus scholarship, she moved to Amsterdam for an additional research in Carlie de Vries's laboratory (Medical Biochemistry department, AMC, university of Amsterdam), where she studied the effect of a cysteine protease inhibitor in the pathology of aorta aneurism, under the supervision of Dr. V. de Waard. In 2012 she obtained her master degree *cum laude* from the University of Naples. In the same year she returned to Amsterdam to begin her PhD program at the department of pathology at AMC, under the supervision of Prof. Dr. Sandrine Florquin, Dr. J.C. Leemans and Dr. M.C. Dessing. In 2014 she was awarded two fellowships for a research collaboration with Prof. Dr. Marco Colonna, that brought her to St. Louis (Missouri, USA) to work at the department of immunology of the prestigious Washington University School of Medicine. She completed her doctoral studies at AMC and the results of her PhD research are the subject of this thesis. On November 2017, together with her partner Jorge, became parents of Angelo Leonardo. Alessandra will continue her research career in kidney diseases at the department of pathology of the Amsterdam UMC, in the group of Prof. Dr. S. Florquin.

A

Acknowledgements

At the end of this amazing experience, I am thankful to so many people who supported me in different ways and I will try to express my gratitude in few words, although it will be hard, I hope that you all know how special you are to me.

First, my sincere gratitude goes to my promotor **prof. dr. S. Florquin**. **Sandrine,** you started as my promotor, then became my supervisor and now you are my boss. You placed your trust in me and I will always be grateful to you. Your immense knowledge, the scientific discussions, your clinical point of view, your exceptional ability to have a helicopter view of many projects and most of all your directness, were essential for the completion of this thesis.

Dr. Dessing, Mark, I still remember our first meeting. I do not know what you saw in that Italian girl with bad English that made you decide that I was suitable for the PhD position. Possibly my enthusiasm, motivation and curiosity convinced you. So I am thankful to have had this opportunity. You always listened to my ideas, though often disagreeing with them. But it was your criticism which motivated me to do better and pushed me to obtain enough publications to finish this book. You have encouraged and supported my decision to visit the Colonna's lab which was a great experience. It challenged me and made me grow in several respects. I wish you all the best in your new career and I am sure you will be as successful as you have been in academia.

Dr. Leemans, Jak, you are the kindest person I ever worked with. You took great care of me when Mark left, even though you were already committed to other projects. I could always walk into your office and have a fruitful scientific discussion and above all receive constant encouragement. I am grateful to have had you read my papers. With your invaluable feedback you helped to turn an early version into a paper which was ready to be submitted for publication. I enjoyed talking to you not only about science but also about my own life, especially during stressful times. Thank you for believing that I was capable of continuing your research, you flatter me! I hope in the future our paths will cross again.

I would also like to extend my gratitude to the members of the committee for the time spent reading my thesis. And to prof. **de Vries. Carlie,** a special thank you for accepting me for an internship in your group. You and **Vivian** were the first inspiring people I had the pleasure to work with in the NL. Thank you so much for your feedbacks and encouragements!

Elena, GRAZIE perche'non sei stata solo un amica, ma anche una guida durante questi anni! mi sembra giusto metterti dopo i grandi, perche' per me tu sei una come loro. Una persona da cui ho tanto da imparare e che mi ha sapientemente consigliato in questi ultimi anni! Grazie perche'se molti progetti hanno preso una strada diversa e sono riusciti con successo e' anche merito tuo. Sono felice che Idris e Angelo sono coetanei e che un giorno potranno andare a scuola calcio insieme☺

To my colleagues of the **RIRE** group, old and new, for creating a great atmosphere in the lab and in the office, but most of all to switch to english everytime I was around! I appreciate it☺ **Nike**, what a privilege it is working with you! A problem solver, an inspiring woman, a great and sweet friend, you are so much more than a colleague! **Joris**, you always have a funny joke and a great sense of humor. It is a pleasure to work with you. Thanks to **Jan,** for the discussions and insightful comments.

Loes thank you for always being available to my last minute requests, and to have isolated many primary cells from me:). **Geurt**, thanks a lot for your critical opinions about my work and the fun time we had in Philly. **Marcel**, thanks for telling me that Mark was looking for a PhD student. I had a lot of fun with you in and outside of the lab. It was great to hear all your entrepreneurial ideas during the years. My favorite is still the meggins:S. I am happy that I was able to show to you and Lotte my roots, my family and friends in Naples but most of all that you were able to taste some good Italian food:P. **Lotte**, you became such a strong woman and I am sure you will be a wonderful mum. **Diba**, thanks to have introduced me to Jorge, I will be grateful for my entire life. **Angelique**, thank you for proofreading my english everytime. **Melissa**, how nice we were pregnant at the same time, it was a completely new world for me, in a different country, but you gave me so much valuable information! Wish you both a fruitful year, full of publications to complete your book! Remember, there is nothing better than a submitted thesis! **Joris and Djera**, you are very bright and I am sure you will have a successful path! Good luck! To people I had the pleasure to meet and that scientifically contributed to this book: **Jesper**, I am glad Mark decided to have a collaboration on the TREM-1 project, you are very talented and I know if I want to know anything about omics, statistics and bioinformatics, a black hole for me, you are the MAN! Good luck in USA. **Cristiana**, che fortuna averti incontrato alla summer school, il tuo commento dopo la mia presentazione ha cambiato le sorti del progetto. Da li' oltre a una proficua collaborazione e'nata una bellissima amicizia che spero continui oltre le distanze☺

To the whole **partyology** crew for the fun time in and out of the lab, the endless borrels, the nights at the Epsteinbar, that made these years gezellig.

Wim thank you so much to make great figures for my publications and for the layout of this book, I know you are very busy but still found some time for me. I appreciate it☺.

Mahnoush, I am happy that you are still working at AMC, you are a bright scientist, very dedicated and I had the pleasure to live with you and discover the great person you are. Good luck in finishing your book.

To the students I supervised that in some respects contributed to this book: **Mascha and Martina**. You were good students, I figured it out after spending many evenings s in re-analyzing your experiments to make sure everything was correct:P

To the international friends I met at AMC: **Vincenzo, Rossella, Goran, Iker, Babu, Cristina, Ana, Andre, Nazanin, Lorena, Emma, Gianni, Thijs, Celine, Leila, Dmitri, Stijntje, Matthijs, Marta, Luca** and many others that I surely forgot. I feel I still have a pregnant brain. THANKS because often you were able to make me forget a tough day at work! I wish I could have all of you back for my promotion for a get-together as in the old days.

To the americans: **Paola and Malinda** that were always up to a trip when I was around and for the great "yoga". Thanks to the people of the Colonna's lab that made my stay unforgettable, in particular to **Alex and Cristina**, my buddies☺ and to the Italian community in St. Louis, in particular to **Claudia**! Grazie per esserti presa cura di me, la mia avventura americana non sarebbe stata la stessa senza di te!!!

Margherita, tu mi sei stata accanto all'inizio di questa avventura, sono stati mesi stupendi in cui ci siamo divertite tantissimo e in cui ho conosciuto la persona speciale che sei. Sono felice che tu abbia conosciuto Giovanni che ti rende felice e ancora piu'sorridente di quello che sei! Che gioia sapere che ci sarai per condividere con me questo giorno cosi'importante!

Marica, pazzerella bella. Tu sei la sensibilita'in persona, che pochi riescono a scoprire, perche'spesso la mascheri bene. Ho avuto la fortuna di conoscerti grazie a Marghe e sono sicura che dopo questo libro saprai un po'di piu'su TREM-1. Sei stata capace di rendere leggere le mie serate stressanti da fine dottorato e ancora oggi riesci sempre a strapparmi un sorriso! Grazie!!!!

Ema, che peccato che sei andato via, grazie per la compagnia, le risate, le correzioni alle lezioni di pilates, i racconti dei tuoi weekend e dei gossip-Monday quando ero in maternita'. Spero che abbia trovato il tuo equilibrio, anche se in tutta onesta'e'strano immaginare che tu non viva piu'ad Amsterdam.

Chiara&Gianluca, siete davvero genuini e sinceri, rarita' incontrare due persone cosi'. Grazie per le cene italiane che mi fanno sentire sempre a casa, soprattutto per la parmigiana e i macarons☺

Duco, you deserve some space here. I still remember the first day at AMC, coming to me at 12 and saying: LUNCH? I thought well this is my breakfast, but let's go to be social. SURE! I was still confused and thought maybe for you it was also breakfast because of the milk, then I learned about this dutch habit!!! Joking aside, from that day on we started a beautiful friendship and together with Jess we were the Weerdestein family. You are a special person, always available to help, listen and cheering me up during these years. After meeting your family, I understood why you are like this. I hope we will be sharing many things in future☺

Jess, our start as housemate was not a great success :D, but this is probably the reason why we became best friends. I loved the girl-time in Weerdestein, going shopping, to brunch, our evening at SPA zuiver, making dinner together and organizing parties, all of this was so much fun with you. Together we developed an exceptional command of the dutch language, which made us think that "openbaar vervoer" for Efteling, meant that they had an open bar in the park!!! Probably because the café belgique was near the class :S Even when you left the NL, we were still sharing many things, it felt you have never left. I know living far away from your love isn't easy, but you were a strong woman and all the sacrifice paid off last july, when you finally moved in with Duco in London. The sparkle in your eyes makes me extremely happy. Thank you both to organize Angelo's baby shower and to make fun of me, together with Jorge, when I was crying during a movie:P

Maria, you are a girl of a few words, but since the first times I met you, I knew you were a sincere person. Even if we don't see each other every day, I know I can always count on you. It was great living together. Thanks for organizing a great surprise for me during the baby shower and for the fun in Spain, Italy, London, and Amsterdam.

Grazie a tutti i miei **cugini e amici** che sono venuti a trovarmi ad Amsterdam. Per quelli che ancora non l'hanno fatto mi dispiace ma ora saro' un po'meno divertente visto che alle 10 max voglio un letto:P. Grazie a **Ivano**, la mia famigia in Olanda, sempre preciso, in orario e che e'sempre disponibile anche all'ultimo minuto. Anche se vive in Olanda e dice di avere un agenda riesce comunque ad essere napoletano! Sono felice che abbia coronato il tuo sogno d'amore con Nathalie.

Grazie alla mia **famiglia** e ai miei **nipoti**, che hanno alleviato i miei momenti di solitudine con una chiamata, un pacco regalo o semplicemente manifestandomi tutto il loro orgoglio e sostegno in questi anni. Siete stati la mia forza! Soprattutto a mia madre, per essermi stata accanto nel giorno piu' bello della mia vita e che corre sempre in mio soccorso.

A **Jorge e Angelo**, il regalo piu' bello che la vita potesse farmi. I vostri sorrisi e l'amore che mi donate sono la mia energia quotidiana. Siete il mio porto sicuro, vi amo.